NORMAL MODES OF REALISTIC EARTH MODELS: AN ADVANCED TREATMENT OF ELASTICITY, ROTATION AND FLUID CORE COMPRESSIBILITY

MD. KAMRUZZAMAN
M. Sc. in Physics, University of Lethbridge, 2015

A thesis submitted
in partial fulfilment of the requirements for the degree of

DOCTOR OF PHILOSOPHY

in

GEOPHYSICS

Department of Physics and Astronomy
University of Lethbridge
LETHBRIDGE, ALBERTA, CANADA

NORMAL MODES OF REALISTIC EARTH MODELS: AN ADVANCED TREATMENT OF ELASTICITY, ROTATION AND FLUID CORE COMPRESSIBILITY

MD. KAMRUZZAMAN

Date of Defense: April 27, 2021

Dr. B. Seyed-Mahmoud Supervisor	Associate Professor	Ph.D.
Dr. A. Akbary-Majdabadno Thesis Examination Committee Member	Professor	Ph.D.
Dr. H. Jiskoot Thesis Examination Committee Member	Professor	Ph.D.
Dr. M. Roussel Internal External Examiner	Professor	Ph.D.
Dr. C. Huang External Examiner	Professor	Ph.D.
Dr. K. Vos Chair, Thesis Examination Committee	Associate Professor	Ph.D.

Dedication

This thesis is dedicated to my lovely son Zayyan.

Abstract

We apply the Galerkin method to solve the linear momentum description (LMD) of the dynamics of the Earth's layers and expand the Galerkin formulation of the LMD to include the first order ellipticity using the Clairaut coordinate system in order to study the Earth's normal modes. We show that the computed frequencies of the inertial modes may be significantly affected by the elasticity of the mantle and inner core. Traditionally, a liquid core with rigid boundaries is considered to study these modes. Our computed periods of the Chandler wobble (CW) and the free core nutation (FCN) are not affected by the density stratification of the fluid core. The computed period of the FCN, 432.28 sd, is almost identical to the observed value. This indicates that the Earth is indeed in hydrostatic equilibrium which is in contrast to previous work suggested that the Earth deviated from hydrostatic equilibrium. The great advantage of our method is that we can ensure the frequencies are converged.

Contributions of Authors

Part I of Chapter 5 is based on a published paper: Inertial modes of an Earth model with a compressible fluid core and elastic mantle and inner core, M. Kamruzzaman and B. Seyed-Mahmoud, J. Geod., 94(4): 1-15, 2020. In this work, I have applied the Galerkin method and have written FORTRAN codes to solve the linear momentum and Poisson's equations with the relevant boundary conditions at the interfaces. My FORTRAN codes would not give the expected results for the elastic (spheroidal) modes, the Slichter modes and the inertial modes because I had not set the first derivatives of the dependent variables to zero at the center of the Earth. I thank Behnam Seyed Mahmoud for suggesting it. Then I computed the periods of these modes, and analyzed the results. Also, Behnam Seyed Mahmoud rechecked my derivations as well as my FORTRAN codes. Next, I wrote the manuscript and Behnam Seyed Mahmoud revised it. The software to integrate the equations in the θ direction was developed by my supervisor.

Acknowledgments

I am indebted to my supervisor Dr. Behnam Seyed-Mahmoud for his supervision, encouragement, suggestion and discussion at every stage of this research work, and for affording me an opportunity to study at the University of Lethbridge. I learned about various modeling techniques for solving geophysical problems using FORTRAN from my supervisor. He will always remain my principal mentor.

I would like to thank my supervisory committee members, Dr. Amir Akbary-Majdabadno and Dr. Hester Jiskoot, for sparing their time to have meetings during the PhD program. I thank you all for the constructive suggestions and encouragements.

I would like to thank my wife Ruksi and my family for mental support in various ways during the PhD program.

I wish to express my gratitude to the School of Graduate Studies and the Faculty of Arts and Science of the University of Lethbridge for their kind hospitality and for providing me facilities at the University of Lethbridge during the PhD program which made this work possible. I would like to thank the administration staff for helping me in various ways during the PhD program.

Contents

List of Tables

List of Figures

List of Abbreviations

IC	Inner Core
OC	Outer Core
MT	Mantle
PREM	Preliminary Reference Earth Model
ICB	Inner Core Boundary
CMB	Core Mantle Boundary
GPS	Global Positioning Systems
VLBI	Very Long Baseline Interferometry
LLR	Lunar Laser Ranging
SOM	Spin Over Mode
TOM	Tilt- Over Mode
CW	Chandler Wobble
NDFW	Nearly Diurnal Free Wobble
FCN	Free Core Nutation
ICW	Inner Core Wobble
FICN	Free Inner Core Nutation

Chapter 1

Introduction

1.1 Overview

The Earth's interior consists of four major layers, the crust, the mantle (MT), the fluid outer core (OC) and the inner core (IC), based on their chemical composition and material properties. The main structural components, which are distinguished by the sharp discontinuities at the boundary interface, of the Earth are shown in Fig 1.1. The solid IC with radius of about 1221.5 km is the deepest region from the Earth's surface, the OC with a mean thickness of about 2258.5 km is a spheroidal shell contained between the IC and MT, and the crust is the thinnest layer of the Earth [1]. S- and P-waves are generated when an Earthquake occurs. The P-wave arrives first to seismometers and then the S-wave. The S-wave is only detected up to an angular distance of about 104° from the epicenter of an Earthquake and the P-wave is not detected between 104° and 140°. This area is called the shadow zone with no waves at all in between. In 1914, Gutenberg figured out that all this was due to the existence of the fluid core because the S-wave cannot transmit through fluids, and also discovered that the solid mantle gives way to the fluid core at a depth of about 2,900 km from the Earth's surface where the P wave decreases in speed while the S wave disappears. This discontinuity is called the Gutenberg discontinuity. This boundary is also referred to the core mantle boundary (CMB). Lehmann [3] analyzed the Earthquake record especially after a 1929 earthquake that occurred in New Zealand, and showed some reflected P-waves in the shadow zone. Previously, seismologists assumed that some faint P-waves in the shadow zone were the result of error of seismometers. She gave an idea that

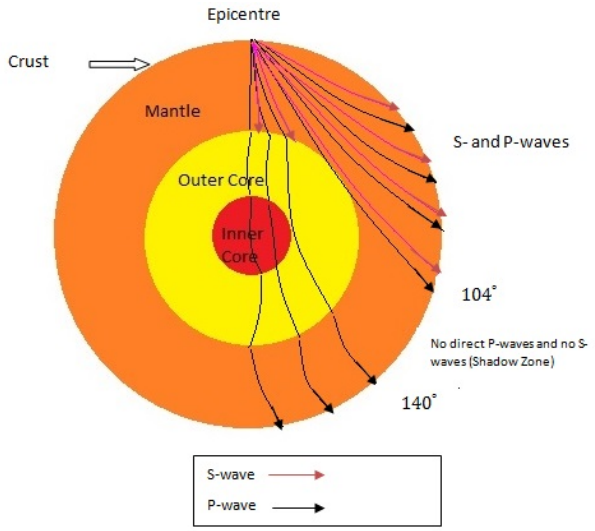

Figure 1.1: Schematic diagram of the Earth's layers. P- and S-wave travel inside the Earth's interior when an Earthquake occurs. Source of this Figure is https://www.iris.edu/hq/inclass/animation/seismic/shadow/zone/basic/introduction

a solid inner core, which would reflect some P-waves in the shadow zone, existed inside the fluid outer core. The boundary between the outer core and inner core is known as the Lehmann discontinuity or the inner core boundary (ICB). In 1954, Lehmann noticed that seismic waves in the Earth's upper mantle (about 200 km from the Earth's surface) travel faster. That region is also known as the Lehmann discontinuity. The boundary between the mantle and crust is called the Mohorovicic' discontinuity or the Moho. Table 1.1 shows the chemical composition and material properties of the Earth's layers. In 1981, Dziewonski and Anderson [1] established the preliminary reference Earth model (PREM) from a compilation of seismic, free oscillation and nutation data. This model provides a basic reference state for many Earth parameters for consistent studies of the Earth, and is widely accepted as a reference Earth model (see details in the section 2.5).

It is well known that the Earth's deep interior is not directly accessible for study and many of its properties are still poorly known. Although the observational and theoretical studies of ray seismology have established accurate profiles for properties such as density, the P-wave and S-wave velocities, some properties such as density stratification parameter and liquid viscosity may not be firmly established because short-period body waves data are

Table 1.1: The chemical composition and material properties of the Earth's layers [1, 2]

Layer	Radius km	Density $\mathrm{kg\,m^{-3}}$	Pressure GPa	Temperature °C	Composition
Crust	25	1020-2900	0-1	27-227	Mostly oxygen, silicon and aluminum
Mantle	2866	3381-5566	1-136	227-3426	Iron- and magnesium-rich silicate minerals
Outer core	2259	9903-12166	136-329	3426-4227	Molten iron and nickel
Inner Core	1221	12763-13088	329-364	4227-7728	Solid iron-nickel alloys

not directly sensitive to those properties [1, 4, 5]. These parameters play an important role in determining the mantle's heterogeneity and mantle flow [6, 7, 8]. In order to establish more accurate Earth models, the theory of ray seismology is complemented by the normal mode theory [9, 10]. The normal modes are the Earth's oscillations which may be excited as a result of a large earthquake, a mass displacement within the Earth or the gravitational pull of secondary bodies (e.g., the sun, the moon and other planets) [11, 12, 13, 14, 15].

The spectrum of the Earth's normal modes consists of:

(i) the short-period free oscillations or the seismic modes which have periods shorter than an hour, and have elasticity as their primary restoring force;

(ii) the intermediate-period (4 hr $< T <$ 7 hr) oscillations such as the Slichter modes which are the translational modes of the IC [16] and which mainly depend on the dynamics of the IC and density jump at the inner core boundary (ICB) [17, 18];

(iii) the long-period, longer than half a day, free oscillations which are considerably affected by the Earth's rotation.

The Earth's possible long-period free oscillations are:

(i) the wobble and nutation modes, which depend on the rotation, composition and shape of the Earth;

(ii) the inertial-gravity modes which have the Coriolis force and the radial component of gravitational force as their restoring force [19];

(iii) the gravity modes with negative buoyancy as their restoring force;

(iv) and the inertial modes, which depend on the Coriolis force as their restoring force.

1.2 Inertial modes

The inertial modes of a rotating, incompressible, homogeneous, inviscid contained fluid with rigid boundaries are described by the Poincaré equation. Among the first who investigated these modes are Bryan [20], Hough [21] and Poincaré [22]. The Poincaré equation is a hyperbolic partial differential equation subject to boundary conditions, a condition that makes the problem ill-posed [23, 24]. The existence of analytical solutions, therefore, depends on the geometry of the container. For example, these solutions exist for a cylinder [25], a sphere [20, 26], a tri-axial ellipsoid [27, 28, 29] and a spheroid of any tilted angle with rotation axis [30]. These solutions do not exist, except for purely toroidal modes, for a spheroidal shell geometry such as the Earth's fluid core. The experimental results, however, suggests that such modes exist in a thick shell [31, 24, 32, 33]. Rieutord [34] used an iterative procedure [see also [35]] to numerically solve the Poincaré problem for a fluid shell of small viscosity. Rieutord and Valdettaro [36] also showed that the axisymetric inertial modes in a spherical shell may be determined by a web of characteristics that reflect at the boundaries. They observed that the web of rays (or characteristics) are formed in the intersection of these surfaces with a meridional plane. They showed that the pattern of rays bifurcates as viscosity moves toward zero and concluded that no asymptotic smooth solutions exist for the limit of zero viscosity.

Seyed Mahmoud et al. [37] considered a compressible and a neutrally stratified fluid to study the inertial modes of rotating and self-gravitating fluid spherical and spherical shell geometries using the Three Potential Description (3PD) of the fluid core dynamics [38].

Their results show that the frequencies of the inertial modes may be affected by such properties as the fluid compressibility and the shape of the container. They also pointed out that the eigenfunctions of these modes are almost identical to those of the Poincaré model. The interactions of inertial-gravity modes of the OC on the wobble and nutation modes for a realistic Earth model was investigated by Rogister and Valette [39]. They truncated the field variables at degree 4 of the spherical harmonics, and their computed modes of the OC were termed pseudo-modes. They show that the frequencies of pseudo-modes of OC depend on the square of the Brunt-V*äisälä* frequency and the Earth's rotation rate. However, except for the frequency of the SOM (spin over mode), truncation at degree 4 of the spherical harmonics is not sufficient when solving for the frequencies of the inertial modes (see table 2 in [37]). Seyed Mahmoud et al. [37] show that the spherical harmonics of degree up to 20 are needed for the free inner core nutation (FICN) of a simple Earth model to converge to a mean value [40]. Recently, Seyed Mahmoud et al. [41] (see also Kamruzzaman [42]) used the 3PD to investigate the influence of density stratification on the frequencies of the inertial modes for several fluid core models with different stratification parameters. They show that the frequency of an inertial mode is a linear function of the stratification parameter. The inertial modes of a contained fluid with elastic boundaries have been first studied by Kamruzzaman and Seyed Mahmoud [43]. They show that the computed dimensionless frequencies of the inertial modes may be significantly affected by the elasticity of the mantle and inner core. For example, the frequencies of the (2,1,1) or the spin-over mode (SOM), (4,1,1), (4,2,1) and (4,3,1) modes are changed from 0.5000, -0.4100, 0.3060 and 0.8540 for a Poincaré model to 0.4995, -0.4208, 0.3150 and 0.8587, respectively. The change in the frequency of the SOM may seem small but it is consistent with the change in the frequency of the free-core nutation (FCN), which is the same mode as the SOM of a wobbling Earth, which changes from ≈ 0.50144 for an Earth model with rigid mantle and inner core to ≈ 0.50116 for an elastic Earth model (see details in part I of the chapter 5). Recently, existing and improving technology was able to detect the gravity

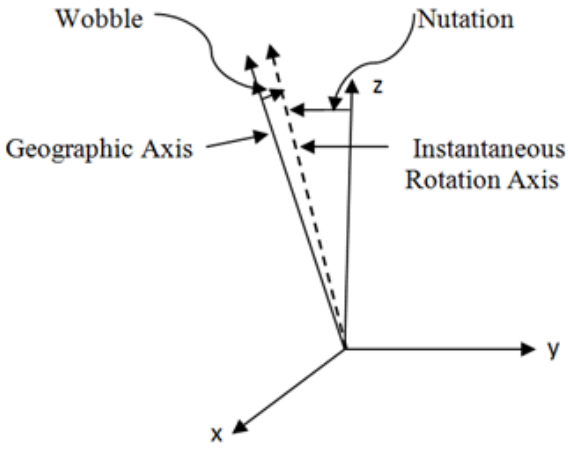

Figure 1.2: Schematic description of the Earth's wobble and nutation. The xyz refers to an inertial reference frame, a solid line depicts the Earth's geographic/rotation axis which is inclined to about 23.5° to the direction of the normal to the Earth's orbital plane around the Sun, and a dotted line is the instantaneous rotation axis.

modes from the time of the Big Bang, and the inertial modes may be detected soon.

1.3 Wobble and Nutation Modes

In astrophysical and geophysical studies, knowledge of the variations in the Earth's orientation, namely wobble/nutation, plays an important part. The oscillatory motion of the rotation axis measured from the inertial reference frame is called nutation, whereas wobble is the oscillatory motion of the rotation axis measured from the rotating reference frame (see Fig. 1.2).

The variation in the Earth's orientation is caused by many factors: the gravitational pull of the secondary bodies (e.g., sun, moons and other planets), Earth's internal structure and shape, Earth's deformations (dynamical effects), ocean tides, and other geophysical impacts such as redistribution of currents, masses, winds, magnetism, hydrology, earthquakes, isostatic rebound, etc [44]. The terms free and forced wobble/nutation refer to the movement of the rotation axis driven by different factors. Free wobble/nutation is due to any internal redistribution of the angular momentum, whereas forced wobble/nutation is caused by the external forces. The periods of the forced nutations have a range from less

than a sidereal day (sd) to thousands of years. The sidereal day is a unit time scale of magnitude, 1 sd = 23 hr, 56 min and 4.0916 seconds, which measures the rotation rate of the Earth with respect to a fixed star, whereas the solar day measures the rotation rate of the Earth with respect to the Sun. The longer periods are 26,000 years, 18.6 years, 9.3 years, annual, semi-annual, and 13.66 sd (fortnightly) nutations. On the other hand, five possible free rotational normal modes exist: the Chandler Wobble (CW), the Tilt-Over Mode (TOM), the Nearly Diurnal Free Wobble (NDFW) or the Free Core Nutation (FCN), the Inner Core Wobble (ICW) and the Free Inner Core Nutation (FICN). The periods of CW, TOM, and FCN depend mainly on the dynamics of the mantle and partly of the fluid core, the whole Earth, and the fluid and inner cores, respectively, while the periods of ICW and FICN depend primarily on the dynamics of the inner core [45]. The CW and ICW are long period prograde motions in the terrestrial (rotating) reference frame, whereas the retrograde FCN and the prograde FICN are long period in the inertial reference frame. The terms prograde and retrograde refer to an object that spins in the same direction as its orbit and an object that spins in the opposite direction as its orbit respectively. Several space geodetic techniques, Global Positioning Systems (GPS), Very Long Baseline Interferometry (VLBI) and Lunar Laser Ranging (LLR), are used to obtain the observed periods of these modes. The observed periods of five possible free rotational normal modes is shown on the Table 1.2. The identification of these modes helps our understanding about the Earth's interior and also to predict the future state of our planet [46, 47, 48, 49].

1.3.1 History of Normal Modes Calculations

Euler first assumed the Earth as a rigid body with a uniform mass distribution, and predicted the period of the free wobble as 306 sd [53]. This is known as a free Eulerian wobble. Subsequently, the Chandler wobble of the Earth with a period of about 435 sd was discovered in 1891 by S. C. Chandler from available astronomical data [50]. The Earth is not rigid; it consists of the solid inner core, fluid outer core, viscous mantle, solid

Table 1.2: The observed periods (sd) of five possible free rotational normal modes

Modes	Period (sd)
CW [50]	435
FCN [51]	-429.07 ± 0.07
FICN [51]	929 ± 31
ICW	Not yet
TOM [21, 52]	1

crust, oceans and atmosphere. Newcomb explained the discrepancy, which is caused by the elasticity of the Earth's solid parts, between the observed and predicted periods [54]. Hough [21] and Poincaré [22] also took into account the presence of the fluid core, and Love considered the elasticity of the Earth to explain the difference [55]. If the presence of the fluid core is considered, the period of the Eulerian wobble is about of 270 sd for a rigid Earth model and the model also yields the free core nutation period of about 350 sd.

In order to establish more realistic Earth models, the variational formulation for the two layers Earth model, a homogeneous fluid core and an elastic, radially inhomogeneous mantle, was given by Jeffreys and Vicente [56]. They calculated the periods of CW at 392.4 sd and NDFW at 0.9978 sd. Molodensky extended this model to add the compressibility of the fluid core (neutral stratification), and computed the periods of CW at 400.87 sd and NDFW at 0.9978 sd [57]. Molodensky's theory was modified by Shen and Mansinha to include non-neutral, both stable and unstable stratification of the fluid core [58]. They showed that the computed periods, both short- and long-periods, of free core oscillations of order 1 and degree 2 depend on the stratification of the core, but the period of NDFW at 0.9978 sd is independent on the core stratification. The NDFW is well known now as the FCN.

Smith [59] derived the set of coupled ordinary differential equations, which describe the dynamics of elastic gravitational motion for a elliptical and rotating Earth in a hydrostatic equilibrium reference frame, based on the linear momentum description (LMD). In this

description, the displacement is represented in the form of two coupling chains in terms of the spheroidal and toroidal components [see equation (2.18)]. The advantage of the LMD is that the dynamics of the fluid core is not pre-assumed to be mainly solid body rotation, which is in contrast to the semi-analytical angular momentum description (AMD) [60]. He applied this theory to compute the periods of the CW as 403.5 sd, and NDFW as 0.9978 sd [52]. He only truncated at harmonics T_3 for these modes, and did not compute the period of ICW accurately.

Wahr extended the normal modes theory [61, 62] based on Smith's formulation [59], and studied the Earth's free and forced nutation. He considered an Earth model in hydrostatic equilibrium. Herring et al. [63] showed that the difference of the observed amplitude, which has been found from the VLBI data of the forced nutations, for the annual nutation with the IAU adopted theory is 2 mas (milliarcsecond). Note that the VLBI method of data analysis makes it possible to find the amplitudes of the nutations at various tidal frequencies with standard errors under 0.1 mas. To minimize the discrepancies of the observed and predicted results, several authors have taken into account the extra dynamical ellipticity (5% higher than PREM) of the core-mantle boundary (CMB) [64, 63], ocean tides [65], energy dissipation and anelasticity of the mantle [66], and atmosphere and oceans [67, 68]. Under these considerations, significant discrepancies of the observed and predicted values still remain, particularly at the semi-annual and fortnightly prograde frequencies [63, 69, 70].

Mathews et al. [71] developed a semi-analytical normal mode theory, based on the AMD, for the Earth model which is a rotating, ocenless, elastic mantle, fluid outer and elastic inner core. In the AMD, they included the dynamical role of an inner core on the fluid core and mantle, whereas the outer core was considered as a predominantly solid body rotation [see their equation (15b) in [71]]. They applied this theory, and computed the periods of the CW, FCN and ICW [72] which are significantly different from the corresponding results of Wahr [61]. They used Sasao's approximation. Recently, Seyed-Mahmoud and Rogister [73] showed that Sasao's approximation is equivalent to ignoring the dynamics

of the mantle when calculating periods of the FICN and ICW. Their work (Mathews et al. [71]) also showed the smaller discrepancies between the predicted and observed values using the modified dynamical ellipticity (about 4.6% higher than PREM) of the PREM, e.g. at the prograde semi-annual and annual, and retrograde 18.6 year and annual nutation series. Even after using the modified ellipticity, the amplitude of the prograde fortnightly nutation still has an uncertainty of about 1 mas. In order to minimize the uncertainties of the amplitudes of forced nutations series; Mathews et al. [74], Herring et al. [75] and Buffett et al. [76] reformulated the model of [71] to include the effects of ocean tides, anelasticity of mantle and electromagnetic couplings, between the fluid core and the solid inner core [i.e. at inner core boundary, (ICB)] and the fluid core and mantle (i.e. at CMB), and using better precision of 20 years of VLBI observed data. The modified model is called MHB2000. In MHB2000, they used the dynamical ellipticities of a fluid core and the Earth, an anelasticity of the mantle, and the electromagnetic coupling constants at ICB and CMB which are determined by a least squares fit. The International Union of Geodesy and Geophysics (IUGG) 2003 nutation series and the IAU 2000 nutation series have adopted this new MHB2000 model. However, the largest uncertainty of the amplitude for the prograde 18.6 year nutation in this model is about 72 μas (microarcsecond), and the period of FCN is 460 sd which is significantly different from the observed value [77].

Rochester and Crossley [78] derived a Lagrangian formulation of the Liouville equations for elastic deformations of an inner core and mantle by combining the analytical features of the AMD in a hydrostatic equilibrium reference frame for low frequency modes. They found the CW period of about 400.3 sd and the ICW period of about 7.5 yr. However, they were not able to compute the periods of inertial-gravity modes of the OC such as the FCN because they omitted the inertial term of the momentum equation. The previous computed period of ICW was about 6.6 yr [72, 74]. Their works [72, 74] took into account the inner core as a solid, but Rochester and Crossley [78] considered the elastic deformations of the Earth's solid parts. Also, Dumberry [79] implemented the theory of [71] by considering

the elastic deformation of an inner core, and found the ICW period as about 7.4 yr. Note that the ICW mode was not still detected by the space geodetic techniques (GPS, VLBI and LLR). Recently, Rochester et al. [60] developed a new mathematical description based on the LMD for the theory of free wobble/nutation modes to include the second order ellipticity using a non-orthogonal (Clairaut) coordinate system. Using this description [60], Crossley and Rochester identified four wobble and nutation modes, the FCN at -456 sd, FICN at 468 sd, CW at 402 sd and ICW at 2842 sd, for a neutrally stratified PREM [45]. They were able to extend the truncation to T_5 rather than the previous T_3 [e.g., [52, 62]], but they were not able to show that the periods of these modes had converged. For example, the period of CW for a 1066A model is 403.17 sd when truncated at T_3 and 416.04 sd at T_5 [45].

1.4 Thesis Outline

The objective of this thesis is to compute the eigenfrequencies and eigenfunctions of the normal modes such as the Slichter modes, the spheroidal modes, the inertial modes and wobble/nutation modes of an Earth model which consists of an elastic IC, a fluid OC and an elastic MT. This thesis is organized into six chapters. In chapter 2, we discuss the governing equations with representation of the field variables of the Earth's layers, including the boundary conditions. In order to study the Earth's normal modes, we consider the Earth models that consist of three layers, the MT, the fluid OC and the IC. We treat the P-, S-wave speed and the density profiles of the MT as one layer.

In chapter 3, we introduce the Galerkin method applicable to a system of simultaneous partial differential equations subject to boundary conditions. This method is then applied, based on the work of Kamruzzaman and Seyed Mahmoud [43], to the dynamical equations. We show that this method may be used to take advantage of the natural boundary condition, and to remove the singularity of the dynamical equations. Then, the matrix representation of the dynamical equations is discussed.

In chapter 4, we discuss the Clairaut coordinate system, and solve the Clairaut equation to find the Earth's ellipticity profile using the Runge-Kutta integration method. We derive the vector and scalar operations, which involve the Galerkin formulation of the dynamical equations, by applying this coordinate system. Then, we expand the Galerkin formulation of the dynamical equations to include the first order ellipticity in the Earth model.

In chapter 5, we discuss the results of this work. This chapter is separated into two parts. In part I, we consider a rotating spherical Earth model with a compressible, inviscid, stratified fluid OC with an elastic MT. Also, we consider a rotating spherical fluid shell contained between an elastic IC and an elastic MT. The procedures for computing non-dimensional frequencies of the normal modes such as the Slichter modes, the spheroidal modes, the inertial modes of both a spherical OC with an elastic MT and spherical shell OC with an elastic IC and MT models are presented. We then present and describe the non-dimensional frequencies and displacement eigenfunctions of these inertial modes, and investigate the effect of the elasticity of the mantle and inner core. Traditionally, a liquid core with rigid boundaries is considered to study these modes. In part II, we consider a rotating spheroidal fluid shell contained between an elastic IC and an elastic MT, and compute the period of the Earth's wobble/nutation modes which are the independent of the density stratification of the OC. Our computed period of the FCN, 432.28 sd, is almost identical to the observed value. The great advantage of our method is that we can ensure the frequencies are converged. Finally, chapter 6 contains conclusions of this work and future direction of possible projects.

Chapter 2

Formulation

In this chapter, we will discuss the governing equations of the Earth's interior including the representation of the field variables of these equations. In section 2.4, the boundary conditions at the geocentre, at the solid-fluid interfaces, and at the Earth's surface will be discussed. Next, we will discuss the Earth models that will be used to investigate the eigenfrequencies and eigenfunctions of the normal modes such as the Slichter modes, the spheroidal modes, the inertial modes, and the wobble/nutation modes of the Earth.

2.1 Governing Equations of the Earth's Interior

In order to study the free oscillation of the Earth's interior, we take the reference state as being one of hydrostatic equilibrium in a coordinate system which rotates with a constant angular velocity Ω about a fixed axis defined by the unit vector $\hat{\mathbf{e}}_3$. In this reference state, the equilibrium pressure p_0, density ρ_0, gravity potential W_0 and the gravity $\mathbf{g}_0$ are related by:

$$\nabla p_0 = \rho_0 \mathbf{g}_0, \tag{2.1}$$

$$\mathbf{g}_0 = \nabla W_0, \tag{2.2}$$

$$\nabla^2 W_0 = -4\pi G\rho_0 + 2\Omega^2, \tag{2.3}$$

where G is the gravitational constant.

Any small disturbance of the Earth's interior gives rise to the free oscillations. The free oscillations of the Earth are described by the conservation laws for mass, linear momentum,

angular momentum and gravitational flux. Smith [59] derived the set of coupled ordinary differential equations which describe the linear dynamics of elastic gravitational motion for a elliptical and rotating Earth in a hydrostatic equilibrium reference frame. These equations can be written as

$$\rho_0 \frac{\partial^2 \mathbf{u}_k}{\partial t^2} + 2\rho_0 \Omega \hat{\mathbf{e}}_3 \times \frac{\partial \mathbf{u}_k}{\partial t} + \rho_0 \Omega^2 \hat{\mathbf{e}}_3 \times (\hat{\mathbf{e}}_3 \times \mathbf{u}_k) - \nabla \cdot (\tilde{\tau})_k + \nabla(p_0 \nabla \cdot \mathbf{u}_k) - \rho_0 \nabla (V_1)_k$$
$$-\rho_0 \mathbf{u}_k \cdot \nabla \nabla (V_0)_k - \nabla \cdot [p_0 (\nabla \mathbf{u}_k)^T] = 0, \tag{2.4}$$

$$\nabla^2 (V_1)_k - 4\pi G \nabla \cdot (\rho_0 \mathbf{u}_k) = 0, \tag{2.5}$$

where $\mathbf{u}_k$, V_{0k}, V_{1k} and $\tilde{\tau}_k$ are respectively the Lagrangian displacement from equilibrium, the equilibrium gravitational potential, the Eulerian perturbation in the gravitational potential and the stress tensor due to deformation in the Earth's k^{th} region, and $k = 1,2,3$ is used as a label for the IC, OC and MT, respectively. Note that the following changes were made to Smith's original notation: $\rho \to \rho_0$, $\mathbf{s} \to \mathbf{u}_k$, $D_t \to \frac{\partial}{\partial t}$, $\Omega_0 \to \Omega \hat{\mathbf{e}}_3$, $\mathbf{T}^e \to \tilde{\tau}_k$, $\phi \to -(V_0)_k$, $\phi_1 \to -(V_1)_k$ and $\gamma \to p_0$. The equilibrium gravitational potential V_0 at $\mathbf{r}$ is

$$V_0 = W_0 - \frac{1}{2} |\Omega \hat{\mathbf{e}}_3 \times \mathbf{r}|^2. \tag{2.6}$$

The stress tensor in the OC takes the form

$$(\tilde{\tau})_2 = \lambda (\nabla \cdot \mathbf{u}_2) \tilde{\mathbf{I}} = (\tilde{\tau}_1)_2, \tag{2.7}$$

and in the elastic IC and MT

$$(\tilde{\tau})_k = (\tilde{\tau}_1)_k + (\tilde{\tau}_2)_k \tag{2.8}$$

with $(\tilde{\tau}_2)_k = 2\mu \{ \nabla \mathbf{u}_k + \nabla \mathbf{u}_k^T \}$, where $\tilde{\mathbf{I}}$ is the unit dyadic and the superscript T defines the transpose of a tensor. Conservation of angular monentum makes sure that the stress tensor $(\tilde{\tau})_k$ is a symmetric tensor. The Lamé parameters, μ and λ are related to the P-wave speed

v_p, S-wave speed v_s, and the density ρ_0 as

$$v_p = \sqrt{\frac{\lambda + 2\mu}{\rho_0}}, \tag{2.9}$$

$$v_s = \sqrt{\frac{\mu}{\rho_0}}. \tag{2.10}$$

Note that $\mu = 0$ in the OC.

Using equations (2.1), (2.2), and (2.6), the equation (2.4) can be written in a compact form

$$\frac{\partial^2 \mathbf{u}_k}{\partial t^2} + 2\Omega\hat{\mathbf{e}}_3 \times \frac{\partial \mathbf{u}_k}{\partial t} + \mathbf{g}_0 \nabla \cdot \mathbf{u}_k - \nabla(\mathbf{u}_k \cdot \mathbf{g}_0 + (V_1)_k) - \frac{1}{\rho_0}\nabla \cdot (\tilde{\tau})_k = 0. \tag{2.11}$$

We assume that all the field variables have $e^{i\omega t}$ dependence because we are dealing with small oscillations, where ω is the angular frequency of a mode which is measured in the rotating reference frame. Under this assumption and doing some mathematical operations in equations (2.5) and (2.11), the linearized dynamical equations describing the oscillatory dynamics of the Earth's interior become

$$\omega^2 \mathbf{u}_k - 2i\omega\Omega\hat{\mathbf{e}}_3 \times \mathbf{u}_k - \mathbf{g}_0 \nabla \cdot \mathbf{u}_k + \nabla(\mathbf{u}_k \cdot \mathbf{g}_0 + (V_1)_k) + \frac{1}{\rho_0}\nabla \cdot (\tilde{\tau})_k = 0, \tag{2.12}$$

$$\nabla^2 (V_1)_k - 4\pi G \nabla \cdot (\rho_0 \mathbf{u}_k) = 0. \tag{2.13}$$

2.1.1 Non-dimensional Form of the Dynamical Equations

For computational purposes, the dimensionless form of the equations (2.12) and (2.13) are

$$\sigma^2 \mathbf{u}'_k - i\sigma\hat{\mathbf{e}}_3 \times \mathbf{u}'_k - \mathbf{g}'_0 \nabla' \cdot \mathbf{u}'_k + \nabla'(\mathbf{u}'_k \cdot \mathbf{g}'_0 + (V_1)'_k) + \frac{1}{\rho'_0}\nabla' \cdot (\tilde{\tau}')_k = 0, \tag{2.14}$$

$$\nabla'^2 (V_1)_k - 4\pi G' \nabla' \cdot (\rho'_0 \mathbf{u}'_k) = 0, \tag{2.15}$$

with

$$\sigma = \frac{\omega}{2\Omega}; \quad \mathbf{u}' = \frac{\mathbf{u}}{R}; \quad \mathbf{g}_0' = \frac{\mathbf{g}_0}{4\Omega^2 R}; \quad \nabla' = R\nabla; \quad V_1' = \frac{V_1}{4\Omega^2 R^2}; \tag{2.16}$$

$$\tilde{\tau}' = \frac{\tilde{\tau}}{4\Omega^2 R^2 \langle \rho_0 \rangle}; \quad \rho_0' = \frac{\rho_0}{\langle \rho_0 \rangle}; \quad G' = \frac{G\langle \rho_0 \rangle}{4\Omega^2}, \tag{2.17}$$

where $\langle \rho_0 \rangle$ and R are the Earth's mean density and mean radius respectively. Note that equations (2.14) and (2.15) are obtained from equations (2.12) and (2.13) by dividing them by $4R\Omega^2$ and $4\Omega^2$, respectively. Hereafter, we will drop the notation $()'$ from all terms of equations (2.14) and (2.15) for convenience.

2.2 Representation of the Vector and Scalar Fields

The displacement eigenfunction $\mathbf{u}_k$ of a normal mode may be expressed as a sum of the spheroidal $\mathbf{S}_k$ and toroidal $\mathbf{T}_k$ vector fields

$$\mathbf{u}_k = \sum_{n=|m|}^{N_k} \left[(\mathbf{S}_n^m)_k + (\mathbf{T}_n^m)_k \right], \tag{2.18}$$

where

$$(\mathbf{S}_n^m)_k = \left[\hat{\mathbf{r}} (U_n^m)_k(r) + r(V_n^m)_k(r)\nabla \right] Y_n^m(\theta, \phi), \tag{2.19}$$

$$(\mathbf{T}_n^m)_k = -(W_n^m)_k(r)\mathbf{r} \times \nabla Y_n^m(\theta, \phi), \tag{2.20}$$

and the $(V_1)_k$ is also expanded as

$$(V_1)_k = \sum_{n=|m|}^{N_k} (X_n^m)_k(r) Y_n^m(\theta, \phi), \tag{2.21}$$

for any m, as we assume azimuthal symmetry. In the above equations (2.19)-(2.21); $Y_n^m(\theta, \phi) = P_n^m(\cos\theta)e^{im\phi}$ are the spherical harmonics of degree n and azimuthal order m, $P_n^m(\cos\theta)$ are the associated Legendre polynomials, θ is the polar angle (see Fig. 2.1), $(U_n^m)_k(r)$,

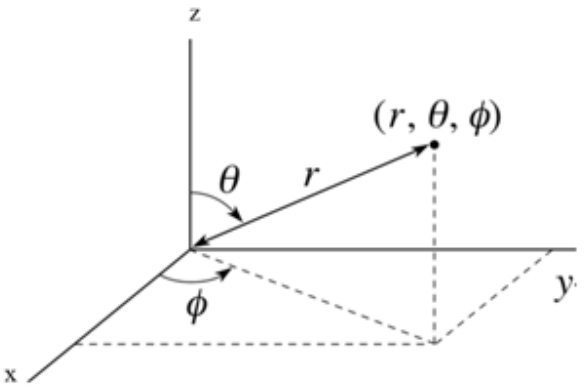

Figure 2.1: The spherical coordinates (r,θ,ϕ) system.

$(V_n^m)_k(r)$, $(W_n^m)_k(r)$ and $(X_n^m)_k(r)$ are the dependent variables which are functions of the radius, and N_k represents the truncation level along the highest degree spherical harmonics included in the angular dependence θ. In theory, N_k extends to infinity.

By definition of the associated Legendre functions, the lowest value n can admit is $|m|$ in equations (2.19) and (2.20). Therefore, the displacement of a normal mode for a rotating Earth can have one of the following forms:

$$\mathbf{u}_k = \sum_{n=|m|}^{N_k} \left[(\mathbf{S}^m_{2n-|m|+1})_k + (\mathbf{T}^m_{2n-|m|})_k \right], \tag{2.22}$$

or

$$\mathbf{u}_k = \sum_{n=|m|}^{N_k} \left[(\mathbf{S}^m_{2n-|m|})_k + (\mathbf{T}^m_{2n-|m|+1})_k \right], \tag{2.23}$$

[see, for example, equations (46) and (47) in [60]]. Because of rotation, the displacement of different harmonic degrees couple according to equations (2.22) and (2.23). The corresponding expression for the $(V_1)_k$ can have

$$(V_1)_k = \sum_{n=|m|}^{N_k} (X^m_{2n-|m|+1})_k Y^m_{2n-|m|+1}(\theta,\phi) \tag{2.24}$$

or

$$(V_1)_k = \sum_{n=|m|}^{N_k} (X^m_{2n-|m|})_k Y^m_{2n-|m|}(\theta,\phi). \tag{2.25}$$

2.3 Representation of the Radially Dependent Variables

The radially dependent functions of equations (2.22) and (2.24) or (2.23) and (2.25) are also expanded as

$$\left\{(U_n^m)_k(r),(V_n^m)_k(r),(W_n^m)_k(r),(X_n^m)_k(r)\right\}=\sum_{l=0}^{L_k}\left\{(C_{n,l}^m)_k,(D_{n,l}^m)_k,(E_{n,l}^m)_k,(F_{n,l}^m)_k\right\}f_l(x), \tag{2.26}$$

for $n=|m|,|m|+1,|m|+2,\cdots,N_k$ in each region; where $(C_{n,l}^m)_k$, $(D_{n,l}^m)_k$, $(E_{n,l}^m)_k$, $(F_{n,l}^m)_k$ are constants, L_k is the truncation level for the radial expansion and $f_l(x)$ are the Legendre polynomials of degree l. Note that the subscript n in the equation (2.26) corresponds to the subscript in the equations (2.22) and (2.24) or (2.23) and (2.25). The argument of x for f_l is $-1\leq x\leq 1$. Now we choose x as

$$x=\frac{2r}{a}-1 \tag{2.27}$$

for the IC,

$$x=\frac{2r-b-a}{b-a} \tag{2.28}$$

for the OC, and

$$x=\frac{2r-R-b}{R-b} \tag{2.29}$$

for the MT, where a and b are the mean radii of ICB and CMB respectively, R is the mean radius of the Earth's outer surface.

2.4 Boundary Conditions

The solutions of equations (2.14) and (2.15) must satisfy the boundary conditions at the interfaces, i.e., surfaces where one or more material properties such as v_p,v_s, and ρ_0 are discontinuous. In addition, $\mathbf{u}_1$ and $(V_1)_1$ must be regular, i.e., their first spatial derivatives

must vanish at the geocenter.

2.4.1 Regularity of the Field Variables at the Geocenter

In order to satisfy the regularity of the dynamical variables at the geocenter, the radial dependence of dynamical variables in the IC must satisfy

$$\frac{d}{dr}\left\{(U_n^m)_1(r),(V_n^m)_1(r),(W_n^m)_1(r),(X_n^m)_1(r)\right\}=0. \tag{2.30}$$

Now by taking the first derivative of equation (2.26) and using equation (2.30), we get

$$\left\{(C_{n,1}^m)_1,(D_{n,1}^m)_1,(E_{n,1}^m)_1,(F_{n,1}^m)_1\right\}=-\sum_{l=2}^{L_1}\left\{(C_{n,l}^m)_1,(D_{n,l}^m)_1,(E_{n,l}^m)_1,(F_{n,l}^m)_1\right\}\frac{df_l}{dx}. \tag{2.31}$$

Next, using equation (2.31) in (2.26), the radial dependent components of equation (2.26) have the form

$$\begin{aligned}\left\{(U_n^m)_1(r),(V_n^m)_1(r),(W_n^m)_1(r),(X_n^m)_1(r)\right\}&=\left\{(C_{n,0})_1^m,(D_{n,0}^m)_1,(E_{n,0}^m)_1,(F_{n,0}^m)_1\right\}\\&+\sum_{l=2}^{L_1}\left\{(C_{n,l}^m)_1,(D_{n,l}^m)_1,(E_{n,l}^m)_1,(F_{n,l}^m)_1\right\}\left(f_l-\frac{df_l}{dx}x\right),\end{aligned} \tag{2.32}$$

for the IC.

2.4.2 Boundary Conditions at the Solid-Fluid Interfaces

The boundary conditions across the solid-fluid interfaces (at ICB and CMB) require that:

1. The normal component of the displacement is continuous,

$$\hat{\mathbf{n}}\cdot\mathbf{u_k}=\hat{\mathbf{n}}\cdot\mathbf{u_{k+1}}; \tag{2.33}$$

2. The normal component of the stress tensor (the stress vector) is continuous,

$$\hat{\mathbf{n}} \cdot \tilde{\tau}_k = \hat{\mathbf{n}} \cdot \tilde{\tau}_{k+1}; \tag{2.34}$$

3. The gravitational potential is continuous,

$$(V_1)_k = (V_1)_{k+1}; \tag{2.35}$$

4. The gravitational flux is continuous,

$$\hat{n} \cdot (\nabla (V_1)_k - 4\pi G \rho_0 \mathbf{u}_k) = \hat{n} \cdot (\nabla (V_1)_{k+1} - 4\pi G \rho_0 \mathbf{u}_{k+1}), \tag{2.36}$$

where $\hat{n}$ is the unit vector normal to the undeformed boundary surface.

2.4.3 Boundary Conditions at the Earth's Surface

At the outer surface of the Earth, the normal component of the stress tensor, $\hat{\mathbf{n}} \cdot \tilde{\tau}_4$, vanishes, and the gravitational potential, $(V_1)_4$, and gravitational flux, $\hat{n} \cdot \nabla (V_1)_4$, outside the Earth ($r > R$) are continuous. In the region $r > R$, Poisson's equation reduces to Laplace's equation and the gravitational potential has the form in spherical coordinates

$$(V_1)_4(r) = \sum_{n=|m|}^{N_k} A_n^m r^{-(n+1)} Y_n^m(\theta, \phi), \tag{2.37}$$

where A_n^m are constants. Therefore, the gravitational flux in this region is

$$\hat{n} \cdot \nabla (V_1)_4(r) = -\sum_{n=|m|}^{N_k} (n+1) A_n^m r^{-(n+2)} Y_n^m(\theta, \phi). \tag{2.38}$$

At the Earth's surface,

$$(V_1)_3(R-) = (V_1)_4(R+), \tag{2.39}$$

which gives

$$(X_n^m)_3(R-) = A_n^m R^{-(n+1)}, \tag{2.40}$$

using equations (2.21) and (2.37), where $R-$ and $R+$ are the radii just inside and just outside the Earth's surface respectively. Hence, using equations (2.38) and (2.40), the gravitational flux at the Earth's surface is

$$\begin{aligned} \hat{n}\cdot(\nabla(V_1)_3 - 4\pi G\rho_0\mathbf{u}_3)|_{R-} &= \hat{n}\cdot\nabla(V_1)_4(R+) \\ &= \sum_{n=|m|}^{N_k} -\frac{n+1}{R}(X_n^m)_3(R-)Y_n^m(\theta,\phi). \end{aligned} \tag{2.41}$$

This means that the gravitational flux at the Earth's surface is written entirely in terms of the gravitational potential just inside the mantle. Note that equations (2.40) and (2.41) are valid for a spherical Earth model. The corresponding form of these equations for a spheroidal Earth model will be shown in section 4.4.

2.5 Earth Models

In this thesis, the Preliminary Reference Earth Model (PREM) [1] is adopted as the base for our Earth model. PREM is a spherical non-rotating Earth model which is divided into 13 concentric layers. The material properties such as the P- and S-wave speed and the density of each layer are a function of the radius. Dziewonski and Anderson [1] constructed this model by inverting the seismological data such as the P- and S-wave speed, and the frequencies of the normal modes. Some properties such as density stratification parameter and liquid viscosity may not be firmly established because short-period body waves data are not directly sensitive to those properties [1, 4, 5]. These parameters play an important role in determining the mantle's heterogeneity and mantle flow [6, 7, 8]. In order to establish more accurate Earth models, the theory of ray seismology is complemented by the normal mode theory [9, 10]. The objective of this thesis is to compute the eigenfrequencies and

eigenfunctions of the normal modes such as the Slichter modes, the spheroidal modes, the inertial modes and wobble/nutation modes of an Earth model which consists of an elastic inner core (IC), a fluid outer core (OC) and an elastic mantle (MT). First, we consider a rotating spherical fluid shell contained between an elastic IC and an elastic MT, and investigate the effects of mantle and inner core elasticity on the frequencies of the inertial modes of a fluid core model with elastic boundaries. Recall that the analytical solutions for the inertial modes of a spherical fluid sphere with rigid boundary are known [80]. Next, we consider a rotating spheroidal fluid shell contained between an elastic IC and an elastic MT, and compute the period of the Earth's wobble/nutation modes.

2.5.1 The S- and P-waves, and the Density Profiles of Inner Core

The P-wave speed v_p and S-wave speed v_s of the inner core of PREM [1] are given as

$$v_p = 11.2622 - 6.3640x^2 \text{ km s}^{-1}, \tag{2.42}$$

and

$$v_s = 3.6678 - 4.4475x^2 \text{ km s}^{-1}, \tag{2.43}$$

where $x = \frac{r}{R}$ and R is the mean radius of the surface of the Earth.

The density profile ρ_0 of the inner core of PREM [1] is

$$\rho_0 = 13.0885 \times 10^3 - 8.8381 \times 10^3 x^2 \text{ kg m}^{-3}. \tag{2.44}$$

2.5.2 The P-wave, and the Density Profiles of Outer Core

The P-wave speed v_p of the fluid core of PREM [1] is given as

$$v_p = (c_0 + c_1 x + c_2 x^2 + c_3 x^3) \text{ km s}^{-1}, \tag{2.45}$$

where $c_0 = 11.0487$, $c_1 = -4.0362$, $c_2 = 4.8023$, and $c_3 = -13.5732$. The density of the fluid core of PREM [1] is

$$\rho_0 = (d_0 + d_1 x + d_2 x^2 + d_3 x^3)\ \mathrm{kg\,m^{-3}}, \tag{2.46}$$

where $d_0 = 12.5815 \times 10^3$, $d_1 = -1.2638 \times 10^3 2$, $d_2 = -3.6426 \times 10^3$, and $d_3 = -5.5281 \times 10^3$.

The presence of the elastic inner core is ignored for simplicity. Since the first derivative of equations (2.45) and (2.46) with respect to r is not zero at $r = 0$, these profiles can not be used for this core model. Kamruzzaman [42], following Seyed-Mahmoud [81], modified the P-wave speed and density profiles for a stratified OC model with no IC. These profiles [42] are

$$v_p = (10.6776 - 8.7572x^2)\ \mathrm{km\,s^{-1}}, \tag{2.47}$$

and

$$\rho_0 = \sum_{j=1}^{12} d_j x^{j-1}\ \mathrm{kg\,m^{-3}}. \tag{2.48}$$

In Tables 2.1, we show the coefficients d_j of the modified density of the OC for different values of stability parameter β which is defined by equation (3.33). Column 2 of table 2.1 is the coefficients d_j for a neutrally ($\beta = 0.0$) stratified OC with no IC model. In columns 3, 4 and 5 of this table, we show the coefficients d_j for different values $\beta = 0.0$, $\beta = -0.001$ and $\beta = +0.001$, respectively, of the OC with IC models. Note that the equation (2.45) is used for the OC with IC models.

2.5.3 The S- and P-waves, and the Density Profiles of Mantle

We consider a one layer ocean-less MT and use the least squares method to modify density and seismic wave velocity profiles of this region. This is justified for our studies as the mantle is nearly rigid compared to the liquid core. In modifying PREM's mantle we make sure that the profiles for the P- and S-wave speeds and the densities (see Fig 2.2)

Table 2.1: The coefficients of the density profile ($\mathrm{kg\,m^{-3}}$) for the different OC models with no inner core (IC), and with IC

	no inner core	with inner core		
d_j	$\beta = 0.0$	$\beta = 0.0$	$\beta = -0.001$	$\beta = +0.001$
d_1	1.2477×10^4	1.2602×10^4	1.2602×10^4	1.2603×10^4
d_2	0.0	-2.8139×10^3	-2.7581×10^3	-2.9028×10^3
d_3	-7.7409×10^3	1.8461×10^4	1.7636×10^4	1.9782×10^4
d_4	5.1132×10^{-2}	-1.5804×10^5	-1.5087×10^5	-1.6955×10^5
d_5	-2.5078×10^3	6.4663×10^5	6.0523×10^5	7.1363×10^5
d_6	1.6271×10^1	-1.8694×10^6	-1.7045×10^6	-2.1399×10^6
d_7	-9.8071×10^2	3.7956×10^6	3.3337×10^6	4.5678×10^6
d_8	5.4545×10^2	-5.2895×10^6	-4.3796×10^6	-6.8492×10^6
d_9	-1.8448×10^3	4.7545×10^6	3.5185×10^6	6.9384×10^6
d_{10}	2.7434×10^3	-2.4150×10^6	-1.3122×10^6	-4.4343×10^6
d_{11}	-2.8131×10^3	4.4199×10^5	-1.4001×10^5	1.5517×10^6
d_{12}	1.2135×10^3	6.3590×10^4	2.0129×10^5	-2.1104×10^5

obey the law of mass conservation and meet the Adams-Williamson condition (2.51) which assumes that the compression is adiabatic and that the Earth is spherically symmetric, homogeneous, and in hydrostatic equilibrium. Consistent with PREM, the modified profiles for the P- and S-wave speed are expressed as polynomials

$$v_p = 36.260 - 96.918x + 143.06x^2 - 74.968x^3 \text{ km s}^{-1}, \tag{2.49}$$

and

$$v_s = 16.756 - 44.306x + 70.904x^2 - 39.215x^3 \text{ km s}^{-1}. \tag{2.50}$$

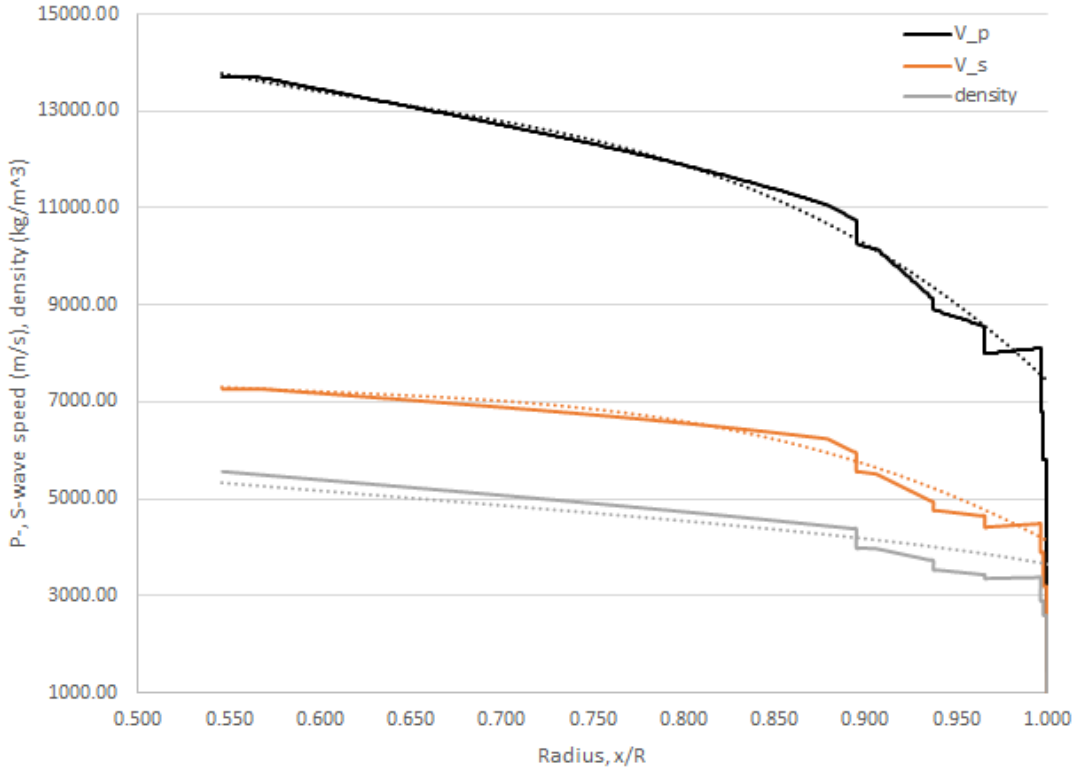

Figure 2.2: The density, P-wave and S-wave speed profiles of the mantle as functions of radius. Solid lines are for PREM and corresponding dot lines are for the modified PREM.

The Adams-Williamson equation [82] for a spherical Earth is

$$\frac{d\rho_0}{dr} = -\frac{g_0\rho_0}{v_p^2 - \frac{4}{3}v_s^2}. \tag{2.51}$$

We choose the density profile as

$$\rho_0 = \sum_{j=1}^{N'} d_j x^{j-1}, \tag{2.52}$$

where $x = \frac{r}{R}$, N' is an integer and d_j are constants. From Eq. (2.52), we get

$$\frac{d\rho_0}{dr} = \frac{d\rho_0}{dx}\frac{dx}{dr} = \frac{1}{R}\sum_{j=2}^{N'}(j-1)d_j x^{j-2}. \tag{2.53}$$

To solve Eq. (2.51) for a best fitting density profile ρ_0, we use a Galerkin method with weight functions x^{i-1} $(i = 1, \cdots, N'-1)$. Using Eq. (2.53), the Galerkin representation of Eq. (2.51) is

$$\sum_{j=2}^{N'}(j-1)d_j \int_{\frac{a}{R}}^{\frac{b}{R}} \frac{v_p^2 - \frac{4}{3}v_s^2}{\rho_0 g_0 R} x^{i+j-3}dx + \int_{\frac{a}{R}}^{\frac{b}{R}} x^{i-1}dx = 0, \tag{2.54}$$

for each i, a is the mean radius of CMB (inner radius of mantle) and b is the mean radius of the outer mantle. Eq. (2.54) can be written as

$$\sum_{j=2}^{N'} A_{ij} d_j = F_i, \tag{2.55}$$

where

$$A_{ij} \equiv (j-1)\int_{\frac{a}{R}}^{\frac{b}{R}} \frac{v_p^2 - \frac{4}{3}v_s^2}{\rho_0 g_0 R} x^{i+j-3}dx, \tag{2.56}$$

and

$$F_i \equiv -\frac{1}{i}\left[\left(\frac{b}{R}\right)^i - \left(\frac{a}{R}\right)^i\right]. \tag{2.57}$$

The gravitational acceleration, g_0, in the mantle is given as

$$g_0(r) = \frac{GM(r)}{r^2}, \tag{2.58}$$

where $M(r)$ is the total mass of the body enclosed by the shell of radius r, and

$$M(r) = MIC + MLC + MM, \tag{2.59}$$

where, MIC = mass of inner core, MLC = mass of liquid core, and MM = mass of mantle which can be written as

$$\begin{aligned} MM(r) &= 4\pi \int_{r_1}^{r_2} \rho_0 r^2 dr, \\ &= 4\pi R^3 \sum_{j=1}^{N'} \frac{d_j}{j+2} \left[x_2^{j+2} - (\frac{a}{R})^{j+2} \right]. \end{aligned} \tag{2.60}$$

In order to find ρ_0 [by Eq. (2.52)] and g_0 [by Eq. (2.58)] in Eq. (2.56), we set the starting values of the coefficients of the density profile: $d_1 = 20.6579 \times 10^3$ kg m^{-3}, $d_2 = -12.9012 \times 10^4$ kg m^{-3}, $d_3 = 44.7085 \times 10^4$kg m^{-3}, $d_4 = -65.8279 \times 10^4$ kg m^{-3}, $d_5 = -31.7742 \times 10^3$ kg m^{-3}, and all other $d_j = 0$. The number of terms in the polynomials representing the aforementioned profiles is arbitrary. We chose 14 for the density because at this number the Adams-Williamson condition was satisfied the fastest. IMSL (International Mathematics and Statistics Library) [83] subroutines DQDAG and DLSARG are then called to solve Eqs. (2.55) and (2.56) respectively for the coefficients $d_2, \cdots, d_{N'}$. To find the value d_1, we use the mass conservation of the mantle as a constraint and proceed as follows:

$$\int_M \rho_0 dV = \frac{4}{3}\pi \langle \rho \rangle (b^3 - a^3), \tag{2.61}$$

where $\langle \rho \rangle$ is the average density of the mantle. Substituting Eq. (2.52) and $dV = r^2 \sin^2\theta dr d\theta d\phi$ in Eq. (2.61), then

$$4\pi R^3 \sum_{j=1}^{N'} d_j \int_{\frac{a}{R}}^{\frac{b}{R}} x^{j+1} dx = \frac{4}{3}\pi \langle \rho \rangle (b^3 - a^3),$$

which can be written as

$$d_1 = \langle \rho \rangle - \frac{3}{\left(\frac{b}{R}\right)^3 - \left(\frac{a}{R}\right)^3} \sum_{j=2}^{N} \frac{d_j}{j+2} \left[\left(\frac{b}{R}\right)^{j+2} - \left(\frac{a}{R}\right)^{j+2} \right]. \tag{2.62}$$

From Eq. (2.51), we get

$$\frac{v_p^2 - \frac{4}{3}v_s^2}{\rho_0 g_0} \frac{d\rho_0}{dr} = -1. \tag{2.63}$$

Once d_j are known, we use the equations (2.49), (2.50), (2.52) and (2.53) to solve for $\frac{v_p^2 - \frac{4}{3}v_s^2}{\rho_0 g_0} \frac{d\rho_0}{dr}$. Let $Z = \frac{v_p^2 - \frac{4}{3}v_s^2}{\rho_0 g_0} \frac{d\rho_0}{dr}$. If $|Z+1| > \varkappa$, where $\varkappa$ is the desired accuracy, we use the new d_j as the starting values, this process is repeated until $|Z+1| \leq \varkappa$. In this thesis, we set $\varkappa = 10^{-6}$, and compute the coefficients of the modified density of the mantle. The modified density of the mantle is

$$\rho_0 = \sum_{i=1}^{14} d_i x^{i-1} \, kgm^{-3}. \tag{2.64}$$

In Tables 2.2, we show the coefficients d_i of the modified density of the mantle. These modified profiles do not significantly affect the periods of the normal modes such as the seismic and Slichter modes (see tables 5.1 and 5.2). Note that the periods of the seismic modes mainly depend on the dynamics of the mantle.

Table 2.2: The coefficients of the density profile ($\mathrm{kg\,m^{-3}}$) for the mantle

d_j	value
d_1	48.877×10^3
d_2	-45.671×10^4
d_3	20.748×10^5
d_4	-51.065×10^5
d_5	70.192×10^5
d_6	-47.512×10^5
d_7	56.739×10^4
d_8	60.499×10^4
d_9	-91.919×10^3
d_{10}	19.516×10^5
d_{11}	-40.945×10^5
d_{12}	31.996×10^5
d_{13}	-10.849×10^5
d_{14}	12.301×10^4

Chapter 3

The Galerkin Method and its Application of to the Governing Equations

In this chapter, following Seyed-Mahmoud [81] and Kamruzzaman [42], we introduce the Galerkin method applicable to a system of simultaneous partial differential equations subject to boundary conditions. We use this method, based on the work of Kamruzzaman and Seyed Mahmoud [43], to solve the dynamical equations and boundary conditions describing the dynamics of the Earth's interior for the normal modes of different Earth's models.

3.1 The Galerkin Method

The Galerkin method was introduced by Russian mathematician Boris Grigoryevich Galerkin. This method is a tool to approximate the solution of an operator equation in the form of a linear combination of the elements of a linearly independent system. This method was applied to the 3PD in [38] for studying the inertial modes of a compressible and stratified fluid core with rigid boundaries in [37, 41, 42], the free wobble/nutation modes of a simple Earth model with a rotating, inviscid, homogeneous and incompressible fluid core contained in a spherical shell with rigid boundaries in [40], and the effect of the Earth's differential rotation of the inner core on the period of the FCN in [84]. The computed periods of wobble/nutation modes in existing methods of previous studies lack proven convergence and the discrepancies between the observed and predicted values are significant. To solve the convergence problem, the Galerkin method will be applied to dynamical equations and

boundary conditions describing the dynamics of a realistic Earth model, where all the field variables are represented by the spherical harmonics. The truncation levels at spherical harmonic become infinite in theory, but in practice they are truncated once convergence is achieved (see e.g., [37, 41, 42]).

We consider a set of functions $X = (X_1, X_2, X_3, \cdots, X_N)$ which satisfies a set of simultaneous PDEs in a region V,

$$\sum_{j=1}^{N} L_{ij} X_j = 0 \tag{3.1}$$

for every i $(i = 1, \cdots, N)$, where L_{ij} are linear (maybe complex) partial differential operators.

Suppose that there are a number of associated boundary conditions satisfied on the boundary S of volume V, such that

$$\sum_{j=1}^{N} B_{ij} X_j = 0 \tag{3.2}$$

for every i $(i = 1, \cdots, N)$, where B_{ij} are linear operators. Using a basis set f_l, $l = 1, \cdots, L$, we introduce trial functions

$$X_j = \sum_{l=1}^{L} C_{jl} f_l \tag{3.3}$$

for every j $(j = 1, \cdots, N)$, which need not a priori satisfy the boundary conditions. The Galerkin method tries to make $\sum_j L_{ij} X_j$ as nearly null as possible by requiring

$$\sum_{j=1}^{N} \sum_{l=1}^{L} \int_V f_l^* L_{ij} C_{jl} f_l dV = 0, \tag{3.4}$$

where $l = 1, \cdots, L$, and * denotes the complex conjugate. Eq. (3.4) can be written in matrix form by setting up 1-1 correspondence of $m = N(l-1) + i$ and $n = N(l-1) + j$,

$$\sum_n G_{mn} a_n = 0, (m = 1, \cdots, LN) \tag{3.5}$$

with $a_n = C_{jl}$, and

$$G_{mn} = \int_V f_l^* L_{ij} f_l dV. \tag{3.6}$$

In general the trial functions do not a priori satisfy the boundary conditions. We choose a set of basis functions ψ_l (i.e., weight functions) equal in number to the basis functions defined in the trial functions X_j is used to reconstruct in Eq. (3.4) as

$$\sum_{j=1}^{N}\sum_{l=1}^{L}[\int_V f_l^* L_{ij} C_{jl} f_l dV + \int_S \psi_l^* B_{ij} C_{jl} f_l dS] = 0, \tag{3.7}$$

which has a form

$$\sum_{j=1}^{N}\sum_{l=1}^{L} F_{lijl} C_{jl} = 0 \tag{3.8}$$

with

$$F_{lijl} = \int_V f_l^* L_{ij} f_l dV + \int_S \psi_l^* B_{ij} f_l dS. \tag{3.9}$$

The surface integral from the boundary conditions may be removed by applying the divergence theorem. When this is possible with a proper choice of weight functions, the boundary conditions are called natural.

3.2 Galerkin Formulation of the Dynamical Equations

(This section is based on the work of Kamruzzaman and Seyed Mahmoud [43].)

In this section we develop a Galerkin method to solve equations (2.13) and (2.14) including the boundary conditions, equations (2.33)-(2.36). Using equations (2.18) and (2.21) along with equation (2.26) and (2.32) as trial functions and applying the Galerkin method, the dynamical equations (2.13) and (2.14) are replaced with the functionals

$$F_{1k} = \int_{V_k} \mathbf{u}_k^* \cdot \left[\sigma^2 \mathbf{u}_k - i\sigma\hat{\mathbf{e}}_3 \times \mathbf{u}_k - \mathbf{g}_0 \nabla \cdot \mathbf{u}_k + \nabla(\mathbf{u}_k \cdot \mathbf{g}_0 + (V_1)_k) + \frac{1}{\rho_0}\nabla \cdot (\tilde{\tau})_k\right] dV \tag{3.10}$$

and

$$F_{2k} = \int_{V_k} (V_1^*)_k \left[\nabla^2 (V_1)_k - 4\pi G \nabla \cdot (\rho_0 \mathbf{u}_k) \right] dV, \tag{3.11}$$

where * indicates the complex conjugate and V_k is the total volume of bounded region by the ICB for $k = 1$, by the ICB and CMB for $k = 2$ and by CMB and the Earth's surface for $k = 3$.

Now, using the identity $\nabla \cdot (f\mathbf{A}) = f\nabla \cdot \mathbf{A} + \mathbf{A} \cdot \nabla f$ on the 4th term of the right-hand side of the equation (3.10) and applying the divergence theorem, we find

$$\begin{aligned} \int_{V_k} \mathbf{u}_k^* \cdot \nabla (\mathbf{u}_k \cdot \mathbf{g}_0 + (V_1)_k) dV &= -\int_{V_k} (\nabla \cdot \mathbf{u}_k^*) \{ \mathbf{u}_k \cdot \mathbf{g}_0 + (V_1)_k \} dV \\ &\quad + \int_{S_k} (\hat{\mathbf{n}} \cdot \mathbf{u}_k^*) \{ \mathbf{u}_k \cdot \mathbf{g}_0 + (V_1)_k \} dS, \end{aligned} \tag{3.12}$$

where S_k is the total surface area of the ICB for $k = 1$, the CMB for $k = 2$ and the Earth's surface for $k = 3$.

Using equation (2.7) on the last term of the right-hand side of equation (3.10), we have

$$\int_{V_k} \frac{1}{\rho_0} \nabla \cdot (\tilde{\tau})_k \cdot \mathbf{u}_k^* dV = \int_{V_k} \frac{1}{\rho_0} [\nabla \cdot \{ (\tilde{\tau}_1)_k + (\tilde{\tau}_2)_k \}] \cdot \mathbf{u}_k^* dV. \tag{3.13}$$

We expand the 1st term of the right-hand side of the above equation to get:

$$\begin{aligned} \nabla \cdot (\frac{1}{\rho_0} (\tilde{\tau}_1)_k \cdot \mathbf{u}_k^*) &= \frac{1}{\rho_0} \nabla \cdot ((\tilde{\tau}_1)_k \cdot \mathbf{u}_k^*) - \frac{\nabla \rho_0}{\rho_0^2} \cdot (\tilde{\tau}_1)_k \cdot \mathbf{u}_k^* \\ &= \frac{1}{\rho_0} \left[(\nabla \cdot (\tilde{\tau}_1)_k) \cdot \mathbf{u}_k^* + (\tilde{\tau}_1)_k : \nabla \mathbf{u}_k^* \right] - \frac{\nabla \rho_0}{\rho_0^2} \cdot (\tilde{\tau}_1)_k \cdot \mathbf{u}_k^*, \end{aligned} \tag{3.14}$$

where : refers to double dot product of two tensors. Therefore

$$\int_{V_k} \frac{1}{\rho_0} \nabla \cdot (\tilde{\tau}_1)_k \cdot \mathbf{u}_k^* dV = \int_{V_k} \left[\frac{\nabla \rho_0}{\rho_0^2} \cdot (\tilde{\tau}_1)_k \cdot \mathbf{u}_k^* - \frac{1}{\rho_0} (\tilde{\tau}_1)_k : \nabla \mathbf{u}_k^* \right] dV + \int_{S_k} \frac{1}{\rho_0} \hat{\mathbf{n}} \cdot (\tilde{\tau}_1)_k \cdot \mathbf{u}_k^* dS. \tag{3.15}$$

Similarly, we can expand the 2nd term of the right-hand side of equation (3.13). However, the term $(\tilde{\tau}_2)_k : \nabla \mathbf{u}_k^*$ leads to the coefficients of $1/\sin^2\theta$, which present a challenge to integrate numerically. In order to bypass this difficulty, we have integrated the 2nd term of the right-hand side of (3.13) directly, and have included the associated boundary condition of this term the following equation (3.7). The r-, θ- and ϕ-components of $\nabla \cdot (\tilde{\tau}_2)_k$ in the spherical coordinate system are given by

$$\begin{aligned}
\left\{\nabla \cdot (\tilde{\tau}_2)_k\right\}_r &= \frac{\partial (\tau_2)_{rr}}{\partial r} + \frac{1}{r}\frac{\partial (\tau_2)_{\theta r}}{\partial \theta} + \frac{1}{r\sin\theta}\frac{\partial (\tau_2)_{\phi r}}{\partial \phi} + \frac{2(\tau_2)_{rr} - (\tau_2)_{\theta\theta} - (\tau_2)_{\phi\phi}}{r} \\
&\quad + \frac{\cot\theta}{r}(\tau_2)_{\theta r}, \qquad (3.16) \\
\left\{\nabla \cdot (\tilde{\tau}_2)_k\right\}_\theta &= \frac{\partial (\tau_2)_{r\theta}}{\partial r} + \frac{1}{r}\frac{\partial (\tau_2)_{\theta\theta}}{\partial \theta} + \frac{1}{r\sin\theta}\frac{\partial (\tau_2)_{\phi\theta}}{\partial \phi} + \frac{3(\tau_2)_{r\theta}}{r} \\
&\quad + \frac{\cot\theta}{r}\left\{(\tau_2)_{\theta\theta} - (\tau_2)_{\phi\phi}\right\}, \qquad (3.17) \\
\left\{\nabla \cdot (\tilde{\tau}_2)_k\right\}_\phi &= \frac{\partial (\tau_2)_{r\phi}}{\partial r} + \frac{1}{r}\frac{\partial (\tau_2)_{\theta\phi}}{\partial \theta} + \frac{1}{r\sin\theta}\frac{\partial (\tau_2)_{\phi\phi}}{\partial \phi} + \frac{3(\tau_2)_{r\phi}}{r} \\
&\quad + \frac{2\cot\theta}{r}(\tau_2)_{\theta\phi}, \qquad (3.18)
\end{aligned}$$

where

$$(\tau_2)_{rr} = 2\mu e_{rr}; \quad (\tau_2)_{\theta\theta} = 2\mu e_{\theta\theta}; \quad (\tau_2)_{\phi\phi} = 2\mu e_{\phi\phi}; \qquad (3.19)$$

$$(\tau_2)_{r\theta} = 2\mu e_{r\theta}; \quad (\tau_2)_{\theta\phi} = 2\mu e_{\theta\phi}; \quad (\tau_2)_{\phi r} = 2\mu e_{\phi r}. \qquad (3.20)$$

In equations (3.19) and (3.20), we have

$$\begin{aligned}
e_{rr} &= \frac{\partial u_r}{\partial r}, \qquad (3.21) \\
e_{\theta\theta} &= \frac{u_r}{r} + \frac{1}{r}\frac{\partial u_\theta}{\partial \theta}, \qquad (3.22) \\
e_{\phi\phi} &= \frac{1}{r\sin\theta}\frac{\partial u_\phi}{\partial \phi} + \frac{u_r}{r} + \frac{\cot\theta u_\theta}{r}, \qquad (3.23)
\end{aligned}$$

$$2e_{r\theta} = \frac{\partial u_\theta}{\partial r} - \frac{u_\theta}{r} + \frac{1}{r}\frac{\partial u_r}{\partial \theta}, \tag{3.24}$$

$$2e_{\theta\phi} = \frac{1}{r}\frac{\partial u_\phi}{\partial \theta} - \frac{\cot\theta u_\phi}{r} + \frac{1}{r\sin\theta}\frac{\partial u_\theta}{\partial \phi}, \tag{3.25}$$

$$2e_{\phi r} = \frac{\partial u_\phi}{\partial r} - \frac{u_\phi}{r} + \frac{1}{r\sin\theta}\frac{\partial u_r}{\partial \phi}, \tag{3.26}$$

where u_r, u_θ and u_ϕ, which are given from the equation (2.18), are the radial, θ and ϕ components of the displacement $\mathbf{u}$ respectively. Note that $e_{r\theta} = e_{\theta r}$, $e_{\theta\phi} = e_{\phi\theta}$, and $e_{\phi r} = e_{r\phi}$ because the stress tensor is a symmetric tensor.

Now, applying the equations (3.12) and (3.15) in equations (3.10), we find

$$\begin{aligned} F_{1k} = & \int_{V_k} \mathbf{u}_k^* \cdot \left[\sigma^2 \mathbf{u}_k - i\sigma \hat{\mathbf{e}}_3 \times \mathbf{u}_k - \mathbf{g}_0 \nabla \cdot \mathbf{u}_k - (\nabla \cdot \mathbf{u}_k^*)\{\mathbf{u}_k \cdot \mathbf{g}_0 + (V_1)_k\} \right] dV \\ & + \int_{S_k} (\hat{\mathbf{n}} \cdot \mathbf{u}_k^*)\{\mathbf{u}_k \cdot \mathbf{g}_0 + (V_1)_k\} dS + \int_{V_k} \left[\frac{\nabla \rho_0}{\rho_0^2} \cdot (\tilde{\tau}_1)_k \cdot \mathbf{u}_k^* - \frac{1}{\rho_0} (\tilde{\tau}_1)_k : \nabla \mathbf{u}_k^* \right] dV \\ & + \int_{S_k} \frac{1}{\rho_0} \hat{\mathbf{n}} \cdot (\tilde{\tau}_1)_k \cdot \mathbf{u}_k^* dS + \int_{V_k} \frac{1}{\rho_0} \mathbf{u}_k^* \cdot (\nabla \cdot (\tilde{\tau}_2)_k) dV - \int_{S_k} \frac{1}{\rho_0} \hat{\mathbf{n}} \cdot (\tilde{\tau}_2)_k \cdot \mathbf{u}_k^* dS. \end{aligned} \tag{3.27}$$

Again, using the identity $\nabla \cdot (f\mathbf{A}) = f\nabla \cdot \mathbf{A} + \mathbf{A} \cdot \nabla f$ on the equation (3.11), and applying the divergence theorem, we find

$$F_{2k} = \int_{S_k} (V_1^*)_k \hat{\mathbf{n}} \cdot \{\nabla (V_1)_k - 4\pi G \rho_0 \mathbf{u}_k\} dS - \int_{V_k} \left[\nabla (V_1)_k - 4\pi G \rho_0 \mathbf{u}_k \right] \cdot \nabla (V_1^*)_k dV. \tag{3.28}$$

An important advantage of the Galerkin method is that application of the divergence theorem replaces the volume integrals involving second order derivatives with surface and volume integrals involving first order derivatives in the form for which the boundary conditions are natural. Also, the derivatives of the material properties at the boundaries, which are not well established in the available Earth models, are removed using the divergence

theorem. The other advantage is that the singularity of the differential equations (2.12) and (2.13) at $r = 0$ is removed using this method.

Applying the boundary conditions [i.e., Eqs. (2.33)] - (2.36)), Eqs. (3.27) and (3.28) become

$$\begin{aligned} F_{11} &= \int_{V_1}\left[\mathbf{u}_1^*\cdot\{\sigma^2\mathbf{u}_1 - i\sigma\hat{\mathbf{e}}_3\times\mathbf{u}_1 - \mathbf{g}_0\nabla\cdot\mathbf{u}_1\} - (\nabla\cdot\mathbf{u}_1^*)\{\mathbf{u}_1\cdot\mathbf{g}_0 + (V_1)_1\}\right]dV \\ &\quad + \int_{S_1}(\hat{\mathbf{n}}\cdot\mathbf{u}_1^*)\{\mathbf{u}_2\cdot\mathbf{g}_0 + (V_1)_2\}_{a+}dS + \int_{V_1}\left[\frac{\nabla\rho_0}{\rho_0^2}\cdot(\tilde{\tau}_1)_1\cdot\mathbf{u}_1^* - \frac{1}{\rho_0}(\tilde{\tau}_1)_1 : \nabla\mathbf{u}_1^*\right]dV \\ &\quad + \int_{S_1}\frac{1}{\rho_0}\{\hat{\mathbf{n}}\cdot(\tilde{\tau}_1)_2\}_{a+}\cdot\mathbf{u}_1^*dS + \int_{V_1}\frac{1}{\rho_0}\mathbf{u}_1^*\cdot(\nabla\cdot(\tilde{\tau}_2)_1)dV, \end{aligned} \tag{3.29}$$

$$F_{21} = \int_{S_1}(V_1^*)_1\hat{\mathbf{n}}\cdot\{\nabla(V_1)_2 - 4\pi G\rho_0\mathbf{u}_2\}_{a+}dS - \int_{V_1}\left[\nabla(V_1)_k - 4\pi G\rho_0\mathbf{u}_k\right]\cdot\nabla(V_1^*)_1dV, \tag{3.30}$$

for the IC, and

$$\begin{aligned} F_{12} &= \int_{V_2}\left[\mathbf{u}_2^*\cdot\{\sigma^2\mathbf{u}_2 - i\sigma\hat{\mathbf{e}}_3\times\mathbf{u}_2 - \mathbf{g}_0\nabla\cdot\mathbf{u}_2\} - (\nabla\cdot\mathbf{u}_2^*)\{\mathbf{u}_2\cdot\mathbf{g}_0 + (V_1)_2\}\right]dV \\ &\quad - \int_{S_1}(\hat{\mathbf{n}}\cdot\mathbf{u}_2^*)\{\mathbf{u}_1\cdot\mathbf{g}_0 + (V_1)_1\}_{a-}dS + \int_{S_2}(\hat{\mathbf{n}}\cdot\mathbf{u}_2^*)\{\mathbf{u}_3\cdot\mathbf{g}_0 + (V_1)_3\}_{b+}dS \\ &\quad + \int_{V_2}\left[\frac{1-\beta}{\rho_0 v_p^2}\mathbf{g}_0\cdot(\tilde{\tau}_1)_2\cdot\mathbf{u}_2^* - \frac{1}{\rho_0}(\tilde{\tau}_1)_2 : \nabla\mathbf{u}_2^*\right]dV - \int_{S_1}\frac{1}{\rho_0}\{\hat{\mathbf{n}}\cdot(\tilde{\tau}_1)_1\}_{a-}\cdot\mathbf{u}_2^*dS \\ &\quad + \int_{S_2}\frac{1}{\rho_0}\{\hat{\mathbf{n}}\cdot(\tilde{\tau}_1)_3\}_{b+}\cdot\mathbf{u}_2^*dS + \int_{S_1}\frac{1}{\rho_0}\{\hat{\mathbf{n}}\cdot(\tilde{\tau}_2)_1\}_{a-}\cdot\mathbf{u}_2^*dS \\ &\quad - \int_{S_2}\frac{1}{\rho_0}\{\hat{\mathbf{n}}\cdot(\tilde{\tau}_2)_3\}_{b+}\cdot\mathbf{u}_2^*dS, \end{aligned} \tag{3.31}$$

$$F_{22} = -\int_{S_1}(V_1^*)_2\hat{\mathbf{n}}\cdot\{\nabla(V_1)_1 - 4\pi G\rho_0\mathbf{u}_1\}_{a-}dS + \int_{S_2}(V_1^*)_2\hat{\mathbf{n}}\cdot\{\nabla(V_1)_3 - 4\pi G\rho_0\mathbf{u}_3\}_{b+}dS$$
$$-\int_{V_2}\left[\nabla(V_1)_2 - 4\pi G\rho_0\mathbf{u}_2\right]\cdot\nabla(V_1^*)_2 dV, \tag{3.32}$$

for the OC, where subscripts $-$ and $+$ refer to the respective radius just inside or outside a respective boundary interface, and we apply the relation

$$\nabla\rho_0 = (1-\beta)\rho_0\frac{\mathbf{g}_0}{v_p^2}, \tag{3.33}$$

into the equation (3.31). The stability parameter β of the OC measures the deviation of the equilibrium density from neutral stratification. The stability parameter is related to the square of the local Brunt-Väisälä frequency N^2, rendered dimensionless by dividing it by $4\Omega^2$, as

$$N^2 = -\frac{\beta g_0^2}{4\Omega^2 v_p^2}. \tag{3.34}$$

A positive value of N^2 (i.e., N is real) would permit a parcel of fluid slightly displaced parallel (or anti-parallel) to $\mathbf{g}_0$ and compressed (or expanded) by the change in pressure, to be lighter (or denser) than the fluid surrounding it, and therefore to perform small oscillations about its original position with frequency N. On the other hand, a negative value of N^2 (i.e., N is imaginary) would result in the displaced parcel as being denser (or lighter) than its new surrounding, and leads to sinking (or rising). Thus one says that if $N^2 > 0$ ($\beta < 0$) then the density profile is stably stratified, if $N^2 < 0$ ($\beta > 0$) then the density profile is unstably stratified and if $N^2 = 0$ ($\beta = 0$) then the density profile is neutrally stratified (i.e., satisfying the Adams-Williamson equation).

Using equations (2.33) - (2.36), equations (3.27) and (3.28) become for the MT

$$\begin{aligned} F_{13} &= \int_{V_3}\Big[\mathbf{u}_3^*\cdot\{\sigma^2\mathbf{u}_3 - i\sigma\hat{\mathbf{e}}_3\times\mathbf{u}_3 - \mathbf{g}_0\nabla\cdot\mathbf{u}_3\} - (\nabla\cdot\mathbf{u}_3^*)\{\mathbf{u}_3\cdot\mathbf{g}_0 + (V_1)_3\}\Big]dV \\ &\quad - \int_{S_2}(\hat{\mathbf{n}}\cdot\mathbf{u}_3^*)\{\mathbf{u}_2\cdot\mathbf{g}_0 + (V_1)_2\}_{b-}dS + \int_{S_3}(\hat{\mathbf{n}}\cdot\mathbf{u}_3^*)\{\mathbf{u}_3\cdot\mathbf{g}_0 + (V_1)_3\}_{R-}dS \\ &\quad + \int_{V_3}\left[\frac{\nabla\rho_0}{\rho_0^2}\cdot(\tilde{\tau}_1)_3\cdot\mathbf{u}_3^* - \frac{1}{\rho_0}(\tilde{\tau}_1)_3 : \nabla\mathbf{u}_3^*\right]dV - \int_{S_2}\frac{1}{\rho_0}\{\hat{\mathbf{n}}\cdot(\tilde{\tau}_1)_2\}_{b-}\cdot\mathbf{u}_3^*dS \\ &\quad + \int_{S_3}\frac{1}{\rho_0}\{\hat{\mathbf{n}}\cdot(\tilde{\tau}_1)_3\}_{R-}\cdot\mathbf{u}_3^*dS + \int\frac{1}{\rho_0}\mathbf{u}_3^*\cdot(\nabla\cdot(\tilde{\tau}_2)_3)dV \\ &\quad - \int_{S_3}\frac{1}{\rho_0}\{\hat{\mathbf{n}}\cdot(\tilde{\tau}_2)_3\}_{R-}\cdot\mathbf{u}_3^*dS, \end{aligned} \tag{3.35}$$

$$\begin{aligned} F_{23} &= -\int_{S_2}(V_1^*)_3\hat{\mathbf{n}}\cdot\{\nabla(V_1)_2 - 4\pi G\rho_0\mathbf{u}_2\}_{b-}dS - \int_{V_3}\Big[\nabla(V_1)_3 - 4\pi G\rho_0\mathbf{u}_3\Big]\cdot\nabla(V_1^*)_3dV \\ &\quad + \int_{S_3}(V_1^*)_3\hat{\mathbf{n}}\cdot\{\nabla(V_1)_3 - 4\pi G\rho_0\mathbf{u}_3\}_{R-}dS. \end{aligned} \tag{3.36}$$

Application of the Galerkin method on functionals F_{1k} and F_{2k} requires that

$$\frac{\partial F_{1k}}{\partial(C_{q,j}^{m*})_k} = 0; \quad \frac{\partial F_{1k}}{\partial(D_{q,j}^{m*})_k} = 0; \quad \frac{\partial F_{1k}}{\partial(E_{q,j}^{m*})_k} = 0; \quad \frac{\partial F_{2k}}{\partial(F_{q,j}^{m*})_k} = 0, \tag{3.37}$$

where $j = 0,2,3,4,\cdots,L_1$ for $k = 1$ and $j = 0,1,2,3,4,\ \cdots,L_k$ for otherwise, and $q = 0,1,2,...,N_k$ for all k's.

3.3 Matrix Representation of the Galerkin Formulation and Eigenvalues

Conditions (3.37) lead to $4\{(N_1+1)L_1 + \sum_{k=2}^{3}(N_k+1)(L_k+1)\} = h$ linear homogeneous equations with the same number of coefficients $(C_{q,j}^{m*})_k$, $(D_{q,j}^{m*})_k$, $(E_{q,j}^{m*})_k$ and $(F_{q,j}^{m*})_k$,

$k = 1, 2, 3$. These linear equations can then be written as a matrix form

$$A\psi = 0, \tag{3.38}$$

where A is a $h \times h$ matrix, and ψ is a $1 \times h$ matrix (column matrix) representing the coefficients $(C^m_{n,l})_k$, $(D^m_{n,l})_k$, $(E^m_{n,l})_k$ and $(F^m_{n,l})_k$. Non-trivial solutions of equation (3.38) exist only if the determinant of A vanishes. The non-dimensional frequencies σ of the normal modes then correspond to the roots of the determinant of A.

Chapter 4

Clairaut Coordinate and their Application to the Galerkin Formulation

In this chapter, we will first discuss the Clairaut coordinate system. Next, we will solve the Clairaut equation to find the Earth's ellipticity profile using the Runge-Kutta integration method. We will derive the vector and scalar operations, the divergence of stress tensor and the boundary conditions at the Earth's surface in this coordinates system. Then, we will expand the Galerkin formulation of dynamical equations to include the first order ellipticity in the Earth model.

4.1 Clairaut Coordinate System

In section 2.1, the reference Earth model is considered in hydrostatic equilibrium which gives the material properties, the Lamé parameters and density, as constant on the equipotential surfaces. The radius of the equipotential surfaces [85] is

$$r = r_0\left[1 - \frac{2}{3}\varepsilon(r_0)P_2(\cos\theta)\right], \tag{4.1}$$

where r_0 is the average equipotential surface's radius, P_2 is the Legendre polynomial of degree 2, r is the magnitude of position vector $\mathbf{r}$, and $\varepsilon(r_0)$ is the ellipticity. The ellipticity profile is given by the Clairaut equation [86]

$$\frac{d^2\varepsilon}{dr_0^2} + \frac{6}{r_0}\frac{\rho_0(r_0)}{\rho_m(r_0)}\frac{d\varepsilon}{dr_0} - \frac{6}{r_0^2}\left[1 - \frac{\rho_0(r_0)}{\rho_m(r_0)}\right]\varepsilon = 0, \tag{4.2}$$

with the boundary conditions [78]:

$$\frac{d\varepsilon}{dr_0} = 0 \quad \text{at} \quad r_0 = 0, \tag{4.3}$$

$$2\varepsilon = \frac{5\Omega^2 R^3}{2GM} - r_0 \frac{d\varepsilon}{dr_0} \quad \text{at} \quad r_0 = R, \tag{4.4}$$

where M is the mass of the Earth, R is the Earth's surface radius, ρ_0 is the density on the equipotential surface of r_0, and ρ_m is the mean density bounded by the same equipotential surface. The ordinary differential equation (4.2) has a singular point at $r_0 = 0$ which presents a challenge to stating numerical integration from $r_0 = 0$. To avoid this difficulty, the Runge-Kutta integration of ordinary differential equation is applied from nearly ($r_0 = 10^{-24}$) the geocenter using the PREM's density profile [1], as if it were valid at some small radius $r_0 = 10^{-24}$ (equal to the first step in integration): i.e. because the ε have zero derivatives at $r_0 = 0$, the Runge-Kutta routine sets $\varepsilon(10^{-24}) = \varepsilon(0)$. To increase accuracy, we make sure to reduce the step size r_0, and the higher number of steps in integration. The ellipticity does not change significantly from the center to ICB, therefore, it is justified that we started integration from near the center rather than the center (see Fig. 4.1). This ellipticity profile gives the ellipticities $\varepsilon(a) = 2.422 \times 10^{-3}$, $\varepsilon(b) = 2.548 \times 10^{-3}$ and $\varepsilon(R) = 3.337 \times 10^{-3}$ at the ICB, CMB and Earth's surface, respectively. The periods of the wobble and nutation modes are sensitive to the values of $\varepsilon(a)$, $\varepsilon(b)$ and $\varepsilon(R)$ [72].

The equipotential surfaces are spherical in the non-rotating Earth model, whereas these surfaces become spheroidal in the rotating Earth model. In order to study a spheroidal Earth model, Seyed-Mahmoud and Moradi [87] studied the effect of first order ellipticity of some low-order inertial modes of the fluid core using a non-orthogonal (Clairaut) coordinate system (r_0, θ, ϕ) for the 3PD. Kopal [88] also applied this coordinate system, and derived the ordinary differential equations governing the freely oscillating star. Wu [89] used a similar coordinate system to explore the dynamics of the fluid core, and studied the wobble and inertia-gravity modes. The transformation from a spherical polar (r, θ, ϕ) coordinate

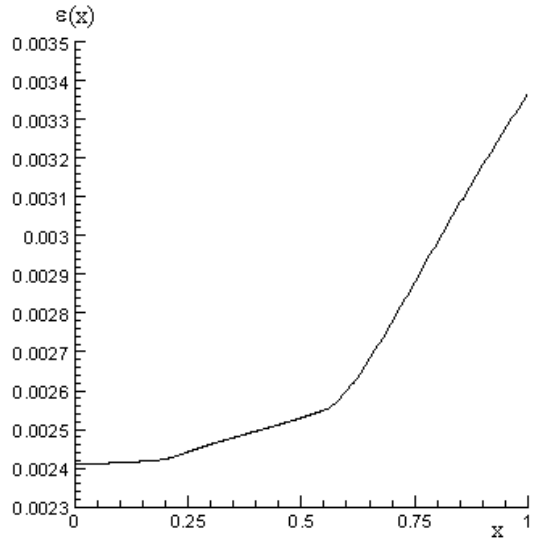

Figure 4.1: The ellipticity profile of the Earth as a function of $x = r/R$.

system to Clairaut coordinates $(r_0, \psi = \theta, \phi)$ system is given by the equations

$$r_0 = r\left[1 + \frac{2}{3}\varepsilon(r_0)P_2(\cos\theta)\right], \tag{4.5}$$

$$\frac{\partial}{\partial r} = \frac{\partial r_0}{\partial r}\frac{\partial}{\partial r_0} = \left[1 + \frac{2}{3}\frac{d}{dr_0}(r_0\varepsilon)P_2(\cos\theta)\right]\frac{\partial}{\partial r_0}, \tag{4.6}$$

$$\frac{\partial}{\partial \theta} = \frac{\partial r_0}{\partial \theta}\frac{\partial}{\partial r_0} + \frac{\partial}{\partial \theta} = \frac{2}{3}r_0\varepsilon P_2^1(\cos\theta)\frac{\partial}{\partial r_0} + \frac{\partial}{\partial \theta}. \tag{4.7}$$

The volume element dV in Clairaut coordinate is given as

$$\begin{aligned} dV &= r^2\frac{\partial r}{\partial r_0}\sin\theta dr_0 d\theta d\phi \\ &= \left[r_0^2 - \frac{2}{3}\frac{d}{dr_0}(r_0^3\varepsilon)P_2\right]\sin\theta dr_0 d\theta d\phi \end{aligned} \tag{4.8}$$

correct to the first order in ε [87].

The unit vector normal to the equipotential surfaces is

$$\hat{n} = \hat{\mathbf{r}} + \frac{2}{3}\varepsilon(r_0)P_2^1(\cos\theta)\hat{\theta} \tag{4.9}$$

correct to the order ε [87]. The argument of $\cos\theta$ for the associated Legendre polynomials $P_n^m(\cos\theta)$ is $-1 \leq \cos\theta \leq 1$. We will write P_n^m instead of $P_n^m(\cos\theta)$ for convenience below.

The equilibrium gravity of the Earth's interior is given by

$$\mathbf{g}_0 = -\left\{\left[1+\frac{2}{3}\frac{d}{dr_0}(r_0\varepsilon)P_2\right]g_0(r_0) - \frac{2}{3}r_0\Omega^2\right\}\hat{r} - \frac{2}{3}\varepsilon P_2^1 g_0(r_0)\hat{\theta} \tag{4.10}$$

correct to the order ε [87]. The non-dimensional form of the gravity is

$$\mathbf{g}_0^{'} = -\left\{\left[1+\frac{2}{3}\frac{d}{dr_0}(r_0\varepsilon)P_2\right]g_0^{'}(r_0) - \frac{1}{6}r_0^{'}\right\}\hat{r} - \frac{2}{3}\varepsilon P_2^1 g_0^{'}(r_0)\hat{\theta}, \tag{4.11}$$

where $\mathbf{g}_0' = \frac{\mathbf{g}_0}{4\Omega^2 R}$, and $r_0^{'} = \frac{r_0}{R}$. Note that equations (4.11) is obtained from equation (4.10) by dividing by $4R\Omega^2$. Hereafter, we will drop the notation $()'$ from all terms of equation (4.11) for convenience.

The surface element dS in Clairaut coordinate is

$$\begin{aligned} dS &= r^2\sin\theta d\theta d\phi \\ &= \left[r_0^2 - \frac{4}{3}\varepsilon P_2\right]\sin\theta d\theta d\phi \end{aligned} \tag{4.12}$$

to the first order in ε.

4.2 Vector and Scalar Operators in Clairaut Coordinate System

Recall that equations (3.27) and (3.28)

$$\begin{aligned} F_{1k} = &\int_{V_k} \mathbf{u}_k^* \cdot \left[\sigma^2 \mathbf{u}_k - i\sigma \hat{\mathbf{e}}_3 \times \mathbf{u}_k - \mathbf{g}_0 \nabla \cdot \mathbf{u}_k - (\nabla \cdot \mathbf{u}_k^*)\{\mathbf{u}_k \cdot \mathbf{g}_0 + (V_1)_k\} \right] dV \\ &+ \int_{S_k} (\hat{\mathbf{n}} \cdot \mathbf{u}_k^*)\{\mathbf{u}_k \cdot \mathbf{g}_0 + (V_1)_k\} dS + \int_{V_k} \left[\frac{\nabla \rho_0}{\rho_0^2} \cdot (\tilde{\tau}_1)_k \cdot \mathbf{u}_k^* - \frac{1}{\rho_0} (\tilde{\tau}_1)_k : \nabla \mathbf{u}_k^* \right] dV \\ &+ \int_{S_k} \frac{1}{\rho_0} \hat{\mathbf{n}} \cdot (\tilde{\tau}_1)_k \cdot \mathbf{u}_k^* dS + \int_{V_k} \frac{1}{\rho_0} \mathbf{u}_k^* \cdot (\nabla \cdot (\tilde{\tau}_2)_k) dV - \int_{S_k} \frac{1}{\rho_0} \hat{\mathbf{n}} \cdot (\tilde{\tau}_2)_k \cdot \mathbf{u}_k^* dS \end{aligned} \tag{4.13}$$

and

$$F_{2k} = \int_{S_k} (V_1^*)_k \hat{\mathbf{n}} \cdot \{\nabla (V_1)_k - 4\pi G \rho_0 \mathbf{u}_k\} dS - \int_{V_k} \left[\nabla (V_1)_k - 4\pi G \rho_0 \mathbf{u}_k \right] \cdot \nabla (V_1^*)_k dV. \tag{4.14}$$

Next, we will first derive the vector and scalar operations, which involve the above equations (4.13) and (4.14), in the Clairaut coordinate system. Then we will find the functionals F_{1k} and F_{2k}. Hereafter, we will drop the subscript k of the field variables in equations (4.13) and (4.14).

4.2.1 Dot Product of Two Vectors

The displacement eigenfunction $\mathbf{u}$ in the spherical coordinate system is given in (2.18)

$$\mathbf{u} = \sum_{n=|m|}^{N} \left[\hat{\mathbf{r}} U_n^m P_n^m + \hat{\theta} \left(\frac{dP_n^m}{d\theta} V_n^m + \frac{im}{\sin\theta} W_n^m P_n^m \right) + \hat{\phi} \left(\frac{im}{\sin\theta} V_n^m P_n^m - \frac{dP_n^m}{d\theta} W_n^m \right) \right] e^{im\phi}. \tag{4.15}$$

By applying equation (4.7) in equation (4.15), then we get the displacement in the Clairaut coordinate system

$$\mathbf{u} = \sum_{n=|m|}^{N} \left[\hat{\mathbf{r}} U_n^m P_n^m + \hat{\theta} \left(\frac{2}{3} r_0 \varepsilon P_2^1 \frac{dV_n^m}{dr_0} P_n^m + V_n^m \frac{dP_n^m}{d\theta} + \frac{im}{\sin\theta} W_n^m P_n^m \right) + \hat{\phi} \left(\frac{im}{\sin\theta} V_n^m P_n^m - \frac{2}{3} r_0 \varepsilon P_2^1 \frac{dW_n^m}{dr_0} P_n^m - W_n^m \frac{dP_n^m}{d\theta} \right) \right] e^{im\phi}. \tag{4.16}$$

The complex conjugate of the displacement is

$$\mathbf{u}^* = \sum_{q=|m|}^{N} \left[\hat{\mathbf{r}} U_q^m P_q^m + \hat{\theta} \left(\frac{2}{3} r_0 \varepsilon P_2^1 \frac{dV_q^m}{dr_0} P_q^m + V_q^m \frac{dP_q^m}{d\theta} - \frac{im}{\sin\theta} W_q^m P_q^m \right) + \hat{\phi} \left(- \frac{im}{\sin\theta} V_q^m P_q^m - \frac{2}{3} r_0 \varepsilon P_2^1 \frac{dW_q^m}{dr_0} P_q^m - W_q^m \frac{dP_q^m}{d\theta} \right) \right] e^{-im\phi}. \tag{4.17}$$

Hence, the dot product of $\mathbf{u}$ and $\mathbf{u}^*$ is

$$\begin{aligned} \mathbf{u}^* \cdot \mathbf{u} = \sum_{q=|m|}^{N} \sum_{n=|m|}^{N} \Bigg[& U_q^m U_n^m P_q^m P_n^m + \left(V_q^m V_n^m + W_q^m W_n^m \right) \left(\frac{dP_n^m}{d\theta} \frac{dP_q^m}{d\theta} + \frac{m^2}{\sin\theta} P_q^m P_n^m \right) \\ & + im \left(V_q^m W_n^m - W_q^m V_n^m \right) \left(\frac{P_q^m}{\sin\theta} \frac{dP_n^m}{d\theta} + \frac{P_n^m}{\sin\theta} \frac{dP_q^m}{d\theta} \right) + \frac{2}{3} r_0 \varepsilon \left(V_q^m \frac{dV_n^m}{dr_0} \right. \\ & \left. + W_q^m \frac{dW_n^m}{dr_0} \right) P_2^1 \frac{dP_q^m}{d\theta} P_n^m + \frac{2}{3} r_0 \varepsilon \left(\frac{dV_q^m}{dr_0} V_n^m + \frac{dW_q^m}{dr_0} W_n^m \right) P_2^1 \frac{dP_n^m}{d\theta} P_n^m \\ & + \frac{2im}{3} r_0 \varepsilon \left(V_q^m \frac{dW_n^m}{dr_0} + \frac{dV_q^m}{dr_0} W_n^m - W_q^m \frac{dV_n^m}{dr_0} - \frac{dW_q^m}{dr_0} V_n^m \right) \frac{P_2^1}{\sin\theta} P_q^m P_n^m \Bigg]. \end{aligned} \tag{4.18}$$

Now, we derive $\mathbf{u} \cdot \mathbf{g}_0$, $\mathbf{u}^* \cdot \mathbf{g}_0$, $\hat{\mathbf{n}} \cdot \mathbf{u}$ and $\hat{\mathbf{n}} \cdot \mathbf{u}^*$ from equations (4.9), (4.11), (4.16) and (4.17) to get

$$\mathbf{u} \cdot \mathbf{g}_0 = \sum_{n=|m|}^{N} \left[- \left\{ \left[1 + \frac{2}{3} \frac{d}{dr_0} (r_0 \varepsilon) P_2 \right] g_0 - \frac{1}{6} r_0 \right\} U_n^m P_n^m - \frac{2}{3} \varepsilon P_2^1 g_0 \left(V_n^m \frac{dP_n^m}{d\theta} + \frac{im}{\sin\theta} W_n^m P_n^m \right) \right] e^{im\phi}, \tag{4.19}$$

$$\mathbf{u}^* \cdot \mathbf{g}_0 = \sum_{q=|m|}^{N} \left[-\left\{ \left[1 + \frac{2}{3}\frac{d}{dr_0}(r_0\varepsilon)P_2 \right] g_0 - \frac{1}{6} r_0 \right\} U_q^m P_q^m \right.$$
$$\left. - \frac{2}{3}\varepsilon P_2^1 g_0 \left(V_q^m \frac{dP_q^m}{d\theta} - \frac{im}{\sin\theta} W_q^m P_q^m \right) \right] e^{-im\phi}, \tag{4.20}$$

$$\hat{\mathbf{n}} \cdot \mathbf{u} = \sum_{n=|m|}^{N} \left[U_n^m P_n^m + \frac{2}{3}\varepsilon P_2^1 \left(V_n^m \frac{dP_n^m}{d\theta} + \frac{im}{\sin\theta} W_n^m P_n^m \right) \right] e^{im\phi}, \tag{4.21}$$

$$\hat{\mathbf{n}} \cdot \mathbf{u}^* = \sum_{q=|m|}^{N} \left[U_q^m P_q^m + \frac{2}{3}\varepsilon P_2^1 \left(V_q^m \frac{dP_q^m}{d\theta} - \frac{im}{\sin\theta} W_q^m P_q^m \right) \right] e^{-im\phi} \tag{4.22}$$

to the first order in ε.

4.2.2 Cross Product of the Unit Vector $\hat{\mathbf{e}}_3$ and the Displacement Vector

The cross product of the unit vector $\hat{\mathbf{e}}_3$ and the displacement eigenfunction $\mathbf{u}$ is

$$\hat{\mathbf{e}}_3 \times \mathbf{u} = \begin{vmatrix} \hat{\mathbf{r}} & \hat{\theta} & \hat{\phi} \\ \cos\theta & -\sin\theta & 0 \\ u_r & u_\theta & u_\phi \end{vmatrix}$$

which is equal to

$$-\sin\theta u_\phi \hat{r} - \cos\theta u_\phi \hat{\theta} + (\cos\theta u_\theta + \sin\theta u_r)\hat{\phi}. \tag{4.23}$$

Now using equations (4.16) and (4.17), and doing some algebra, we get

$$\begin{aligned}\mathbf{u}^*\cdot\hat{\mathbf{e}}_3\times\mathbf{u} = \sum_{q=|m|}^{N}\sum_{n=|m|}^{N}\Bigg[& -im\left(U_q^mV_n^m+V_q^mU_n^m\right)P_q^mP_n^m+\left(V_q^mW_n^m-W_q^mV_n^m\right)\\ & \times\cos\theta\left(\frac{dP_n^m}{d\theta}\frac{dP_q^m}{d\theta}+\frac{m^2}{\sin\theta}P_q^mP_n^m\right)-im\left(V_q^mV_n^m+W_q^mW_n^m\right)\\ & \times\cos\theta\left(\frac{P_q^m}{\sin\theta}\frac{dP_n^m}{d\theta}+\frac{P_n^m}{\sin\theta}\frac{dP_q^m}{d\theta}\right)+U_q^mW_n^m\sin\theta\frac{dP_n^m}{d\theta}P_q^m-W_q^mU_n^m\sin\theta\frac{dP_q^m}{d\theta}P_n^m\\ & +\frac{2}{3}r_0\varepsilon\left(V_q^m\frac{dW_n^m}{dr_0}-W_q^m\frac{dV_n^m}{dr_0}\right)\cos\theta P_2^1\frac{dP_q^m}{d\theta}P_n^m+\frac{2}{3}r_0\varepsilon\left(\frac{dV_q^m}{dr_0}W_n^m-\frac{dW_q^m}{dr_0}V_n^m\right)\\ & \times\cos\theta P_2^1\frac{dP_n^m}{d\theta}P_n^m+\frac{2}{3}r_0\varepsilon\left(U_q^m\frac{dW_n^m}{dr_0}-\frac{dW_q^m}{dr_0}U_n^m\right)\sin\theta P_2^1P_n^mP_q^m-\frac{2im}{3}r_0\varepsilon\\ & \times\left(V_q^m\frac{dV_n^m}{dr_0}+\frac{dV_q^m}{dr_0}V_n^m+W_q^m\frac{dW_n^m}{dr_0}+\frac{dW_q^m}{dr_0}W_n^m\right)\frac{\cos\theta}{\sin\theta}P_2^1P_q^mP_n^m\Bigg]. \end{aligned}\tag{4.24}$$

4.2.3 Divergence of the Displacement Vector

The divergence of the displacement in the spherical coordinate system is given by

$$\nabla\cdot\mathbf{u}=\frac{1}{r^2}\frac{\partial}{\partial r}(r^2u_r)+\frac{1}{r\sin\theta}\frac{\partial}{\partial\theta}(\sin\theta u_\theta)+\frac{1}{r\sin\theta}\frac{\partial}{\partial\phi}(u_\phi).\tag{4.25}$$

Using equations (4.5)-(4.7) and (4.16) in (4.25), the divergence of $\mathbf{u}$ in the Clairaut coordinate system is

$$\begin{aligned}\nabla\cdot\mathbf{u}=\sum_{n=|m|}^{N}\Bigg[& \left(\frac{dU_n^m}{dr_0}+\frac{2U_n^m-n(n+1)V_n^m}{r_0}\right)P_n^m+\frac{2}{3}\varepsilon\left(\frac{dU_n^m}{dr_0}+\frac{2U_n^m-n(n+1)V_n^m}{r_0}\right)P_2P_n^m\\ & +\frac{2}{3}r_0\frac{d\varepsilon}{dr_0}\frac{dU_n^m}{dr_0}P_2P_n^m+\frac{4}{3}\varepsilon\frac{dV_n^m}{dr_0}P_2^1\frac{dP_n^m}{d\theta}-4\varepsilon\frac{dV_n^m}{dr_0}P_2P_n^m\Bigg]e^{im\phi}\end{aligned}\tag{4.26}$$

correct to the first order in ε, where we use the associated Legendre differential equation

$$\frac{d^2P_n^m}{d\theta^2}+\frac{\cos\theta}{\sin\theta}+\left[n(n+1)-\frac{m^2}{\sin^2\theta}\right]P_n^m=0.\tag{4.27}$$

Similarly, we get

$$\nabla\cdot\mathbf{u}^{*}=\sum_{q=|m|}^{N}\left[\left(\frac{dU_q^m}{dr_0}+\frac{2U_q^m-q(q+1)V_q^m}{r_0}\right)P_q^m+\frac{2}{3}\varepsilon\left(\frac{dU_q^m}{dr_0}+\frac{2U_q^m-q(q+1)V_q^m}{r_0}\right)P_2P_q^m\right.$$
$$\left.+\frac{2}{3}r_0\frac{d\varepsilon}{dr_0}\frac{dU_q^m}{dr_0}P_2P_q^m+\frac{4}{3}\varepsilon\frac{dV_q^m}{dr_0}P_2^1\frac{dP_q^m}{d\theta}-4\varepsilon\frac{dV_q^m}{dr_0}P_2P_q^m\right]e^{-im\phi} \tag{4.28}$$

correct to the first order in ε.

4.2.4 Gradient of a Scalar Field

The gradient of the gravitational potential V_1 in the spherical coordinate system is

$$\nabla V_1=\hat{\mathbf{r}}\frac{\partial V_1}{\partial r}+\hat{\theta}\frac{1}{r}\frac{\partial V_1}{\partial\theta}+\hat{\phi}\frac{1}{r\sin\theta}\frac{\partial V_1}{\partial\phi}. \tag{4.29}$$

Using equation (2.21) in equation (4.29), we get

$$\nabla V_1=\sum_{n=|m|}^{N}\left[\hat{\mathbf{r}}\frac{dX_n^m}{dr}P_n^m+\hat{\theta}\frac{1}{r}\frac{dP_n^m}{d\theta}X_n^m+\hat{\phi}\frac{im}{r\sin\theta}X_n^mP_n^m\right]e^{im\phi}. \tag{4.30}$$

Again, using equations (4.5)-(4.7) in (4.30), the Clairaut form of equation (4.30) is

$$\begin{aligned}\nabla V_1 &= \sum_{n=|m|}^{N}\left[\hat{\mathbf{r}}\left\{1+\frac{2}{3}\frac{d}{dr_0}(r_0\varepsilon)P_2\right\}\frac{dX_n^m}{dr_0}P_n^m+\hat{\theta}\frac{1}{r_0}\left\{X_n^m\frac{dP_n^m}{d\theta}+\frac{2}{3}\varepsilon X_n^mP_2\frac{dP_n^m}{d\theta}\right.\right.\\ &\left.\left.+\frac{2}{3}r_0\varepsilon\frac{dX_n^m}{dr_0}P_2^1P_n^m\right\}+\hat{\phi}\frac{im}{r_0\sin\theta}\left(1+\frac{2}{3}\varepsilon P_2\right)X_n^mP_n^m\right]e^{im\phi}\end{aligned} \tag{4.31}$$

to the first order in ε. Similarly,

$$\begin{aligned}\nabla V_1^{*} &= \sum_{q=|m|}^{N}\left[\hat{\mathbf{r}}\left\{1+\frac{2}{3}\frac{d}{dr_0}(r_0\varepsilon)P_2\right\}\frac{dX_q^m}{dr_0}P_q^m+\hat{\theta}\frac{1}{r_0}\left\{X_q^m\frac{dP_q^m}{d\theta}+\frac{2}{3}\varepsilon X_q^mP_2\frac{dP_q^m}{d\theta}\right.\right.\\ &\left.\left.+\frac{2}{3}r_0\varepsilon\frac{dX_q^m}{dr_0}P_2^1P_q^m\right\}-\hat{\phi}\frac{im}{r_0\sin\theta}\left(1+\frac{2}{3}\varepsilon P_2\right)X_q^mP_q^m\right]e^{-im\phi}\end{aligned} \tag{4.32}$$

to the first order in ε.

Since the density, ρ_0, is a function of r only, therefore the gradient of density in the Clairaut coordinate system is

$$\nabla\rho_0 = \hat{\mathbf{r}}\left\{1+\frac{2}{3}\frac{d}{dr_0}(r_0\varepsilon)P_2\right\}\frac{d\rho_0}{dr_0}+\hat{\theta}\frac{2}{3}\varepsilon P_2^1\frac{d\rho_0}{dr_0} \tag{4.33}$$

to the first order in ε.

4.3 Divergence of the Stress Tensor in the Clairaut Coordinate System

In section 3.2, the Galerkin formulation of divergence of the stress is separated into two parts i.e., $\nabla\cdot\tilde{\tau}_1$ and $\nabla\cdot\tilde{\tau}_2$ [see equation (3.13)]. In this section, we will show the implementation of these two parts in the Clairaut Coordinates System.

4.3.1 Divergence of $\tilde{\tau}_1$

The Galerkin formulation of $\frac{1}{\rho_0}\nabla\cdot\tilde{\tau}_1$ leads the three terms: $\frac{\nabla\rho_0}{\rho_0^2}\cdot\tilde{\tau}_1\cdot\mathbf{u}^*$, $\frac{1}{\rho_0}\tilde{\tau}_1:\nabla\mathbf{u}^*$, and $\frac{1}{\rho_0}\hat{\mathbf{n}}\cdot\tilde{\tau}_1\cdot\mathbf{u}^*$. Next, we will derive these terms in the Clairaut coordinate system as follows. From equation(2.7), we get

$$\tilde{\tau}_1 = \lambda(\nabla\cdot\mathbf{u})\tilde{I} = \lambda(\nabla\cdot\mathbf{u})(\hat{r}\hat{r}+\hat{\theta}\hat{\theta}+\hat{\phi}\hat{\phi}), \tag{4.34}$$

which gives

$$(\tau_1)_{rr} = (\tau_1)_{\theta\theta} = (\tau_1)_{\phi\phi} = \lambda(\nabla\cdot\mathbf{u}). \tag{4.35}$$

The dot product of $\tilde{\tau}_1$ and $\mathbf{u}^*$ is

$$\tilde{\tau}_1\cdot\mathbf{u}^* = (\tau_1)_{rr}u_r^*\hat{r}+(\tau_1)_{\theta\theta}u_\theta^*\hat{\theta}+(\tau_1)_{\phi\phi}u_\phi^*\hat{\phi}. \tag{4.36}$$

Using equations (4.33), (4.35) and (4.36), we get

$$\begin{aligned}\frac{\nabla\rho_0}{\rho_0^2}\cdot\tilde{\tau}_1\cdot\mathbf{u}^* &= \frac{1}{\rho_0^2}\left\{1+\frac{2}{3}\frac{d}{dr_0}(r_0\varepsilon)P_2\right\}\frac{d\rho_0}{dr_0}\lambda(\nabla\cdot\mathbf{u})u_r^* + \frac{1}{\rho_0^2}\frac{2}{3}\varepsilon P_2^1\frac{d\rho_0}{dr_0}\lambda(\nabla\cdot\mathbf{u})u_\theta^* \\ &= \frac{\lambda}{\rho_0^2}\frac{d\rho_0}{dr_0}(\nabla\cdot\mathbf{u})\left[\left\{1+\frac{2}{3}\frac{d}{dr_0}(r_0\varepsilon)P_2\right\}u_r^* + \frac{2}{3}\varepsilon P_2^1 u_\theta^*\right] \qquad (4.37)\end{aligned}$$

to the first order in ε, where u_r^*, u_θ^* and $\nabla\cdot\mathbf{u}$ are given from equations (4.17) and (4.26). Therefore, we get

$$\begin{aligned}\frac{\nabla\rho_0}{\rho_0^2}\cdot\tilde{\tau}_1\cdot\mathbf{u}^* = \frac{\lambda}{\rho_0^2}\frac{d\rho_0}{dr_0}\sum_{q=|m|}^{N}\sum_{n=|m|}^{N}\Bigg[U_q^m\Bigg\{&\left(\frac{dU_n^m}{dr_0}+\frac{2U_n^m-n(n+1)V_n^m}{r_0}\right)P_n^m + \frac{2}{3}\varepsilon\Bigg(\frac{dU_n^m}{dr_0} \\ &+\frac{2U_n^m-n(n+1)V_n^m}{r_0}\Bigg)P_2P_n^m + \frac{2}{3}r_0\frac{d\varepsilon}{dr_0}\frac{dU_n^m}{dr_0}P_2P_n^m + \frac{4}{3}\varepsilon\frac{dV_n^m}{dr_0}P_2^1\frac{dP_n^m}{d\theta} \\ &-4\varepsilon\frac{dV_n^m}{dr_0}P_2P_n^m + \frac{2}{3}\frac{d}{dr_0}(r_0\varepsilon)\left(\frac{dU_n^m}{dr_0}+\frac{2U_n^m-n(n+1)V_n^m}{r_0}\right)P_2P_n^m\Bigg\}P_q^m \\ &+\frac{2}{3}\varepsilon V_q^m\left(\frac{dU_n^m}{dr_0}+\frac{2U_n^m-n(n+1)V_n^m}{r_0}\right)P_2^1\frac{dP_q^m}{d\theta}P_n^m \\ &-\frac{2im}{3}\varepsilon W_q^m\left(\frac{dU_n^m}{dr_0}+\frac{2U_n^m-n(n+1)V_n^m}{r_0}\right)\frac{P_2^1}{\sin\theta}P_n^mP_q^m\Bigg]. \qquad (4.38)\end{aligned}$$

The double dot product of $\tilde{\tau}_1$ and $\nabla\mathbf{u}^*$ in the spherical coordinate system is given by

$$\tilde{\tau}_1:\nabla\mathbf{u}^* = (\tau_1)_{rr}\frac{\partial u_r^*}{\partial r} + (\tau_1)_{\theta\theta}\left(\frac{1}{r}\frac{\partial u_\theta^*}{\partial\theta}+\frac{u_r^*}{r}\right) + (\tau_1)_{\phi\phi}\left(\frac{1}{r\sin\theta}\frac{\partial u_\phi^*}{\partial\phi}+\frac{u_r^*}{r}+\frac{u_\theta^*\cot\theta}{r}\right).$$

Since $(\tau_1)_{rr} = (\tau_1)_{\theta\theta} = (\tau_1)_{\phi\phi} = \lambda(\nabla\cdot\mathbf{u})$, then we get

$$\begin{aligned}\tilde{\tau}_1:\nabla\mathbf{u}^* &= \lambda(\nabla\cdot\mathbf{u})\left[\frac{\partial u_r^*}{\partial r}+\left(\frac{1}{r}\frac{\partial u_\theta^*}{\partial\theta}+\frac{u_r^*}{r}\right)+\left(\frac{1}{r\sin\theta}\frac{\partial u_\phi^*}{\partial\phi}+\frac{u_r^*}{r}+\frac{u_\theta^*\cot\theta}{r}\right)\right], \\ &= \lambda(\nabla\cdot\mathbf{u})\lambda(\nabla\cdot\mathbf{u}^*). \qquad (4.39)\end{aligned}$$

Substituting equations (4.26) and (4.28) into equation (4.39), then we get the $\tilde{\tau}_1:\nabla\mathbf{u}^*$ in

the Clairaut coordinate system

$$\begin{aligned}
\tilde{\tau}_1 : \nabla \mathbf{u}^* = \lambda \sum_{q=|m|}^{N} \sum_{n=|m|}^{N} \Bigg[& \left(\frac{dU_q^m}{dr_0} + \frac{2U_q^m}{r_0} \right) \Bigg\{ \left(\frac{dU_n^m}{dr_0} + \frac{2U_n^m - n(n+1)V_n^m}{r_0} \right) P_n^m \\
& + \frac{4}{3}\varepsilon \left(\frac{dU_n^m}{dr_0} + \frac{2U_n^m - n(n+1)V_n^m}{r_0} \right) P_2 P_n^m + \frac{2}{3} r_0 \frac{d\varepsilon}{dr_0} \frac{dU_n^m}{dr_0} P_2 P_n^m \\
& + \frac{4}{3}\varepsilon \frac{dV_n^m}{dr_0} P_2^1 \frac{dP_n^m}{d\theta} - 4\varepsilon \frac{dV_n^m}{dr_0} P_2 P_n^m \Bigg\} P_q^m - V_q^m \left(\frac{q(q+1)}{r_0} \right) \\
& \times \Bigg\{ \left(\frac{dU_n^m}{dr_0} + \frac{2U_n^m - n(n+1)V_n^m}{r_0} \right) P_n^m + \frac{4}{3}\varepsilon \left(\frac{dU_n^m}{dr_0} + \frac{2U_n^m - n(n+1)V_n^m}{r_0} \right) P_2 P_n^m \\
& + \frac{2}{3} r_0 \frac{d\varepsilon}{dr_0} \frac{dU_n^m}{dr_0} P_2 P_n^m + \frac{4}{3}\varepsilon \frac{dV_n^m}{dr_0} P_2^1 \frac{dP_n^m}{d\theta} - 4\varepsilon \frac{dV_n^m}{dr_0} P_2 P_n^m \Bigg\} P_q^m \\
& + \frac{2}{3} r_0 \frac{d\varepsilon}{dr_0} \frac{dU_q^m}{dr_0} \left(\frac{dU_n^m}{dr_0} + \frac{2U_n^m - n(n+1)V_n^m}{r_0} \right) P_2 P_n^m P_q^m \\
& + \frac{4}{3}\varepsilon \frac{dV_q^m}{dr_0} \left(\frac{dU_n^m}{dr_0} + \frac{2U_n^m - n(n+1)V_n^m}{r_0} \right) P_2^1 \frac{dP_q^m}{d\theta} P_n^m \\
& - 4\varepsilon \frac{dV_q^m}{dr_0} \left(\frac{dU_n^m}{dr_0} + \frac{2U_n^m - n(n+1)V_n^m}{r_0} \right) P_2 P_n^m P_q^m \Bigg].
\end{aligned} \tag{4.40}$$

Again, we get from equations (4.9) and (4.36)

$$\begin{aligned}
\hat{\mathbf{n}} \cdot \tilde{\tau}_1 \cdot \mathbf{u}^* &= \left(\hat{\mathbf{r}} + \frac{2}{3}\varepsilon P_2^1 \hat{\theta} \right) \cdot \left((\tau_1)_{rr} u_r^* \hat{r} + (\tau_1)_{\theta\theta} u_\theta^* \hat{\theta} + (\tau_1)_{\phi\phi} u_\phi^* \hat{\phi} \right), \\
&= (\tau_1)_{rr} u_r^* + \frac{2}{3}\varepsilon P_2^1 (\tau_1)_{\theta\theta} u_\theta^*.
\end{aligned} \tag{4.41}$$

Using equation (4.35) in (4.41), therefore, we get

$$\hat{\mathbf{n}} \cdot \tilde{\tau}_1 \cdot \mathbf{u}^* = \lambda (\nabla \cdot \mathbf{u}) \left(u_r^* + \frac{2}{3}\varepsilon P_2^1 u_\theta^* \right) \tag{4.42}$$

to the first order in ε, where u_r^*, u_θ^* and $\nabla \cdot \mathbf{u}$ are given from equations (4.17) and (4.26).

Therefore, we get

$$\begin{aligned}\hat{\mathbf{n}}\cdot\tilde{\tau}_1\cdot\mathbf{u}^* = \lambda\sum_{q=|m|}^{N}\sum_{n=|m|}^{N}\Bigg[U_q^m\Bigg\{\left(\frac{dU_n^m}{dr_0}+\frac{2U_n^m-n(n+1)V_n^m}{r_0}\right)P_n^m+\frac{2}{3}\varepsilon\Bigg(\frac{dU_n^m}{dr_0}\\ +\frac{2U_n^m-n(n+1)V_n^m}{r_0}\Bigg)P_2P_n^m+\frac{2}{3}r_0\frac{d\varepsilon}{dr_0}\frac{dU_n^m}{dr_0}P_2P_n^m+\frac{4}{3}\varepsilon\frac{dV_n^m}{dr_0}P_2^1\frac{dP_n^m}{d\theta}\\ -4\varepsilon\frac{dV_n^m}{dr_0}P_2P_n^m\Bigg\}P_q^m+\frac{2}{3}\varepsilon V_q^m\left(\frac{dU_n^m}{dr_0}+\frac{2U_n^m-n(n+1)V_n^m}{r_0}\right)P_2^1\frac{dP_q^m}{d\theta}P_n^m\\ -\frac{2im}{3}\varepsilon W_q^m\left(\frac{dU_n^m}{dr_0}+\frac{2U_n^m-n(n+1)V_n^m}{r_0}\right)\frac{P_2^1}{\sin\theta}P_n^mP_q^m\Bigg].\end{aligned} \tag{4.43}$$

Hence, we see from equation (4.43) [also see Eq. (4.70)] that the derivatives of material properties at the boundaries, which are not well established in the available Earth models, are removed. This is one of the advantages of using the Galerkin method as we mentioned in section 3.2.

4.3.2 Divergence of $\tilde{\tau}_2$

The Galerkin formulation of $\nabla\cdot\tilde{\tau}_2$, which is zero for the OC because $\mu=0$ in the OC, and boundary conditions to it will be derived as follows. Recall that the r, θ and ϕ components of $\nabla\cdot(\tilde{\tau}_2)$ in the spherical coordinate system are given by equations (3.16)-(3.18) i.e.,

$$\begin{aligned}\left\{\nabla\cdot\tilde{\tau}_2\right\}_r =&\frac{\partial(\tau_2)_{rr}}{\partial r}+\frac{1}{r}\frac{\partial(\tau_2)_{\theta r}}{\partial\theta}+\frac{1}{r\sin\theta}\frac{\partial(\tau_2)_{\phi r}}{\partial\phi}+\frac{2(\tau_2)_{rr}-(\tau_2)_{\theta\theta}-(\tau_2)_{\phi\phi}}{r}\\ &+\frac{\cot\theta}{r}(\tau_2)_{\theta r},\end{aligned} \tag{4.44}$$

$$\begin{aligned}\left\{\nabla\cdot\tilde{\tau}_2\right\}_\theta =&\frac{\partial(\tau_2)_{r\theta}}{\partial r}+\frac{1}{r}\frac{\partial(\tau_2)_{\theta\theta}}{\partial\theta}+\frac{1}{r\sin\theta}\frac{\partial(\tau_2)_{\phi\theta}}{\partial\phi}+\frac{3(\tau_2)_{r\theta}}{r}\\ &+\frac{\cot\theta}{r}\left\{(\tau_2)_{\theta\theta}-(\tau_2)_{\phi\phi}\right\},\end{aligned} \tag{4.45}$$

$$\left\{\nabla\cdot\tilde{\tau}_2\right\}_\phi = \frac{\partial(\tau_2)_{r\phi}}{\partial r} + \frac{1}{r}\frac{\partial(\tau_2)_{\theta\phi}}{\partial\theta} + \frac{1}{r\sin\theta}\frac{\partial(\tau_2)_{\phi\phi}}{\partial\phi} + \frac{3(\tau_2)_{r\phi}}{r} + \frac{2\cot\theta}{r}(\tau_2)_{\theta\phi}. \tag{4.46}$$

Here the components of the stress tensor $\tilde{\tau}_2$ are given by equations (3.19)-(3.26)

$$(\tau_2)_{rr} = 2\mu\frac{\partial u_r}{\partial r}, \tag{4.47}$$

$$(\tau_2)_{\theta\theta} = 2\mu\left[\frac{u_r}{r} + \frac{1}{r}\frac{\partial u_\theta}{\partial\theta}\right], \tag{4.48}$$

$$(\tau_2)_{\phi\phi} = 2\mu\left[\frac{1}{r\sin\theta}\frac{\partial u_\phi}{\partial\phi} + \frac{u_r}{r} + \frac{\cot\theta u_\theta}{r}\right], \tag{4.49}$$

$$(\tau_2)_{r\theta} = \mu\left[\frac{\partial u_\theta}{\partial r} - \frac{u_\theta}{r} + \frac{1}{r}\frac{\partial u_r}{\partial\theta}\right], \tag{4.50}$$

$$(\tau_2)_{\theta\phi} = \mu\left[\frac{1}{r}\frac{\partial u_\phi}{\partial\theta} - \frac{\cot\theta u_\phi}{r} + \frac{1}{r\sin\theta}\frac{\partial u_\theta}{\partial\phi}\right], \tag{4.51}$$

$$(\tau_2)_{\phi r} = \mu\left[\frac{\partial u_\phi}{\partial r} - \frac{u_\phi}{r} + \frac{1}{r\sin\theta}\frac{\partial u_r}{\partial\phi}\right]. \tag{4.52}$$

Using equations (4.5)-(4.7), Clairaut's form of equations (4.44)-(4.46) is

$$\left\{\nabla\cdot\tilde{\tau}_2\right\}_r = \left[1+\frac{2}{3}\frac{d}{dr_0}(r_0\varepsilon)P_2\right]\frac{\partial(\tau_2)_{rr}}{\partial r_0} + \frac{1}{r_0}\left(1+\frac{2}{3}\varepsilon P_2\right)\left[\frac{2}{3}r_0\varepsilon P_2^1\frac{\partial(\tau_2)_{\theta r}}{\partial r_0} + \frac{\partial(\tau_2)_{\theta r}}{\partial\theta} + \frac{1}{\sin\theta}\frac{\partial(\tau_2)_{\phi r}}{\partial\phi} + 2(\tau_2)_{rr} - (\tau_2)_{\theta\theta} - (\tau_2)_{\phi\phi} + \cot\theta(\tau_2)_{\theta r}\right], \tag{4.53}$$

$$\left\{\nabla\cdot\tilde{\tau}_2\right\}_\theta = \left[1+\frac{2}{3}\frac{d}{dr_0}(r_0\varepsilon)P_2\right]\frac{\partial(\tau_2)_{r\theta}}{\partial r_0} + \frac{1}{r_0}\left(1+\frac{2}{3}\varepsilon P_2\right)\left[\frac{2}{3}r_0\varepsilon P_2^1\frac{\partial(\tau_2)_{\theta\theta}}{\partial r_0} + \frac{\partial(\tau_2)_{\theta\theta}}{\partial\theta} + \frac{1}{\sin\theta}\frac{\partial(\tau_2)_{\phi\theta}}{\partial\phi} + 3(\tau_2)_{r\theta} + \cot\theta\left\{(\tau_2)_{\theta\theta} - (\tau_2)_{\phi\phi}\right\}\right], \tag{4.54}$$

$$\left\{\nabla\cdot\tilde{\tau}_2\right\}_{\phi}=\left[1+\frac{2}{3}\frac{d}{dr_0}(r_0\varepsilon)P_2\right]\frac{\partial(\tau_2)_{r\phi}}{\partial r_0}+\frac{1}{r_0}\left(1+\frac{2}{3}\varepsilon P_2\right)\left[\frac{2}{3}r_0\varepsilon P_2^1\frac{\partial(\tau_2)_{\theta\phi}}{\partial r_0}\right.$$
$$\left.+\frac{\partial(\tau_2)_{\theta\phi}}{\partial\theta}+\frac{1}{\sin\theta}\frac{\partial(\tau_2)_{\phi\phi}}{\partial\phi}+3(\tau_2)_{r\phi}+2\cot\theta(\tau_2)_{\theta\phi}\right]. \tag{4.55}$$

Again, using equations (4.5)-(4.7) and (4.16) in (4.47)-(4.52), the components of $\tilde{\tau}_2$ in the Clairaut coordinates system become

$$(\tau_2)_{rr}=2\mu\left[1+\frac{2}{3}\frac{d}{dr_0}(r_0\varepsilon)P_2\right]\frac{\partial u_r}{\partial r_0},$$
$$=2\mu\left[1+\frac{2}{3}\frac{d}{dr_0}(r_0\varepsilon)P_2\right]\sum_{n=|m|}^{N}\frac{dU_n^m}{dr_0}P_n^m e^{im\phi}, \tag{4.56}$$

$$(\tau_2)_{\theta\theta}=\frac{2\mu}{r_0}\left(1+\frac{2}{3}\varepsilon P_2\right)\left[u_r+\frac{2}{3}r_0P_2^1\frac{\partial u_\theta}{\partial r_0}+\frac{\partial u_\theta}{\partial\theta}\right],$$
$$=\frac{2\mu}{r_0}\sum_{n=|m|}^{N}\left[U_n^mP_n^m+V_n^m\frac{d^2P_n^m}{d\theta^2}+\frac{im}{\sin\theta}W_n^m\frac{dP_n^m}{d\theta}-\frac{im}{\sin\theta}W_n^m\cot\theta P_n^m\right.$$
$$+\frac{2}{3}r_0\varepsilon\left\{\frac{dV_n^m}{dr_0}P_n^m+2\frac{dV_n^m}{dr_0}P_2^1\frac{dP_n^m}{d\theta}+im\frac{dW_n^m}{dr_0}\frac{P_2^1}{\sin\theta}P_n^m\right\}+\frac{2}{3}\varepsilon\left\{U_n^mP_n^m+V_n^m\frac{d^2P_n^m}{d\theta^2}\right.$$
$$\left.\left.-4r_0\frac{dV_n^m}{dr_0}P_n^m+\frac{im}{\sin\theta}W_n^m\frac{dP_n^m}{d\theta}-\frac{im}{\sin\theta}W_n^m\cot\theta P_n^m\right\}P_2\right]e^{im\phi}, \tag{4.57}$$

$$(\tau_2)_{\phi\phi}=\frac{2\mu}{r_0}\left(1+\frac{2}{3}\varepsilon P_2\right)\left[\frac{1}{\sin\theta}\frac{\partial u_\phi}{\partial\phi}+u_r+\cot\theta u_\theta\right],$$
$$=\frac{2\mu}{r_0}\sum_{n=|m|}^{N}\left[U_n^mP_n^m-\frac{m^2}{\sin^2\theta}V_n^mP_n^m+V_n^m\cot\theta\frac{dP_n^m}{d\theta}-\frac{im}{\sin\theta}W_n^m\frac{dP_n^m}{d\theta}+imW_n^m\frac{\cot\theta}{\sin\theta}P_n^m\right.$$
$$+\frac{2}{3}r_0\varepsilon\left\{\frac{dV_n^m}{dr_0}\cot\theta P_2^1P_n^m-im\frac{dW_n^m}{dr_0}\frac{P_2^1}{\sin\theta}P_n^m\right\}+\frac{2}{3}\varepsilon\left\{U_n^mP_n^m-\frac{m^2}{\sin^2\theta}V_n^mP_n^m\right.$$
$$\left.\left.+V_n^m\cot\theta\frac{dP_n^m}{d\theta}-\frac{im}{\sin\theta}W_n^m\frac{dP_n^m}{d\theta}+imW_n^m\frac{\cot\theta}{\sin\theta}P_n^m\right\}P_2\right]e^{im\phi}, \tag{4.58}$$

$$
\begin{aligned}
(\tau_2)_{r\theta} &= \mu\left[\left\{1+\frac{2}{3}\frac{d}{dr_0}(r_0\varepsilon)P_2^1\right\}\frac{\partial u_\theta}{\partial r_0}-\frac{1}{r_0}\left(1+\frac{2}{3}\varepsilon P_2\right)\left\{u_\theta-\frac{2}{3}r_0P_2^1\frac{\partial u_r}{\partial r_0}-\frac{\partial u_r}{\partial\theta}\right\}\right],\\
&= \mu\sum_{n=|m|}^{N}\left[\frac{dV_n^m}{dr_0}\frac{dP_n^m}{d\theta}+\frac{im}{\sin\theta}\frac{dW_n^m}{dr_0}P_n^m-\frac{1}{r_0}\left\{V_n^m\frac{dP_n^m}{d\theta}+\frac{im}{\sin\theta}W_n^mP_n^m-U_n^m\frac{dP_n^m}{d\theta}\right\}\right.\\
&+\frac{2}{3}\frac{d}{dr_0}(r_0\varepsilon)\left\{\frac{dV_n^m}{dr_0}\frac{dP_n^m}{d\theta}+\frac{im}{\sin\theta}\frac{dW_n^m}{dr_0}P_n^m\right\}P_2-\frac{2}{3r_0}\varepsilon\left\{V_n^m\frac{dP_n^m}{d\theta}+\frac{im}{\sin\theta}W_n^mP_n^m\right.\\
&\left.\left.-U_n^m\frac{dP_n^m}{d\theta}\right\}P_2+\frac{2}{3}\left\{\frac{d}{dr_0}(r_0\varepsilon)\frac{dV_n^m}{dr_0}+r_0\varepsilon\frac{d^2V_n^m}{dr_0^2}-\varepsilon\frac{dV_n^m}{dr_0}+\varepsilon\frac{dU_n^m}{dr_0}\right\}P_2^1P_n^m\right]e^{im\phi},
\end{aligned}
\tag{4.59}
$$

$$
\begin{aligned}
(\tau_2)_{\theta\phi} &= \frac{\mu}{r_0}\left(1+\frac{2}{3}\varepsilon P_2\right)\left[\frac{2}{3}r_0P_2^1\frac{\partial u_\phi}{\partial r_0}+\frac{\partial u_\phi}{\partial\theta}-\cot\theta u_\phi+\frac{1}{\sin\theta}\frac{\partial u_\theta}{\partial\phi}\right],\\
&= \frac{\mu}{r_0}\sum_{n=|m|}^{N}\left[\frac{2im}{\sin\theta}V_n^m\frac{dP_n^m}{d\theta}-2imV_n^m\frac{\cot\theta}{\sin\theta}-W_n^m\frac{d^2P_n^m}{d\theta^2}-W_n^m\frac{m^2}{\sin^2\theta}+W_n^m\cot\theta\frac{dP_n^m}{d\theta}\right.\\
&-\frac{2}{3}\varepsilon r_0\frac{dW_n^m}{dr_0}P_n^m+\frac{2}{3}\varepsilon\left\{2imV_n^m\frac{1}{\sin\theta}\frac{dP_n^m}{d\theta}-2imV_n^m\frac{\cot\theta}{\sin\theta}P_n^m-W_n^m\frac{d^2P_n^m}{d\theta^2}\right.\\
&\left.+W_n^m\cot\theta\frac{dP_n^m}{d\theta}-W_n^m\frac{m^2}{\sin^2\theta}P_n^m+4r_0\frac{dW_n^m}{dr_0}P_n^m\right\}P_2+\frac{2}{3}r_0\varepsilon\left\{2im\frac{dV_n^m}{dr_0}\frac{1}{\sin\theta}P_n^m\right.\\
&\left.\left.-2\frac{dW_n^m}{dr_0}\frac{dP_n^m}{d\theta}+\frac{dW_n^m}{dr_0}\cot\theta P_n^m\right\}P_2^1\right]e^{im\phi},
\end{aligned}
\tag{4.60}
$$

$$
\begin{aligned}
(\tau_2)_{\phi r} &= \mu\left[\left\{1+\frac{2}{3}\frac{d}{dr_0}(r_0\varepsilon)P_2^1\right\}\frac{\partial u_\phi}{\partial r_0}-\frac{1}{r_0}\left(1+\frac{2}{3}\varepsilon P_2\right)\left\{u_\phi-\frac{1}{\sin\theta}\frac{\partial u_r}{\partial\phi}\right\}\right],\\
&= \mu\sum_{n=|m|}^{N}\left[\frac{im}{\sin\theta}\frac{dV_n^m}{dr_0}P_n^m-\frac{dW_n^m}{dr_0}\frac{dP_n^m}{d\theta}-\frac{1}{r_0}\left\{\frac{im}{\sin\theta}V_n^mP_n^m-W_n^m\frac{dP_n^m}{d\theta}-\frac{im}{\sin\theta}U_n^mP_n^m\right\}\right.\\
&+\frac{2}{3}\frac{d}{dr_0}(r_0\varepsilon)\left\{\frac{im}{\sin\theta}\frac{dV_n^m}{dr_0}P_n^m-\frac{dW_n^m}{dr_0}\frac{dP_n^m}{d\theta}\right\}P_2-\frac{2}{3r_0}\varepsilon\left\{\frac{im}{\sin\theta}V_n^mP_n^m-W_n^m\frac{dP_n^m}{d\theta}\right.\\
&\left.\left.-\frac{im}{\sin\theta}U_n^mP_n^m\right\}P_2-\frac{2}{3}\left\{\frac{d}{dr_0}(r_0\varepsilon)\frac{dW_n^m}{dr_0}+r_0\varepsilon\frac{d^2W_n^m}{dr_0^2}-\varepsilon\frac{dW_n^m}{dr_0}\right\}P_2^1P_n^m\right]e^{im\phi}
\end{aligned}
\tag{4.61}
$$

to the first order in ε, where we use the relation

$$\frac{dP_2^1}{d\theta} = 1 - 4P_2. \tag{4.62}$$

Now, using equations (4.56)-(4.61) in (4.53), and doing some algebra, we get the r component of $\nabla \cdot (\tilde{\tau}_2)$

$$\begin{aligned}
\left\{\nabla\cdot\tilde{\tau}_2\right\}_r = \sum_{n=|m|}^{N} \mu\Bigg[\Bigg\{ & 2\frac{d^2U_n^m}{dr_0^2} - n(n+1)U_n^m - 4U_n^m + \frac{4}{r_0}\frac{dU_n^m}{dr_0} + \frac{2}{3r_0}\varepsilon\frac{dU_n^m}{dr_0} - n(n+1) \\
& \times\left(\frac{1}{r_0}\frac{dV_n^m}{dr_0} - 3V_n^m\right) + \frac{2}{3r_0}\left(\frac{d}{dr_0}(r_0\varepsilon)\frac{dV_n^m}{dr_0} + r_0\varepsilon\frac{dV_n^m}{dr_0^2} - 3\varepsilon\frac{dV_n^m}{dr_0}\right)\Bigg\}P_n^m \\
& + \Bigg\{\frac{8}{3}\frac{d}{dr_0}(r_0\varepsilon)\frac{d^2U_n^m}{dr_0^2} + \frac{4}{3}\frac{d^2}{dr_0^2}(r_0\varepsilon)\frac{d^2}{dr_0^2}(r_0\varepsilon)\frac{dU_n^m}{dr_0} + \frac{8}{3r_0}\Bigg(- \frac{d}{dr_0}(r_0\varepsilon)\frac{dV_n^m}{dr_0} \\
& - r_0\varepsilon\frac{d^2V_n^m}{dr_0^2} + 3\varepsilon\frac{dV_n^m}{dr_0}\Bigg) - n(n+1)\Bigg(\frac{2}{3r_0}\frac{d}{dr_0}(r_0\varepsilon)\frac{dV_n^m}{dr_0} + \frac{2}{3r_0}\varepsilon\frac{dV_n^m}{dr_0} \\
& - 4\varepsilon V_n^m\Bigg) - \frac{4}{3}n(n+1)\varepsilon U_n^m + \frac{8}{3}\left(\frac{1}{r_0}\frac{d}{dr_0}(r_0\varepsilon)\frac{dU_n^m}{dr_0} - 2\varepsilon U_n^m\right)\Bigg\}P_2P_n^m \\
& + \frac{4}{3r_0}\left\{\varepsilon\frac{dU_n^m}{dr_0} + r_0\varepsilon\frac{d^2V_n^m}{d^2r_0} + \frac{d}{dr_0}(r_0\varepsilon)\frac{dV_n^m}{dr_0} - 3\varepsilon\frac{dV_n^m}{dr_0}\right\}P_2^1\frac{dP_n^m}{d\theta} \\
& + \frac{2}{3r_0}\left\{\varepsilon\frac{dU_n^m}{dr_0} + r_0\varepsilon\frac{d^2V_n^m}{d^2r_0} + \frac{d}{dr_0}(r_0\varepsilon)\frac{dV_n^m}{dr_0} - 3\varepsilon\frac{dV_n^m}{dr_0}\right\}P_2^1\cot\theta P_n^m\Bigg]e^{im\phi} \\
& + \sum_{n=|m|}^{N}\frac{d\mu}{dr_0}\Bigg[2\frac{dU_n^m}{dr_0}P_n^m + \frac{2}{3}\varepsilon\left\{\frac{U_n^m}{r_0} - \frac{V_n^m}{r_0} + \frac{dV_n^m}{dr_0}\right\}P_2^1\frac{dP_n^m}{d\theta} \\
& + \frac{8}{3}\frac{d}{dr_0}(r_0\varepsilon)\frac{dU_n^m}{dr_0}P_2P_n^m + \frac{2im}{3}\varepsilon\left\{\frac{dW_n^m}{dr_0} - \frac{W_n^m}{r_0}\right\}\frac{P_2^1}{\sin\theta}P_n^m\Bigg]e^{im\phi}
\end{aligned} \tag{4.63}$$

in the Clairaut coordinates system to the first order in ε, where the associated Legendre differential equation (4.27) is used.

Similarly, the θ component of $\nabla \cdot (\tilde{\tau}_2)$ is obtained from equations (4.56)-(4.61) and

(4.54)

$$
\begin{aligned}
\left\{\nabla\cdot\tilde{\tau}_2\right\}_\theta = \sum_{n=|m|}^{N}\mu\Bigg[&\left\{\frac{1}{r_0}\frac{dU_n^m}{dr_0}+\frac{4}{r_n^2}U_n^m+\frac{d^2V_n^m}{dr_0^2}+\frac{2}{r_0}\frac{dV_n^m}{dr_0}-\frac{2}{r_0^2}n(n+1)V_n^m\right.\\
&\left.+\frac{4}{r_0}\varepsilon\frac{dV_n^m}{dr_0}\right\}\frac{dP_n^m}{d\theta}+im\left\{\frac{d^2W_n^m}{dr_0^2}+\frac{2}{r_0}\frac{dW_n^m}{dr_0}-\frac{n(n+1)}{r_0^2}W_n^m+\frac{2}{3r_0}\varepsilon\frac{dW_n^m}{dr_0}\right\}\\
&\times\frac{P_n^m}{\sin\theta}+\frac{4}{3r_0}\varepsilon\frac{dV_n^m}{dr_0}\cot\theta P_n^m+\left\{\left(\frac{2}{3}\varepsilon\frac{d^2U_n^m}{dr_0^2}+\frac{2}{3r_0}\frac{d}{dr_0}(r_0\varepsilon)\frac{dU_n^m}{dr_0}\right.\right.\\
&+\frac{4}{3r_0}\varepsilon\frac{dU_n^m}{dr_0}+\frac{2}{3}\frac{d^2}{dr_0^2}(r_0\varepsilon)\frac{dV_n^m}{dr_0}+\frac{4}{3}\frac{d}{dr_0}(r_0\varepsilon)\frac{d^2V_n^m}{dr_0^2}+\frac{4}{3}\varepsilon\frac{d^2V_n^m}{dr_0^2}\\
&\left.+\frac{2}{3}r_0\varepsilon\frac{d^3V_n^m}{dr_0^3}-\frac{20}{3r_0}\varepsilon\frac{dV_n^m}{dr_0}+\frac{4}{3r_0}\frac{d}{dr_0}(r_0\varepsilon)\frac{dV_n^m}{dr_0}\right)P_n^m+\frac{4}{3r_0}\varepsilon\frac{dV_n^m}{dr_0}\frac{d^2P_n^m}{d\theta^2}\\
&-\frac{4}{3r_0}\varepsilon\frac{dV_n^m}{dr_0}\frac{m^2}{\sin^2\theta}P_n^m-\frac{4}{3r_0}\varepsilon\frac{dV_n^m}{dr_0}\cot^2\theta P_n^m+\frac{8}{3r_0}\varepsilon\frac{dV_n^m}{dr_0}\frac{d^2P_n^m}{d\theta^2}\\
&+\frac{8}{3r_0}\varepsilon\frac{dV_n^m}{dr_0}\cot\theta\frac{dP_n^m}{d\theta}+\frac{4im}{3r_0}\varepsilon\frac{dW_n^m}{dr_0}\frac{1}{\sin\theta}\frac{dP_n^m}{d\theta}+\frac{2im}{3r_0}\varepsilon\frac{dW_n^m}{dr_0}\frac{\cot\theta}{\sin\theta}P_n^m\Bigg\}P_2^1\\
&+\left\{\left(\frac{2}{3r_0}\varepsilon\frac{dU_n^m}{dr_0}+\frac{2}{3r_0}\frac{d}{dr_0}(r_0\varepsilon)\frac{dU_n^m}{dr_0}+\frac{16}{3r_0^2}\varepsilon U_n^m+\frac{2}{3}\frac{d^2}{dr_0^2}(r_0\varepsilon)\frac{dV_n^m}{dr_0}\right.\right.\\
&\left.+\frac{4}{3}\frac{d}{dr_0}(r_0\varepsilon)\frac{d^2V_n^m}{dr_0^2}+\frac{4}{3r_0}\frac{d}{dr_0}(r_0\varepsilon)\frac{dV_n^m}{dr_0}-\frac{44}{3r_0}\varepsilon\frac{dV_n^m}{dr_0}-\frac{8}{3r_0^2}n(n+1)\varepsilon V_n^m\right)\\
&\times\frac{dP_n^m}{d\theta}-\frac{16}{3r_0}\varepsilon\frac{dV_n^m}{dr_0}\cot\theta P_n^m+im\left(\frac{2}{3}\frac{d^2}{dr_0^2}(r_0\varepsilon)\frac{dW_n^m}{dr_0}+\frac{4}{3}\frac{d}{dr_0}(r_0\varepsilon)\frac{d^2W_n^m}{dr_0^2}\right.\\
&\left.\left.+\frac{4}{3r_0}\frac{d}{dr_0}(r_0\varepsilon)\frac{dW_n^m}{dr_0}-\frac{4}{3r_0}\varepsilon\frac{dW_n^m}{dr_0}-\frac{4}{3r_0^2}n(n+1)\varepsilon W_n^m\right)\frac{P_n^m}{\sin\theta}\right\}P_2\Bigg]e^{im\phi}\\
&+\sum_{n=|m|}^{N}\frac{d\mu}{dr_0}\Bigg[\left\{\frac{U_n^m}{r_0}+\frac{dV_n^m}{dr_0}-\frac{V_n^m}{r_0}\right\}\frac{dP_n^m}{d\theta}+im\left\{\frac{dW_n^m}{dr_0}-\frac{W_n^m}{r_0}\right\}\frac{P_n^m}{\sin\theta}\\
&\left\{\left(\frac{2}{3}\varepsilon\frac{dU_n^m}{dr_0}+\frac{4}{3r_0}\varepsilon U_n^m+\frac{2}{3}\frac{d}{dr_0}(r_0\varepsilon)\frac{dV_n^m}{dr_0}+\frac{2}{3}r_0\varepsilon\frac{d^2V_n^m}{dr_0^2}-\frac{2}{3}\varepsilon\frac{dV_n^m}{dr_0}\right)P_n^m\right.\\
&+\frac{4}{3r_0}\varepsilon V_n^m\frac{d^2P_n^m}{d\theta^2}+\frac{4im}{3r_0}\varepsilon W_n^m\frac{1}{\sin\theta}\frac{dP_n^m}{d\theta}-\frac{4im}{3r_0}\varepsilon W_n^m\frac{\cos\theta}{\sin^2\theta}P_n^m\Bigg\}P_2^1\\
&+\left\{\left(\frac{2}{3r_0}\varepsilon U_n^m+\frac{2}{3r_0}\frac{d}{dr_0}(r_0\varepsilon)U_n^m+\frac{4}{3}\frac{d}{dr_0}(r_0\varepsilon)\frac{dV_n^m}{dr_0}-\frac{2}{3r_0}\varepsilon V_n^m\right.\right.
\end{aligned}
$$

$$-\frac{2}{3r_0}\frac{d}{dr_0}(r_0\varepsilon)V_n^m\Big)\frac{dP_n^m}{d\theta}+im\Bigg(\frac{4}{3}\frac{d}{dr_0}(r_0\varepsilon)\frac{dW_n^m}{dr_0}-\frac{2}{3r_0}\varepsilon W_n^m$$
$$-\frac{2}{3r_0}\frac{d}{dr_0}(r_0\varepsilon)W_n^m\Big)\frac{P_n^m}{\sin\theta}\Bigg\}P_2\Bigg]e^{im\phi}. \tag{4.64}$$

The ϕ component of $\nabla\cdot(\tilde{\tau}_2)$ is

$$\begin{aligned}
\left\{\nabla\cdot\tilde{\tau}_2\right\}_\phi = \sum_{n=|m|}^{N}\mu\Bigg[im\Bigg\{&\frac{1}{r_0}\frac{dU_n^m}{dr_0}+\frac{4}{r_n^2}U_n^m+\frac{d^2V_n^m}{dr_0^2}+\frac{2}{r_0}\frac{dV_n^m}{dr_0}-\frac{2}{r_0^2}n(n+1)V_n^m\\
&+\frac{4}{r_0}\varepsilon\frac{dV_n^m}{dr_0}\Bigg\}\frac{P_n^m}{\sin\theta}-\Bigg\{\frac{d^2W_n^m}{dr_0^2}+\frac{2}{r_0}\frac{dW_n^m}{dr_0}-\frac{n(n+1)}{r_0^2}W_n^m+\frac{2}{r_0}\varepsilon\frac{dW_n^m}{dr_0}\Bigg\}\frac{dP_n^m}{d\theta}\\
&-\frac{2}{3r_0}\varepsilon\frac{dW_n^m}{dr_0}\cot\theta P_n^m+\Bigg\{\frac{8im}{3r_0}\varepsilon\frac{dV_n^m}{dr_0}\frac{1}{\sin\theta}\frac{dP_n^m}{d\theta}+\frac{4im}{3r_0}\varepsilon\frac{dV_n^m}{dr_0}\frac{\cot\theta}{\sin\theta}P_n^m\\
&\Bigg(-\frac{2}{3}\frac{d^2}{dr_0^2}(r_0\varepsilon)\frac{dW_n^m}{dr_0}-\frac{4}{3}\frac{d}{dr_0}(r_0\varepsilon)\frac{d^2W_n^m}{dr_0^2}-\frac{4}{3}\varepsilon\frac{d^2W_n^m}{dr_0^2}-\frac{2}{3}r_0\varepsilon\frac{d^3W_n^m}{dr_0^3}\\
&+\frac{10}{3r_0}\varepsilon\frac{dW_n^m}{dr_0}-\frac{4}{3r_0}\frac{d}{dr_0}(r_0\varepsilon)\frac{dW_n^m}{dr_0}\Bigg)P_n^m-\frac{2}{r_0}\varepsilon\frac{dW_n^m}{dr_0}\frac{d^2P_n^m}{d\theta^2}\\
&+\frac{2}{3r_0}\varepsilon\frac{dW_n^m}{dr_0}\frac{m^2}{\sin^2\theta}P_n^m+\frac{2}{3r_0}\varepsilon\frac{dW_n^m}{dr_0}\cot^2\theta P_n^m-\frac{4}{3r_0}\varepsilon\frac{dW_n^m}{dr_0}\cot\theta\frac{dP_n^m}{d\theta}\Bigg\}P_2^1\\
&+\Bigg\{im\Bigg(\frac{2}{3r_0}\varepsilon\frac{dU_n^m}{dr_0}+\frac{2}{3r_0}\frac{d}{dr_0}(r_0\varepsilon)\frac{dU_n^m}{dr_0}+\frac{16}{3r_0^2}\varepsilon U_n^m+\frac{2}{3}\frac{d^2}{dr_0^2}(r_0\varepsilon)\frac{dV_n^m}{dr_0}\\
&+\frac{4}{3}\frac{d}{dr_0}(r_0\varepsilon)\frac{d^2V_n^m}{dr_0^2}+\frac{4}{3r_0}\frac{d}{dr_0}(r_0\varepsilon)\frac{dV_n^m}{dr_0}-\frac{4}{r_0}\varepsilon\frac{dV_n^m}{dr_0}-\frac{8}{3r_0^2}n(n+1)\varepsilon V_n^m\Bigg)\\
&\times\frac{P_n^m}{\sin\theta}+\Bigg(-\frac{2}{3}\frac{d^2}{dr_0^2}(r_0\varepsilon)\frac{dW_n^m}{dr_0}-\frac{4}{3}\frac{d}{dr_0}(r_0\varepsilon)\frac{d^2W_n^m}{dr_0^2}-\frac{4}{3r_0}\frac{d}{dr_0}(r_0\varepsilon)\frac{dW_n^m}{dr_0}\\
&+\frac{20}{3r_0}\varepsilon\frac{dW_n^m}{dr_0}+\frac{4}{3r_0^2}n(n+1)\varepsilon W_n^m\Bigg)\frac{dP_n^m}{d\theta}+\frac{8}{3r_0}\varepsilon\frac{dW_n^m}{dr_0}\cot\theta P_n^m\Bigg\}P_2\Bigg]e^{im\phi}\\
&+\sum_{n=|m|}^{N}\frac{d\mu}{dr_0}\Bigg[im\Bigg\{\frac{U_n^m}{r_0}+\frac{dV_n^m}{dr_0}-\frac{V_n^m}{r_0}\Bigg\}\frac{P_n^m}{\sin\theta}-\Bigg\{\frac{dW_n^m}{dr_0}-\frac{W_n^m}{r_0}\Bigg\}\frac{dP_n^m}{d\theta}\\
&+\Bigg\{\frac{4im}{3r_0}\varepsilon V_n^m\frac{1}{\sin\theta}\frac{dP_n^m}{d\theta}-\frac{4im}{3r_0}\varepsilon V_n^m\frac{\cos\theta}{\sin^2\theta}P_n^m+\Bigg(-\frac{2}{3}\frac{d}{dr_0}(r_0\varepsilon)\frac{dW_n^m}{dr_0}\\
&-\frac{2}{3}r_0\varepsilon\frac{d^2W_n^m}{dr_0^2}+\frac{2}{3}\varepsilon\frac{dW_n^m}{dr_0}\Bigg)P_n^m+\frac{2}{3r_0}\varepsilon W_n^m\Bigg(-\frac{d^2P_n^m}{d\theta^2}+\cot\theta\frac{dP_n^m}{d\theta}
\end{aligned}$$

$$
\begin{aligned}
&- \frac{m^2}{\sin^2\theta} P_n^m \Big) \Big\} P_2^1 + \Big\{ im \Big(\frac{2}{3r_0} \varepsilon U_n^m + \frac{2}{3r_0} \frac{d}{dr_0} (r_0\varepsilon) U_n^m + \frac{4}{3} \frac{d}{dr_0} (r_0\varepsilon) \frac{dV_n^m}{dr_0} \\
&- \frac{2}{3r_0} \varepsilon V_n^m - \frac{2}{3r_0} \frac{d}{dr_0} (r_0\varepsilon) V_n^m \Big) \frac{P_n^m}{\sin\theta} - \Big(\frac{4}{3} \frac{d}{dr_0} (r_0\varepsilon) \frac{dW_n^m}{dr_0} - \frac{2}{3r_0} \varepsilon W_n^m \\
&- \frac{2}{3r_0} \frac{d}{dr_0} (r_0\varepsilon) W_n^m \Big) \frac{dP_n^m}{d\theta} \Big\} P_2 \Big] e^{im\phi}. \qquad (4.65)
\end{aligned}
$$

The dot product of $\mathbf{u}^*$ and $\nabla \cdot \tilde{\tau}_2$ is

$$
\mathbf{u}^* \cdot (\nabla \cdot \tilde{\tau}_2) = u_r^* \big\{ \nabla \cdot \tilde{\tau}_2 \big\}_r + u_\theta^* \big\{ \nabla \cdot \tilde{\tau}_2 \big\}_\phi + u_\phi^* \big\{ \nabla \cdot \tilde{\tau}_2 \big\}_\phi. \qquad (4.66)
$$

Using equations (4.17), and (4.63)-(4.65) in equation (4.66),

$$
\begin{aligned}
\mathbf{u}^* \cdot (\nabla \cdot \tilde{\tau}_2) = \sum_{q=|m|}^{N} \sum_{n=|m|}^{N} U_q^m \mu \Big[\Big\{ & 2 \frac{d^2 U_n^m}{dr_0^2} - n(n+1) U_n^m - 4 U_n^m + \frac{4}{r_0} \frac{dU_n^m}{dr_0} + \frac{2}{3r_0} \varepsilon \frac{dU_n^m}{dr_0} \\
& - n(n+1) \Big(\frac{1}{r_0} \frac{dV_n^m}{dr_0} - 3V_n^m \Big) + \frac{2}{3r_0} \Big(\frac{d}{dr_0} (r_0\varepsilon) \frac{dV_n^m}{dr_0} + r_0 \varepsilon \frac{dV_n^m}{dr_0^2} \\
& - 3\varepsilon \frac{dV_n^m}{dr_0} \Big) \Big\} P_n^m + \Big\{ \frac{8}{3} \frac{d}{dr_0} (r_0\varepsilon) \frac{d^2 U_n^m}{dr_0^2} + \frac{4}{3} \frac{d^2}{dr_0^2} (r_0\varepsilon) \frac{d^2}{dr_0^2} (r_0\varepsilon) \frac{dU_n^m}{dr_0} \\
& + \frac{8}{3r_0} \Big(- \frac{d}{dr_0} (r_0\varepsilon) \frac{dV_n^m}{dr_0} - r_0 \varepsilon \frac{d^2 V_n^m}{dr_0^2} + 3\varepsilon \frac{dV_n^m}{dr_0} \Big) - n(n+1) \\
& \times \Big(\frac{2}{3r_0} \frac{d}{dr_0} (r_0\varepsilon) \frac{dV_n^m}{dr_0} + \frac{2}{3r_0} \varepsilon \frac{dV_n^m}{dr_0} - 4\varepsilon V_n^m \Big) - \frac{4}{3} n(n+1) \varepsilon U_n^m \\
& + \frac{8}{3} \Big(\frac{1}{r_0} \frac{dU_n^m}{dr_0} - 2\varepsilon U_n^m \Big) \Big\} P_2 P_n^m + \frac{4}{3r_0} \Big\{ \varepsilon \frac{dU_n^m}{dr_0} + r_0 \varepsilon \frac{d^2 V_n^m}{d^2 r_0} \\
& + \frac{d}{dr_0} (r_0\varepsilon) \frac{dV_n^m}{dr_0} - 3\varepsilon \frac{dV_n^m}{dr_0} \Big\} P_2^1 \frac{dP_n^m}{d\theta} + \frac{2}{3r_0} \Big\{ \varepsilon \frac{dU_n^m}{dr_0} + r_0 \varepsilon \frac{d^2 V_n^m}{d^2 r_0} \\
& + \frac{d}{dr_0} (r_0\varepsilon) \frac{dV_n^m}{dr_0} - 3\varepsilon \frac{dV_n^m}{dr_0} \Big\} P_2^1 \cot\theta P_n^m \Big] P_q^m \\
& + \sum_{q=|m|}^{N} \sum_{n=|m|}^{N} U_q^m \frac{d\mu}{dr_0} \Big[2 \frac{dU_n^m}{dr_0} P_n^m + \frac{2}{3} \varepsilon \Big\{ \frac{U_n^m}{r_0} - \frac{V_n^m}{r_0} + \frac{dV_n^m}{dr_0} \Big\} P_2^1 \frac{dP_n^m}{d\theta} \\
& + \frac{8}{3} \frac{d}{dr_0} (r_0\varepsilon) \frac{dU_n^m}{dr_0} P_2 P_n^m + \frac{2im}{3} \varepsilon \Big\{ \frac{dW_n^m}{dr_0} - \frac{W_n^m}{r_0} \Big\} \frac{P_2^1}{\sin\theta} P_n^m \Big] P_q^m
\end{aligned}
$$

$$+\sum_{q=|m|}^{N}\sum_{n=|m|}^{N}\frac{dV_q^m}{dr_0}\left(\frac{2}{3}r_0\mu\varepsilon\right)\left[\left\{\frac{1}{r_0}\frac{dU_n^m}{dr_0}+\frac{4}{r_n^2}U_n^m+\frac{d^2V_n^m}{dr_0^2}+\frac{2}{r_0}\frac{dV_n^m}{dr_0}\right.\right.$$

$$\left.-\frac{2}{r_0^2}n(n+1)V_n^m\right\}P_2^1\frac{dP_n^m}{d\theta}P_q^m+im\left\{\frac{d^2W_n^m}{dr_0^2}+\frac{2}{r_0}\frac{dW_n^m}{dr_0}-\frac{n(n+1)}{r_0^2}W_n^m\right\}$$

$$\left.\times\frac{P_2^1}{\sin\theta}P_n^mP_q^m\right]+\sum_{q=|m|}^{N}\sum_{n=|m|}^{N}V_q^m\mu\left[\left\{\frac{1}{r_0}\frac{dU_n^m}{dr_0}+\frac{4}{r_n^2}U_n^m+\frac{d^2V_n^m}{dr_0^2}+\frac{2}{r_0}\frac{dV_n^m}{dr_0}\right.\right.$$

$$\left.-\frac{2}{r_0^2}n(n+1)V_n^m+\frac{4}{r_0}\varepsilon\frac{dV_n^m}{dr_0}\right\}\left(\frac{dP_n^m}{d\theta}\frac{dP_q^m}{d\theta}+\frac{m^2}{\sin^2\theta}P_n^mP_q^m\right)-\frac{8m^2}{r_0}\varepsilon\frac{dV_n^m}{dr_0}P_n^mP_q^m$$

$$+im\left\{\frac{d^2W_n^m}{dr_0^2}+\frac{2}{r_0}\frac{dW_n^m}{dr_0}-\frac{n(n+1)}{r_0^2}W_n^m\right\}\left(\frac{P_n^m}{\sin\theta}\frac{dP_q^m}{d\theta}+\frac{P_q^m}{\sin\theta}\frac{dP_n^m}{d\theta}\right)$$

$$+\frac{4im}{r_0}\varepsilon\frac{dW_n^m}{dr_0}\sin\theta\frac{dP_n^m}{d\theta}P_q^m+\left\{\left(\frac{2}{3}\varepsilon\frac{d^2U_n^m}{dr_0^2}+\frac{2}{3r_0}\frac{d}{dr_0}(r_0\varepsilon)\frac{dU_n^m}{dr_0}+\frac{4}{3r_0}\varepsilon\frac{dU_n^m}{dr_0}\right.\right.$$

$$+\frac{2}{3}\frac{d^2}{dr_0^2}(r_0\varepsilon)\frac{dV_n^m}{dr_0}+\frac{4}{3}\frac{d}{dr_0}(r_0\varepsilon)\frac{d^2V_n^m}{dr_0^2}+\frac{4}{3}\varepsilon\frac{d^2V_n^m}{dr_0^2}+\frac{2}{3}r_0\varepsilon\frac{d^3V_n^m}{dr_0^3}$$

$$\left.-\frac{20}{3r_0}\varepsilon\frac{dV_n^m}{dr_0}+\frac{4}{3r_0}\frac{d}{dr_0}(r_0\varepsilon)\frac{dV_n^m}{dr_0}\right)\frac{dP_q^m}{d\theta}P_n^m-\frac{4}{3r_0}\varepsilon\frac{dV_n^m}{dr_0}\cot\theta\left(\frac{dP_n^m}{d\theta}\frac{dP_q^m}{d\theta}\right.$$

$$\left.+\frac{m^2}{\sin^2\theta}P_n^mP_q^m\right)-\frac{4}{r_0}n(n+1)\varepsilon\frac{dV_n^m}{dr_0}\frac{dP_q^m}{d\theta}P_n^m-\frac{4}{3r_0}\varepsilon\frac{dV_n^m}{dr_0}\frac{dP_q^m}{d\theta}P_n^m$$

$$-\frac{4}{3r_0}\varepsilon\frac{dV_n^m}{dr_0}\frac{m^2}{\sin^2\theta}\left(P_n^m\frac{dP_q^m}{d\theta}+P_q^m\frac{dP_n^m}{d\theta}\right)-im\left(-\frac{2}{3}\frac{d^2}{dr_0^2}(r_0\varepsilon)\frac{dW_n^m}{dr_0}-\frac{4}{3}\varepsilon\frac{d^2W_n^m}{dr_0^2}\right.$$

$$-\frac{4}{3}\frac{d}{dr_0}(r_0\varepsilon)\frac{d^2W_n^m}{dr_0^2}-\frac{2}{3}r_0\varepsilon\frac{d^3W_n^m}{dr_0^3}+\frac{10}{3r_0}\varepsilon\frac{dW_n^m}{dr_0}-\frac{4}{3r_0}\frac{d}{dr_0}(r_0\varepsilon)\frac{dW_n^m}{dr_0}\left.\right)\frac{P_n^m}{\sin\theta}P_q^m$$

$$+\frac{4im}{3r_0}\varepsilon\frac{dW_n^m}{dr_0}\frac{1}{\sin\theta}\left(\frac{dP_n^m}{d\theta}\frac{dP_q^m}{d\theta}+\frac{m^2}{\sin^2\theta}P_n^mP_q^m\right)-\frac{2im}{3r_0}\varepsilon\frac{dW_n^m}{dr_0}\frac{P_n^m}{\sin\theta}P_q^m$$

$$\left.-\frac{2im}{r_0}\varepsilon n(n+1)\frac{dW_n^m}{dr_0}\frac{P_n^m}{\sin\theta}P_q^m\right\}P_2^1+\left\{\left(\frac{2}{3r_0}\varepsilon\frac{dU_n^m}{dr_0}+\frac{2}{3r_0}\frac{d}{dr_0}(r_0\varepsilon)\frac{dU_n^m}{dr_0}\right.\right.$$

$$+\frac{16}{3r_0^2}\varepsilon U_n^m+\frac{2}{3}\frac{d^2}{dr_0^2}(r_0\varepsilon)\frac{dV_n^m}{dr_0}+\frac{4}{3}\frac{d}{dr_0}(r_0\varepsilon)\frac{d^2V_n^m}{dr_0^2}+\frac{4}{3r_0}\frac{d}{dr_0}(r_0\varepsilon)\frac{dV_n^m}{dr_0}$$

$$\left.-\frac{44}{3r_0}\varepsilon\frac{dV_n^m}{dr_0}-\frac{8}{3r_0^2}n(n+1)\varepsilon V_n^m\right)\left(\frac{dP_n^m}{d\theta}\frac{dP_q^m}{d\theta}+\frac{m^2}{\sin^2\theta}P_n^mP_q^m\right)$$

$$-\frac{16}{3r_0}\varepsilon\frac{dV_n^m}{dr_0}\cot\theta P_n^m+im\left(\frac{2}{3}\frac{d^2}{dr_0^2}(r_0\varepsilon)\frac{dW_n^m}{dr_0}+\frac{4}{3}\frac{d}{dr_0}(r_0\varepsilon)\frac{d^2W_n^m}{dr_0^2}\right.$$

$$+\frac{4}{3r_0}\frac{d}{dr_0}(r_0\varepsilon)\frac{dW_n^m}{dr_0}-\frac{8}{3r_0}\varepsilon\frac{dW_n^m}{dr_0}-\frac{4}{3r_0^2}n(n+1)\varepsilon W_n^m\Bigg)$$

$$\times\left(\frac{P_n^m}{\sin\theta}\frac{dP_q^m}{d\theta}+\frac{P_q^m}{\sin\theta}\frac{dP_n^m}{d\theta}\right)\Bigg\}P_2\Bigg]+\sum_{q=|m|}^{N}\sum_{n=|m|}^{N}\frac{dV_q^m}{dr_0}\left(\frac{2}{3}\frac{d\mu}{dr_0}r_0\varepsilon\right)$$

$$\times\left[\left\{\frac{U_n^m}{r_0}+\frac{dV_n^m}{dr_0}-\frac{V_n^m}{r_0}\right\}P_2^1\frac{dP_n^m}{d\theta}+im\left\{\frac{dW_n^m}{dr_0}-\frac{W_n^m}{r_0}\right\}\frac{P_2^1}{\sin\theta}P_n^mP_q^m\right]$$

$$+\sum_{q=|m|}^{N}\sum_{n=|m|}^{N}V_q^m\frac{d\mu}{dr_0}\left[\left\{\frac{U_n^m}{r_0}+\frac{dV_n^m}{dr_0}-\frac{V_n^m}{r_0}\right\}\left(\frac{dP_n^m}{d\theta}\frac{dP_q^m}{d\theta}+\frac{m^2}{\sin^2\theta}P_n^mP_q^m\right)\right.$$

$$+im\left\{\frac{dW_n^m}{dr_0}-\frac{W_n^m}{r_0}\right\}\left(\frac{P_n^m}{\sin\theta}\frac{dP_q^m}{d\theta}+\frac{P_q^m}{\sin\theta}\frac{dP_n^m}{d\theta}\right)+\left\{\left(\frac{2}{3}\varepsilon\frac{dU_n^m}{dr_0}+\frac{4}{3r_0}\varepsilon U_n^m\right.\right.$$

$$+\frac{2}{3}\frac{d}{dr_0}(r_0\varepsilon)\frac{dV_n^m}{dr_0}+\frac{2}{3}r_0\varepsilon\frac{d^2V_n^m}{dr_0^2}-\frac{2}{3}\varepsilon\frac{dV_n^m}{dr_0}\Bigg)P_n^m\frac{dP_q^m}{d\theta}-\frac{4}{3r_0}\varepsilon V_n^m\cot\theta$$

$$\times\left(\frac{dP_n^m}{d\theta}\frac{dP_q^m}{d\theta}+\frac{m^2}{\sin^2\theta}P_n^mP_q^m\right)+\frac{4}{3r_0}\varepsilon V_n^m\frac{m^2}{\sin^2\theta}\left(\frac{dP_n^m}{d\theta}P_q^m+\frac{dP_q^m}{d\theta}P_n^m\right)$$

$$-\frac{4}{3r_0}n(n+1)\varepsilon V_n^mP_n^m\frac{dP_q^m}{d\theta}-im\Bigg(-\frac{2}{3}\frac{d}{dr_0}(r_0\varepsilon)\frac{dW_n^m}{dr_0}-\frac{2}{3}r_0\varepsilon\frac{d^2W_n^m}{dr_0^2}$$

$$+\frac{2}{3}\varepsilon\frac{dW_n^m}{dr_0}\Bigg)\frac{P_n^m}{\sin\theta}P_q^m+\frac{4im}{3r_0}\varepsilon W_n^m\frac{1}{\sin\theta}\left(\frac{dP_n^m}{d\theta}\frac{dP_q^m}{d\theta}+\frac{m^2}{\sin^2\theta}P_n^mP_q^m\right)$$

$$-\frac{2im}{3r_0}n(n+1)\varepsilon W_n^m\frac{P_n^m}{\sin\theta}P_q^m-\frac{4im}{3r_0}\varepsilon W_n^m\frac{\cos\theta}{\sin\theta}\left(\frac{dP_n^m}{d\theta}P_q^m+\frac{dP_q^m}{d\theta}P_n^m\right)\Bigg\}P_2^1$$

$$+\Bigg\{\Bigg(\frac{2}{3r_0}\varepsilon U_n^m+\frac{2}{3r_0}\frac{d}{dr_0}(r_0\varepsilon)U_n^m+\frac{4}{3}\frac{d}{dr_0}(r_0\varepsilon)\frac{dV_n^m}{dr_0}-\frac{2}{3r_0}\varepsilon V_n^m$$

$$-\frac{2}{3r_0}\frac{d}{dr_0}(r_0\varepsilon)V_n^m\Bigg)\left(\frac{dP_n^m}{d\theta}\frac{dP_q^m}{d\theta}+\frac{m^2}{\sin^2\theta}P_n^mP_q^m\right)+im\Bigg(\frac{4}{3}\frac{d}{dr_0}(r_0\varepsilon)\frac{dW_n^m}{dr_0}$$

$$-\frac{2}{3r_0}\varepsilon W_n^m-\frac{2}{3r_0}\frac{d}{dr_0}(r_0\varepsilon)W_n^m\Bigg)\left(\frac{P_n^m}{\sin\theta}\frac{dP_q^m}{d\theta}+\frac{P_q^m}{\sin\theta}\frac{dP_n^m}{d\theta}\right)\Bigg\}P_2\Bigg]$$

$$+\sum_{q=|m|}^{N}\sum_{n=|m|}^{N}\frac{dW_q^m}{dr_0}\left(\frac{2}{3}r_0\varepsilon\mu\right)\Bigg[-im\left\{\frac{1}{r_0}\frac{dU_n^m}{dr_0}+\frac{4}{r_n^2}U_n^m+\frac{d^2V_n^m}{dr_0^2}+\frac{2}{r_0}\frac{dV_n^m}{dr_0}\right.$$

$$-\frac{2}{r_0^2}n(n+1)V_n^m\Bigg\}\frac{P_2^1}{\sin\theta}P_n^mP_q^m+\left\{\frac{d^2W_n^m}{dr_0^2}+\frac{2}{r_0}\frac{dW_n^m}{dr_0}-\frac{n(n+1)}{r_0^2}W_n^m\right\}P_2^1\frac{dP_n^m}{d\theta}P_q^m\Bigg]$$

$$+\sum_{q=|m|}^{N}\sum_{n=|m|}^{N}W_q^m\mu\Bigg[-im\left\{\frac{1}{r_0}\frac{dU_n^m}{dr_0}+\frac{4}{r_n^2}U_n^m+\frac{d^2V_n^m}{dr_0^2}+\frac{2}{r_0}\frac{dV_n^m}{dr_0}-\frac{2}{r_0^2}n(n+1)V_n^m\right.$$

$$+\frac{4}{r_0}\varepsilon\frac{dV_n^m}{dr_0}++\frac{4}{3r_0}\varepsilon\frac{dV_n^m}{dr_0}-\frac{2}{r_0^2}n(n+1)\varepsilon V_n^m\Bigg\}\left(\frac{P_n^m}{\sin\theta}\frac{dP_q^m}{d\theta}+\frac{P_q^m}{\sin\theta}\frac{dP_n^m}{d\theta}\right)$$

$$+\frac{8im}{r_0}\varepsilon\frac{dV_n^m}{dr_0}\sin\theta\frac{dP_q^m}{d\theta}P_n^m+\left\{\frac{d^2W_n^m}{dr_0^2}+\frac{2}{r_0}\frac{dW_n^m}{dr_0}-\frac{n(n+1)}{r_0^2}W_n^m+\frac{10}{3r_0}\varepsilon\frac{dW_n^m}{dr_0}\right\}$$

$$\times\left(\frac{dP_n^m}{d\theta}\frac{dP_q^m}{d\theta}+\frac{m^2}{\sin^2\theta}P_n^mP_q^m\right)-\frac{4m^2}{r_0}\varepsilon\frac{dW_n^m}{dr_0}P_n^mP_q^m+\left\{-im\left(\frac{2}{3}\varepsilon\frac{d^2U_n^m}{dr_0^2}\right.\right.$$

$$+\frac{2}{3r_0}\frac{d}{dr_0}(r_0\varepsilon)\frac{dU_n^m}{dr_0}+\frac{4}{3r_0}\varepsilon\frac{dU_n^m}{dr_0}+\frac{2}{3}\frac{d^2}{dr_0^2}(r_0\varepsilon)\frac{dV_n^m}{dr_0}+\frac{4}{3}\frac{d}{dr_0}(r_0\varepsilon)\frac{d^2V_n^m}{dr_0^2}$$

$$+\frac{4}{3}\varepsilon\frac{d^2V_n^m}{dr_0^2}+\frac{2}{3}r_0\varepsilon\frac{d^3V_n^m}{dr_0^3}-\frac{20}{3r_0}\varepsilon\frac{dV_n^m}{dr_0}+\frac{4}{3r_0}\frac{d}{dr_0}(r_0\varepsilon)\frac{dV_n^m}{dr_0}-\frac{4}{3r_0}\varepsilon\frac{dV_n^m}{dr_0}$$

$$\left.-\frac{4}{r_0}n(n+1)\varepsilon\frac{dV_n^m}{dr_0}\right)\frac{1}{\sin\theta}P_n^mP_q^m-\frac{8im}{3r_0}\varepsilon\frac{dV_n^m}{dr_0}\frac{1}{\sin\theta}\left(\frac{dP_n^m}{d\theta}\frac{dP_q^m}{d\theta}+\frac{m^2}{\sin^2\theta}P_n^mP_q^m\right)$$

$$-\left(-\frac{2}{3}\frac{d^2}{dr_0^2}(r_0\varepsilon)\frac{dW_n^m}{dr_0}-\frac{4}{3}\frac{d}{dr_0}(r_0\varepsilon)\frac{d^2W_n^m}{dr_0^2}-\frac{4}{3}\varepsilon\frac{d^2W_n^m}{dr_0^2}-\frac{2}{3}r_0\varepsilon\frac{d^3W_n^m}{dr_0^3}\right.$$

$$\left.+\frac{10}{3r_0}\varepsilon\frac{dW_n^m}{dr_0}-\frac{4}{3r_0}\frac{d}{dr_0}(r_0\varepsilon)\frac{dW_n^m}{dr_0}+\frac{2}{3r_0}\varepsilon\frac{dW_n^m}{dr_0}+\frac{2}{r_0}n(n+1)\varepsilon\frac{dW_n^m}{dr_0}\right)\frac{dP_q^m}{d\theta}P_n^m$$

$$+\frac{4}{3r_0}\varepsilon\frac{dW_n^m}{dr_0}\frac{m^2}{\sin^2\theta}\left(P_n^m\frac{dP_q^m}{d\theta}+P_q^m\frac{dP_n^m}{d\theta}\right)+\frac{2}{3r_0}\varepsilon\frac{dW_n^m}{dr_0}$$

$$\left.\times\cot\theta\left(\frac{dP_n^m}{d\theta}\frac{dP_n^m}{d\theta}+\frac{m^2}{\sin^2\theta}P_n^mP_q^m\right)\right\}P_2^1$$

$$+\left\{-im\left(\frac{2}{3r_0}\varepsilon\frac{dU_n^m}{dr_0}+\frac{2}{3r_0}\frac{d}{dr_0}(r_0\varepsilon)\frac{dU_n^m}{dr_0}+\frac{16}{3r_0^2}\varepsilon U_n^m+\frac{2}{3}\frac{d^2}{dr_0^2}(r_0\varepsilon)\frac{dV_n^m}{dr_0}\right.\right.$$

$$\left.+\frac{4}{3}\frac{d}{dr_0}(r_0\varepsilon)\frac{d^2V_n^m}{dr_0^2}+\frac{4}{3r_0}\frac{d}{dr_0}(r_0\varepsilon)\frac{dV_n^m}{dr_0}-\frac{4}{r_0}\varepsilon\frac{dV_n^m}{dr_0}-\frac{8}{3r_0^2}n(n+1)\varepsilon V_n^m\right)$$

$$\times\left(\frac{P_n^m}{\sin\theta}\frac{dP_q^m}{d\theta}+\frac{P_q^m}{\sin\theta}\frac{dP_n^m}{d\theta}\right)-\frac{8im}{3r_0}\varepsilon\frac{dV_n^m}{dr_0}\left(\frac{P_n^m}{\sin\theta}\frac{dP_q^m}{d\theta}+\frac{P_q^m}{\sin\theta}\frac{dP_n^m}{d\theta}\right)$$

$$-\left(-\frac{2}{3}\frac{d^2}{dr_0^2}(r_0\varepsilon)\frac{dW_n^m}{dr_0}-\frac{4}{3}\frac{d}{dr_0}(r_0\varepsilon)\frac{d^2W_n^m}{dr_0^2}-\frac{4}{3r_0}\frac{d}{dr_0}(r_0\varepsilon)\frac{dW_n^m}{dr_0}\right.$$

$$\left.\left.+\frac{4}{r_0}\varepsilon\frac{dW_n^m}{dr_0}+\frac{4}{3r_0^2}n(n+1)\varepsilon W_n^m\right)\left(\frac{dP_n^m}{d\theta}\frac{dP_q^m}{d\theta}+\frac{m^2}{\sin^2\theta}P_n^mP_q^m\right)\right\}P_2\Bigg]$$

$$+\sum_{q=|m|}^{N}\sum_{n=|m|}^{N}\frac{dW_q^m}{dr_0}\left(\frac{2}{3}r_0\varepsilon\frac{d\mu}{dr_0}\right)\Bigg[-im\left\{\frac{U_n^m}{r_0}+\frac{dV_n^m}{dr_0}-\frac{V_n^m}{r_0}\right\}\frac{P_2^1}{\sin\theta}P_n^mP_q^m$$

$$+\left\{\frac{dW_n^m}{dr_0}-\frac{W_n^m}{r_0}\right\}P_2^1\frac{dP_n^m}{d\theta}P_q^m\Bigg]+\sum_{q=|m|}^{N}\sum_{n=|m|}^{N}W_q^m\frac{d\mu}{dr_0}\Bigg[-im\Bigg\{\frac{U_n^m}{r_0}+\frac{dV_n^m}{dr_0}$$
$$-\frac{V_n^m}{r_0}\Bigg\}\left(\frac{P_n^m}{\sin\theta}\frac{dP_q^m}{d\theta}+\frac{P_q^m}{\sin\theta}\frac{dP_n^m}{d\theta}\right)+\left\{\frac{dW_n^m}{dr_0}-\frac{W_n^m}{r_0}\right\}\left(\frac{dP_n^m}{d\theta}\frac{dP_q^m}{d\theta}$$
$$+\frac{m^2}{\sin^2\theta}P_n^mP_q^m\right)-im\Bigg\{\left(\frac{2}{3}\varepsilon\frac{dU_n^m}{dr_0}+\frac{4}{3r_0}\varepsilon U_n^m+\frac{2}{3}\frac{d}{dr_0}(r_0\varepsilon)\frac{dV_n^m}{dr_0}\right.$$
$$\left.+\frac{2}{3}r_0\varepsilon\frac{d^2V_n^m}{dr_0^2}-\frac{2}{3}\varepsilon\frac{dV_n^m}{dr_0}-\frac{4}{3r_0}n(n+1)\varepsilon V_n^m\right)\frac{P_n^m}{\sin\theta}P_q^m+\frac{4im}{3r_0}\varepsilon V_n^m$$
$$\times\cot\theta\left(\frac{P_q^m}{\sin\theta}\frac{dP_n^m}{d\theta}+\frac{P_n^m}{\sin\theta}\frac{dP_q^m}{d\theta}\right)-\frac{4im}{3r_0}\varepsilon V_n^m\frac{1}{\sin\theta}\left(\frac{dP_n^m}{d\theta}\frac{dP_q^m}{d\theta}+\frac{m^2}{\sin^2\theta}P_n^mP_q^m\right)$$
$$-\left(-\frac{2}{3}\frac{d}{dr_0}(r_0\varepsilon)\frac{dW_n^m}{dr_0}-\frac{2}{3}r_0\varepsilon\frac{d^2W_n^m}{dr_0^2}+\frac{2}{3}\varepsilon\frac{dW_n^m}{dr_0}\right)P_n^m\frac{dP_q^m}{d\theta}$$
$$-\frac{2}{3r_0}n(n+1)\varepsilon W_n^mP_n^m\frac{dP_n^m}{d\theta}+\frac{4}{3r_0}\varepsilon W_n^m\frac{m^2}{\sin\theta}\left(\frac{P_q^m}{\sin\theta}\frac{dP_n^m}{d\theta}+\frac{P_n^m}{\sin\theta}\frac{dP_q^m}{d\theta}\right)$$
$$-\frac{4}{3r_0}\varepsilon W_n^m\cot\theta\left(\frac{dP_n^m}{d\theta}\frac{dP_q^m}{d\theta}+\frac{m^2}{\sin^2\theta}P_n^m\right)\Bigg\}P_2^1$$
$$+\Bigg\{-im\left(\frac{2}{3r_0}\varepsilon U_n^m+\frac{2}{3r_0}\frac{d}{dr_0}(r_0\varepsilon)U_n^m+\frac{4}{3}\frac{d}{dr_0}(r_0\varepsilon)\frac{dV_n^m}{dr_0}-\frac{2}{3r_0}\varepsilon V_n^m\right.$$
$$\left.-\frac{2}{3r_0}\frac{d}{dr_0}(r_0\varepsilon)V_n^m\right)\left(\frac{P_q^m}{\sin\theta}\frac{dP_n^m}{d\theta}+\frac{P_n^m}{\sin\theta}\frac{dP_q^m}{d\theta}\right)+\left(\frac{4}{3}\frac{d}{dr_0}(r_0\varepsilon)\frac{dW_n^m}{dr_0}\right.$$
$$\left.-\frac{2}{3r_0}\varepsilon W_n^m-\frac{2}{3r_0}\frac{d}{dr_0}(r_0\varepsilon)W_n^m\right)\left(\frac{dP_n^m}{d\theta}\frac{dP_q^m}{d\theta}+\frac{m^2}{\sin^2\theta}P_n^mP_q^m\right)\Bigg\}P_2\Bigg]. \tag{4.67}$$

The normal component of the stress tensor $\tilde{\tau}_2$ is given as

$$\hat{\mathbf{n}}\cdot\tilde{\tau}_2=\left(\hat{\mathbf{r}}+\frac{2}{3}\varepsilon P_2^1\hat{\theta}\right)\cdot\Big\{(\tau_2)_{rr}\hat{r}\hat{r}+(\tau_2)_{r\theta}\hat{r}\hat{\theta}+(\tau_2)_{r\phi}\hat{r}\hat{\phi}+(\tau_2)_{\theta r}\hat{\theta}\hat{r}$$
$$+(\tau_2)_{\theta\theta}\hat{\theta}\hat{\theta}+(\tau_2)_{\theta\phi}\hat{\theta}\hat{\phi}+(\tau_2)_{\phi r}\hat{\phi}\hat{r}+(\tau_2)_{\phi\theta}\hat{\phi}\hat{\theta}+(\tau_2)_{\phi\phi}\hat{\phi}\hat{\phi},$$
$$=\left((\tau_2)_{rr}+\frac{2}{3}\varepsilon P_2^1(\tau_2)_{\theta r}\right)\hat{r}+\left((\tau_2)_{r\theta}+\frac{2}{3}\varepsilon P_2^1(\tau_2)_{\theta\theta}\right)\hat{\theta}$$
$$+\left((\tau_2)_{r\phi}+\frac{2}{3}\varepsilon P_2^1(\tau_2)_{\theta\phi}\right)\hat{\phi}. \tag{4.68}$$

The dot product of $\hat{\mathbf{n}}\cdot\tilde{\tau}_2$ and $\mathbf{u}^*$ is expressed by

$$\hat{\mathbf{n}}\cdot\tilde{\tau}_2\cdot\mathbf{u}^* = \left((\tau_2)_{rr}+\frac{2}{3}\varepsilon P_2^1(\tau_2)_{\theta r}\right)u_r^* + \left((\tau_2)_{r\theta}+\frac{2}{3}\varepsilon P_2^1(\tau_2)_{\theta\theta}\right)u_\theta^* + \left((\tau_2)_{r\phi}+\frac{2}{3}\varepsilon P_2^1(\tau_2)_{\theta\phi}\right)u_\phi^*. \tag{4.69}$$

Using equations (4.17), (4.56)-(4.61) in (4.69), we get

$$\begin{aligned}
\hat{\mathbf{n}}\cdot\tilde{\tau}_2\cdot\mathbf{u}^* = \sum_{q=|m|}^{N}\sum_{n=|m|}^{N}\Bigg[& 2\mu U_q^m\Bigg\{\frac{dU_n^m}{dr_0}P_n^m+\frac{2}{3}\frac{d}{dr_0}(r_0\varepsilon)\frac{dU_n^m}{dr_0}P_2P_n^m-2im\varepsilon\left(\frac{dW_n^m}{dr_0}-\frac{1}{r_0}W_n^m\right)\\
& \times\cos\theta P_n^m+\frac{2}{3}\varepsilon\left(\frac{dV_n^m}{dr_0}-\frac{1}{r_0}V_n^m-\frac{1}{r_0}U_n^m\right)P_2^1\frac{dP_n^m}{d\theta}\Bigg\}P_q^m+\frac{dV_q^m}{dr_0}\frac{\mu\varepsilon}{r_0}\Bigg\{-2im\Bigg(\frac{dW_n^m}{dr_0}\\
& -\frac{1}{r_0}W_n^m\Bigg)\cos\theta P_n^m+\frac{2}{3}\left(\frac{dV_n^m}{dr_0}-\frac{1}{r_0}V_n^m-\frac{1}{r_0}U_n^m\right)P_2^1\frac{dP_n^m}{d\theta}\Bigg\}P_q^m+V_q^m\mu\Bigg\{\frac{2}{3}\Bigg(\varepsilon\frac{dU_n^m}{dr_0}\\
& +\frac{2\varepsilon}{r_0}U_n^m+r_0\varepsilon\frac{d^2V_n^m}{dr_0^2}+\frac{d}{dr_0}(r_0\varepsilon)\frac{dV_n^m}{dr_0}-\varepsilon\frac{dV_n^m}{dr_0}\Bigg)P_2^1\frac{dP_q^m}{d\theta}P_n^m+\Bigg(\frac{U_n^m}{r_0}+\frac{dV_n^m}{dr_0}\\
& -\frac{V_n^m}{r_0}\Bigg)\left(\frac{dP_n^m}{d\theta}\frac{dP_q^m}{d\theta}+\frac{m^2}{\sin^2\theta}P_n^mP_q^m\right)+\frac{2}{3}\left(\frac{\varepsilon}{r_0}U_n^m+\frac{d}{dr_0}(r_0\varepsilon)\frac{dV_n^m}{dr_0}-\frac{\varepsilon}{r_0}V_n^m\right)\\
& \times\left(\frac{dP_n^m}{d\theta}\frac{dP_q^m}{d\theta}+\frac{m^2}{\sin^2\theta}P_n^mP_q^m\right)P_2+im\left(\frac{dW_n^m}{dr_0}-\frac{1}{r_0}W_n^m\right)\left(\frac{P_n^m}{\sin\theta}\frac{dP_q^m}{d\theta}+\frac{P_q^m}{\sin\theta}\frac{dP_n^m}{d\theta}\right)\\
& +\frac{2im}{3}\left(\frac{d}{dr_0}(r_0\varepsilon)\frac{dW_n^m}{dr_0}-\frac{\varepsilon}{r_0}W_n^m\right)\left(\frac{P_n^m}{\sin\theta}\frac{dP_q^m}{d\theta}+\frac{P_q^m}{\sin\theta}\frac{dP_n^m}{d\theta}\right)P_2\\
& +\frac{2im}{3}\left(\frac{d}{dr_0}(r_0\varepsilon)\frac{dW_n^m}{dr_0}+r_0\varepsilon\frac{d^2W_n^m}{dr_0^2}-\varepsilon\frac{dW_n^m}{dr_0}\right)\frac{P_2^1}{\sin\theta}P_n^mP_q^m-\frac{4}{3r_0}\varepsilon V_n^m\\
& \times\cot\theta\left(\frac{dP_n^m}{d\theta}\frac{dP_q^m}{d\theta}+\frac{m^2}{\sin^2\theta}P_n^mP_q^m\right)P_2^1-\frac{4}{3r_0}n(n+1)\varepsilon V_n^mP_n^m\frac{dP_q^m}{d\theta}P_2^1+\frac{4}{3r_0}\varepsilon V_n^m\\
& \times\frac{m^2}{\sin\theta}\left(\frac{P_n^m}{\sin\theta}\frac{dP_q^m}{d\theta}+\frac{P_q^m}{\sin\theta}\frac{dP_n^m}{d\theta}\right)P_2^1-\frac{4im}{3r_0}\varepsilon W_n^m\cot\theta\left(\frac{P_n^m}{\sin\theta}\frac{dP_q^m}{d\theta}+\frac{P_q^m}{\sin\theta}\frac{dP_n^m}{d\theta}\right)P_2^1\\
& -\frac{2im}{3r_0}n(n+1)\varepsilon W_n^m\frac{P_2^1}{\sin\theta}P_n^mP_q^m+\frac{4im}{3r_0}\varepsilon W_n^m\left(\frac{dP_n^m}{d\theta}\frac{dP_q^m}{d\theta}+\frac{m^2}{\sin^2\theta}P_n^mP_q^m\right)\frac{P_2^1}{\sin\theta}\Bigg\}\\
& +\frac{dW_q^m}{dr_0}\frac{2\mu\varepsilon}{3}\Bigg\{-im\left(U_n^m+r_0\frac{dV_n^m}{dr_0}-V_n^m\right)\frac{P_2^1}{\sin\theta}P_n^mP_q^m+\left(r_0\frac{dW_n^m}{dr_0}-W_n^m\right)P_2^1\frac{dP_n^m}{d\theta}P_q^m\Bigg\}
\end{aligned}$$

$$+W_q^m\mu\Bigg\{im\Bigg(-\frac{U_n^m}{r_0}-\frac{dV_n^m}{dr_0}+\frac{V_n^m}{r_0}\Bigg)\Bigg(\frac{P_n^m}{\sin\theta}\frac{dP_q^m}{d\theta}+\frac{P_q^m}{\sin\theta}\frac{dP_n^m}{d\theta}\Bigg)-\frac{2im}{3}\Bigg(\varepsilon\frac{dU_n^m}{dr_0}$$
$$+\frac{2}{r_0}\varepsilon U_n^m+r_0\varepsilon\frac{d^2V_n^m}{dr_0^2}+\frac{d}{dr_0}(r_0\varepsilon)\frac{dV_n^m}{dr_0}-\varepsilon\frac{dV_n^m}{dr_0}\Bigg)\frac{P_2^1}{\sin\theta}P_n^mP_q^m+\frac{2im}{3}\Bigg(-\frac{\varepsilon U_n^m}{r_0}$$
$$-\frac{d}{dr_0}(r_0\varepsilon)\frac{dV_n^m}{dr_0}+\frac{\varepsilon V_n^m}{r_0}\Bigg)\Bigg(\frac{P_n^m}{\sin\theta}\frac{dP_q^m}{d\theta}+\frac{P_q^m}{\sin\theta}\frac{dP_n^m}{d\theta}\Bigg)P_2+\Bigg(\frac{dW_n^m}{dr_0}-\frac{W_n^m}{r_0}\Bigg)$$
$$\times\Bigg(\frac{dP_n^m}{d\theta}\frac{dP_q^m}{d\theta}+\frac{m^2}{\sin^2\theta}P_n^mP_q^m\Bigg)+\frac{2}{3}\Bigg(\frac{d}{dr_0}(r_0\varepsilon)\frac{dW_n^m}{dr_0}-\frac{\varepsilon W_n^m}{r_0}\Bigg)\Bigg(\frac{dP_n^m}{d\theta}\frac{dP_q^m}{d\theta}$$
$$+\frac{m^2}{\sin^2\theta}P_n^mP_q^m\Bigg)P_2+\frac{2}{3}\Bigg(r_0\varepsilon\frac{d^2W_n^m}{dr_0^2}+\frac{d}{dr_0}(r_0\varepsilon)\frac{dW_n^m}{dr_0}-\varepsilon\frac{dW_n^m}{dr_0}\Bigg)P_2^1\frac{dP_q^m}{d\theta}P_n^m$$
$$-\frac{4im}{r_0}\varepsilon V_n^m\cos^2\theta\Bigg(\frac{P_n^m}{\sin\theta}\frac{dP_q^m}{d\theta}+\frac{P_q^m}{\sin\theta}\frac{dP_n^m}{d\theta}\Bigg)-\frac{4im}{r_0}n(n+1)\varepsilon V_n^m\cos\theta P_n^mP_q^m$$
$$+\frac{4im}{r_0}\varepsilon V_n^m\cos\theta\Bigg(\frac{dP_n^m}{d\theta}\frac{dP_q^m}{d\theta}+\frac{m^2}{\sin^2\theta}P_n^mP_q^m\Bigg)+\frac{4m^2}{3r_0}\varepsilon W_n^m\Bigg(\frac{P_n^m}{\sin\theta}\frac{dP_q^m}{d\theta}+\frac{P_q^m}{\sin\theta}\frac{dP_n^m}{d\theta}\Bigg)$$
$$\times\frac{P_2^1}{\sin\theta}+\frac{4}{r_0}\varepsilon W_n^m\cos^2\theta\Bigg(\frac{dP_n^m}{d\theta}\frac{dP_q^m}{d\theta}+\frac{m^2}{\sin^2\theta}P_n^mP_q^m\Bigg)$$
$$-\frac{2}{3r_0}n(n+1)\varepsilon W_n^mP_2^1\frac{dP_q^m}{d\theta}P_n^m\Bigg\}\Bigg]. \tag{4.70}$$

4.4 Boundary Conditions at the Earth's Surface in the Clairaut Coordinate System

In subsection 2.4.3, we mentioned that the normal component of the stress tensor $\hat{\mathbf{n}}\cdot\tilde{\tau}_4$ vanishes; and the gravitational potential $(V_1)_4$ and gravitational flux $\hat{n}\cdot\nabla(V_1)_4$ outside the Earth ($r>R$) are continuous. In the region $r>R$, Poisson's equation reduces to Laplace's equation. Recall that the gravitational potential (Eq. (2.37)) in the spherical coordinate system is

$$(V_1)_4(r)=\sum_{n=|m|}^{N_k}A_n^mr^{-(n+1)}Y_n^m(\theta,\phi), \tag{4.71}$$

where A_n^m are constants.

Using equation (4.1) in (4.71) and applying a Taylor expansion up to the first order in

ε, the gravitational potential in the Clairaut coordinate system is

$$(V_1)_4(r) = \sum_{n=|m|}^{N_k} A_n^m r_0^{-(n+1)} \left(1 + \frac{2}{3}(n+1)\varepsilon P_2\right) Y_n^m(\theta,\phi) \tag{4.72}$$

correct to the first order in ε [87].

Using equations (4.5)-(4.7) in (4.29), the gradient of the gravitational potential V_1 in the Clairaut coordinate system is

$$\begin{aligned} \nabla V_1 &= \hat{\mathbf{r}}\left(1 + \frac{2}{3}\frac{d}{dr_0}(r_0\varepsilon)P_2\right)\frac{\partial V_1}{\partial r_0} + \hat{\theta}\frac{1}{r_0}\left(\frac{2}{3}r_0\varepsilon P_2^1\frac{\partial}{\partial r_0} + \frac{\partial}{\partial\theta} + \frac{2}{3}\varepsilon P_2\frac{\partial}{\partial\theta}\right)V_1 \\ &\quad + \hat{\phi}\frac{1}{r_0\sin\theta}\left(1 + \frac{2}{3}\varepsilon P_2\right)\frac{\partial V_1}{\partial\phi}, \end{aligned} \tag{4.73}$$

correct to the first order in ε [87].

Using equation (4.9) in equation (4.73), the gravitational flux is expressed as

$$\hat{\mathbf{n}}\cdot\nabla V_1 = \left(1 + \frac{2}{3}\frac{d}{dr_0}(r_0\varepsilon)P_2\right)\frac{\partial V_1}{\partial r_0} + \frac{2}{3r_0}\varepsilon P_2^1\frac{\partial V_1}{\partial\theta}, \tag{4.74}$$

correct to the first order in ε [87].

Again, using (4.72) in (4.75), we get

$$\begin{aligned} \hat{\mathbf{n}}\cdot\nabla(V_1)_4 &= \sum_{n=|m|}^{N_k} A_n^m\left[\left\{-(n+1)r_0^{-(n+2)}\left(1 + \frac{2}{3}(n+1)\varepsilon P_2\right) + \frac{2}{3}(n+1)r_0^{-(n+1)}\frac{d\varepsilon}{dr_0}P_2\right. \right. \\ &\quad \left. \left. -\frac{2}{3}(n+1)\frac{d}{dr_0}(r_0\varepsilon)r_0^{-(n+2)}P_2\right\}Y_n^m + \frac{2}{3}r_0^{-(n+2)}\varepsilon P_2^1\frac{dP_n^m}{d\theta}e^{im\phi}\right]. \end{aligned} \tag{4.75}$$

At the Earth's surface,

$$(V_1)_3(R-) = (V_1)_4(R+), \tag{4.76}$$

which gives

$$(X_n^m)_3(R-) = A_n^m r_0^{-(n+1)}\left(1 + \frac{2}{3}(n+1)\varepsilon P_2\right), \tag{4.77}$$

where equations (2.21) and (4.72) are used. Hence, using equations (4.75) and (4.77), the gravitational flux at the Earth's surface is

$$\begin{aligned}\hat{n}\cdot(\nabla(V_1)_3 - 4\pi G\rho_0\mathbf{u}_3)|_{R-} &= \hat{n}\cdot\nabla(V_1)_4(R+) \\ &= \sum_{n=|m|}^{N_k}\Bigg[-\frac{n+1}{R}\left\{1+\frac{2}{3}\varepsilon P_2\right\}(X_n^m)_3(R-)Y_n^m \\ &\quad +\frac{2}{3R}\varepsilon(X_n^m)_3(R-)P_2^1\frac{dP_n^m}{d\theta}e^{im\phi}\Bigg]. \qquad (4.78)\end{aligned}$$

If we set $\varepsilon = 0$ in the above equations (4.72)-(4.78), then they are valid for a spherical Earth model as we derived in subsection 2.4.3.

4.5 Application of Clairaut Coordinate to Galerkin Functional Forms for the Dynamical Equations of the Earth's Elastic Inner Core and Mantle

In this section, we will expand the Galerkin functional forms of the momentum equation and the Poisson equation for an elastic IC and MT of the Earth model correct to the first order in ellipticity. Using equations (4.18), (4.24), (4.17)-(4.22), (4.26)-(4.28), (4.38), (4.40), (4.43), (4.67), (4.70) in equation (4.13), we arrive at the Galerkin functional form of the momentum equation

$$\begin{aligned}F_{1k} = \int_{(r_0)_k}^{(r_0)_{k+1}}\int_0^{\pi}\int_0^{2\pi}\sum_{q=|m|}^{N_k}\sum_{n=|m|}^{N_k}\Bigg[&\sigma^2\left\{U_q^mU_n^mP_q^mP_n^m+\left(V_q^mV_n^m+W_q^mW_n^m\right)\left(\frac{dP_n^m}{d\theta}\frac{dP_q^m}{d\theta}\right.\right. \\ &\left.+\frac{m^2}{\sin\theta}P_q^mP_n^m\right)+im\left(V_q^mW_n^m-W_q^mV_n^m\right)\left(\frac{P_q^m}{\sin\theta}\frac{dP_n^m}{d\theta}+\frac{P_n^m}{\sin\theta}\frac{dP_q^m}{d\theta}\right)+\frac{2}{3}r_0\varepsilon\left(V_q^m\frac{dV_n^m}{dr_0}\right. \\ &\left.+W_q^m\frac{dW_n^m}{dr_0}\right)P_2^1\frac{dP_q^m}{d\theta}P_n^m+\frac{2}{3}r_0\varepsilon\left(\frac{dV_q^m}{dr_0}V_n^m+\frac{dW_q^m}{dr_0}W_n^m\right)P_2^1\frac{dP_n^m}{d\theta}P_n^m+\frac{2im}{3}r_0\varepsilon\left(V_q^m\frac{dW_n^m}{dr_0}\right. \\ &\left.\left.+\frac{dV_q^m}{dr_0}W_n^m-W_q^m\frac{dV_n^m}{dr_0}-\frac{dW_q^m}{dr_0}V_n^m\right)\frac{P_2^1}{\sin\theta}P_q^mP_n^m\right\}-\sigma\left\{m\left(U_q^mV_n^m+V_q^mU_n^m\right)P_q^mP_n^m\right.\end{aligned}$$

$$+i\left(V_q^m W_n^m - W_q^m V_n^m\right)\cos\theta\left(\frac{dP_n^m}{d\theta}\frac{dP_q^m}{d\theta}+\frac{m^2}{\sin\theta}P_q^m P_n^m\right)+m\left(V_q^m V_n^m + W_q^m W_n^m\right)$$

$$\times\cos\theta\left(\frac{P_q^m}{\sin\theta}\frac{dP_n^m}{d\theta}+\frac{P_n^m}{\sin\theta}\frac{dP_q^m}{d\theta}\right)+iU_q^m W_n^m\sin\theta\frac{dP_n^m}{d\theta}P_q^m - iW_q^m U_n^m\sin\theta\frac{dP_q^m}{d\theta}P_n^m$$

$$+\frac{2i}{3}r_0\varepsilon\left(V_q^m\frac{dW_n^m}{dr_0}-W_q^m\frac{dV_n^m}{dr_0}\right)\cos\theta P_2^1\frac{dP_q^m}{d\theta}P_n^m+\frac{2i}{3}r_0\varepsilon\left(\frac{dV_q^m}{dr_0}W_n^m-\frac{dW_q^m}{dr_0}V_n^m\right)$$

$$\times\cos\theta P_2^1\frac{dP_n^m}{d\theta}P_n^m+\frac{2i}{3}r_0\varepsilon\left(U_q^m\frac{dW_n^m}{dr_0}-\frac{dW_q^m}{dr_0}U_n^m\right)\sin\theta P_2^1 P_n^m P_q^m+\frac{2m}{3}r_0\varepsilon\left(V_q^m\frac{dV_n^m}{dr_0}\right.$$

$$\left.+\frac{dV_q^m}{dr_0}V_n^m+W_q^m\frac{dW_n^m}{dr_0}+\frac{dW_q^m}{dr_0}W_n^m\right)\frac{\cos\theta}{\sin\theta}P_2^1 P_q^m P_n^m\Bigg\}+U_q^m\left(g_0-\frac{r_0}{6}\right)\Bigg\{\left(\frac{dU_n^m}{dr_0}\right.$$

$$\left.+\frac{2U_n^m-n(n+1)V_n^m}{r_0}\right)P_n^m P_q^m+\frac{2}{3}\varepsilon\left(\frac{dU_n^m}{dr_0}+\frac{2U_n^m-n(n+1)V_n^m}{r_0}\right)P_2 P_n^m P_q^m$$

$$+\frac{2}{3}r_0\frac{d\varepsilon}{dr_0}\frac{dU_n^m}{dr_0}P_2 P_n^m P_q^m+\frac{4}{3}\varepsilon\frac{dV_n^m}{dr_0}P_2^1\frac{dP_n^m}{d\theta}P_q^m-4\varepsilon\frac{dV_n^m}{dr_0}P_2 P_n^m P_q^m\Bigg\}$$

$$+U_q^m\left(\frac{2}{3}\frac{d}{dr_0}(r_0\varepsilon)g_0\right)\left(\frac{dU_n^m}{dr_0}+\frac{2U_n^m-n(n+1)V_n^m}{r_0}\right)P_2 P_n^m P_q^m+V_q^m\left(\frac{2}{3}\varepsilon g_0\right)$$

$$\times\left(\frac{dU_n^m}{dr_0}+\frac{2U_n^m-n(n+1)V_n^m}{r_0}\right)P_2^1\frac{dP_q^m}{d\theta}P_n^m-W_q^m\left(\frac{2im}{3}\varepsilon g_0\right)\left(\frac{dU_n^m}{dr_0}\right.$$

$$\left.+\frac{2U_n^m-n(n+1)V_n^m}{r_0}\right)\frac{P_2^1}{\sin\theta}P_q^m P_n^m-\left(\frac{dU_q^m}{dr_0}+\frac{2U_q^m}{r_0}\right)\Bigg\{-\left(g_0-\frac{r_0}{6}\right)U_n^m P_n^m P_q^m$$

$$-\frac{2}{3}\frac{d}{dr_0}(r_0\varepsilon)g_0U_n^m P_2 P_n^m P_q^m-\frac{2}{3}\varepsilon g_0 V_n^m P_2^1\frac{dP_n^m}{d\theta}P_q^m-\frac{2im}{3}\varepsilon g_0 W_n^m\frac{P_2^1}{\sin\theta}P_n^m P_q^m$$

$$+X_n^m P_n^m P_q^m\Bigg\}+V_q^m\left(\frac{q(q+1)}{r_0}\right)\Bigg\{-\left(g_0-\frac{r_0}{6}\right)U_n^m P_n^m P_q^m-\frac{2}{3}\frac{d}{dr_0}(r_0\varepsilon)g_0U_n^m P_2 P_n^m P_q^m$$

$$-\frac{2}{3}\varepsilon g_0 V_n^m P_2^1\frac{dP_n^m}{d\theta}P_q^m-\frac{2im}{3}\varepsilon g_0 W_n^m\frac{P_2^1}{\sin\theta}P_n^m P_q^m+X_n^m P_n^m P_q^m\Bigg\}-\frac{2}{3}\varepsilon\left(\frac{dU_q^m}{dr_0}+\frac{2U_q^m}{r_0}\right)$$

$$\times\Bigg\{-\left(g_0-\frac{r_0}{6}\right)U_n^m P_2 P_n^m P_q^m+X_n^m P_2 P_n^m P_q^m\Bigg\}+\frac{2}{3}\varepsilon V_q^m\left(\frac{q(q+1)}{r_0}\right)\Bigg\{-\left(g_0-\frac{r_0}{6}\right)$$

$$\times U_n^m P_2 P_n^m P_q^m+X_n^m P_2 P_n^m P_q^m\Bigg\}+\frac{2}{3}\frac{dU_q^m}{dr_0}r_0\frac{d\varepsilon}{dr_0}\Bigg\{\left(g_0-\frac{r_0}{6}\right)U_n^m P_2 P_n^m P_q^m-X_n^m P_2 P_n^m P_q^m\Bigg\}$$

$$+4\varepsilon\frac{dV_q^m}{dr_0}\Bigg\{-\left(g_0-\frac{r_0}{6}\right)U_n^m P_2 P_n^m P_q^m+X_n^m P_2 P_n^m P_q^m\Bigg\}-\frac{4}{3}\varepsilon\frac{dV_q^m}{dr_0}\Bigg\{-\left(g_0-\frac{r_0}{6}\right)U_n^m$$

$$\times P_2^1\frac{dP_q^m}{d\theta}P_n^m+X_n^m P_2^1\frac{dP_q^m}{d\theta}P_n^m\Bigg\}\Bigg]r_0^2\sin\theta dr_0 d\theta d\phi$$

$$
-\int_{(r_0)_k}^{(r_0)_{k+1}}\int_0^{\pi}\int_0^{2\pi}\sum_{q=|m|}^{N_k}\sum_{n=|m|}^{N_k}\frac{2}{3}\frac{d}{dr_0}(r_0^3\varepsilon)\Bigg[\sigma^2\Bigg\{U_q^mU_n^mP_2P_q^mP_n^m+\Bigg(V_q^mV_n^m+W_q^mW_n^m\Bigg)
$$

$$
\times\Bigg(\frac{dP_n^m}{d\theta}\frac{dP_q^m}{d\theta}+\frac{m^2}{\sin\theta}P_q^mP_n^m\Bigg)P_2+im\Bigg(V_q^mW_n^m-W_q^mV_n^m\Bigg)\Bigg(\frac{P_q^m}{\sin\theta}\frac{dP_n^m}{d\theta}+\frac{P_n^m}{\sin\theta}\frac{dP_q^m}{d\theta}\Bigg)P_2
$$

$$
-\sigma\Bigg\{m\Bigg(U_q^mV_n^m+V_q^mU_n^m\Bigg)P_2P_q^mP_n^m+i\Bigg(V_q^mW_n^m-W_q^mV_n^m\Bigg)P_2\cos\theta\Bigg(\frac{dP_n^m}{d\theta}\frac{dP_q^m}{d\theta}
$$

$$
+\frac{m^2}{\sin\theta}P_q^mP_n^m\Bigg)+m\Bigg(V_q^mV_n^m+W_q^mW_n^m\Bigg)\cos\theta P_2\Bigg(\frac{P_q^m}{\sin\theta}\frac{dP_n^m}{d\theta}+\frac{P_n^m}{\sin\theta}\frac{dP_q^m}{d\theta}\Bigg)
$$

$$
+iU_q^mW_n^mP_2\sin\theta\frac{dP_n^m}{d\theta}P_q^m-iW_q^mU_n^mP_2\sin\theta\frac{dP_q^m}{d\theta}P_n^m\Bigg\}+U_q^m\Bigg(g_0-\frac{r_0}{6}\Bigg)\Bigg(\frac{dU_n^m}{dr_0}
$$

$$
+\frac{2U_n^m-n(n+1)V_n^m}{r_0}\Bigg)P_2P_n^mP_q^m-\Bigg(\frac{dU_q^m}{dr_0}+\frac{2U_q^m}{r_0}\Bigg)\Bigg\{-\Bigg(g_0-\frac{r_0}{6}\Bigg)U_n^m+X_n^m\Bigg\}
$$

$$
\times P_2P_n^mP_q^m+V_q^m\Bigg(\frac{q(q+1)}{r_0}\Bigg)\Bigg\{-\Bigg(g_0-\frac{r_0}{6}\Bigg)U_n^m+X_n^m\Bigg\}P_2P_n^mP_q^m\Bigg]\sin\theta dr_0d\theta d\phi
$$

$$
+\int_{(r_0)_k}^{(r_0)_{k+1}}\int_0^{\pi}\int_0^{2\pi}\sum_{q=|m|}^{N_k}\sum_{n=|m|}^{N_k}\frac{\lambda}{\rho_0^2}\frac{d\rho_0}{dr_0}\Bigg[U_q^m\Bigg\{\Bigg(\frac{dU_n^m}{dr_0}+\frac{2U_n^m-n(n+1)V_n^m}{r_0}\Bigg)P_n^mP_q^m
$$

$$
+\frac{2}{3}\varepsilon\Bigg(\frac{dU_n^m}{dr_0}+\frac{2U_n^m-n(n+1)V_n^m}{r_0}\Bigg)P_2P_n^mP_q^m+\frac{2}{3}r_0\frac{d\varepsilon}{dr_0}\frac{dU_n^m}{dr_0}P_2P_n^mP_q^m+\frac{4}{3}\varepsilon\frac{dV_n^m}{dr_0}
$$

$$
\times P_2^1\frac{dP_n^m}{d\theta}P_q^m-4\varepsilon\frac{dV_n^m}{dr_0}P_2P_n^mP_q^m+\frac{2}{3}\frac{d}{dr_0}(r_0\varepsilon)\Bigg(\frac{dU_n^m}{dr_0}+\frac{2U_n^m-n(n+1)V_n^m}{r_0}\Bigg)P_2P_n^mP_q^m\Bigg\}
$$

$$
+\frac{2}{3}\varepsilon V_q^m\Bigg(\frac{dU_n^m}{dr_0}+\frac{2U_n^m-n(n+1)V_n^m}{r_0}\Bigg)P_2^1\frac{dP_q^m}{d\theta}P_n^m-\frac{2im}{3}\varepsilon W_q^m\Bigg(\frac{dU_n^m}{dr_0}
$$

$$
+\frac{2U_n^m-n(n+1)V_n^m}{r_0}\Bigg)\frac{P_2^1}{\sin\theta}P_n^mP_q^m\Bigg]r_0^2\sin\theta dr_0d\theta d\phi
$$

$$
-\int_{(r_0)_k}^{(r_0)_{k+1}}\int_0^{\pi}\int_0^{2\pi}\sum_{q=|m|}^{N_k}\sum_{n=|m|}^{N_k}\frac{2}{3}\frac{d}{dr_0}(r_0^3\varepsilon)\frac{\lambda}{\rho_0^2}\frac{d\rho_0}{dr_0}\Bigg[U_q^m\Bigg(\frac{dU_n^m}{dr_0}+\frac{2U_n^m-n(n+1)V_n^m}{r_0}\Bigg)
$$

$$
\times P_2P_n^mP_q^m\Bigg]\sin\theta dr_0d\theta d\phi
$$

$$
-\int_{(r_0)_k}^{(r_0)_{k+1}}\int_0^{\pi}\int_0^{2\pi}\sum_{q=|m|}^{N_k}\sum_{n=|m|}^{N_k}\frac{\lambda}{\rho_0}\Bigg[\Bigg(\frac{dU_q^m}{dr_0}+\frac{2U_q^m}{r_0}\Bigg)\Bigg\{\Bigg(\frac{dU_n^m}{dr_0}+\frac{2U_n^m-n(n+1)V_n^m}{r_0}\Bigg)
$$

$$
\times P_n^mP_q^m+\frac{4}{3}\varepsilon\Bigg(\frac{dU_n^m}{dr_0}+\frac{2U_n^m-n(n+1)V_n^m}{r_0}\Bigg)P_2P_n^mP_q^m+\frac{2}{3}r_0\frac{d\varepsilon}{dr_0}\frac{dU_n^m}{dr_0}P_2P_n^mP_q^m+\frac{4}{3}\varepsilon\frac{dV_n^m}{dr_0}
$$

$$\times P_2^1 \frac{dP_n^m}{d\theta} P_q^m - 4\varepsilon \frac{dV_n^m}{dr_0} P_2 P_n^m P_q^m \Bigg\} - V_q^m \left(\frac{q(q+1)}{r_0} \right) \Bigg\{ \left(\frac{dU_n^m}{dr_0} + \frac{2U_n^m - n(n+1)V_n^m}{r_0} \right)$$

$$\times P_n^m P_q^m + \frac{4}{3}\varepsilon \left(\frac{dU_n^m}{dr_0} + \frac{2U_n^m - n(n+1)V_n^m}{r_0} \right) P_2 P_n^m P_q^m + \frac{2}{3} r_0 \frac{d\varepsilon}{dr_0} \frac{dU_n^m}{dr_0} P_2 P_n^m P_q^m$$

$$+ \frac{4}{3}\varepsilon \frac{dV_n^m}{dr_0} P_2^1 \frac{dP_n^m}{d\theta} P_q^m - 4\varepsilon \frac{dV_n^m}{dr_0} P_2 P_n^m P_q^m \Bigg\} + \frac{2}{3} r_0 \frac{d\varepsilon}{dr_0} \frac{dU_q^m}{dr_0} \left(\frac{dU_n^m}{dr_0} + \frac{2U_n^m - n(n+1)V_n^m}{r_0} \right)$$

$$\times P_2 P_n^m P_q^m + \frac{4}{3}\varepsilon \frac{dV_q^m}{dr_0} \left(\frac{dU_n^m}{dr_0} + \frac{2U_n^m - n(n+1)V_n^m}{r_0} \right) P_2^1 \frac{dP_q^m}{d\theta} P_n^m$$

$$- 4\varepsilon \frac{dV_q^m}{dr_0} \left(\frac{dU_n^m}{dr_0} + \frac{2U_n^m - n(n+1)V_n^m}{r_0} \right) P_2 P_n^m P_q^m \Bigg] r_0^2 \sin\theta dr_0 d\theta d\phi$$

$$+ \int_{(r_0)_k}^{(r_0)_{k+1}} \int_0^{\pi} \int_0^{2\pi} \sum_{q=|m|}^{N_k} \sum_{n=|m|}^{N_k} \frac{2}{3} \frac{d}{dr_0} (r_0^3 \varepsilon) \frac{\lambda}{\rho_0} \Bigg[\left(\frac{dU_q^m}{dr_0} + \frac{2U_q^m}{r_0} \right) \left(\frac{dU_n^m}{dr_0} \right.$$

$$\left. + \frac{2U_n^m - n(n+1)V_n^m}{r_0} \right) P_2 P_n^m P_q^m - V_q^m \left(\frac{q(q+1)}{r_0} \right) \left(\frac{dU_n^m}{dr_0} + \frac{2U_n^m - n(n+1)V_n^m}{r_0} \right)$$

$$\times P_2 P_n^m P_q^m \Bigg] \sin\theta dr_0 d\theta d\phi$$

$$+ \int_{(r_0)_k}^{(r_0)_{k+1}} \int_0^{\pi} \int_0^{2\pi} \sum_{q=|m|}^{N_k} \sum_{n=|m|}^{N_k} U_q^m \frac{\mu}{\rho_0} \Bigg[\Bigg\{ 2\frac{d^2 U_n^m}{dr_0^2} - n(n+1)U_n^m - 4U_n^m + \frac{4}{r_0} \frac{dU_n^m}{dr_0}$$

$$+ \frac{2}{3r_0}\varepsilon \frac{dU_n^m}{dr_0} - n(n+1) \left(\frac{1}{r_0} \frac{dV_n^m}{dr_0} - 3V_n^m \right) + \frac{2}{3r_0} \left(\frac{d}{dr_0}(r_0\varepsilon) \frac{dV_n^m}{dr_0} + r_0\varepsilon \frac{dV_n^m}{dr_0^2} \right.$$

$$\left. - 3\varepsilon \frac{dV_n^m}{dr_0} \right) \Bigg\} P_n^m + \Bigg\{ \frac{8}{3} \frac{d}{dr_0}(r_0\varepsilon) \frac{d^2 U_n^m}{dr_0^2} + \frac{4}{3} \frac{d^2}{dr_0^2}(r_0\varepsilon) \frac{d^2}{dr_0^2}(r_0\varepsilon) \frac{dU_n^m}{dr_0} + \frac{8}{3r_0} \left(-r_0\varepsilon \frac{d^2 V_n^m}{dr_0^2} \right.$$

$$- \frac{d}{dr_0}(r_0\varepsilon) \frac{dV_n^m}{dr_0} + 3\varepsilon \frac{dV_n^m}{dr_0} \Bigg) - n(n+1) \left(\frac{2}{3r_0} \frac{d}{dr_0}(r_0\varepsilon) \frac{dV_n^m}{dr_0} + \frac{2}{3r_0}\varepsilon \frac{dV_n^m}{dr_0} - 4\varepsilon V_n^m \right)$$

$$- \frac{4}{3} n(n+1)\varepsilon U_n^m + \frac{8}{3} \left(\frac{1}{r_0} \frac{d}{dr_0}(r_0\varepsilon) \frac{dU_n^m}{dr_0} - 2\varepsilon U_n^m \right) \Bigg\} P_2 P_n^m + \frac{4}{3r_0} \Bigg\{ \varepsilon \frac{dU_n^m}{dr_0} + r_0\varepsilon \frac{d^2 V_n^m}{d^2 r_0}$$

$$+ \frac{d}{dr_0}(r_0\varepsilon) \frac{dV_n^m}{dr_0} - 3\varepsilon \frac{dV_n^m}{dr_0} \Bigg\} P_2^1 \frac{dP_n^m}{d\theta} + \frac{2}{3r_0} \Bigg\{ \varepsilon \frac{dU_n^m}{dr_0} + r_0\varepsilon \frac{d^2 V_n^m}{d^2 r_0} + \frac{d}{dr_0}(r_0\varepsilon) \frac{dV_n^m}{dr_0}$$

$$- 3\varepsilon \frac{dV_n^m}{dr_0} \Bigg\} P_2^1 \cot\theta P_n^m \Bigg] P_q^m r_0^2 \sin\theta dr_0 d\theta d\phi$$

$$- \int_{(r_0)_k}^{(r_0)_{k+1}} \int_0^{\pi} \int_0^{2\pi} \sum_{q=|m|}^{N_k} \sum_{n=|m|}^{N_k} U_q^m \frac{2}{3} \frac{d}{dr_0}(r_0^3\varepsilon) \frac{\mu}{\rho_0} \Bigg[2\frac{d^2 U_n^m}{dr_0^2} - n(n+1)U_n^m - 4U_n^m$$

$$+\frac{4}{r_0}\frac{dU_n^m}{dr_0}-n(n+1)\left(\frac{1}{r_0}\frac{dV_n^m}{dr_0}-3V_n^m\right)\Bigg]P_2P_n^mP_q^m\sin\theta dr_0d\theta d\phi$$

$$+\int_{(r_0)_k}^{(r_0)_{k+1}}\int_0^{\pi}\int_0^{2\pi}\sum_{q=|m|}^{N_k}\sum_{n=|m|}^{N_k}U_q^m\frac{d\mu}{dr_0}\frac{1}{\rho_0}\Bigg[2\frac{dU_n^m}{dr_0}P_n^m+\frac{2}{3}\varepsilon\left\{\frac{U_n^m}{r_0}-\frac{V_n^m}{r_0}+\frac{dV_n^m}{dr_0}\right\}P_2^1\frac{dP_n^m}{d\theta}$$

$$+\frac{8}{3}\frac{d}{dr_0}(r_0\varepsilon)\frac{dU_n^m}{dr_0}P_2P_n^m+\frac{2im}{3}\varepsilon\left\{\frac{dW_n^m}{dr_0}-\frac{W_n^m}{r_0}\right\}\frac{P_2^1}{\sin\theta}P_n^m\Bigg]P_q^mr_0^2\sin\theta dr_0d\theta d\phi$$

$$-\int_{(r_0)_k}^{(r_0)_{k+1}}\int_0^{\pi}\int_0^{2\pi}\sum_{q=|m|}^{N_k}\sum_{n=|m|}^{N_k}U_q^m\frac{4}{3}\frac{d}{dr_0}(r_0^3\varepsilon)\frac{d\mu}{dr_0}\frac{1}{\rho_0}\frac{dU_n^m}{dr_0}P_2P_n^mP_q^m\sin\theta dr_0d\theta d\phi$$

$$+\int_{(r_0)_k}^{(r_0)_{k+1}}\int_0^{\pi}\int_0^{2\pi}\sum_{q=|m|}^{N_k}\sum_{n=|m|}^{N_k}\frac{dV_q^m}{dr_0}\left(\frac{2}{3\rho_0}r_0\mu\varepsilon\right)\Bigg[\left\{\frac{1}{r_0}\frac{dU_n^m}{dr_0}+\frac{4}{r_n^2}U_n^m+\frac{d^2V_n^m}{dr_0^2}\right.$$

$$\left.+\frac{2}{r_0}\frac{dV_n^m}{dr_0}-\frac{2}{r_0^2}n(n+1)V_n^m\right\}P_2^1\frac{dP_n^m}{d\theta}P_q^m+im\left\{\frac{d^2W_n^m}{dr_0^2}+\frac{2}{r_0}\frac{dW_n^m}{dr_0}-\frac{n(n+1)}{r_0^2}W_n^m\right\}$$

$$\times\frac{P_2^1}{\sin\theta}P_n^mP_q^m\Bigg]r_0^2\sin\theta dr_0d\theta d\phi$$

$$+\int_{(r_0)_k}^{(r_0)_{k+1}}\int_0^{\pi}\int_0^{2\pi}\sum_{q=|m|}^{N_k}\sum_{n=|m|}^{N_k}V_q^m\frac{\mu}{\rho_0}\Bigg[\left\{\frac{1}{r_0}\frac{dU_n^m}{dr_0}+\frac{4}{r_n^2}U_n^m+\frac{d^2V_n^m}{dr_0^2}+\frac{2}{r_0}\frac{dV_n^m}{dr_0}\right.$$

$$\left.-\frac{2}{r_0^2}n(n+1)V_n^m+\frac{4}{r_0}\varepsilon\frac{dV_n^m}{dr_0}\right\}\left(\frac{dP_n^m}{d\theta}\frac{dP_q^m}{d\theta}+\frac{m^2}{\sin^2\theta}P_n^mP_q^m\right)-\frac{8m^2}{r_0}\varepsilon\frac{dV_n^m}{dr_0}P_n^mP_q^m$$

$$+im\left\{\frac{d^2W_n^m}{dr_0^2}+\frac{2}{r_0}\frac{dW_n^m}{dr_0}-\frac{n(n+1)}{r_0^2}W_n^m\right\}\left(\frac{P_n^m}{\sin\theta}\frac{dP_q^m}{d\theta}+\frac{P_q^m}{\sin\theta}\frac{dP_n^m}{d\theta}\right)+\frac{4im}{r_0}\varepsilon\frac{dW_n^m}{dr_0}$$

$$\times\sin\theta\frac{dP_n^m}{d\theta}P_q^m+\Bigg\{\left(\frac{2}{3}\varepsilon\frac{d^2U_n^m}{dr_0^2}+\frac{2}{3r_0}\frac{d}{dr_0}(r_0\varepsilon)\frac{dU_n^m}{dr_0}+\frac{4}{3r_0}\varepsilon\frac{dU_n^m}{dr_0}+\frac{2}{3}\frac{d^2}{dr_0^2}(r_0\varepsilon)\frac{dV_n^m}{dr_0}\right.$$

$$\left.+\frac{4}{3}\varepsilon\frac{d^2V_n^m}{dr_0^2}+\frac{4}{3}\frac{d}{dr_0}(r_0\varepsilon)\frac{d^2V_n^m}{dr_0^2}+\frac{2}{3}r_0\varepsilon\frac{d^3V_n^m}{dr_0^3}-\frac{20}{3r_0}\varepsilon\frac{dV_n^m}{dr_0}+\frac{4}{3r_0}\frac{d}{dr_0}(r_0\varepsilon)\frac{dV_n^m}{dr_0}\right)$$

$$\times\frac{dP_q^m}{d\theta}P_n^m-\frac{4}{3r_0}\varepsilon\frac{dV_n^m}{dr_0}\cot\theta\left(\frac{dP_n^m}{d\theta}\frac{dP_q^m}{d\theta}+\frac{m^2}{\sin^2\theta}P_n^mP_q^m\right)-\frac{4}{r_0}n(n+1)\varepsilon\frac{dV_n^m}{dr_0}\frac{dP_q^m}{d\theta}P_n^m$$

$$-\frac{4}{3r_0}\varepsilon\frac{dV_n^m}{dr_0}\frac{dP_q^m}{d\theta}P_n^m+\frac{8}{3r_0}\varepsilon\frac{dV_n^m}{dr_0}\frac{m^2}{\sin^2\theta}\left(P_n^m\frac{dP_q^m}{d\theta}+P_q^m\frac{dP_n^m}{d\theta}\right)+im\left(\frac{2}{3}\frac{d^2}{dr_0^2}(r_0\varepsilon)\frac{dW_n^m}{dr_0}\right.$$

$$\left.+\frac{4}{3}\varepsilon\frac{d^2W_n^m}{dr_0^2}+\frac{4}{3}\frac{d}{dr_0}(r_0\varepsilon)\frac{d^2W_n^m}{dr_0^2}-\frac{2}{3}r_0\varepsilon\frac{d^3W_n^m}{dr_0^3}-\frac{10}{3r_0}\varepsilon\frac{dW_n^m}{dr_0}+\frac{4}{3r_0}\frac{d}{dr_0}(r_0\varepsilon)\frac{dW_n^m}{dr_0}\right)$$

$$\times\frac{P_n^m}{\sin\theta}P_q^m+\frac{4im}{3r_0}\varepsilon\frac{dW_n^m}{dr_0}\frac{1}{\sin\theta}\left(\frac{dP_n^m}{d\theta}\frac{dP_q^m}{d\theta}+\frac{m^2}{\sin^2\theta}P_n^mP_q^m\right)-\frac{2im}{3r_0}\varepsilon\frac{dW_n^m}{dr_0}\frac{P_n^m}{\sin\theta}P_q^m$$

$$
-\frac{2im}{r_0}\varepsilon n(n+1)\frac{dW_n^m}{dr_0}\frac{P_n^m}{\sin\theta}P_q^m\Bigg\}P_2^1+\Bigg\{\Bigg(\frac{2}{3r_0}\varepsilon\frac{dU_n^m}{dr_0}+\frac{2}{3r_0}\frac{d}{dr_0}(r_0\varepsilon)\frac{dU_n^m}{dr_0}+\frac{16}{3r_0^2}\varepsilon U_n^m
$$

$$
+\frac{2}{3}\frac{d^2}{dr_0^2}(r_0\varepsilon)\frac{dV_n^m}{dr_0}+\frac{4}{3}\frac{d}{dr_0}(r_0\varepsilon)\frac{d^2V_n^m}{dr_0^2}+\frac{4}{3r_0}\frac{d}{dr_0}(r_0\varepsilon)\frac{dV_n^m}{dr_0}-\frac{8}{3r_0^2}n(n+1)\varepsilon V_n^m
$$

$$
-\frac{44}{3r_0}\varepsilon\frac{dV_n^m}{dr_0}\Bigg)\Bigg(\frac{dP_n^m}{d\theta}\frac{dP_q^m}{d\theta}+\frac{m^2}{\sin^2\theta}P_n^mP_q^m\Bigg)+im\Bigg(-\frac{8}{3r_0}\varepsilon\frac{dW_n^m}{dr_0}+\frac{2}{3}\frac{d^2}{dr_0^2}(r_0\varepsilon)\frac{dW_n^m}{dr_0}
$$

$$
+\frac{4}{3}\frac{d}{dr_0}(r_0\varepsilon)\frac{d^2W_n^m}{dr_0^2}+\frac{4}{3r_0}\frac{d}{dr_0}(r_0\varepsilon)\frac{dW_n^m}{dr_0}-\frac{4}{3r_0^2}n(n+1)\varepsilon W_n^m\Bigg)\Bigg(\frac{P_n^m}{\sin\theta}\frac{dP_q^m}{d\theta}
$$

$$
+\frac{P_q^m}{\sin\theta}\frac{dP_n^m}{d\theta}\Bigg)\Bigg\}P_2\Bigg]r_0^2\sin\theta dr_0d\theta d\phi
$$

$$
-\int_{(r_0)_k}^{(r_0)_{k+1}}\int_0^{\pi}\int_0^{2\pi}\sum_{q=|m|}^{N_k}\sum_{n=|m|}^{N_k}V_q^m\Bigg(\frac{2\mu}{3\rho_0}\frac{d}{dr_0}(r_0^3\varepsilon)\Bigg)\Bigg[\Bigg\{\frac{1}{r_0}\frac{dU_n^m}{dr_0}+\frac{4}{r_n^2}U_n^m+\frac{d^2V_n^m}{dr_0^2}
$$

$$
+\frac{2}{r_0}\frac{dV_n^m}{dr_0}-\frac{2}{r_0^2}n(n+1)V_n^m\Bigg\}P_2\Bigg(\frac{dP_n^m}{d\theta}\frac{dP_q^m}{d\theta}+\frac{m^2}{\sin^2\theta}P_n^mP_q^m\Bigg)+im\Bigg\{\frac{d^2W_n^m}{dr_0^2}+\frac{2}{r_0}\frac{dW_n^m}{dr_0}
$$

$$
-\frac{n(n+1)}{r_0^2}W_n^m\Bigg\}P_2\Bigg(\frac{P_n^m}{\sin\theta}\frac{dP_q^m}{d\theta}+\frac{P_q^m}{\sin\theta}\frac{dP_n^m}{d\theta}\Bigg)\Bigg]\sin\theta dr_0d\theta d\phi
$$

$$
+\int_{(r_0)_k}^{(r_0)_{k+1}}\int_0^{\pi}\int_0^{2\pi}\sum_{q=|m|}^{N_k}\sum_{n=|m|}^{N_k}\frac{dV_q^m}{dr_0}\Bigg(\frac{2}{3}\frac{1}{\rho_0}\frac{d\mu}{dr_0}r_0\varepsilon\Bigg)\Bigg[\Bigg\{\frac{U_n^m}{r_0}+\frac{dV_n^m}{dr_0}-\frac{V_n^m}{r_0}\Bigg\}P_2^1\frac{dP_n^m}{d\theta}P_q^m
$$

$$
+im\Bigg\{\frac{dW_n^m}{dr_0}-\frac{W_n^m}{r_0}\Bigg\}\frac{P_2^1}{\sin\theta}P_n^mP_q^m\Bigg]r_0^2\sin\theta dr_0d\theta d\phi
$$

$$
+\int_{(r_0)_k}^{(r_0)_{k+1}}\int_0^{\pi}\int_0^{2\pi}\sum_{q=|m|}^{N_k}\sum_{n=|m|}^{N_k}V_q^m\frac{1}{\rho_0}\frac{d\mu}{dr_0}\Bigg[\Bigg\{\frac{U_n^m}{r_0}+\frac{dV_n^m}{dr_0}-\frac{V_n^m}{r_0}\Bigg\}\Bigg(\frac{dP_n^m}{d\theta}\frac{dP_q^m}{d\theta}
$$

$$
+\frac{m^2}{\sin^2\theta}P_n^mP_q^m\Bigg)+im\Bigg\{\frac{dW_n^m}{dr_0}-\frac{W_n^m}{r_0}\Bigg\}\Bigg(\frac{P_n^m}{\sin\theta}\frac{dP_q^m}{d\theta}+\frac{P_q^m}{\sin\theta}\frac{dP_n^m}{d\theta}\Bigg)+\Bigg\{\Bigg(\frac{2}{3}\varepsilon\frac{dU_n^m}{dr_0}
$$

$$
+\frac{4}{3r_0}\varepsilon U_n^m-\frac{2}{3}\varepsilon\frac{dV_n^m}{dr_0}+\frac{2}{3}\frac{d}{dr_0}(r_0\varepsilon)\frac{dV_n^m}{dr_0}+\frac{2}{3}r_0\varepsilon\frac{d^2V_n^m}{dr_0^2}\Bigg)P_n^m\frac{dP_q^m}{d\theta}-\frac{4}{3r_0}\varepsilon V_n^m\cot\theta
$$

$$
\times\Bigg(\frac{dP_n^m}{d\theta}\frac{dP_q^m}{d\theta}+\frac{m^2}{\sin^2\theta}P_n^mP_q^m\Bigg)+\frac{4}{3r_0}\varepsilon V_n^m\frac{m^2}{\sin^2\theta}\Bigg(\frac{dP_n^m}{d\theta}P_q^m+\frac{dP_q^m}{d\theta}P_n^m\Bigg)
$$

$$
-\frac{4}{3r_0}n(n+1)\varepsilon V_n^mP_n^m\frac{dP_q^m}{d\theta}+im\Bigg(\frac{2}{3}r_0\varepsilon\frac{d^2W_n^m}{dr_0^2}+\frac{2}{3}\frac{d}{dr_0}(r_0\varepsilon)\frac{dW_n^m}{dr_0}-\frac{2}{3}\varepsilon\frac{dW_n^m}{dr_0}\Bigg)\frac{P_n^m}{\sin\theta}P_q^m
$$

$$
+\frac{4im}{3r_0}\varepsilon W_n^m\frac{1}{\sin\theta}\Bigg(\frac{dP_n^m}{d\theta}\frac{dP_q^m}{d\theta}+\frac{m^2}{\sin^2\theta}P_n^mP_q^m\Bigg)-\frac{2im}{3r_0}n(n+1)\varepsilon W_n^m\frac{P_n^m}{\sin\theta}P_q^m
$$

$$
-\frac{4im}{3r_0}\varepsilon W_n^m\frac{\cot\theta}{\sin\theta}\left(\frac{dP_n^m}{d\theta}P_q^m+\frac{dP_q^m}{d\theta}P_n^m\right)\Bigg\}P_2^1+\Bigg\{\left(\frac{2}{3r_0}\varepsilon U_n^m+\frac{2}{3r_0}\frac{d}{dr_0}(r_0\varepsilon)U_n^m\right.
$$

$$
+\frac{4}{3}\frac{d}{dr_0}(r_0\varepsilon)\frac{dV_n^m}{dr_0}-\frac{2}{3r_0}\varepsilon V_n^m-\frac{2}{3r_0}\frac{d}{dr_0}(r_0\varepsilon)V_n^m\Bigg)\left(\frac{dP_n^m}{d\theta}\frac{dP_q^m}{d\theta}+\frac{m^2}{\sin^2\theta}P_n^mP_q^m\right)
$$

$$
+im\left(\frac{4}{3}\frac{d}{dr_0}(r_0\varepsilon)\frac{dW_n^m}{dr_0}-\frac{2}{3r_0}\varepsilon W_n^m-\frac{2}{3r_0}\frac{d}{dr_0}(r_0\varepsilon)W_n^m\right)\left(\frac{P_n^m}{\sin\theta}\frac{dP_q^m}{d\theta}+\frac{P_q^m}{\sin\theta}\frac{dP_n^m}{d\theta}\right)\Bigg\}P_2\Bigg]
$$

$$
\times r_0^2\sin\theta dr_0d\theta d\phi
$$

$$
-\int_{(r_0)_k}^{(r_0)_{k+1}}\int_0^{\pi}\int_0^{2\pi}\sum_{q=|m|}^{N_k}\sum_{n=|m|}^{N_k}V_q^m\left(\frac{2}{3\rho_0}\frac{d}{dr_0}(r_0^3\varepsilon)\frac{d\mu}{dr_0}\right)\Bigg[\left\{\frac{U_n^m}{r_0}+\frac{dV_n^m}{dr_0}-\frac{V_n^m}{r_0}\right\}P_2
$$

$$
\times\left(\frac{dP_n^m}{d\theta}\frac{dP_q^m}{d\theta}+\frac{m^2}{\sin^2\theta}P_n^mP_q^m\right)+im\left\{\frac{dW_n^m}{dr_0}-\frac{W_n^m}{r_0}\right\}P_2\left(\frac{P_n^m}{\sin\theta}\frac{dP_q^m}{d\theta}+\frac{P_q^m}{\sin\theta}\frac{dP_n^m}{d\theta}\right)\Bigg]
$$

$$
\times\sin\theta dr_0d\theta d\phi
$$

$$
+\int_{(r_0)_k}^{(r_0)_{k+1}}\int_0^{\pi}\int_0^{2\pi}\sum_{q=|m|}^{N_k}\sum_{n=|m|}^{N_k}\frac{dW_q^m}{dr_0}\left(\frac{2}{3\rho_0}r_0\varepsilon\mu\right)\Bigg[-im\left\{\frac{1}{r_0}\frac{dU_n^m}{dr_0}+\frac{4}{r_n^2}U_n^m+\frac{d^2V_n^m}{dr_0^2}\right.
$$

$$
\left.+\frac{2}{r_0}\frac{dV_n^m}{dr_0}-\frac{2}{r_0^2}n(n+1)V_n^m\right\}\frac{P_2^1}{\sin\theta}P_n^mP_q^m+\left\{\frac{d^2W_n^m}{dr_0^2}+\frac{2}{r_0}\frac{dW_n^m}{dr_0}-\frac{n(n+1)}{r_0^2}W_n^m\right\}
$$

$$
\times P_2^1\frac{dP_n^m}{d\theta}P_q^m\Bigg]r_0^2\sin\theta dr_0d\theta d\phi
$$

$$
+\int_{(r_0)_k}^{(r_0)_{k+1}}\int_0^{\pi}\int_0^{2\pi}\sum_{q=|m|}^{N_k}\sum_{n=|m|}^{N_k}W_q^m\frac{\mu}{\rho_0}\Bigg[-im\left\{\frac{1}{r_0}\frac{dU_n^m}{dr_0}+\frac{4}{r_n^2}U_n^m+\frac{d^2V_n^m}{dr_0^2}+\frac{2}{r_0}\frac{dV_n^m}{dr_0}\right.
$$

$$
\left.-\frac{2}{r_0^2}n(n+1)V_n^m+\frac{4}{r_0}\varepsilon\frac{dV_n^m}{dr_0}++\frac{4}{3r_0}\varepsilon\frac{dV_n^m}{dr_0}-\frac{2}{r_0^2}n(n+1)\varepsilon V_n^m\right\}\left(\frac{P_n^m}{\sin\theta}\frac{dP_q^m}{d\theta}+\frac{P_q^m}{\sin\theta}\right.
$$

$$
\left.\times\frac{dP_n^m}{d\theta}\right)+\frac{8im}{r_0}\varepsilon\frac{dV_n^m}{dr_0}\sin\theta\frac{dP_q^m}{d\theta}P_n^m+\left\{\frac{d^2W_n^m}{dr_0^2}+\frac{2}{r_0}\frac{dW_n^m}{dr_0}-\frac{n(n+1)}{r_0^2}W_n^m+\frac{10}{3r_0}\varepsilon\frac{dW_n^m}{dr_0}\right\}
$$

$$
\times\left(\frac{dP_n^m}{d\theta}\frac{dP_q^m}{d\theta}+\frac{m^2}{\sin^2\theta}P_n^mP_q^m\right)-\frac{4m^2}{r_0}\varepsilon\frac{dW_n^m}{dr_0}P_n^mP_q^m+\Bigg\{-im\Bigg(\frac{2}{3}\varepsilon\frac{d^2U_n^m}{dr_0^2}+\frac{4}{3r_0}\varepsilon\frac{dU_n^m}{dr_0}
$$

$$
+\frac{2}{3r_0}\frac{d}{dr_0}(r_0\varepsilon)\frac{dU_n^m}{dr_0}+\frac{2}{3}\frac{d^2}{dr_0^2}(r_0\varepsilon)\frac{dV_n^m}{dr_0}+\frac{4}{3}\frac{d}{dr_0}(r_0\varepsilon)\frac{d^2V_n^m}{dr_0^2}+\frac{4}{3}\varepsilon\frac{d^2V_n^m}{dr_0^2}+\frac{2}{3}r_0\varepsilon\frac{d^3V_n^m}{dr_0^3}
$$

$$
-\frac{20}{3r_0}\varepsilon\frac{dV_n^m}{dr_0}+\frac{4}{3r_0}\frac{d}{dr_0}(r_0\varepsilon)\frac{dV_n^m}{dr_0}-\frac{4}{3r_0}\varepsilon\frac{dV_n^m}{dr_0}-\frac{4}{r_0}n(n+1)\varepsilon\frac{dV_n^m}{dr_0}\Bigg)\frac{1}{\sin\theta}P_n^mP_q^m
$$

$$
-\frac{8im}{3r_0}\varepsilon\frac{dV_n^m}{dr_0}\frac{1}{\sin\theta}\left(\frac{dP_n^m}{d\theta}\frac{dP_q^m}{d\theta}+\frac{m^2}{\sin^2\theta}P_n^mP_q^m\right)-\left(-\frac{2}{3}\frac{d^2}{dr_0^2}(r_0\varepsilon)\frac{dW_n^m}{dr_0}-\frac{4}{3}\varepsilon\frac{d^2W_n^m}{dr_0^2}\right.
$$

$$
-\frac{4}{3}\frac{d}{dr_0}(r_0\varepsilon)\frac{d^2W_n^m}{dr_0^2}-\frac{2}{3}r_0\varepsilon\frac{d^3W_n^m}{dr_0^3}+\frac{10}{3r_0}\varepsilon\frac{dW_n^m}{dr_0}-\frac{4}{3r_0}\frac{d}{dr_0}(r_0\varepsilon)\frac{dW_n^m}{dr_0}+\frac{2}{3r_0}\varepsilon\frac{dW_n^m}{dr_0}
$$

$$
\left.+\frac{2}{r_0}n(n+1)\varepsilon\frac{dW_n^m}{dr_0}\right)\frac{dP_q^m}{d\theta}P_n^m+\frac{4}{3r_0}\varepsilon\frac{dW_n^m}{dr_0}\frac{m^2}{\sin^2\theta}\left(P_n^m\frac{dP_q^m}{d\theta}+P_q^m\frac{dP_n^m}{d\theta}\right)+\frac{2}{3r_0}\varepsilon\frac{dW_n^m}{dr_0}
$$

$$
\times\cot\theta\left(\frac{dP_n^m}{d\theta}\frac{dP_n^m}{d\theta}+\frac{m^2}{\sin^2\theta}P_n^mP_q^m\right)\Bigg\}P_2^1+\Bigg\{-im\left(\frac{2}{3r_0}\varepsilon\frac{dU_n^m}{dr_0}+\frac{16}{3r_0^2}\varepsilon U_n^m-\frac{4}{r_0}\varepsilon\frac{dV_n^m}{dr_0}\right.
$$

$$
+\frac{2}{3r_0}\frac{d}{dr_0}(r_0\varepsilon)\frac{dU_n^m}{dr_0}+\frac{2}{3}\frac{d^2}{dr_0^2}(r_0\varepsilon)\frac{dV_n^m}{dr_0}+\frac{4}{3}\frac{d}{dr_0}(r_0\varepsilon)\frac{d^2V_n^m}{dr_0^2}+\frac{4}{3r_0}\frac{d}{dr_0}(r_0\varepsilon)\frac{dV_n^m}{dr_0}
$$

$$
\left.-\frac{8}{3r_0^2}n(n+1)\varepsilon V_n^m\right)\left(\frac{P_n^m}{\sin\theta}\frac{dP_q^m}{d\theta}+\frac{P_q^m}{\sin\theta}\frac{dP_n^m}{d\theta}\right)-\frac{8im}{3r_0}\varepsilon\frac{dV_n^m}{dr_0}\left(\frac{P_n^m}{\sin\theta}\frac{dP_q^m}{d\theta}+\frac{P_q^m}{\sin\theta}\frac{dP_n^m}{d\theta}\right)
$$

$$
-\left(-\frac{2}{3}\frac{d^2}{dr_0^2}(r_0\varepsilon)\frac{dW_n^m}{dr_0}-\frac{4}{3}\frac{d}{dr_0}(r_0\varepsilon)\frac{d^2W_n^m}{dr_0^2}+\frac{4}{r_0}\varepsilon\frac{dW_n^m}{dr_0}-\frac{4}{3r_0}\frac{d}{dr_0}(r_0\varepsilon)\frac{dW_n^m}{dr_0}\right.
$$

$$
\left.+\frac{4}{3r_0^2}n(n+1)\varepsilon W_n^m\right)\left(\frac{dP_n^m}{d\theta}\frac{dP_q^m}{d\theta}+\frac{m^2}{\sin^2\theta}P_n^mP_q^m\right)\Bigg\}P_2\Bigg]r_0^2\sin\theta dr_0d\theta d\phi
$$

$$
-\int_{(r_0)_k}^{(r_0)_{k+1}}\int_0^{\pi}\int_0^{2\pi}\sum_{q=|m|}^{N_k}\sum_{n=|m|}^{N_k}W_q^m\left(\frac{2\mu}{3\rho_0}\frac{d}{dr_0}(r_0^3\varepsilon)\right)\Bigg[-im\Bigg\{\frac{1}{r_0}\frac{dU_n^m}{dr_0}+\frac{4}{r_n^2}U_n^m+\frac{d^2V_n^m}{dr_0^2}
$$

$$
+\frac{2}{r_0}\frac{dV_n^m}{dr_0}-\frac{2}{r_0^2}n(n+1)V_n^m\Bigg\}P_2\left(\frac{P_n^m}{\sin\theta}\frac{dP_q^m}{d\theta}+\frac{P_q^m}{\sin\theta}\frac{dP_n^m}{d\theta}\right)+\Bigg\{\frac{d^2W_n^m}{dr_0^2}+\frac{2}{r_0}\frac{dW_n^m}{dr_0}
$$

$$
-\frac{n(n+1)}{r_0^2}W_n^m\Bigg\}P_2\left(\frac{dP_n^m}{d\theta}\frac{dP_q^m}{d\theta}+\frac{m^2}{\sin^2\theta}P_n^mP_q^m\right)\Bigg]\sin\theta dr_0d\theta d\phi
$$

$$
+\int_{(r_0)_k}^{(r_0)_{k+1}}\int_0^{\pi}\int_0^{2\pi}\sum_{q=|m|}^{N_k}\sum_{n=|m|}^{N_k}\frac{dW_q^m}{dr_0}\left(\frac{2}{3\rho_0}r_0\varepsilon\frac{d\mu}{dr_0}\right)\Bigg[-im\Bigg\{\frac{U_n^m}{r_0}+\frac{dV_n^m}{dr_0}-\frac{V_n^m}{r_0}\Bigg\}
$$

$$
\times\frac{P_2^1}{\sin\theta}P_n^mP_q^m+\Bigg\{\frac{dW_n^m}{dr_0}-\frac{W_n^m}{r_0}\Bigg\}P_2^1\frac{dP_n^m}{d\theta}P_q^m\Bigg]r_0^2\sin\theta dr_0d\theta d\phi
$$

$$
+\int_{(r_0)_k}^{(r_0)_{k+1}}\int_0^{\pi}\int_0^{2\pi}\sum_{q=|m|}^{N_k}\sum_{n=|m|}^{N_k}W_q^m\frac{1}{\rho_0}\frac{d\mu}{dr_0}\Bigg[-im\Bigg\{\frac{U_n^m}{r_0}+\frac{dV_n^m}{dr_0}-\frac{V_n^m}{r_0}\Bigg\}\left(\frac{P_n^m}{\sin\theta}\frac{dP_q^m}{d\theta}\right.
$$

$$
\left.+\frac{P_q^m}{\sin\theta}\frac{dP_n^m}{d\theta}\right)+\Bigg\{\frac{dW_n^m}{dr_0}-\frac{W_n^m}{r_0}\Bigg\}\left(\frac{dP_n^m}{d\theta}\frac{dP_q^m}{d\theta}+\frac{m^2}{\sin^2\theta}P_n^mP_q^m\right)+\Bigg\{-im\left(\frac{2}{3}\varepsilon\frac{dU_n^m}{dr_0}\right.
$$

$$
\left.+\frac{4}{3r_0}\varepsilon U_n^m+\frac{2}{3}\frac{d}{dr_0}(r_0\varepsilon)\frac{dV_n^m}{dr_0}+\frac{2}{3}r_0\varepsilon\frac{d^2V_n^m}{dr_0^2}-\frac{2}{3}\varepsilon\frac{dV_n^m}{dr_0}-\frac{4}{3r_0}n(n+1)\varepsilon V_n^m\right)\frac{P_n^m}{\sin\theta}P_q^m
$$

$$+\frac{4im}{3r_0}\varepsilon V_n^m\cot\theta\left(\frac{P_q^m}{\sin\theta}\frac{dP_n^m}{d\theta}+\frac{P_n^m}{\sin\theta}\frac{dP_q^m}{d\theta}\right)-\frac{4im}{3r_0}\varepsilon V_n^m\frac{1}{\sin\theta}\left(\frac{dP_n^m}{d\theta}\frac{dP_q^m}{d\theta}+\frac{m^2}{\sin^2\theta}P_n^mP_q^m\right)$$

$$+\left(\frac{2}{3}\frac{d}{dr_0}(r_0\varepsilon)\frac{dW_n^m}{dr_0}+\frac{2}{3}r_0\varepsilon\frac{d^2W_n^m}{dr_0^2}-\frac{2}{3}\varepsilon\frac{dW_n^m}{dr_0}\right)P_n^m\frac{dP_q^m}{d\theta}-\frac{2}{3r_0}n(n+1)\varepsilon W_n^mP_n^m\frac{dP_q^m}{d\theta}$$

$$+\frac{4}{3r_0}\varepsilon W_n^m\frac{m^2}{\sin\theta}\left(\frac{P_q^m}{\sin\theta}\frac{dP_n^m}{d\theta}+\frac{P_n^m}{\sin\theta}\frac{dP_q^m}{d\theta}\right)-\frac{4}{3r_0}\varepsilon W_n^m\cot\theta\left(\frac{dP_n^m}{d\theta}\frac{dP_q^m}{d\theta}+\frac{m^2}{\sin^2\theta}P_n^m\right)\Bigg\}$$

$$\times P_2^1+\Bigg\{-im\Bigg(\frac{2}{3r_0}\varepsilon U_n^m+\frac{2}{3r_0}\frac{d}{dr_0}(r_0\varepsilon)U_n^m+\frac{4}{3}\frac{d}{dr_0}(r_0\varepsilon)\frac{dV_n^m}{dr_0}-\frac{2}{3r_0}\varepsilon V_n^m$$

$$-\frac{2}{3r_0}\frac{d}{dr_0}(r_0\varepsilon)V_n^m\Bigg)\left(\frac{P_q^m}{\sin\theta}\frac{dP_n^m}{d\theta}+\frac{P_n^m}{\sin\theta}\frac{dP_q^m}{d\theta}\right)+\Bigg(\frac{4}{3}\frac{d}{dr_0}(r_0\varepsilon)\frac{dW_n^m}{dr_0}-\frac{2}{3r_0}\varepsilon W_n^m$$

$$-\frac{2}{3r_0}\frac{d}{dr_0}(r_0\varepsilon)W_n^m\Bigg)\left(\frac{dP_n^m}{d\theta}\frac{dP_q^m}{d\theta}+\frac{m^2}{\sin^2\theta}P_n^mP_q^m\right)\Bigg\}P_2\Bigg]r_0^2\sin\theta dr_0d\theta d\phi$$

$$-\int_{(r_0)_k}^{(r_0)_{k+1}}\int_0^\pi\int_0^{2\pi}\sum_{q=|m|}^{N_k}\sum_{n=|m|}^{N_k}\frac{dW_q^m}{dr_0}\left(\frac{2}{3\rho_0}\frac{d}{dr_0}(r_0^3\varepsilon)\frac{d\mu}{dr_0}\right)\Bigg[-im\Bigg\{\frac{U_n^m}{r_0}+\frac{dV_n^m}{dr_0}-\frac{V_n^m}{r_0}\Bigg\}$$

$$\times P_2\left(\frac{P_n^m}{\sin\theta}\frac{dP_q^m}{d\theta}+\frac{P_q^m}{\sin\theta}\frac{dP_n^m}{d\theta}\right)+\left\{\frac{dW_n^m}{dr_0}-\frac{W_n^m}{r_0}\right\}P_2\left(\frac{dP_n^m}{d\theta}\frac{dP_q^m}{d\theta}+\frac{m^2}{\sin^2\theta}P_n^mP_q^m\right)\Bigg]$$

$$\times\sin\theta dr_0d\theta d\phi$$

$$+\int_0^\pi\int_0^{2\pi}\sum_{q=|m|}^{N_k}\sum_{n=|m|}^{N_k}\Bigg[U_q^m\Bigg\{-\left(g_0-\frac{r_0}{6}\right)U_n^mP_n^mP_q^m+\frac{4}{3}\varepsilon\left(g_0-\frac{r_0}{6}\right)U_n^mP_2P_n^mP_q^m$$

$$-\frac{2}{3}\frac{d}{dr_0}(r_0\varepsilon)g_0U_n^mP_2P_n^mP_q^m-\frac{2}{3}\varepsilon g_0V_n^mP_2^1\frac{dP_n^m}{d\theta}P_q^m-\frac{2im}{3}\varepsilon g_0W_n^m\frac{P_2^1}{\sin\theta}P_n^mP_q^m$$

$$+X_n^mP_n^mP_q^m-\frac{4}{3}\varepsilon X_n^mP_2P_n^mP_q^m\Bigg\}+\frac{2}{3}\varepsilon V_q^m\Bigg\{-\left(g_0-\frac{r_0}{6}\right)U_n^m+X_n^m\Bigg\}P_2^1\frac{dP_q^m}{d\theta}P_n^m$$

$$+2im\varepsilon W_q^m\Bigg\{-\left(g_0-\frac{r_0}{6}\right)U_n^m+X_n^m\Bigg\}\cos\theta P_n^mP_q^m\Bigg]r_0^2\sin\theta d\theta d\phi$$

$$+\int_0^\pi\int_0^{2\pi}\sum_{q=|m|}^{N_k}\sum_{n=|m|}^{N_k}\lambda\Bigg[U_q^m\Bigg\{\left(\frac{dU_n^m}{dr_0}+\frac{2U_n^m-n(n+1)V_n^m}{r_0}\right)P_n^m-\frac{2}{3}\varepsilon\Bigg(\frac{dU_n^m}{dr_0}$$

$$+\frac{2U_n^m-n(n+1)V_n^m}{r_0}\Bigg)P_2P_n^m+\frac{2}{3}r_0\frac{d\varepsilon}{dr_0}\frac{dU_n^m}{dr_0}P_2P_n^m+\frac{4}{3}\varepsilon\frac{dV_n^m}{dr_0}P_2^1\frac{dP_n^m}{d\theta}$$

$$-4\varepsilon\frac{dV_n^m}{dr_0}P_2P_n^m\Bigg\}P_q^m+\frac{2}{3}\varepsilon V_q^m\left(\frac{dU_n^m}{dr_0}+\frac{2U_n^m-n(n+1)V_n^m}{r_0}\right)P_2^1\frac{dP_q^m}{d\theta}P_n^m$$

$$
-\frac{2im}{3}\varepsilon W_q^m\left(\frac{dU_n^m}{dr_0}+\frac{2U_n^m-n(n+1)V_n^m}{r_0}\right)\frac{P_2^1}{\sin\theta}P_n^mP_q^m\Bigg]r_0^2\sin\theta d\theta d\phi
$$

$$
-\int_0^{\pi}\int_0^{2\pi}\sum_{q=|m|}^{N_k}\sum_{n=|m|}^{N_k}\Bigg[2\mu U_q^m\Bigg\{\frac{dU_n^m}{dr_0}P_n^m-\frac{4}{3}\varepsilon\frac{dU_n^m}{dr_0}P_2P_n^m+\frac{2}{3}\frac{d}{dr_0}(r_0\varepsilon)\frac{dU_n^m}{dr_0}P_2P_n^m
$$

$$
-2im\varepsilon\left(\frac{dW_n^m}{dr_0}-\frac{1}{r_0}W_n^m\right)\cos\theta P_n^m+\frac{2}{3}\varepsilon\left(\frac{dV_n^m}{dr_0}-\frac{1}{r_0}V_n^m-\frac{1}{r_0}U_n^m\right)P_2^1\frac{dP_n^m}{d\theta}\Bigg\}P_q^m
$$

$$
+\frac{dV_q^m}{dr_0}\frac{\mu\varepsilon}{r_0}\Bigg\{-2im\left(\frac{dW_n^m}{dr_0}-\frac{1}{r_0}W_n^m\right)\cos\theta P_n^m+\frac{2}{3}\left(\frac{dV_n^m}{dr_0}-\frac{1}{r_0}V_n^m-\frac{1}{r_0}U_n^m\right)P_2^1\frac{dP_n^m}{d\theta}\Bigg\}P_q^m
$$

$$
+V_q^m\mu\Bigg\{\frac{2}{3}\left(\varepsilon\frac{dU_n^m}{dr_0}+\frac{2\varepsilon}{r_0}U_n^m+r_0\varepsilon\frac{d^2V_n^m}{dr_0^2}+\frac{d}{dr_0}(r_0\varepsilon)\frac{dV_n^m}{dr_0}-\varepsilon\frac{dV_n^m}{dr_0}\right)P_2^1\frac{dP_q^m}{d\theta}P_n^m
$$

$$
+\left(\frac{U_n^m}{r_0}+\frac{dV_n^m}{dr_0}-\frac{V_n^m}{r_0}\right)\left(\frac{dP_n^m}{d\theta}\frac{dP_q^m}{d\theta}+\frac{m^2}{\sin^2\theta}P_n^mP_q^m\right)-\frac{4}{3}\varepsilon\left(\frac{U_n^m}{r_0}+\frac{dV_n^m}{dr_0}-\frac{V_n^m}{r_0}\right)
$$

$$
\times P_2\left(\frac{dP_n^m}{d\theta}\frac{dP_q^m}{d\theta}+\frac{m^2}{\sin^2\theta}P_n^mP_q^m\right)+\frac{2}{3}\left(\frac{\varepsilon}{r_0}U_n^m+\frac{d}{dr_0}(r_0\varepsilon)\frac{dV_n^m}{dr_0}-\frac{\varepsilon}{r_0}V_n^m\right)\left(\frac{dP_n^m}{d\theta}\frac{dP_q^m}{d\theta}\right.
$$

$$
\left.+\frac{m^2}{\sin^2\theta}P_n^mP_q^m\right)P_2+im\left(\frac{dW_n^m}{dr_0}-\frac{1}{r_0}W_n^m\right)\left(\frac{P_n^m}{\sin\theta}\frac{dP_q^m}{d\theta}+\frac{P_q^m}{\sin\theta}\frac{dP_n^m}{d\theta}\right)-\frac{4im}{3}\varepsilon\left(\frac{dW_n^m}{dr_0}\right.
$$

$$
\left.-\frac{1}{r_0}W_n^m\right)P_2\left(\frac{P_n^m}{\sin\theta}\frac{dP_q^m}{d\theta}+\frac{P_q^m}{\sin\theta}\frac{dP_n^m}{d\theta}\right)+\frac{2im}{3}\left(\frac{d}{dr_0}(r_0\varepsilon)\frac{dW_n^m}{dr_0}-\frac{\varepsilon}{r_0}W_n^m\right)\left(\frac{P_n^m}{\sin\theta}\frac{dP_q^m}{d\theta}\right.
$$

$$
\left.+\frac{P_q^m}{\sin\theta}\frac{dP_n^m}{d\theta}\right)P_2+\frac{2im}{3}\left(\frac{d}{dr_0}(r_0\varepsilon)\frac{dW_n^m}{dr_0}+r_0\varepsilon\frac{d^2W_n^m}{dr_0^2}-\varepsilon\frac{dW_n^m}{dr_0}\right)\frac{P_2^1}{\sin\theta}P_n^mP_q^m-\frac{4}{3r_0}\varepsilon V_n^m
$$

$$
\times\cot\theta\left(\frac{dP_n^m}{d\theta}\frac{dP_q^m}{d\theta}+\frac{m^2}{\sin^2\theta}P_n^mP_q^m\right)P_2^1-\frac{4}{3r_0}n(n+1)\varepsilon V_n^mP_n^m\frac{dP_q^m}{d\theta}P_2^1+\frac{4}{3r_0}\varepsilon V_n^m
$$

$$
\times\frac{m^2}{\sin\theta}\left(\frac{P_n^m}{\sin\theta}\frac{dP_q^m}{d\theta}+\frac{P_q^m}{\sin\theta}\frac{dP_n^m}{d\theta}\right)P_2^1-\frac{4im}{3r_0}\varepsilon W_n^m\cot\theta\left(\frac{P_n^m}{\sin\theta}\frac{dP_q^m}{d\theta}+\frac{P_q^m}{\sin\theta}\frac{dP_n^m}{d\theta}\right)P_2^1
$$

$$
-\frac{2im}{3r_0}n(n+1)\varepsilon W_n^m\frac{P_2^1}{\sin\theta}P_n^mP_q^m+\frac{4im}{3r_0}\varepsilon W_n^m\left(\frac{dP_n^m}{d\theta}\frac{dP_q^m}{d\theta}+\frac{m^2}{\sin^2\theta}P_n^mP_q^m\right)\frac{P_2^1}{\sin\theta}\Bigg\}
$$

$$
+\frac{dW_q^m}{dr_0}\frac{2\mu\varepsilon}{3}\Bigg\{-im\left(U_n^m+r_0\frac{dV_n^m}{dr_0}-V_n^m\right)\frac{P_2^1}{\sin\theta}P_n^mP_q^m+\left(r_0\frac{dW_n^m}{dr_0}-W_n^m\right)P_2^1\frac{dP_n^m}{d\theta}P_q^m\Bigg\}
$$

$$
+W_q^m\mu\Bigg\{im\left(-\frac{U_n^m}{r_0}-\frac{dV_n^m}{dr_0}+\frac{V_n^m}{r_0}\right)\left(\frac{P_n^m}{\sin\theta}\frac{dP_q^m}{d\theta}+\frac{P_q^m}{\sin\theta}\frac{dP_n^m}{d\theta}\right)-\frac{4im}{3}\varepsilon\left(-\frac{U_n^m}{r_0}-\frac{dV_n^m}{dr_0}\right.
$$

$$
\left.+\frac{V_n^m}{r_0}\right)P_2\left(\frac{P_n^m}{\sin\theta}\frac{dP_q^m}{d\theta}+\frac{P_q^m}{\sin\theta}\frac{dP_n^m}{d\theta}\right)-\frac{2im}{3}\left(\varepsilon\frac{dU_n^m}{dr_0}+\frac{2}{r_0}\varepsilon U_n^m+r_0\varepsilon\frac{d^2V_n^m}{dr_0^2}-\varepsilon\frac{dV_n^m}{dr_0}\right.
$$

$$+\frac{d}{dr_0}(r_0\varepsilon)\frac{dV_n^m}{dr_0}\Bigg)\frac{P_2^1}{\sin\theta}P_n^mP_q^m+\frac{2im}{3}\Bigg(-\frac{\varepsilon U_n^m}{r_0}-\frac{d}{dr_0}(r_0\varepsilon)\frac{dV_n^m}{dr_0}+\frac{\varepsilon V_n^m}{r_0}\Bigg)\Bigg(\frac{P_n^m}{\sin\theta}\frac{dP_q^m}{d\theta}$$
$$+\frac{P_q^m}{\sin\theta}\frac{dP_n^m}{d\theta}\Bigg)P_2+\left(\frac{dW_n^m}{dr_0}-\frac{W_n^m}{r_0}\right)\left(\frac{dP_n^m}{d\theta}\frac{dP_q^m}{d\theta}+\frac{m^2}{\sin^2\theta}P_n^mP_q^m\right)-\frac{4}{3}\varepsilon\left(\frac{dW_n^m}{dr_0}-\frac{W_n^m}{r_0}\right)$$
$$\times P_2\left(\frac{dP_n^m}{d\theta}\frac{dP_q^m}{d\theta}+\frac{m^2}{\sin^2\theta}P_n^mP_q^m\right)+\frac{2}{3}\left(\frac{d}{dr_0}(r_0\varepsilon)\frac{dW_n^m}{dr_0}-\frac{\varepsilon W_n^m}{r_0}\right)\left(\frac{dP_n^m}{d\theta}\frac{dP_q^m}{d\theta}\right.$$
$$\left.+\frac{m^2}{\sin^2\theta}P_n^mP_q^m\right)P_2+\frac{2}{3}\left(r_0\varepsilon\frac{d^2W_n^m}{dr_0^2}+\frac{d}{dr_0}(r_0\varepsilon)\frac{dW_n^m}{dr_0}-\varepsilon\frac{dW_n^m}{dr_0}\right)P_2^1\frac{dP_q^m}{d\theta}P_n^m$$
$$-\frac{4im}{r_0}\varepsilon V_n^m\cos^2\theta\left(\frac{P_n^m}{\sin\theta}\frac{dP_q^m}{d\theta}+\frac{P_q^m}{\sin\theta}\frac{dP_n^m}{d\theta}\right)-\frac{4im}{r_0}n(n+1)\varepsilon V_n^m\cos\theta P_n^mP_q^m$$
$$+\frac{4im}{r_0}\varepsilon V_n^m\cos\theta\left(\frac{dP_n^m}{d\theta}\frac{dP_q^m}{d\theta}+\frac{m^2}{\sin^2\theta}P_n^mP_q^m\right)+\frac{4m^2}{3r_0}\varepsilon W_n^m\left(\frac{P_n^m}{\sin\theta}\frac{dP_q^m}{d\theta}+\frac{P_q^m}{\sin\theta}\frac{dP_n^m}{d\theta}\right)$$
$$\times\frac{P_2^1}{\sin\theta}+\frac{4}{r_0}\varepsilon W_n^m\cos^2\theta\left(\frac{dP_n^m}{d\theta}\frac{dP_q^m}{d\theta}+\frac{m^2}{\sin^2\theta}P_n^mP_q^m\right)$$
$$\left.-\frac{2}{3r_0}n(n+1)\varepsilon W_n^mP_2^1\frac{dP_q^m}{d\theta}P_n^m\right\}\Bigg]r_0^2\sin d\theta d\phi, \tag{4.79}$$

where the subscript $k=1$ of the limits [i.e., $(r_0)_1$ and $(r_0)_2$] for the radial integration corresponds to the IC, whereas $k=2$ and $k=3$ correspond to the OC and the MT, respectively.

Now, using integration by parts among the spherical harmonics, then we get

$$\int_0^\pi\frac{1}{\sin\theta}\left(P_q^m\frac{dP_n^m}{d\theta}+P_n^m\frac{dP_q^m}{d\theta}\right)\sin\theta d\theta=P_n^mP_q^m|_0^\pi=0,\quad\text{if } m\neq0 \tag{4.80}$$

$$\int_0^\pi\frac{\cos\theta}{\sin\theta}\left(P_q^m\frac{dP_n^m}{d\theta}+P_n^m\frac{dP_q^m}{d\theta}\right)\sin\theta d\theta=\cos\theta P_n^mP_q^m|_0^\pi+\int_0^\pi P_n^mP_q^m\sin\theta d\theta, \tag{4.81}$$

$$\int_0^\pi\frac{P_2}{\sin\theta}\left(P_q^m\frac{dP_n^m}{d\theta}+P_n^m\frac{dP_q^m}{d\theta}\right)\sin\theta d\theta=P_2P_n^mP_q^m|_0^\pi+\int_0^\pi3\cos\theta P_n^mP_q^m\sin\theta d\theta, \tag{4.82}$$

$$\int_0^\pi\frac{\cos\theta}{\sin\theta}\left(P_q^m\frac{dP_n^m}{d\theta}+P_n^m\frac{dP_q^m}{d\theta}\right)P_2\sin\theta d\theta=\cos\theta P_2P_n^mP_q^m|_0^\pi$$
$$+\int_0^\pi\Big(1+3P_2\Big)P_n^mP_q^m\sin\theta d\theta, \tag{4.83}$$

$$\int_0^\pi \left(\frac{dP_q^m}{d\theta}\frac{dP_n^m}{d\theta}+\frac{m^2}{\sin^2\theta}P_n^m P_q^m\right)\sin\theta d\theta = \int_0^\pi n(n+1)P_n^m P_q^m \sin\theta d\theta, \tag{4.84}$$

$$\int_0^\pi \cos\theta\left(\frac{dP_q^m}{d\theta}\frac{dP_n^m}{d\theta}+\frac{m^2}{\sin^2\theta}P_n^m P_q^m\right)\sin\theta d\theta = \int_0^\pi \left(\sin\theta\frac{dP_n^m}{d\theta}+n(n+1)\right.$$
$$\left.\times\cos\theta P_n^m\right)P_q^m\sin\theta d\theta, \tag{4.85}$$

$$\int_0^\pi P_2\left(\frac{dP_q^m}{d\theta}\frac{dP_n^m}{d\theta}+\frac{m^2}{\sin^2\theta}P_q^m P_n^m\right)\sin\theta d\theta = \int_0^\pi n(n+1)P_2 P_q^m P_n^m\sin\theta d\theta$$
$$-\int_0^\pi P_2^1\frac{dP_n^m}{d\theta}P_q^m\sin\theta d\theta \tag{4.86}$$

$$\int_0^\pi P_2\cos\theta\left(\frac{dP_q^m}{d\theta}\frac{dP_n^m}{d\theta}+\frac{m^2}{\sin^2\theta}P_n^m P_q^m\right)\sin\theta d\theta = \int_0^\pi n(n+1)\cos\theta P_2 P_n^m P_q^m\sin\theta d\theta$$
$$-\frac{3}{2}\int_0^\pi P_2^1\cos\theta\frac{dP_n^m}{d\theta}P_q^m\sin\theta d\theta$$
$$-\frac{1}{2}\int_0^\pi \sin\theta\frac{dP_n^m}{d\theta}P_q^m\sin\theta d\theta, \tag{4.87}$$

$$\int_0^\pi P_2^1\frac{dP_q^m}{d\theta}P_n^m\sin\theta d\theta = \int_0^\pi\left(6P_2P_n^m - P_2^1\frac{dP_n^m}{d\theta}\right)P_q^m\sin\theta d\theta, \tag{4.88}$$

$$\int_0^\pi \sin\theta\frac{dP_q^m}{d\theta}P_n^m\sin\theta d\theta = -\int_0^\pi\left(2\cos\theta P_n^m+\sin\theta\frac{dP_n^m}{d\theta}\right)P_q^m\sin\theta d\theta \tag{4.89}$$

$$\int_0^\pi P_2\sin\theta\frac{dP_q^m}{d\theta}P_n^m\sin\theta d\theta = -\int_0^\pi\left(2\cos\theta P_2P_n^m+P_2\sin\theta\frac{dP_n^m}{d\theta}+\sin\theta P_2^1P_n^m\right)P_q^m\sin\theta d\theta \tag{4.90}$$

$$\int_0^\pi \cos\theta P_2^1\frac{dP_q^m}{d\theta}P_n^m\sin\theta d\theta = \int_0^\pi\left(-2\cos\theta P_n^m+8\cos\theta P_2P_n^m+\cos\theta P_2^1\frac{dP_n^m}{d\theta}\right)P_q^m\sin\theta d\theta \tag{4.91}$$

Using equations (4.80)-(4.91) in (4.79), we get

$$
\begin{aligned}
F_{1k} =& 2\pi \int_{(r_0)_k}^{(r_0)_{k+1}} \int_0^{\pi} \sum_{q=|m|}^{N_k} \sum_{n=|m|}^{N_k} \Bigg[\sigma^2 \Bigg\{ U_q^m U_n^m P_q^m P_n^m + n(n+1) \left(V_q^m V_n^m + W_q^m W_n^m \right) P_q^m P_n^m \\
&+ \frac{2}{3} r_0 \varepsilon \left(V_q^m \frac{dV_n^m}{dr_0} + W_q^m \frac{dW_n^m}{dr_0} \right) \left(6P_2 P_n^m - P_2^1 \frac{dP_n^m}{d\theta} \right) P_q^m + \frac{2}{3} r_0 \varepsilon \left(\frac{dV_q^m}{dr_0} V_n^m + \frac{dW_q^m}{dr_0} W_n^m \right) \\
&\times P_2^1 \frac{dP_n^m}{d\theta} P_n^m - 2imr_0 \varepsilon \left(V_q^m \frac{dW_n^m}{dr_0} + \frac{dV_q^m}{dr_0} W_n^m - W_q^m \frac{dV_n^m}{dr_0} - \frac{dW_q^m}{dr_0} V_n^m \right) \cos\theta P_q^m P_n^m \Bigg\} \\
&- \sigma \Bigg\{ m \left(U_q^m V_n^m + V_q^m U_n^m \right) P_q^m P_n^m + i \left(V_q^m W_n^m - W_q^m V_n^m \right) \left(\sin\theta \frac{dP_n^m}{d\theta} + n(n+1) \right. \\
&\times \cos\theta P_n^m \Big) + m \left(V_q^m V_n^m + W_q^m W_n^m \right) P_q^m P_n^m + i U_q^m W_n^m \sin\theta \frac{dP_n^m}{d\theta} P_q^m + i W_q^m U_n^m \\
&\times \left(2\cos\theta P_n^m + \sin\theta \frac{dP_n^m}{d\theta} \right) P_q^m + \frac{2i}{3} r_0 \varepsilon \left(V_q^m \frac{dW_n^m}{dr_0} - W_q^m \frac{dV_n^m}{dr_0} \right) \Big(-2\cos\theta P_n^m \\
&+ 8\cos\theta P_2 P_n^m + \cos\theta P_2^1 \frac{dP_n^m}{d\theta} \Big) P_q^m + \frac{2i}{3} r_0 \varepsilon \left(\frac{dV_q^m}{dr_0} W_n^m - \frac{dW_q^m}{dr_0} V_n^m \right) \cos\theta P_2^1 \frac{dP_n^m}{d\theta} P_n^m \\
&+ \frac{2i}{3} r_0 \varepsilon \left(U_q^m \frac{dW_n^m}{dr_0} - \frac{dW_q^m}{dr_0} U_n^m \right) \sin\theta P_2^1 P_n^m P_q^m - \frac{2m}{3} r_0 \varepsilon \left(V_q^m \frac{dV_n^m}{dr_0} + \frac{dV_q^m}{dr_0} V_n^m \right. \\
&+ W_q^m \frac{dW_n^m}{dr_0} + \frac{dW_q^m}{dr_0} W_n^m \Big) \left(1 + 2P_2 \right) P_q^m P_n^m \Bigg\} + U_q^m \left(g_0 - \frac{r_0}{6} \right) \Bigg\{ \Bigg(\frac{dU_n^m}{dr_0} \\
&+ \frac{2U_n^m - n(n+1)V_n^m}{r_0} \Bigg) P_n^m P_q^m + \frac{2}{3} \varepsilon \left(\frac{dU_n^m}{dr_0} + \frac{2U_n^m - n(n+1)V_n^m}{r_0} \right) P_2 P_n^m P_q^m \\
&+ \frac{2}{3} r_0 \frac{d\varepsilon}{dr_0} \frac{dU_n^m}{dr_0} P_2 P_n^m P_q^m + \frac{4}{3} \varepsilon \frac{dV_n^m}{dr_0} P_2^1 \frac{dP_n^m}{d\theta} P_q^m - 4\varepsilon \frac{dV_n^m}{dr_0} P_2 P_n^m P_q^m \Bigg\} \\
&+ U_q^m \left(\frac{2}{3} \frac{d}{dr_0} (r_0 \varepsilon) g_0 \right) \left(\frac{dU_n^m}{dr_0} + \frac{2U_n^m - n(n+1)V_n^m}{r_0} \right) P_2 P_n^m P_q^m + V_q^m \left(\frac{2}{3} \varepsilon g_0 \right) \\
&\times \left(\frac{dU_n^m}{dr_0} + \frac{2U_n^m - n(n+1)V_n^m}{r_0} \right) \left(6P_2 P_n^m - P_2^1 \frac{dP_n^m}{d\theta} \right) P_q^m + W_q^m \left(2im\varepsilon g_0 \right) \Bigg(\frac{dU_n^m}{dr_0} \\
&+ \frac{2U_n^m - n(n+1)V_n^m}{r_0} \Bigg) \cos\theta P_q^m P_n^m - \left(\frac{dU_q^m}{dr_0} + \frac{2U_q^m}{r_0} \right) \Bigg\{ - \left(g_0 - \frac{r_0}{6} \right) U_n^m P_n^m P_q^m \\
&- \frac{2}{3} \frac{d}{dr_0} (r_0 \varepsilon) g_0 U_n^m P_2 P_n^m P_q^m - \frac{2}{3} \varepsilon g_0 V_n^m P_2^1 \frac{dP_n^m}{d\theta} P_q^m + 2im\varepsilon g_0 W_n^m \cos\theta P_n^m P_q^m \\
&+ X_n^m P_n^m P_q^m \Bigg\} + V_q^m \left(\frac{q(q+1)}{r_0} \right) \Bigg\{ - \left(g_0 - \frac{r_0}{6} \right) U_n^m P_n^m P_q^m - \frac{2}{3} \frac{d}{dr_0} (r_0 \varepsilon) g_0 U_n^m P_2 P_n^m P_q^m
\end{aligned}
$$

$$-\frac{2}{3}\varepsilon g_0 V_n^m P_2^1 \frac{dP_n^m}{d\theta} P_q^m + 2im\varepsilon g_0 W_n^m \cos\theta P_n^m P_q^m + X_n^m P_n^m P_q^m \Big\} - \frac{2}{3}\varepsilon \left(\frac{dU_q^m}{dr_0} + \frac{2U_q^m}{r_0} \right)$$

$$\times \left\{ -\left(g_0 - \frac{r_0}{6} \right) U_n^m + X_n^m \right\} P_2 P_n^m P_q^m + \frac{2}{3}\varepsilon V_q^m \left(\frac{q(q+1)}{r_0} \right) \left\{ -\left(g_0 - \frac{r_0}{6} \right) U_n^m + X_n^m \right\}$$

$$\times P_2 P_n^m P_q^m + \frac{2}{3}\frac{dU_q^m}{dr_0} r_0 \frac{d\varepsilon}{dr_0} \left\{ \left(g_0 - \frac{r_0}{6} \right) U_n^m - X_n^m \right\} P_2 P_n^m P_q^m + 4\varepsilon \frac{dV_q^m}{dr_0} \left\{ -\left(g_0 - \frac{r_0}{6} \right) \right.$$

$$\left. \times U_n^m + X_n^m \right\} P_2 P_n^m P_q^m - \frac{4}{3}\varepsilon \frac{dV_q^m}{dr_0} \left\{ -\left(g_0 - \frac{r_0}{6} \right) U_n^m + X_n^m \right\} \left(6P_2 P_n^m - P_2^1 \frac{dP_n^m}{d\theta} \right) P_q^m \Big]$$

$$\times r_0^2 \sin\theta dr_0 d\theta$$

$$-2\pi \int_{(r_0)_k}^{(r_0)_{k+1}} \int_0^\pi \sum_{q=|m|}^{N_k} \sum_{n=|m|}^{N_k} \frac{2}{3}\frac{d}{dr_0}(r_0^3\varepsilon) \Big[\sigma^2 \Big\{ U_q^m U_n^m P_2 P_q^m P_n^m + \left(V_q^m V_n^m + W_q^m W_n^m \right)$$

$$\times \left(n(n+1) P_2 P_n^m P_q^m - P_2^1 \frac{dP_n^m}{d\theta} P_q^m \right) + 3im \left(V_q^m W_n^m - W_q^m V_n^m \right) \cos\theta P_n^m P_q^m$$

$$-\sigma \Big\{ m \left(U_q^m V_n^m + V_q^m U_n^m \right) P_2 P_q^m P_n^m + i \left(V_q^m W_n^m - W_q^m V_n^m \right) \Big(n(n+1) P_2 \cos\theta P_n^m P_q^m$$

$$-\frac{2}{3} P_2^1 \cos\theta \frac{dP_n^m}{d\theta} P_q^m - \frac{1}{2}\sin\theta \frac{dP_n^m}{d\theta} P_q^m \Big) + m \left(V_q^m V_n^m + W_q^m W_n^m \right) \left(1 + 3P_2 \right) P_n^m P_q^m$$

$$+ iU_q^m W_n^m P_2 \sin\theta \frac{dP_n^m}{d\theta} P_q^m + iW_q^m U_n^m \left(2\cos\theta P_2 P_n^m + P_2 \sin\theta \frac{dP_n^m}{d\theta} + \sin\theta P_2^1 P_n^m \right) P_q^m \Big\}$$

$$+ U_q^m \left(g_0 - \frac{r_0}{6} \right) \left(\frac{dU_n^m}{dr_0} + \frac{2U_n^m - n(n+1)V_n^m}{r_0} \right) P_2 P_n^m P_q^m - \left(\frac{dU_q^m}{dr_0} + \frac{2U_q^m}{r_0} \right)$$

$$\times \left\{ -\left(g_0 - \frac{r_0}{6} \right) U_n^m + X_n^m \right\} P_2 P_n^m P_q^m + V_q^m \left(\frac{q(q+1)}{r_0} \right) \left\{ -\left(g_0 - \frac{r_0}{6} \right) U_n^m + X_n^m \right\}$$

$$\times P_2 P_n^m P_q^m \Big] \sin\theta dr_0 d\theta$$

$$+2\pi \int_{(r_0)_k}^{(r_0)_{k+1}} \int_0^\pi \sum_{q=|m|}^{N_k} \sum_{n=|m|}^{N_k} \frac{\lambda}{\rho_0^2}\frac{d\rho_0}{dr_0} \Big[U_q^m \Big\{ \left(\frac{dU_n^m}{dr_0} + \frac{2U_n^m - n(n+1)V_n^m}{r_0} \right) P_n^m P_q^m$$

$$+\frac{2}{3}\varepsilon \left(\frac{dU_n^m}{dr_0} + \frac{2U_n^m - n(n+1)V_n^m}{r_0} \right) P_2 P_n^m P_q^m + \frac{2}{3} r_0 \frac{d\varepsilon}{dr_0} \frac{dU_n^m}{dr_0} P_2 P_n^m P_q^m + \frac{4}{3}\varepsilon \frac{dV_n^m}{dr_0}$$

$$\times P_2^1 \frac{dP_n^m}{d\theta} P_q^m - 4\varepsilon \frac{dV_n^m}{dr_0} P_2 P_n^m P_q^m + \frac{2}{3}\frac{d}{dr_0}(r_0\varepsilon) \left(\frac{dU_n^m}{dr_0} + \frac{2U_n^m - n(n+1)V_n^m}{r_0} \right) P_2 P_n^m P_q^m \Big\}$$

$$+\frac{2}{3}\varepsilon V_q^m \left(\frac{dU_n^m}{dr_0} + \frac{2U_n^m - n(n+1)V_n^m}{r_0} \right) \left(6P_2 P_n^m - P_2^1 \frac{dP_n^m}{d\theta} \right) P_q^m + 2im\varepsilon W_q^m \left(\frac{dU_n^m}{dr_0} \right.$$

$$+\frac{2U_n^m-n(n+1)V_n^m}{r_0}\Bigg)\cos\theta P_n^m P_q^m\Bigg]r_0^2\sin\theta dr_0 d\theta$$

$$-2\pi\int_{(r_0)_k}^{(r_0)_{k+1}}\int_0^{\pi}\sum_{q=|m|}^{N_k}\sum_{n=|m|}^{N_k}\frac{2}{3}\frac{d}{dr_0}(r_0^3\varepsilon)\frac{\lambda}{\rho_0^2}\frac{d\rho_0}{dr_0}\Bigg[U_q^m\Bigg(\frac{dU_n^m}{dr_0}+\frac{2U_n^m-n(n+1)V_n^m}{r_0}\Bigg)$$

$$\times P_2 P_n^m P_q^m\Bigg]\sin\theta dr_0 d\theta$$

$$-2\pi\int_{(r_0)_k}^{(r_0)_{k+1}}\int_0^{\pi}\sum_{q=|m|}^{N_k}\sum_{n=|m|}^{N_k}\frac{\lambda}{\rho_0}\Bigg[\Bigg(\frac{dU_q^m}{dr_0}+\frac{2U_q^m}{r_0}\Bigg)\Bigg\{\Bigg(\frac{dU_n^m}{dr_0}+\frac{2U_n^m-n(n+1)V_n^m}{r_0}\Bigg)$$

$$\times P_n^m P_q^m+\frac{4}{3}\varepsilon\Bigg(\frac{dU_n^m}{dr_0}+\frac{2U_n^m-n(n+1)V_n^m}{r_0}\Bigg)P_2 P_n^m P_q^m+\frac{2}{3}r_0\frac{d\varepsilon}{dr_0}\frac{dU_n^m}{dr_0}P_2 P_n^m P_q^m+\frac{4}{3}\varepsilon\frac{dV_n^m}{dr_0}$$

$$\times P_2^1\frac{dP_n^m}{d\theta}P_q^m-4\varepsilon\frac{dV_n^m}{dr_0}P_2 P_n^m P_q^m\Bigg\}-V_q^m\Bigg(\frac{q(q+1)}{r_0}\Bigg)\Bigg\{\Bigg(\frac{dU_n^m}{dr_0}+\frac{2U_n^m-n(n+1)V_n^m}{r_0}\Bigg)$$

$$\times P_n^m P_q^m+\frac{4}{3}\varepsilon\Bigg(\frac{dU_n^m}{dr_0}+\frac{2U_n^m-n(n+1)V_n^m}{r_0}\Bigg)P_2 P_n^m P_q^m+\frac{2}{3}r_0\frac{d\varepsilon}{dr_0}\frac{dU_n^m}{dr_0}P_2 P_n^m P_q^m$$

$$+\frac{4}{3}\varepsilon\frac{dV_n^m}{dr_0}P_2^1\frac{dP_n^m}{d\theta}P_q^m-4\varepsilon\frac{dV_n^m}{dr_0}P_2 P_n^m P_q^m\Bigg\}+\frac{2}{3}r_0\frac{d\varepsilon}{dr_0}\frac{dU_q^m}{dr_0}\Bigg(\frac{dU_n^m}{dr_0}+\frac{2U_n^m-n(n+1)V_n^m}{r_0}\Bigg)$$

$$\times P_2 P_n^m P_q^m+\frac{4}{3}\varepsilon\frac{dV_q^m}{dr_0}\Bigg(\frac{dU_n^m}{dr_0}+\frac{2U_n^m-n(n+1)V_n^m}{r_0}\Bigg)\Bigg(6P_2 P_n^m-P_2^1\frac{dP_n^m}{d\theta}\Bigg)P_q^m$$

$$-4\varepsilon\frac{dV_q^m}{dr_0}\Bigg(\frac{dU_n^m}{dr_0}+\frac{2U_n^m-n(n+1)V_n^m}{r_0}\Bigg)P_2 P_n^m P_q^m\Bigg]r_0^2\sin\theta dr_0 d\theta$$

$$+2\pi\int_{(r_0)_k}^{(r_0)_{k+1}}\int_0^{\pi}\sum_{q=|m|}^{N_k}\sum_{n=|m|}^{N_k}\frac{2}{3}\frac{d}{dr_0}(r_0^3\varepsilon)\frac{\lambda}{\rho_0}\Bigg[\Bigg(\frac{dU_q^m}{dr_0}+\frac{2U_q^m}{r_0}\Bigg)\Bigg(\frac{dU_n^m}{dr_0}$$

$$+\frac{2U_n^m-n(n+1)V_n^m}{r_0}\Bigg)P_2 P_n^m P_q^m-V_q^m\Bigg(\frac{q(q+1)}{r_0}\Bigg)\Bigg(\frac{dU_n^m}{dr_0}+\frac{2U_n^m-n(n+1)V_n^m}{r_0}\Bigg)$$

$$\times P_2 P_n^m P_q^m\Bigg]\sin\theta dr_0 d\theta$$

$$+2\pi\int_{(r_0)_k}^{(r_0)_{k+1}}\int_0^{\pi}\sum_{q=|m|}^{N_k}\sum_{n=|m|}^{N_k}U_q^m\frac{\mu}{\rho_0}\Bigg[\Bigg\{2\frac{d^2U_n^m}{dr_0^2}-n(n+1)U_n^m-4U_n^m+\frac{4}{r_0}\frac{dU_n^m}{dr_0}$$

$$+\frac{2}{3r_0}\varepsilon\frac{dU_n^m}{dr_0}-n(n+1)\Bigg(\frac{1}{r_0}\frac{dV_n^m}{dr_0}-3V_n^m\Bigg)+\frac{2}{3r_0}\Bigg(\frac{d}{dr_0}(r_0\varepsilon)\frac{dV_n^m}{dr_0}+r_0\varepsilon\frac{dV_n^m}{dr_0^2}$$

$$-3\varepsilon\frac{dV_n^m}{dr_0}\Bigg)\Bigg\}P_n^m+\Bigg\{\frac{8}{3}\frac{d}{dr_0}(r_0\varepsilon)\frac{d^2U_n^m}{dr_0^2}+\frac{4}{3}\frac{d^2}{dr_0^2}(r_0\varepsilon)\frac{d^2}{dr_0^2}(r_0\varepsilon)\frac{dU_n^m}{dr_0}+\frac{8}{3r_0}\Bigg(-r_0\varepsilon\frac{d^2V_n^m}{dr_0^2}$$

$$
-\frac{d}{dr_0}(r_0\varepsilon)\frac{dV_n^m}{dr_0}+3\varepsilon\frac{dV_n^m}{dr_0}\Bigg)-n(n+1)\Bigg(\frac{2}{3r_0}\frac{d}{dr_0}(r_0\varepsilon)\frac{dV_n^m}{dr_0}+\frac{2}{3r_0}\varepsilon\frac{dV_n^m}{dr_0}-4\varepsilon V_n^m\Bigg)
$$

$$
-\frac{4}{3}n(n+1)\varepsilon U_n^m+\frac{8}{3}\Bigg(\frac{1}{r_0}\frac{d}{dr_0}(r_0\varepsilon)\frac{dU_n^m}{dr_0}-2\varepsilon U_n^m\Bigg)\Bigg\}P_2P_n^m+\frac{4}{3r_0}\Bigg\{\varepsilon\frac{dU_n^m}{dr_0}+r_0\varepsilon\frac{d^2V_n^m}{d^2r_0}
$$

$$
+\frac{d}{dr_0}(r_0\varepsilon)\frac{dV_n^m}{dr_0}-3\varepsilon\frac{dV_n^m}{dr_0}\Bigg\}P_2^1\frac{dP_n^m}{d\theta}-\frac{2}{3r_0}\Bigg\{\varepsilon\frac{dU_n^m}{dr_0}+r_0\varepsilon\frac{d^2V_n^m}{d^2r_0}+\frac{d}{dr_0}(r_0\varepsilon)\frac{dV_n^m}{dr_0}
$$

$$
-3\varepsilon\frac{dV_n^m}{dr_0}\Bigg\}\Bigg(1+2P_2\Bigg)P_n^m\Bigg]P_q^m r_0^2\sin\theta dr_0d\theta
$$

$$
-2\pi\int_{(r_0)_k}^{(r_0)_{k+1}}\int_0^\pi\sum_{q=|m|}^{N_k}\sum_{n=|m|}^{N_k}U_q^m\frac{2}{3}\frac{d}{dr_0}(r_0^3\varepsilon)\frac{\mu}{\rho_0}\Bigg[2\frac{d^2U_n^m}{dr_0^2}-n(n+1)U_n^m-4U_n^m
$$

$$
+\frac{4}{r_0}\frac{dU_n^m}{dr_0}-n(n+1)\Bigg(\frac{1}{r_0}\frac{dV_n^m}{dr_0}-3V_n^m\Bigg)\Bigg]P_2P_n^mP_q^m\sin\theta dr_0d\theta
$$

$$
+2\pi\int_{(r_0)_k}^{(r_0)_{k+1}}\int_0^\pi\sum_{q=|m|}^{N_k}\sum_{n=|m|}^{N_k}U_q^m\frac{d\mu}{dr_0}\frac{1}{\rho_0}\Bigg[2\frac{dU_n^m}{dr_0}P_n^m+\frac{2}{3}\varepsilon\Bigg\{\frac{U_n^m}{r_0}-\frac{V_n^m}{r_0}+\frac{dV_n^m}{dr_0}\Bigg\}P_2^1\frac{dP_n^m}{d\theta}
$$

$$
+\frac{8}{3}\frac{d}{dr_0}(r_0\varepsilon)\frac{dU_n^m}{dr_0}P_2P_n^m-2im\varepsilon\Bigg\{\frac{dW_n^m}{dr_0}-\frac{W_n^m}{r_0}\Bigg\}\cos\theta P_n^m\Bigg]P_q^m r_0^2\sin\theta dr_0d\theta
$$

$$
-2\pi\int_{(r_0)_k}^{(r_0)_{k+1}}\int_0^\pi\sum_{q=|m|}^{N_k}\sum_{n=|m|}^{N_k}U_q^m\frac{4}{3}\frac{d}{dr_0}(r_0^3\varepsilon)\frac{d\mu}{dr_0}\frac{1}{\rho_0}\frac{dU_n^m}{dr_0}P_2P_n^mP_q^m\sin\theta dr_0d\theta
$$

$$
+2\pi\int_{(r_0)_k}^{(r_0)_{k+1}}\int_0^\pi\sum_{q=|m|}^{N_k}\sum_{n=|m|}^{N_k}\frac{dV_q^m}{dr_0}\Bigg(\frac{2}{3\rho_0}r_0\mu\varepsilon\Bigg)\Bigg[\Bigg\{\frac{1}{r_0}\frac{dU_n^m}{dr_0}+\frac{4}{r_n^2}U_n^m+\frac{d^2V_n^m}{dr_0^2}
$$

$$
+\frac{2}{r_0}\frac{dV_n^m}{dr_0}-\frac{2}{r_0^2}n(n+1)V_n^m\Bigg\}P_2^1\frac{dP_n^m}{d\theta}P_q^m-3im\Bigg\{\frac{d^2W_n^m}{dr_0^2}+\frac{2}{r_0}\frac{dW_n^m}{dr_0}-\frac{n(n+1)}{r_0^2}W_n^m\Bigg\}
$$

$$
\times\cos\theta P_n^mP_q^m\Bigg]r_0^2\sin\theta dr_0d\theta
$$

$$
+2\pi\int_{(r_0)_k}^{(r_0)_{k+1}}\int_0^\pi\sum_{q=|m|}^{N_k}\sum_{n=|m|}^{N_k}V_q^m\frac{\mu}{\rho_0}\Bigg[\Bigg\{\frac{1}{r_0}\frac{dU_n^m}{dr_0}+\frac{4}{r_n^2}U_n^m+\frac{d^2V_n^m}{dr_0^2}+\frac{2}{r_0}\frac{dV_n^m}{dr_0}+\frac{4}{r_0}\varepsilon\frac{dV_n^m}{dr_0}
$$

$$
-\frac{2}{r_0^2}n(n+1)V_n^m\Bigg\}n(n+1)P_n^mP_q^m-\frac{8m^2}{r_0}\varepsilon\frac{dV_n^m}{dr_0}P_n^mP_q^m+\frac{4im}{r_0}\varepsilon\frac{dW_n^m}{dr_0}\sin\theta\frac{dP_n^m}{d\theta}P_q^m
$$

$$
+\Bigg(\frac{2}{3}\varepsilon\frac{d^2U_n^m}{dr_0^2}+\frac{2}{3r_0}\frac{d}{dr_0}(r_0\varepsilon)\frac{dU_n^m}{dr_0}+\frac{4}{3r_0}\varepsilon\frac{dU_n^m}{dr_0}+\frac{2}{3}\frac{d^2}{dr_0^2}(r_0\varepsilon)\frac{dV_n^m}{dr_0}+\frac{4}{3}\varepsilon\frac{d^2V_n^m}{dr_0^2}
$$

$$
+\frac{4}{3}\frac{d}{dr_0}(r_0\varepsilon)\frac{d^2V_n^m}{dr_0^2}+\frac{2}{3}r_0\varepsilon\frac{d^3V_n^m}{dr_0^3}-\frac{20}{3r_0}\varepsilon\frac{dV_n^m}{dr_0}+\frac{4}{3r_0}\frac{d}{dr_0}(r_0\varepsilon)\frac{dV_n^m}{dr_0}\Bigg)\Bigg(6P_2P_n^mP_q^m
$$

$$
\begin{aligned}
&- P_2^1 \frac{dP_n^m}{d\theta} P_q^m \Bigg) + \frac{4}{3r_0}\varepsilon \frac{dV_n^m}{dr_0} n(n+1) P_n^m P_q^m + \frac{8}{3r_0}\varepsilon \frac{dV_n^m}{dr_0} n(n+1) P_2 P_n^m P_q^m - \frac{8}{3r_0}\varepsilon \frac{dV_n^m}{dr_0} \\
&\times P_2^1 \frac{dP_n^m}{d\theta} P_q^m - \frac{4}{r_0} n(n+1)\varepsilon \frac{dV_n^m}{dr_0} \left(6 P_2 P_n^m P_q^m - P_2^1 \frac{dP_n^m}{d\theta} P_q^m \right) - \frac{4}{3r_0}\varepsilon \frac{dV_n^m}{dr_0} \Bigg(6 P_2 P_n^m P_q^m \\
&- P_2^1 \frac{dP_n^m}{d\theta} P_q^m \Bigg) - \frac{8m^2}{r_0}\varepsilon \frac{dV_n^m}{dr_0} P_n^m P_q^m - 3im \Bigg(\frac{2}{3} \frac{d^2}{dr_0^2}(r_0\varepsilon) \frac{dW_n^m}{dr_0} + \frac{4}{3}\varepsilon \frac{d^2 W_n^m}{dr_0^2} - \frac{2}{3} r_0 \varepsilon \frac{d^3 W_n^m}{dr_0^3} \\
&+ \frac{4}{3} \frac{d}{dr_0}(r_0\varepsilon) \frac{d^2 W_n^m}{dr_0^2} - \frac{10}{3r_0}\varepsilon \frac{dW_n^m}{dr_0} + \frac{4}{3r_0} \frac{d}{dr_0}(r_0\varepsilon) \frac{dW_n^m}{dr_0} \Bigg) \cos\theta P_n^m P_q^m - \frac{4im}{r_0}\varepsilon \frac{dW_n^m}{dr_0} \\
&\times \sin\theta \frac{dP_n^m}{d\theta} P_q^m - \frac{4im}{r_0}\varepsilon \frac{dW_n^m}{dr_0} n(n+1) \cos\theta P_n^m P_q^m + \frac{2im}{r_0}\varepsilon \frac{dW_n^m}{dr_0} \cos\theta P_n^m P_q^m \\
&+ \frac{6im}{r_0}\varepsilon n(n+1) \frac{dW_n^m}{dr_0} \cos\theta P_n^m P_q^m + \Bigg(\frac{2}{3r_0}\varepsilon \frac{dU_n^m}{dr_0} + \frac{2}{3r_0} \frac{d}{dr_0}(r_0\varepsilon) \frac{dU_n^m}{dr_0} + \frac{16}{3r_0^2}\varepsilon U_n^m \\
&+ \frac{2}{3} \frac{d^2}{dr_0^2}(r_0\varepsilon) \frac{dV_n^m}{dr_0} + \frac{4}{3} \frac{d}{dr_0}(r_0\varepsilon) \frac{d^2 V_n^m}{dr_0^2} + \frac{4}{3r_0} \frac{d}{dr_0}(r_0\varepsilon) \frac{dV_n^m}{dr_0} - \frac{8}{3r_0^2} n(n+1)\varepsilon V_n^m \\
&- \frac{44}{3r_0}\varepsilon \frac{dV_n^m}{dr_0} \Bigg) \left(n(n+1) P_2 P_n^m P_q^m - P_2^1 \frac{dP_n^m}{d\theta} P_q^m \right) + 3im \Bigg(- \frac{8}{3r_0}\varepsilon \frac{dW_n^m}{dr_0} + \frac{2}{3} \frac{d^2}{dr_0^2}(r_0\varepsilon) \\
&\times \frac{dW_n^m}{dr_0} + \frac{4}{3} \frac{d}{dr_0}(r_0\varepsilon) \frac{d^2 W_n^m}{dr_0^2} + \frac{4}{3r_0} \frac{d}{dr_0}(r_0\varepsilon) \frac{dW_n^m}{dr_0} - \frac{4}{3r_0^2} n(n+1)\varepsilon W_n^m \Bigg) \cos\theta P_n^m P_q^m \Bigg] \\
&\times r_0^2 \sin\theta dr_0 d\theta \\
&- 2\pi \int_{(r_0)_k}^{(r_0)_{k+1}} \int_0^\pi \sum_{q=|m|}^{N_k} \sum_{n=|m|}^{N_k} V_q^m \left(\frac{2\mu}{3\rho_0} \frac{d}{dr_0}(r_0^3\varepsilon) \right) \Bigg[\Bigg\{ \frac{1}{r_0} \frac{dU_n^m}{dr_0} + \frac{4}{r_n^2} U_n^m + \frac{d^2 V_n^m}{dr_0^2} \\
&+ \frac{2}{r_0} \frac{dV_n^m}{dr_0} - \frac{2}{r_0^2} n(n+1) V_n^m \Bigg\} \left(n(n+1) P_2 P_n^m P_q^m - P_2^1 \frac{dP_n^m}{d\theta} P_q^m \right) + 3im \Bigg\{ \frac{d^2 W_n^m}{dr_0^2} \\
&+ \frac{2}{r_0} \frac{dW_n^m}{dr_0} - \frac{n(n+1)}{r_0^2} W_n^m \Bigg\} \cos\theta P_n^m P_q^m \Bigg] \sin\theta dr_0 d\theta \\
&+ 2\pi \int_{(r_0)_k}^{(r_0)_{k+1}} \int_0^\pi \sum_{q=|m|}^{N_k} \sum_{n=|m|}^{N_k} \frac{dV_q^m}{dr_0} \left(\frac{2}{3} \frac{1}{\rho_0} \frac{d\mu}{dr_0} r_0 \varepsilon \right) \Bigg[\Bigg\{ \frac{U_n^m}{r_0} + \frac{dV_n^m}{dr_0} - \frac{V_n^m}{r_0} \Bigg\} P_2^1 \frac{dP_n^m}{d\theta} P_q^m \\
&- 3im \Bigg\{ \frac{dW_n^m}{dr_0} - \frac{W_n^m}{r_0} \Bigg\} \cos\theta P_n^m P_q^m \Bigg] r_0^2 \sin\theta dr_0 d\theta \\
&+ 2\pi \int_{(r_0)_k}^{(r_0)_{k+1}} \int_0^\pi \sum_{q=|m|}^{N_k} \sum_{n=|m|}^{N_k} V_q^m \frac{1}{\rho_0} \frac{d\mu}{dr_0} \Bigg[\Bigg\{ \frac{U_n^m}{r_0} + \frac{dV_n^m}{dr_0} - \frac{V_n^m}{r_0} \Bigg\} n(n+1) P_n^m P_q^m
\end{aligned}
$$

$$+\left(\frac{2}{3}\varepsilon\frac{dU_n^m}{dr_0}+\frac{4}{3r_0}\varepsilon U_n^m-\frac{2}{3}\varepsilon\frac{dV_n^m}{dr_0}+\frac{2}{3}\frac{d}{dr_0}(r_0\varepsilon)\frac{dV_n^m}{dr_0}+\frac{2}{3}r_0\varepsilon\frac{d^2V_n^m}{dr_0^2}\right)\left(6P_2P_n^mP_q^m\right.$$

$$\left.-P_2^1\frac{dP_n^m}{d\theta}P_q^m\right)+\frac{4}{3r_0}\varepsilon V_n^m n(n+1)P_n^mP_q^m+\frac{8}{3r_0}\varepsilon V_n^m\left(n(n+1)P_2P_n^mP_q^m-P_2^1\frac{dP_n^m}{d\theta}P_q^m\right)$$

$$-\frac{4m^2}{r_0}\varepsilon V_n^mP_n^mP_q^m-\frac{4}{3r_0}n(n+1)\varepsilon V_n^m\left(6P_2P_n^mP_q^m-P_2^1\frac{dP_n^m}{d\theta}P_q^m\right)-3im\left(\frac{2}{3}r_0\varepsilon\frac{d^2W_n^m}{dr_0^2}\right.$$

$$\left.+\frac{2}{3}\frac{d}{dr_0}(r_0\varepsilon)\frac{dW_n^m}{dr_0}-\frac{2}{3}\varepsilon\frac{dW_n^m}{dr_0}\right)\cos\theta P_n^mP_q^m-\frac{4im}{r_0}\varepsilon W_n^m\left(\sin\theta\frac{dP_n^m}{d\theta}P_q^m+n(n+1)\right.$$

$$\left.\times\cos\theta P_n^mP_q^m\right)+\frac{2im}{r_0}n(n+1)\varepsilon W_n^m\cos\theta P_n^mP_q^m+\frac{8im}{r_0}\varepsilon W_n^m\cos\theta P_n^mP_q^m+\left(\frac{2}{3r_0}\varepsilon U_n^m\right.$$

$$+\frac{2}{3r_0}\frac{d}{dr_0}(r_0\varepsilon)U_n^m+\frac{4}{3}\frac{d}{dr_0}(r_0\varepsilon)\frac{dV_n^m}{dr_0}-\frac{2}{3r_0}\varepsilon V_n^m-\frac{2}{3r_0}\frac{d}{dr_0}(r_0\varepsilon)V_n^m\Big)\Big(n(n+1)P_2P_n^mP_q^m$$

$$\left.-P_2^1\frac{dP_n^m}{d\theta}P_q^m\right)+3im\left(\frac{4}{3}\frac{d}{dr_0}(r_0\varepsilon)\frac{dW_n^m}{dr_0}-\frac{2}{3r_0}\varepsilon W_n^m-\frac{2}{3r_0}\frac{d}{dr_0}(r_0\varepsilon)W_n^m\right)\cos\theta P_n^mP_q^m\Big]$$

$$\times r_0^2\sin\theta dr_0d\theta$$

$$-2\pi\int_{(r_0)_k}^{(r_0)_{k+1}}\int_0^\pi\sum_{q=|m|}^{N_k}\sum_{n=|m|}^{N_k}V_q^m\left(\frac{2}{3\rho_0}\frac{d}{dr_0}(r_0^3\varepsilon)\frac{d\mu}{dr_0}\right)\left[\left\{\frac{U_n^m}{r_0}+\frac{dV_n^m}{dr_0}-\frac{V_n^m}{r_0}\right\}\right.$$

$$\left.\times\left(n(n+1)P_2P_n^mP_q^m-P_2^1\frac{dP_n^m}{d\theta}P_q^m\right)+3im\left\{\frac{dW_n^m}{dr_0}-\frac{W_n^m}{r_0}\right\}\cos\theta P_n^mP_q^m\right]\sin\theta dr_0d\theta$$

$$+2\pi\int_{(r_0)_k}^{(r_0)_{k+1}}\int_0^\pi\sum_{q=|m|}^{N_k}\sum_{n=|m|}^{N_k}\frac{dW_q^m}{dr_0}\left(\frac{2}{3\rho_0}r_0\varepsilon\mu\right)\left[3im\left\{\frac{1}{r_0}\frac{dU_n^m}{dr_0}+\frac{4}{r_n^2}U_n^m+\frac{d^2V_n^m}{dr_0^2}\right.\right.$$

$$\left.+\frac{2}{r_0}\frac{dV_n^m}{dr_0}-\frac{2}{r_0^2}n(n+1)V_n^m\right\}\cos\theta P_n^mP_q^m+\left\{\frac{d^2W_n^m}{dr_0^2}+\frac{2}{r_0}\frac{dW_n^m}{dr_0}-\frac{n(n+1)}{r_0^2}W_n^m\right\}$$

$$\left.\times P_2^1\frac{dP_n^m}{d\theta}P_q^m\right]r_0^2\sin\theta dr_0d\theta$$

$$+2\pi\int_{(r_0)_k}^{(r_0)_{k+1}}\int_0^\pi\sum_{q=|m|}^{N_k}\sum_{n=|m|}^{N_k}W_q^m\frac{\mu}{\rho_0}\left[-\frac{8im}{r_0}\varepsilon\frac{dV_n^m}{dr_0}\left(2\cos\theta P_n^mP_q^m+\sin\theta\frac{dP_n^m}{d\theta}P_q^m\right)\right.$$

$$+\left\{\frac{d^2W_n^m}{dr_0^2}+\frac{2}{r_0}\frac{dW_n^m}{dr_0}-\frac{n(n+1)}{r_0^2}W_n^m+\frac{10}{3r_0}\varepsilon\frac{dW_n^m}{dr_0}\right\}n(n+1)P_n^mP_q^m-\frac{4m^2}{r_0}\varepsilon\frac{dW_n^m}{dr_0}P_n^mP_q^m$$

$$+3im\left(\frac{2}{3}\varepsilon\frac{d^2U_n^m}{dr_0^2}+\frac{4}{3r_0}\varepsilon\frac{dU_n^m}{dr_0}+\frac{2}{3r_0}\frac{d}{dr_0}(r_0\varepsilon)\frac{dU_n^m}{dr_0}+\frac{2}{3}\frac{d^2}{dr_0^2}(r_0\varepsilon)\frac{dV_n^m}{dr_0}+\frac{2}{3}r_0\varepsilon\frac{d^3V_n^m}{dr_0^3}\right.$$

$$+\frac{4}{3}\frac{d}{dr_0}(r_0\varepsilon)\frac{d^2V_n^m}{dr_0^2}+\frac{4}{3}\varepsilon\frac{d^2V_n^m}{dr_0^2}-\frac{20}{3r_0}\varepsilon\frac{dV_n^m}{dr_0}+\frac{4}{3r_0}\frac{d}{dr_0}(r_0\varepsilon)\frac{dV_n^m}{dr_0}-\frac{4}{3r_0}\varepsilon\frac{dV_n^m}{dr_0}$$

$$-\frac{4}{r_0}n(n+1)\varepsilon\frac{dV_n^m}{dr_0}\Bigg)\cos\theta P_n^m P_q^m+\frac{8im}{r_0}\varepsilon\frac{dV_n^m}{dr_0}\left(\sin\theta\frac{dP_n^m}{d\theta}+n(n+1)\cos\theta P_n^m P_q^m\right)$$

$$-\Bigg(-\frac{2}{3}\frac{d^2}{dr_0^2}(r_0\varepsilon)\frac{dW_n^m}{dr_0}-\frac{4}{3}\varepsilon\frac{d^2W_n^m}{dr_0^2}-\frac{4}{3}\frac{d}{dr_0}(r_0\varepsilon)\frac{d^2W_n^m}{dr_0^2}-\frac{2}{3}r_0\varepsilon\frac{d^3W_n^m}{dr_0^3}+\frac{10}{3r_0}\varepsilon\frac{dW_n^m}{dr_0}$$

$$-\frac{4}{3r_0}\frac{d}{dr_0}(r_0\varepsilon)\frac{dW_n^m}{dr_0}+\frac{2}{3r_0}\varepsilon\frac{dW_n^m}{dr_0}+\frac{2}{r_0}n(n+1)\varepsilon\frac{dW_n^m}{dr_0}\Bigg)\left(6P_2P_n^mP_q^m-P_2^1\frac{dP_n^m}{d\theta}P_q^m\right)$$

$$-\frac{4m^2}{r_0}\varepsilon\frac{dW_n^m}{dr_0}P_n^mP_q^m-\frac{2}{3r_0}\varepsilon\frac{dW_n^m}{dr_0}n(n+1)P_n^mP_q^m-\frac{4}{3r_0}\varepsilon\frac{dW_n^m}{dr_0}\Bigg(n(n+1)P_2P_n^mP_q^m$$

$$-P_2^1\frac{dP_n^m}{d\theta}P_q^m\Bigg)-3im\Bigg(\frac{2}{3r_0}\varepsilon\frac{dU_n^m}{dr_0}+\frac{16}{3r_0^2}\varepsilon U_n^m-\frac{4}{r_0}\varepsilon\frac{dV_n^m}{dr_0}+\frac{2}{3r_0}\frac{d}{dr_0}(r_0\varepsilon)\frac{dU_n^m}{dr_0}$$

$$+\frac{2}{3}\frac{d^2}{dr_0^2}(r_0\varepsilon)\frac{dV_n^m}{dr_0}+\frac{4}{3}\frac{d}{dr_0}(r_0\varepsilon)\frac{d^2V_n^m}{dr_0^2}+\frac{4}{3r_0}\frac{d}{dr_0}(r_0\varepsilon)\frac{dV_n^m}{dr_0}-\frac{8}{3r_0^2}n(n+1)\varepsilon V_n^m\Bigg)$$

$$\times\cos\theta P_n^mP_q^m-\frac{8im}{r_0}\varepsilon\frac{dV_n^m}{dr_0}\cos\theta P_n^mP_q^m-\Bigg(-\frac{2}{3}\frac{d^2}{dr_0^2}(r_0\varepsilon)\frac{dW_n^m}{dr_0}-\frac{4}{3}\frac{d}{dr_0}(r_0\varepsilon)\frac{d^2W_n^m}{dr_0^2}$$

$$+\frac{4}{r_0}\varepsilon\frac{dW_n^m}{dr_0}-\frac{4}{3r_0}\frac{d}{dr_0}(r_0\varepsilon)\frac{dW_n^m}{dr_0}+\frac{4}{3r_0^2}n(n+1)\varepsilon W_n^m\Bigg)\Bigg(n(n+1)P_2P_n^mP_q^m$$

$$-P_2^1\frac{dP_n^m}{d\theta}P_q^m\Bigg)\Bigg]r_0^2\sin\theta dr_0d\theta$$

$$-2\pi\int_{(r_0)_k}^{(r_0)_{k+1}}\int_0^\pi\sum_{q=|m|}^{N_k}\sum_{n=|m|}^{N_k}W_q^m\left(\frac{2\mu}{3\rho_0}\frac{d}{dr_0}(r_0^3\varepsilon)\right)\Bigg[-im\Bigg\{\frac{1}{r_0}\frac{dU_n^m}{dr_0}+\frac{4}{r_n^2}U_n^m+\frac{d^2V_n^m}{dr_0^2}$$

$$+\frac{2}{r_0}\frac{dV_n^m}{dr_0}-\frac{2}{r_0^2}n(n+1)V_n^m\Bigg\}\cos\theta P_n^mP_q^m+\Bigg\{\frac{d^2W_n^m}{dr_0^2}+\frac{2}{r_0}\frac{dW_n^m}{dr_0}-\frac{n(n+1)}{r_0^2}W_n^m\Bigg\}$$

$$\times\left(n(n+1)P_2P_n^mP_q^m-P_2^1\frac{dP_n^m}{d\theta}P_q^m\right)\Bigg]\Bigg]\sin\theta dr_0d\theta$$

$$+2\pi\int_{(r_0)_k}^{(r_0)_{k+1}}\int_0^\pi\sum_{q=|m|}^{N_k}\sum_{n=|m|}^{N_k}\frac{dW_q^m}{dr_0}\left(\frac{2}{3\rho_0}r_0\varepsilon\frac{d\mu}{dr_0}\right)\Bigg[3im\Bigg\{\frac{U_n^m}{r_0}+\frac{dV_n^m}{dr_0}-\frac{V_n^m}{r_0}\Bigg\}$$

$$\times\cos\theta P_n^mP_q^m+\Bigg\{\frac{dW_n^m}{dr_0}-\frac{W_n^m}{r_0}\Bigg\}P_2^1\frac{dP_n^m}{d\theta}P_q^m\Bigg]r_0^2\sin\theta dr_0d\theta$$

$$+2\pi\int_{(r_0)_k}^{(r_0)_{k+1}}\int_0^\pi\sum_{q=|m|}^{N_k}\sum_{n=|m|}^{N_k}W_q^m\frac{1}{\rho_0}\frac{d\mu}{dr_0}\Bigg[\Bigg\{\frac{dW_n^m}{dr_0}-\frac{W_n^m}{r_0}\Bigg\}n(n+1)P_n^mP_q^m+3im$$

$$\times\left(\frac{2}{3}\varepsilon\frac{dU_n^m}{dr_0}+\frac{4}{3r_0}\varepsilon U_n^m+\frac{2}{3}\frac{d}{dr_0}(r_0\varepsilon)\frac{dV_n^m}{dr_0}+\frac{2}{3}r_0\varepsilon\frac{d^2V_n^m}{dr_0^2}-\frac{2}{3}\varepsilon\frac{dV_n^m}{dr_0}-\frac{4}{3r_0}n(n+1)\varepsilon V_n^m\right)$$

$$\times\cos\theta P_n^m P_q^m-\frac{8im}{r_0}\varepsilon V_n^m\cos\theta P_n^m P_q^m+\frac{4im}{r_0}\varepsilon V_n^m\left(\sin\theta\frac{dP_n^m}{d\theta}P_q^m+n(n+1)\cos\theta P_n^m P_q^m\right)$$

$$+\left(\frac{2}{3}\frac{d}{dr_0}(r_0\varepsilon)\frac{dW_n^m}{dr_0}+\frac{2}{3}r_0\varepsilon\frac{d^2W_n^m}{dr_0^2}-\frac{2}{3}\varepsilon\frac{dW_n^m}{dr_0}-\frac{2}{3r_0}n(n+1)\varepsilon W_n^m\right)\left(P_2P_n^mP_q^m\right.$$

$$\left.-P_2^1\frac{dP_n^m}{d\theta}P_q^m\right)-\frac{4m^2}{r_0}\varepsilon W_n^m P_n^m P_q^m+\frac{4}{3r_0}\varepsilon W_n^m n(n+1)P_n^m P_q^m+\frac{8}{3r_0}\varepsilon W_n^m\left(n(n+1)\right.$$

$$\left.\times P_2P_n^mP_q^m-P_2^1\frac{dP_n^m}{d\theta}P_q^m\right)-3im\left(\frac{2}{3r_0}\varepsilon U_n^m+\frac{2}{3r_0}\frac{d}{dr_0}(r_0\varepsilon)U_n^m+\frac{4}{3}\frac{d}{dr_0}(r_0\varepsilon)\frac{dV_n^m}{dr_0}\right.$$

$$\left.-\frac{2}{3r_0}\varepsilon V_n^m-\frac{2}{3r_0}\frac{d}{dr_0}(r_0\varepsilon)V_n^m\right)\cos\theta P_n^m P_q^m+\left(\frac{4}{3}\frac{d}{dr_0}(r_0\varepsilon)\frac{dW_n^m}{dr_0}-\frac{2}{3r_0}\varepsilon W_n^m\right.$$

$$\left.-\frac{2}{3r_0}\frac{d}{dr_0}(r_0\varepsilon)W_n^m\right)\left(n(n+1)P_2P_n^mP_q^m-P_2^1\frac{dP_n^m}{d\theta}P_q^m\right)\Bigg]r_0^2\sin\theta dr_0d\theta$$

$$-2\pi\int_{(r_0)_k}^{(r_0)_{k+1}}\int_0^\pi\sum_{q=|m|}^{N_k}\sum_{n=|m|}^{N_k}\frac{dW_q^m}{dr_0}\left(\frac{2}{3\rho_0}\frac{d}{dr_0}(r_0^3\varepsilon)\frac{d\mu}{dr_0}\right)\Bigg[-im\left\{\frac{U_n^m}{r_0}+\frac{dV_n^m}{dr_0}-\frac{V_n^m}{r_0}\right\}$$

$$\times\cos\theta P_n^m P_q^m+\left\{\frac{dW_n^m}{dr_0}-\frac{W_n^m}{r_0}\right\}\left(n(n+1)P_2P_n^mP_q^m-P_2^1\frac{dP_n^m}{d\theta}P_q^m\right)\Bigg]\sin\theta dr_0d\theta$$

$$+2\pi\int_0^\pi\sum_{q=|m|}^{N_k}\sum_{n=|m|}^{N_k}\Bigg[U_q^m\Bigg\{-\left(g_0-\frac{r_0}{6}\right)U_n^mP_n^mP_q^m+\frac{4}{3}\varepsilon\left(g_0-\frac{r_0}{6}\right)U_n^mP_2P_n^mP_q^m$$

$$-\frac{2}{3}\frac{d}{dr_0}(r_0\varepsilon)g_0U_n^mP_2P_n^mP_q^m-\frac{2}{3}\varepsilon g_0V_n^mP_2^1\frac{dP_n^m}{d\theta}P_q^m+2im\varepsilon g_0W_n^m\cos\theta P_n^mP_q^m+X_n^mP_n^mP_q^m$$

$$-\frac{4}{3}\varepsilon X_n^mP_2P_n^mP_q^m\Bigg\}+\frac{2}{3}\varepsilon V_q^m\Bigg\{-\left(g_0-\frac{r_0}{6}\right)U_n^m+X_n^m\Bigg\}\left(6P_2P_n^mP_q^m-P_2^1\frac{dP_n^m}{d\theta}P_q^m\right)$$

$$+2im\varepsilon W_q^m\Bigg\{-\left(g_0-\frac{r_0}{6}\right)U_n^m+X_n^m\Bigg\}\cos\theta P_n^mP_q^m\Bigg]r_0^2\sin\theta d\theta$$

$$+2\pi\int_0^\pi\sum_{q=|m|}^{N_k}\sum_{n=|m|}^{N_k}\lambda\Bigg[U_q^m\Bigg\{\left(\frac{dU_n^m}{dr_0}+\frac{2U_n^m-n(n+1)V_n^m}{r_0}\right)P_n^m-\frac{2}{3}\varepsilon\left(\frac{dU_n^m}{dr_0}\right.$$

$$\left.+\frac{2U_n^m-n(n+1)V_n^m}{r_0}\right)P_2P_n^m+\frac{2}{3}r_0\frac{d\varepsilon}{dr_0}\frac{dU_n^m}{dr_0}P_2P_n^m+\frac{4}{3}\varepsilon\frac{dV_n^m}{dr_0}P_2^1\frac{dP_n^m}{d\theta}-4\varepsilon\frac{dV_n^m}{dr_0}P_2P_n^m\Bigg\}$$

$$\times P_q^m+\frac{2}{3}\varepsilon V_q^m\left(\frac{dU_n^m}{dr_0}+\frac{2U_n^m-n(n+1)V_n^m}{r_0}\right)\left(6P_2P_n^mP_q^m-P_2^1\frac{dP_n^m}{d\theta}P_q^m\right)$$

$$+2im\varepsilon W_q^m\left(\frac{dU_n^m}{dr_0}+\frac{2U_n^m-n(n+1)V_n^m}{r_0}\right)\cos\theta P_n^m P_q^m\Bigg]r_0^2\sin\theta d\theta$$

$$-2\pi\int_0^{\pi}\sum_{q=|m|}^{N_k}\sum_{n=|m|}^{N_k}\Bigg[2\mu U_q^m\Bigg\{\frac{dU_n^m}{dr_0}P_n^m-\frac{4}{3}\varepsilon\frac{dU_n^m}{dr_0}P_2P_n^m+\frac{2}{3}\frac{d}{dr_0}(r_0\varepsilon)\frac{dU_n^m}{dr_0}P_2P_n^m$$

$$-2im\varepsilon\left(\frac{dW_n^m}{dr_0}-\frac{1}{r_0}W_n^m\right)\cos\theta P_n^m+\frac{2}{3}\varepsilon\left(\frac{dV_n^m}{dr_0}-\frac{1}{r_0}V_n^m-\frac{1}{r_0}U_n^m\right)P_2^1\frac{dP_n^m}{d\theta}\Bigg\}P_q^m$$

$$+\frac{dV_q^m}{dr_0}\frac{\mu\varepsilon}{r_0}\Bigg\{-2im\left(\frac{dW_n^m}{dr_0}-\frac{1}{r_0}W_n^m\right)\cos\theta P_n^m+\frac{2}{3}\left(\frac{dV_n^m}{dr_0}-\frac{1}{r_0}V_n^m-\frac{1}{r_0}U_n^m\right)P_2^1\frac{dP_n^m}{d\theta}\Bigg\}$$

$$\times P_q^m+V_q^m\mu\Bigg\{\frac{2}{3}\left(\varepsilon\frac{dU_n^m}{dr_0}+\frac{2\varepsilon}{r_0}U_n^m+r_0\varepsilon\frac{d^2V_n^m}{dr_0^2}+\frac{d}{dr_0}(r_0\varepsilon)\frac{dV_n^m}{dr_0}-\varepsilon\frac{dV_n^m}{dr_0}\right)\Bigg(6P_2P_n^mP_q^m$$

$$-P_2^1\frac{dP_n^m}{d\theta}P_q^m\Bigg)+\left(\frac{U_n^m}{r_0}+\frac{dV_n^m}{dr_0}-\frac{V_n^m}{r_0}\right)n(n+1)P_n^mP_q^m-\frac{4}{3}\varepsilon\left(\frac{U_n^m}{r_0}+\frac{dV_n^m}{dr_0}-\frac{V_n^m}{r_0}\right)$$

$$\times\left(n(n+1)P_2P_n^mP_q^m-P_2^1\frac{dP_n^m}{d\theta}P_q^m\right)+\frac{2}{3}\left(\frac{\varepsilon}{r_0}U_n^m+\frac{d}{dr_0}(r_0\varepsilon)\frac{dV_n^m}{dr_0}-\frac{\varepsilon}{r_0}V_n^m\right)\Bigg(n(n+1)$$

$$\times P_2P_n^mP_q^m-P_2^1\frac{dP_n^m}{d\theta}P_q^m\Bigg)-4im\varepsilon\left(\frac{dW_n^m}{dr_0}-\frac{1}{r_0}W_n^m\right)\cos\theta P_n^mP_q^m+2im\Bigg(\frac{d}{dr_0}(r_0\varepsilon)\frac{dW_n^m}{dr_0}$$

$$-\frac{\varepsilon}{r_0}W_n^m\Bigg)\cos\theta P_n^mP_q^m-2im\left(\frac{d}{dr_0}(r_0\varepsilon)\frac{dW_n^m}{dr_0}+r_0\varepsilon\frac{d^2W_n^m}{dr_0^2}-\varepsilon\frac{dW_n^m}{dr_0}\right)\cos\theta P_n^mP_q^m$$

$$+\frac{4}{3r_0}\varepsilon V_n^m n(n+1)P_n^mP_q^m+\frac{8}{3r_0}\varepsilon V_n^m\left(n(n+1)P_2P_n^mP_q^m-P_2^1\frac{dP_n^m}{d\theta}P_q^m\right)-\frac{4}{3r_0}n(n+1)\varepsilon$$

$$\times V_n^m\left(6P_2P_n^mP_q^m-P_2^1\frac{dP_n^m}{d\theta}P_q^m\right)-\frac{4m^2}{r_0}\varepsilon V_n^mP_n^mP_q^m+\frac{8im}{r_0}\varepsilon W_n^m\cos\theta P_n^mP_q^m$$

$$+\frac{2im}{r_0}n(n+1)\varepsilon W_n^m\cos\theta P_n^mP_q^m-\frac{4im}{r_0}\varepsilon W_n^m\left(\sin\theta\frac{dP_n^m}{d\theta}P_q^m+n(n+1)\cos\theta P_n^mP_q^m\right)\Bigg\}$$

$$+\frac{dW_q^m}{dr_0}\frac{2\mu\varepsilon}{3}\Bigg\{3im\left(U_n^m+r_0\frac{dV_n^m}{dr_0}-V_n^m\right)\cos\theta P_n^mP_q^m+\left(r_0\frac{dW_n^m}{dr_0}-W_n^m\right)P_2^1\frac{dP_n^m}{d\theta}P_q^m\Bigg\}$$

$$+W_q^m\mu\Bigg\{-4im\varepsilon\left(-\frac{U_n^m}{r_0}-\frac{dV_n^m}{dr_0}+\frac{V_n^m}{r_0}\right)\cos\theta P_n^mP_q^m+2im\Bigg(\varepsilon\frac{dU_n^m}{dr_0}+\frac{2}{r_0}\varepsilon U_n^m$$

$$+r_0\varepsilon\frac{d^2V_n^m}{dr_0^2}-\varepsilon\frac{dV_n^m}{dr_0}+\frac{d}{dr_0}(r_0\varepsilon)\frac{dV_n^m}{dr_0}\Bigg)\cos\theta P_n^mP_q^m+2im\Bigg(-\frac{\varepsilon U_n^m}{r_0}-\frac{d}{dr_0}(r_0\varepsilon)\frac{dV_n^m}{dr_0}$$

$$+\frac{\varepsilon V_n^m}{r_0}\Bigg)\cos\theta P_n^mP_q^m+\left(\frac{dW_n^m}{dr_0}-\frac{W_n^m}{r_0}\right)n(n+1)P_n^mP_q^m-\frac{4}{3}\varepsilon\left(\frac{dW_n^m}{dr_0}-\frac{W_n^m}{r_0}\right)$$

$$\times\left(n(n+1)P_2P_n^mP_q^m-P_2^1\frac{dP_n^m}{d\theta}P_q^m\right)+\frac{2}{3}\left(\frac{d}{dr_0}(r_0\varepsilon)\frac{dW_n^m}{dr_0}-\frac{\varepsilon W_n^m}{r_0}\right)\Bigg(n(n+1)P_2P_n^mP_q^m$$

$$
\begin{aligned}
&- P_2^1 \frac{dP_n^m}{d\theta} P_q^m \Bigg) + \frac{2}{3}\left(r_0 \varepsilon \frac{d^2 W_n^m}{dr_0^2} + \frac{d}{dr_0}(r_0\varepsilon)\frac{dW_n^m}{dr_0} - \varepsilon \frac{dW_n^m}{dr_0} \right)\left(6P_2 P_n^m P_q^m - P_2^1 \frac{dP_n^m}{d\theta} P_q^m \right) \\
&- \frac{8im}{r_0}\varepsilon V_n^m \cos\theta P_n^m P_q^m - \frac{4im}{r_0} n(n+1)\varepsilon V_n^m \cos\theta P_n^m P_q^m - \frac{4m^2}{r_0}\varepsilon W_n^m P_n^m P_q^m + \frac{4im}{r_0}\varepsilon V_n^m \\
&\times \left(\sin\theta \frac{dP_n^m}{d\theta} P_q^m + n(n+1)\cos\theta P_n^m P_q^m \right) + \frac{8}{3r_0}\varepsilon W_n^m \left(n(n+1) P_2 P_n^m P_q^m - P_2^1 \frac{dP_n^m}{d\theta} P_q^m \right) \\
&+ \frac{4}{3r_0}\varepsilon W_n^m n(n+1) P_n^m P_q^m - \frac{2}{3r_0} n(n+1)\varepsilon W_n^m \left(6P_2 P_n^m P_q^m - P_2^1 \frac{dP_n^m}{d\theta} P_q^m \right) \Bigg\} \Bigg] r_0^2 \sin d\theta,
\end{aligned}
\tag{4.92}
$$

where we used the relations:

$$
\cos^2\theta = \frac{1}{3}(2P_2 + 1), \tag{4.93}
$$

$$
\frac{P_2^1}{\sin\theta} = -3\cos\theta \tag{4.94}
$$

$$
\cot\theta P_2^1 = -(2P_2 + 1). \tag{4.95}
$$

Similarly, using equations (2.24), (4.8), (4.9), (4.12), (4.15), (4.31), (4.32), and (4.80)-(4.91) in equation (4.14), then we get the Galerkin functional form of the Poisson equation

$$
\begin{aligned}
F_{2k} =& 2\pi \int_0^{\pi} \sum_{q=|m|}^{N_k} \sum_{n=|m|}^{N_k} X_q^m \Bigg[\frac{dX_n^m}{dr_0} P_n^m - \frac{4}{3}\varepsilon \frac{dX_n^m}{dr_0} P_2 P_n^m + \frac{2}{3}\frac{d}{dr_0}(r_0\varepsilon)\frac{dX_n^m}{dr_0} P_2 P_n^m + \frac{2}{3r_0}\varepsilon X_n^m \\
&\times P_2^1 \frac{dP_n^m}{d\theta} - 4\pi G\rho_0 \left\{ U_n^m P_n^m - \frac{4}{3}\varepsilon U_n^m P_2 P_n^m + \frac{2}{3}\varepsilon V_n^m P_2^1 \frac{dP_n^m}{d\theta} - 2im\varepsilon W_n^m \cos\theta P_n^m \right\} \Bigg] P_q^m \\
&\times r_0^2 \sin\theta d\theta \\
&- 2\pi \int_{(r_0)_k}^{(r_0)_{k+1}} \int_0^{\pi} \sum_{q=|m|}^{N_k} \sum_{n=|m|}^{N_k} \Bigg[\frac{dX_q^m}{dr_0}\frac{dX_n^m}{dr_0} P_n^m P_q^m + \frac{1}{r_0^2} n(n+1) X_n^m X_q^m P_n^m P_q^m \\
&+ \frac{4}{3}\frac{d}{dr_0}(r_0\varepsilon)\frac{dX_q^m}{dr_0}\frac{dX_n^m}{dr_0} P_2 P_n^m P_q^m + \frac{2}{3r_0}\varepsilon X_q^m \frac{dX_n^m}{dr_0} P_2^1 \frac{dP_q^m}{d\theta} P_n^m + \frac{2}{3r_0}\varepsilon \frac{dX_n^m}{dr_0} X_n^m P_2^1 \frac{dP_n^m}{d\theta} P_q^m \\
&+ \frac{3}{4r_0^2}\varepsilon X_q^m X_n^m \left(n(n+1) P_2 P_n^m P_q^m - P_2^1 \frac{dP_n^m}{d\theta} P_q^m \right) \Bigg] r_0^2 \sin\theta dr_0 d\theta
\end{aligned}
$$

$$+2\pi\int_{(r_0)_k}^{(r_0)_{k+1}}\int_0^{\pi}\sum_{q=|m|}^{N_k}\sum_{n=|m|}^{N_k}\frac{2}{3}\frac{d}{dr_0}(r_0^3\varepsilon)\left[\frac{dX_q^m}{dr_0}\frac{dX_n^m}{dr_0}P_2P_n^mP_q^m+\frac{1}{r_0^2}X_q^mX_n^m\left(n(n+1)\right.\right.$$

$$\left.\left.\times P_2P_n^mP_q^m-P_2^1\frac{dP_n^m}{d\theta}P_q^m\right)\right]\sin\theta dr_0d\theta$$

$$+2\pi\int_{(r_0)_k}^{(r_0)_{k+1}}\int_0^{\pi}\sum_{q=|m|}^{N_k}\sum_{n=|m|}^{N_k}4\pi G\rho_0\left[\frac{dX_q^m}{dr_0}\left\{U_n^mP_n^mP_q^m+\frac{d}{dr_0}(r_0\varepsilon)U_n^mP_2P_n^mP_q^m\right\}\right.$$

$$+X_q^m\left\{\frac{n(n+1)}{r_0}V_n^mP_n^mP_q^m+\frac{2}{3r_0}V_n^m\left(n(n+1)P_2P_n^mP_q^m-P_2^1\frac{dP_n^m}{d\theta}P_q^m\right)+\frac{2}{3}\varepsilon\frac{dV_n^m}{dr_0}\right.$$

$$\left.\times\left(6P_2P_n^mP_q^m-P_2^1\frac{dP_n^m}{d\theta}P_q^m\right)\right\}+\frac{2}{3}\varepsilon\frac{dX_q^m}{dr_0}V_n^mP_2^1\frac{dP_n^m}{d\theta}P_q^m+2im\varepsilon\left\{\frac{1}{r_0}X_q^mW_n^m-X_q^m\frac{dW_n^m}{dr_0}\right.$$

$$\left.\left.-\frac{dX_q^m}{dr_0}W_n^m\right\}\cos\theta P_n^mP_q^m\right]r_0^2\sin\theta dr_0d\theta d\phi$$

$$-2\pi\int_{(r_0)_k}^{(r_0)_{k+1}}\int_0^{\pi}\sum_{q=|m|}^{N_k}\sum_{n=|m|}^{N_k}\frac{8}{3}\pi G\rho_0\frac{d}{dr_0}(r_0^3\varepsilon)\left[\frac{dX_q^m}{dr_0}U_n^mP_2P_n^mP_q^m+\frac{1}{r_0}X_q^mV_n^m\right.$$

$$\left.\times\left(n(n+1)P_2P_n^mP_q^m-P_2^1\frac{dP_n^m}{d\theta}P_q^m\right)+\frac{3im}{r_0}X_q^mW_n^m\cos\theta P_n^mP_q^m\right]\sin\theta dr_0d\theta. \qquad (4.96)$$

If we set $\varepsilon=0$ in equations (4.92) and (4.96), then equations (4.92) and (4.96) are valid for a spherical Earth model. In sections 3.2 and 3.3 of chapter 3, we show that the Galerkin functionals [(4.92) and (4.96)] give three sets of equations for the IC, the OC and the MT. These sets of equations lead to $4\{(N_1+1)L_1+\sum_{k=2}^{3}(N_k+1)(L_k+1)\}$ algebraic linear and homogeneous equations with same number of coefficients. These linear equations can then be written in matrix form. The roots of the determinant of the matrix are the non-dimensional frequencies σ of the normal modes. First, we consider the spherical Earth model, and compute the non-dimensional frequencies of the normal modes such as the Slichter modes, the spheroidal modes, the inertial modes of both the spherical OC with an elastic MT and spherical shell OC with an elastic IC and MT models as we will discuss in part I of the next chapter.

4.6 The Dynamical Equations of the Earth's Fluid Core for a Spheroidal Earth Model

The dynamical equations of the fluid core are given by equations (2.7), (2.12) and (2.13)

$$\omega^2\mathbf{u}_k - 2i\omega\Omega\hat{\mathbf{e}}_3\times\mathbf{u}_k - \mathbf{g}_0\nabla\cdot\mathbf{u}_k + \nabla(\mathbf{u}_k\cdot\mathbf{g}_0 + (V_1)_k) + \frac{1}{\rho_0}\nabla\cdot(\lambda\nabla\cdot\mathbf{u}_k\tilde{1}) = 0, \tag{4.97}$$

$$\nabla^2(V_1)_k - 4\pi G\nabla\cdot(\rho_0\mathbf{u}_k) = 0. \tag{4.98}$$

Kamruzzaman and Seyed Mahmoud [43] have computed the frequencies of the normal modes such as the Slichter modes, the spheroidal modes, the inertial modes of both the spherical OC with an elastic MT and spherical shell OC with an elastic IC and MT models using equations (4.97) and (4.98) of the OC. However, these equations are unable to describe the OC flow i.e., the inertial modes of the OC for a spheroidal Earth model (e.g, Seyed-Mahmoud and Rochester [38], Rochester and Crossley [78], Rochester et al. [60]). We have scaled analysis of equations (4.97) and (4.98) in terms of the ellipticity because the wobble and nutation modes depend on the shape of the Earth i.e., the ellipticity of the Earth. For low frequency (long period) modes: $\omega\sim\varepsilon\Omega$ [78], and we get from equation (4.4) $\Omega^2\sim\varepsilon G\rho_0$. Therefore

1st Term: $\omega^2\mathbf{u}\sim\varepsilon^2\Omega^2\mathbf{u} = \varepsilon^3 G\rho_0\mathbf{u}$

2nd Term: $\omega\Omega\hat{\mathbf{e}}_3\times\mathbf{u}\sim\varepsilon\Omega^2\hat{\mathbf{e}}_3\times\mathbf{u} = \varepsilon^2 G\rho_0\hat{\mathbf{e}}_3\times\mathbf{u}$

We show that the 1st and 2nd terms of equation (4.97) are 3rd and 2nd order in terms of ellipticity, respectively, whereas the other terms are 1st order [78]. This means that the 3rd, 4th and 5th terms of this equation dominate in terms of ellipticity. However, the inertial modes of the OC mainly depends on the Coriolis term (2nd term). That is why, equations (4.97) and (4.98) are unable to describe the OC flow for a spheroidal Earth model. To overcome this problem, the dynamical equations of the fluid core may be written in the

form [78]

$$\sigma^2\mathbf{u} - i\sigma\hat{\mathbf{e}}_3\times\mathbf{u} - \beta\mathbf{g}_0\nabla\cdot\mathbf{u} - \nabla\zeta = 0, \tag{4.99}$$

$$\zeta + \frac{\lambda}{\rho_0}\nabla\cdot\mathbf{u} + \mathbf{u}\cdot\mathbf{g}_0 + V_1 = 0, \tag{4.100}$$

$$\nabla^2 V_1 - \frac{4\pi G\rho_0^2}{\lambda}\left(\zeta + V_1 + \beta\mathbf{u}\cdot\mathbf{g}_0\right) = 0, \tag{4.101}$$

where the subscript k of the field variables in equations (4.99)-(4.101) is dropped for convenience, and ζ is the reduced pressure. Note that Rochester and Crossley [78] did not account for the inertial term (1st term) of the momentum equation (4.99), and computed the eigenperiods for the CW and ICW. However, their formulation is insufficient for computing the periods of the inertial-gravity modes of the OC such as the FCN. To justify the above equations of the fluid core, we will compute the eigenfrequencies of the inertial modes of the OC with a rigid boundary for a spheroidal Earth model as shown in section 5.3.

The Galerkin functional forms of equations (4.99) - (4.101) are

$$F_1 = \int_V \mathbf{u}^*\cdot\left[\sigma^2\mathbf{u} - i\sigma\hat{\mathbf{e}}_3\times\mathbf{u} - \beta\mathbf{g}_0\nabla\cdot\mathbf{u} - \nabla\zeta\right]dV, \tag{4.102}$$

$$F_2 = \int_V \zeta^*\frac{\rho_0}{\lambda}\left[\zeta + \mathbf{u}\cdot\mathbf{g}_0 + V_1\right]dV + \int_S \zeta^*(\hat{n}\cdot\mathbf{u})dS - \int_V \mathbf{u}\cdot\nabla\zeta^* dV, \tag{4.103}$$

$$F_3 = \int_S V_1^*(\hat{n}\cdot\nabla V_1)dS - \int_V \nabla V_1^*\cdot\nabla V_1 dV + \int_V V_1^*\frac{4\pi G\rho_0^2}{\lambda}\left(\zeta + V_1 + \beta\mathbf{u}\cdot\mathbf{g}_0\right)dV, \tag{4.104}$$

where the identity $\nabla\cdot(f\mathbf{A}) = f\nabla\cdot\mathbf{A} + \mathbf{A}\cdot\nabla f$ and the divergence theorem are used. The trial function of ζ corresponding to equations (2.22) and (2.23) can have

$$\zeta = \sum_{p=|m|}^{N_2} Z^m_{2p-|m|+1} Y^m_{2p-|m|+1}(\theta,\phi), \tag{4.105}$$

or

$$\zeta = \sum_{p=|m|}^{N_2} Z^m_{2p-|m|} Y^m_{2p-|m|}(\theta,\phi). \tag{4.106}$$

Hereafter, we will use the subscript n instead of the subscripts for equations (4.105) and (4.106). The radially dependent functions in equation (4.105) or (4.106) are expanded as

$$Z^m_n(r) = \sum_{l=0}^{L_2} K^m_{n,l}\, f_l(x), \tag{4.107}$$

for $n = |m|, |m|+1, |m|+2, \cdots, N_2$; where $K^m_{n,l}$ are constants, L_2 is the truncation level for the radial expansion and $f_l(x)$ are the Legendre polynomials of degree l. The argument of x for f_l is $-1 \leq x \leq 1$. The expression for x is given by equation (2.28).

The Galerkin formation of the dynamical equations of an elastic IC and MT leads to the boundary conditions at the ICB and CMB on the fluid side which are

$$BC_{fluid} = \pm \int_{S_k} (\hat{\mathbf{n}} \cdot \mathbf{u}^*)\{\mathbf{u} \cdot \mathbf{g}_0 + V_1\}_{r_k} dS \pm \int_{S_k} \frac{1}{\rho_0} \{\hat{\mathbf{n}} \cdot \tilde{\tau}_1\}_{r_k} \cdot \mathbf{u}^* dS, \tag{4.108}$$

[see equations (3.29) and (3.35)]. The '+' sign of equation (4.108) corresponds to the the ICB at $r_1 = a+$, and the '$-$' sign corresponds to the CMB at $r_2 = b-$.

Since $\hat{\mathbf{n}} \cdot \tilde{\mathbf{1}} \cdot \mathbf{u}^* = \hat{\mathbf{n}} \cdot \mathbf{u}^*$, and using equations (2.7) and (4.100) in (4.108), we get

$$BC_{fluid} = \pm \int_{S_k} (\hat{\mathbf{n}} \cdot \mathbf{u}^*)(-\zeta) dS. \tag{4.109}$$

This means that the boundary conditions at the ICB and CMB on the fluid side due to the dynamical equations of an elastic IC and MT are written in terms of the reduced pressure just inside of the OC.

4.7 Application of Clairaut Coordinate to Galerkin Functional Forms for the Dynamical Equations of the Earth's Fluid Core

In this section, we will expand the equations (4.102)-(4.104) in terms of the Clairaut coordinate. We already expanded all analogous terms relevant in equations (4.102)-(4.104) in terms of the Clairaut oordinate in sections 4.2 - 4.5. Using equations (4.5) - (4.8), (4.10), (4.17) -(4.18), (4.24), (4.80) - (4.91) and (4.107) in (4.102), we get

$$
\begin{aligned}
F_1 =& 2\pi\int_a^b\int_0^{\pi}\sum_{q=|m|}^{N_2}\sum_{n=|m|}^{N_2}\Bigg[\sigma^2\Bigg\{U_q^m U_n^m P_q^m P_n^m + n(n+1)\left(V_q^m V_n^m + W_q^m W_n^m\right)P_q^m P_n^m \\
&+ \frac{2}{3}r_0\varepsilon\left(V_q^m\frac{dV_n^m}{dr_0} + W_q^m\frac{dW_n^m}{dr_0}\right)\left(6P_2P_n^m - P_2^1\frac{dP_n^m}{d\theta}\right)P_q^m + \frac{2}{3}r_0\varepsilon\left(\frac{dV_q^m}{dr_0}V_n^m + \frac{dW_q^m}{dr_0}W_n^m\right) \\
&\times P_2^1\frac{dP_n^m}{d\theta}P_n^m - 2imr_0\varepsilon\left(V_q^m\frac{dW_n^m}{dr_0} + \frac{dV_q^m}{dr_0}W_n^m - W_q^m\frac{dV_n^m}{dr_0} - \frac{dW_q^m}{dr_0}V_n^m\right)\cos\theta P_q^m P_n^m\Bigg\} \\
&- \sigma\Bigg\{m\left(U_q^m V_n^m + V_q^m U_n^m\right)P_q^m P_n^m + i\left(V_q^m W_n^m - W_q^m V_n^m\right)\Bigg(\sin\theta\frac{dP_n^m}{d\theta} + n(n+1) \\
&\times\cos\theta P_n^m\Bigg) + m\left(V_q^m V_n^m + W_q^m W_n^m\right)P_q^m P_n^m + iU_q^m W_n^m\sin\theta\frac{dP_n^m}{d\theta}P_q^m + iW_q^m U_n^m \\
&\times\left(2\cos\theta P_n^m + \sin\theta\frac{dP_n^m}{d\theta}\right)P_q^m + \frac{2i}{3}r_0\varepsilon\left(V_q^m\frac{dW_n^m}{dr_0} - W_q^m\frac{dV_n^m}{dr_0}\right)\Bigg(-2\cos\theta P_n^m \\
&+ 8\cos\theta P_2P_n^m + \cos\theta P_2^1\frac{dP_n^m}{d\theta}\Bigg)P_q^m + \frac{2i}{3}r_0\varepsilon\left(\frac{dV_q^m}{dr_0}W_n^m - \frac{dW_q^m}{dr_0}V_n^m\right)\cos\theta P_2^1\frac{dP_n^m}{d\theta}P_n^m \\
&+ \frac{2i}{3}r_0\varepsilon\left(U_q^m\frac{dW_n^m}{dr_0} - \frac{dW_q^m}{dr_0}U_n^m\right)\sin\theta P_2^1 P_n^m P_q^m - \frac{2m}{3}r_0\varepsilon\left(V_q^m\frac{dV_n^m}{dr_0} + \frac{dV_q^m}{dr_0}V_n^m\right. \\
&\left.+ W_q^m\frac{dW_n^m}{dr_0} + \frac{dW_q^m}{dr_0}W_n^m\right)\left(1+2P_2\right)P_q^m P_n^m\Bigg\} + U_q^m\beta\left(g_0 - \frac{r_0}{6}\right)\Bigg\{\Bigg(\frac{dU_n^m}{dr_0} \\
&+ \frac{2U_n^m - n(n+1)V_n^m}{r_0}\Bigg)P_n^m P_q^m + \frac{2}{3}\varepsilon\left(\frac{dU_n^m}{dr_0} + \frac{2U_n^m - n(n+1)V_n^m}{r_0}\right)P_2P_n^m P_q^m \\
&+ \frac{2}{3}r_0\frac{d\varepsilon}{dr_0}\frac{dU_n^m}{dr_0}P_2P_n^m P_q^m + \frac{4}{3}\varepsilon\frac{dV_n^m}{dr_0}P_2^1\frac{dP_n^m}{d\theta}P_q^m - 4\varepsilon\frac{dV_n^m}{dr_0}P_2P_n^m P_q^m\Bigg\} \\
&+ U_q^m\beta\left(\frac{2}{3}\frac{d}{dr_0}(r_0\varepsilon)g_0\right)\left(\frac{dU_n^m}{dr_0} + \frac{2U_n^m - n(n+1)V_n^m}{r_0}\right)P_2P_n^m P_q^m + V_q^m\beta\left(\frac{2}{3}\varepsilon g_0\right)
\end{aligned}
$$

$$\times\left(\frac{dU_n^m}{dr_0}+\frac{2U_n^m-n(n+1)V_n^m}{r_0}\right)\left(6P_2P_n^m-P_2^1\frac{dP_n^m}{d\theta}\right)P_q^m+W_q^m\beta\left(2im\varepsilon g_0\right)\left(\frac{dU_n^m}{dr_0}\right.$$
$$\left.+\frac{2U_n^m-n(n+1)V_n^m}{r_0}\right)\cos\theta P_q^mP_n^m\Bigg]r_0^2\sin\theta dr_0d\theta$$
$$-2\pi\int_a^b\int_0^\pi\sum_{q=|m|}^{N_2}\sum_{n=|m|}^{N_2}\frac{2}{3}\frac{d}{dr_0}(r_0^3\varepsilon)\Bigg[\sigma^2\Bigg\{U_q^mU_n^mP_2P_q^mP_n^m+\left(V_q^mV_n^m+W_q^mW_n^m\right)$$
$$\times\left(n(n+1)P_2P_n^mP_q^m-P_2^1\frac{dP_n^m}{d\theta}P_q^m\right)+3im\left(V_q^mW_n^m-W_q^mV_n^m\right)\cos\theta P_n^mP_q^m$$
$$-\sigma\Bigg\{m\left(U_q^mV_n^m+V_q^mU_n^m\right)P_2P_q^mP_n^m+i\left(V_q^mW_n^m-W_q^mV_n^m\right)\left(n(n+1)P_2\cos\theta P_n^mP_q^m\right.$$
$$-\frac{2}{3}P_2^1\cos\theta\frac{dP_n^m}{d\theta}P_q^m-\frac{1}{2}\sin\theta\frac{dP_n^m}{d\theta}P_q^m\Bigg)+m\left(V_q^mV_n^m+W_q^mW_n^m\right)\left(1+3P_2\right)P_n^mP_q^m$$
$$+iU_q^mW_n^mP_2\sin\theta\frac{dP_n^m}{d\theta}P_q^m+iW_q^mU_n^m\left(2\cos\theta P_2P_n^m+P_2\sin\theta\frac{dP_n^m}{d\theta}+\sin\theta P_2^1P_n^m\right)P_q^m\Bigg\}$$
$$+U_q^m\beta\left(g_0-\frac{r_0}{6}\right)\left(\frac{dU_n^m}{dr_0}+\frac{2U_n^m-n(n+1)V_n^m}{r_0}\right)P_2P_n^mP_q^m\Bigg]\sin\theta dr_0d\theta$$
$$-2\pi\int_a^b\int_0^\pi\sum_{q=|m|}^{N_2}\sum_{n=|m|}^{N_2}\Bigg[U_q^m\left\{\frac{dZ_n^m}{dr_0}P_n^mP_q^m+\frac{d}{dr_0}(r_0\varepsilon)\frac{dZ_n^m}{dr_0}P_2P_n^mP_q^m\right\}$$
$$+V_q^m\Bigg\{\frac{n(n+1)}{r_0}Z_n^mP_n^mP_q^m+\frac{2}{3r_0}Z_n^m\left(n(n+1)P_2P_n^mP_q^m-P_2^1\frac{dP_n^m}{d\theta}P_q^m\right)+\frac{2}{3}\varepsilon\frac{dZ_n^m}{dr_0}$$
$$\times\left(6P_2P_n^mP_q^m-P_2^1\frac{dP_n^m}{d\theta}P_q^m\right)\Bigg\}+\frac{2}{3}\varepsilon\frac{dV_q^m}{dr_0}Z_n^mP_2^1\frac{dP_n^m}{d\theta}P_q^m-2im\varepsilon\Bigg\{\frac{1}{r_0}W_q^mZ_n^m-W_q^m\frac{dZ_n^m}{dr_0}$$
$$-\frac{dW_q^m}{dr_0}Z_n^m\Bigg\}\cos\theta P_n^mP_q^m\Bigg]r_0^2\sin\theta dr_0d\theta$$
$$+2\pi\int_a^b\int_0^\pi\sum_{q=|m|}^{N_2}\sum_{n=|m|}^{N_2}\frac{2}{3}\frac{d}{dr_0}(r_0^3\varepsilon)\Bigg[U_q^m\frac{dZ_n^m}{dr_0}P_2P_n^mP_q^m+\frac{1}{r_0}V_q^mZ_n^m\Bigg(n(n+1)P_2P_n^mP_q^m$$
$$-P_2^1\frac{dP_n^m}{d\theta}P_q^m\Bigg)-\frac{3im}{r_0}W_q^mZ_n^m\cos\theta P_n^mP_q^m\Bigg]\sin\theta dr_0d\theta. \tag{4.110}$$

Again, using equations (2.21), (4.8) -(4.12), (4.16) and (4.19) -(4.21) in equation (4.103),

$$
\begin{aligned}
F_2 = {} & 2\pi \int_a^b \int_0^\pi \sum_{q=|m|}^{N_2} \sum_{n=|m|}^{N_2} Z_q^m \frac{\rho_0}{\lambda} \left[Z_n^m P_n^m P_q^m - \left\{ \left(1 + \frac{2}{3} \frac{d}{dr_0} (r_0 \varepsilon) P_2 \right) g_0 - \frac{1}{6} r_0 \right\} U_n^m P_n^m P_q^m \right. \\
& \left. - \frac{2}{3} \varepsilon g_0 V_n^m P_2^1 \frac{dP_n^m}{d\theta} P_q^m + 2im\varepsilon g_0 W_n^m \cos\theta P_n^m P_q^m + X_n^m P_n^m P_q^m \right] r_0^2 \sin\theta dr_0 d\theta \\
& - 2\pi \int_a^b \int_0^\pi \sum_{q=|m|}^{N_2} \sum_{n=|m|}^{N_2} \frac{2}{3} \frac{d}{dr_0} (r_0^3 \varepsilon) Z_q^m \frac{\rho_0}{\lambda} \left[Z_n^m P_2 P_n^m P_q^m - \left\{ g_0 - \frac{1}{6} r_0 \right\} U_n^m P_2 P_n^m P_q^m \right. \\
& \left. + X_n^m P_2 P_n^m P_q^m \right] \sin\theta dr_0 d\theta \\
& \pm 2\pi \int_0^\pi \sum_{q=|m|}^{N_2} \sum_{n=|m|}^{N_2} Z_q^m(r_k) \left[U_n^m P_n^m P_q^m - \frac{4}{3} \varepsilon U_n^m P_2 P_n^m P_q^m + \frac{2}{3} \varepsilon P_2^1 V_n^m \frac{dP_n^m}{d\theta} P_q^m \right. \\
& \left. - 2im\varepsilon W_n^m \cos\theta P_n^m P_q^m \right]_{r_k} r_k^2 \sin\theta d\theta \\
& - 2\pi \int_a^b \int_0^\pi \sum_{q=|m|}^{N_2} \sum_{n=|m|}^{N_2} \left[\frac{dZ_q^m}{dr_0} \left\{ U_n^m P_n^m P_q^m + \frac{d}{dr_0} (r_0 \varepsilon) U_n^m P_2 P_n^m P_q^m \right\} \right. \\
& + Z_q^m \left\{ \frac{n(n+1)}{r_0} V_n^m P_n^m P_q^m + \frac{2}{3r_0} V_n^m \left(n(n+1) P_2 P_n^m P_q^m - P_2^1 \frac{dP_n^m}{d\theta} P_q^m \right) + \frac{2}{3} \varepsilon \frac{dV_n^m}{dr_0} \right. \\
& \left. \times \left(6 P_2 P_n^m P_q^m - P_2^1 \frac{dP_n^m}{d\theta} P_q^m \right) \right\} + \frac{2}{3} \varepsilon \frac{dZ_q^m}{dr_0} V_n^m P_2^1 \frac{dP_n^m}{d\theta} P_q^m + 2im\varepsilon \left\{ \frac{1}{r_0} Z_q^m W_n^m - X_q^m \frac{dW_n^m}{dr_0} \right. \\
& \left. \left. - \frac{dX_q^m}{dr_0} W_n^m \right\} \cos\theta P_n^m P_q^m \right] r_0^2 \sin\theta dr_0 d\theta \\
& + 2\pi \int_a^b \int_0^\pi \sum_{q=|m|}^{N_2} \sum_{n=|m|}^{N_2} \frac{2}{3} \frac{d}{dr_0} (r_0^3 \varepsilon) \left[\frac{dZ_q^m}{dr_0} U_n^m P_2 P_n^m P_q^m + \frac{1}{r_0} Z_q^m V_n^m \left(n(n+1) P_2 P_n^m P_q^m \right. \right. \\
& \left. \left. - P_2^1 \frac{dP_n^m}{d\theta} P_q^m \right) + \frac{3im}{r_0} Z_q^m W_n^m \cos\theta P_n^m P_q^m \right] \sin\theta dr_0 d\theta, \qquad (4.111)
\end{aligned}
$$

where '+' sign corresponds to the the ICB at $r_1 = a+$, and the '$-$' sign corresponds to the CMB at $r_2 = b-$.

Similarly, equation (4.104) gives

$$
\begin{aligned}
F_3 = \pm 2\pi \int_0^{\pi} \sum_{q=|m|}^{N_2} \sum_{n=|m|}^{N_2} X_q^m(r_k) \Bigg[& \frac{dX_n^m}{dr_0} P_n^m - \frac{4}{3}\varepsilon \frac{dX_n^m}{dr_0} P_2 P_n^m + \frac{2}{3}\frac{d}{dr_0}(r_0\varepsilon)\frac{dX_n^m}{dr_0} P_2 P_n^m \\
& + \frac{2}{3r_0}\varepsilon X_n^m P_2^1 \frac{dP_n^m}{d\theta} \Bigg]_{r_k} P_q^m r_k^2 \sin\theta d\theta \\
& - 2\pi \int_a^b \int_0^{\pi} \sum_{q=|m|}^{N_2} \sum_{n=|m|}^{N_2} \Bigg[\frac{dX_q^m}{dr_0}\frac{dX_n^m}{dr_0} P_n^m P_q^m + \frac{1}{r_0^2} n(n+1) X_n^m X_q^m P_n^m P_q^m \\
& + \frac{4}{3}\frac{d}{dr_0}(r_0\varepsilon)\frac{dX_q^m}{dr_0}\frac{dX_n^m}{dr_0} P_2 P_n^m P_q^m + \frac{2}{3r_0}\varepsilon X_q^m \frac{dX_n^m}{dr_0} P_2^1 \frac{dP_q^m}{d\theta} P_n^m + \frac{2}{3r_0}\varepsilon \frac{dX_n^m}{dr_0} X_n^m P_2^1 \frac{dP_n^m}{d\theta} P_q^m \\
& + \frac{3}{4r_0^2}\varepsilon X_q^m X_n^m \left(n(n+1) P_2 P_n^m P_q^m - P_2^1 \frac{dP_n^m}{d\theta} P_q^m \right) \Bigg] r_0^2 \sin\theta dr_0 d\theta \\
& + 2\pi \int_a^b \int_0^{\pi} \sum_{q=|m|}^{N_2} \sum_{n=|m|}^{N_2} \frac{2}{3}\frac{d}{dr_0}(r_0^3\varepsilon) \Bigg[\frac{dX_q^m}{dr_0}\frac{dX_n^m}{dr_0} P_2 P_n^m P_q^m + \frac{1}{r_0^2} X_q^m X_n^m \Bigg(n(n+1) P_2 P_n^m P_q^m \\
& - P_2^1 \frac{dP_n^m}{d\theta} P_q^m \Bigg) \Bigg] \sin\theta dr_0 d\theta \\
& + 2\pi \int_a^b \int_0^{\pi} \sum_{q=|m|}^{N_2} \sum_{n=|m|}^{N_2} \frac{4\pi G\rho_0^2}{\lambda} X_q^m \Bigg[Z_n^m P_n^m P_q^m - \beta \Bigg\{ \left(1 + \frac{2}{3}\frac{d}{dr_0}(r_0\varepsilon) P_2 \right) g_0 - \frac{1}{6} r_0 \Bigg\} U_n^m \\
& \times P_n^m P_q^m - \frac{2}{3}\varepsilon g_0 \beta V_n^m P_2^1 \frac{dP_n^m}{d\theta} P_q^m + 2im\varepsilon g_0 \beta W_n^m \cos\theta P_n^m P_q^m + X_n^m P_n^m P_q^m \Bigg] r_0^2 \sin\theta dr_0 d\theta \\
& - 2\pi \int_a^b \int_0^{\pi} \sum_{q=|m|}^{N_2} \sum_{n=|m|}^{N_2} \frac{8}{3}\frac{\pi G\rho_0^2}{\lambda}\frac{d}{dr_0}(r_0^3\varepsilon) Z_q^m \Bigg[Z_n^m P_2 P_n^m P_q^m - \beta \Bigg\{ g_0 - \frac{1}{6} r_0 \Bigg\} U_n^m P_2 P_n^m P_q^m \\
& + X_n^m P_2 P_n^m P_q^m \Bigg] \sin\theta dr_0 d\theta. \qquad (4.112)
\end{aligned}
$$

The Galerkin functionals for an elastic IC and MT [equations (4.92) and (4.96)], and a compressible OC [equations (4.110) - (4.112)] give to $4(N_1+1)L_1 + 5(N_2+1)(L_2+1) + 4(N_3+1)(L_3+1)$ algebraic linear and homogeneous equations with same number of coefficients. These linear equations can then be written in a matrix form. The roots of the determinant of the matrix are the non-dimensional frequencies σ of the normal modes for a spheroidal Earth model as we will discuss in part II of the next chapter.

4.8 Integration of Galerkin Functional Forms for the Dynamical Equations

The Galerkin functional has a form

$$F = \int_{(r_0)_k}^{(r_0)_{k+1}} \int_0^{\pi} \Bigg[S1_n(r_0) P_n^m + S2_n(r_0)\cos\theta P_n^m + S3_n(r_0)\sin\theta \frac{dP_n^m}{d\theta} + S4_n(r_0) P_2 P_n^m$$
$$+ S5_n(r_0) P_2^1 \frac{dP_n^m}{\theta} + S6_n(r_0)\left(6P_2P_n^m - P_2^1\frac{dP_n^m}{\theta}\right) + S7_n(r_0)\cos\theta P_2 P_n^m + S8_n(r_0)\sin\theta P_2^1 P_n^m$$
$$+ S9_n(r_0)\cos\theta P_2^1 \frac{dP_n^m}{d\theta} + S10_n(r_0)\sin\theta P_2 \frac{dP_n^m}{d\theta}\Bigg] P_q^m \sin\theta dr_0 d\theta, \tag{4.113}$$

where $S1_n$, $S2_n$, ..., $S10_n$ compose on the radial dependent variables U_n^m, V_n^m, W_n^m, X_n^m, and Z_n^m. In order to integrate equation (4.113) with respect to θ, we need the following identities:

$$\cos\theta P_n^m = G_n^m P_{n-1}^m + H_n^m P_{n+1}^m, \tag{4.114}$$

$$\sin\theta \frac{dP_n^m}{d\theta} = -(n+1)G_n^m P_{n-1}^m + nH_n^m P_{n+1}^m, \tag{4.115}$$

$$P_2 P_n^m = A_n^m P_{n-2}^m + B_n^m P_n^m + C_n^m P_{n+2}^m, \tag{4.116}$$

$$P_2^1 \frac{dP_n^m}{d\theta} = 2(n+1)A_n^m P_{n-2}^m + 3B_n^m P_n^m - 2nC_n^m P_{n+2}^m, \tag{4.117}$$

$$6P_2P_n^m - P_2^1\frac{dP_n^m}{\theta} = (4-2n)A_n^m P_{n-2}^m + 3B_n^m P_n^m + (2n+6)C_n^m P_{n+2}^m, \tag{4.118}$$

$$\cos\theta P_2 P_n^m = A_n^m G_{n-2}^m P_{n-3}^m + \left[2(n+1)A_n^m H_{n-2}^m + 3B_n^m G_n^m\right] P_{n-1}^m$$
$$+ \left[3B_n^m H_n^m - 2nC_n^m G_{n+2}^m\right] P_{n+1}^m - 2nC_n^m H_{n+2}^m P_{n+3}^m, \tag{4.119}$$

$$\sin\theta P_2^1 P_n^m = 3G_n^m G_{n-1}^m G_{n-2}^m P_{n-3}^m + 3G_n^m\left[G_{n-1}^m H_{n-2}^m + G_n^m H_{n-1}^m + G_{n+1}^m H_n^m - 1\right] P_{n-1}^m$$
$$+ 3H_n^m\left[G_n^m H_{n-1}^m + G_{n+1}^m H_n^m + G_{n+2}^m H_{n+1}^m - 1\right] P_{n+1}^m + 3H_n^m H_{n+1}^m H_{n+2}^m P_{n+3}^m, \tag{4.120}$$

$$\cos\theta P_2^1 \frac{dP_n^m}{d\theta} = 2(n+1)A_n^m G_{n-2}^m P_{n-3}^m + \left[2(n+1)A_n^m H_{n-2}^m + 3B_n^m G_n^m\right] P_{n-1}^m + \left[3B_n^m H_n^m - 2nC_n^m G_{n+2}^m\right] P_{n+1}^m - 2nC_n^m H_{n+2}^m P_{n+3}^m \tag{4.121}$$

$$P_2 \sin\theta \frac{dP_n^m}{d\theta} = -(n+1)A_{n-1}^m G_n^m P_{n-3}^m + \left[nA_{n+1}^m H_n^m - (n+1)B_{n-1}^m G_n^m\right] P_{n-1}^m + \left[nB_{n+1}^m H_n^m - (n+1)C_{n-1}^m G_n^m\right] P_{n+1}^m + nC_{n+1}^m H_n^m P_{n+3}^m, \tag{4.122}$$

where

$$G_n^m = \frac{n+m}{2n+1}, \tag{4.123}$$

$$H_n^m = \frac{n+1-m}{2n+1}, \tag{4.124}$$

$$A_n^m = \frac{3}{2}\frac{(n+m)(n+m-1)}{(2n+1)(2n-1)}, \tag{4.125}$$

$$B_n^m = \frac{n(n+1)-3m^2}{(2n+3)(2n-1)}, \tag{4.126}$$

$$C_n^m = \frac{3}{2}\frac{(n+2-m)(n+1-m)}{(2n+3)(2n+1)}. \tag{4.127}$$

Using equations (4.114) - (4.122) in equation (4.113), the Galerkin functional takes a form

$$F = \int_{(r_0)_k}^{(r_0)_{k+1}} S_n(r)dr \int_0^{\pi} P_n^m P_q^m \sin\theta d\theta. \tag{4.128}$$

The orthogonality relation is given by

$$\int_0^{\pi} P_n^m P_q^m \sin\theta d\theta = \frac{2}{2q+1}\frac{(q+m)!}{(q-m)!}\delta_{q,n}, \tag{4.129}$$

where $\delta_{q,n}$ is the Kronecker delta, which is zero for $n \neq q$ and 1 for $n = q$. Now the orthogonality relation is applied to the equation (4.128), and we remove the θ dependence from the equation (4.128). We apply this technique to develop an algorithm based on the work of Seyed-Mahmoud [81] to integrate the Galerkin functional forms with respect to

θ. The algorithm is given in Appendix A. After integrating the Galerkin functional forms with respect to θ, we use the IMSL [83] subroutine DQDAG, which is an adaptive scheme based on Gauss-Kronrod quadrature rule, to integrate the Galerkin functional forms with respect to r.

Chapter 5

Numerical results

This chapter is separated into two parts. In part I, we will first consider a rotating spherical Earth model with a compressible, inviscid, stratified fluid OC with an elastic MT. Next, we consider a rotating spherical fluid shell contained between an elastic inner core and mantle. The procedures for computing non-dimensional frequencies of the normal modes such as the Slichter modes, the spheroidal modes, the inertial modes of both the spherical OC with an elastic MT and spherical shell OC with an elastic IC and MT models will be presented. We will then present the non-dimensional frequencies and the displacement eigenfunctions of some of these inertial modes. In part II, we will consider a rotating spheroidal fluid shell contained between an elastic inner core and mantle, and will compute the period of the Earth's wobble/nutation modes.

Part I

Numerical Results for Spherical Earth Models

The following part is reprinted from the work of Kamruzzaman and Seyed Mahmoud [43]. As a first project of my PhD work, I have used the LMD of the dynamics of the Earth in order to investigate the effects of mantle and inner core elasticity on the frequencies of some of the inertial modes of a spherical Earth model with a liquid core. No one has done that before. Traditionally, a liquid core with rigid boundaries is considered to study these modes. Initially, I have applied the Galerkin method and have written FORTRAN codes to solve the linear momentum and Poisson's equations with the relevant boundary conditions at the interfaces. Unfortunately, my FORTRAN codes were not given the expected results for the elastic (spheroidal) modes, the Slichter modes and the inertial modes because I did not set the first derivatives of the dependent variables to zero at the center of the Earth. I thank Behnam Seyed Mahmoud for suggesting it. Then I have computed the periods of the seismic and Slichter modes and the frequencies of some of the inertial modes of that model, and have analyzed the results. Also, Behnam Seyed Mahmoud has rechecked my derivations as well as my FORTRAN codes. Next, I have written the manuscript and have submitted for a publication.

5.1 Numerical Validation

In this work, we first compute the periods of the seismic and Slichter modes and compare the results to the known values in order to validate our approach. Next, we compute the eigenfrequencies and the displacement eigenfunctions for some of the inertial modes of a realistic Earth model with elastic inner core and mantle. We then compare the results with the analytical results for a Poincaré core model and other core models (when available) to show the effects of elastic boundaries on the eigenfrequencies and eigenfunctions of these modes.

We first consider a SNREI (spherical, non-rotating, elastic and isotropic) Earth model and compute the elastic and Slichter modes of this model. In this model, the displacement

Table 5.1: The periods (min) of the seismic modes of a SNREI Earth model

Author	${}_0S_2$	${}_0S_3$	${}_0S_4$	${}_0S_5$
Dziewonski and Anderson [1]	53.89	35.57	25.76	19.84
This work	53.58	35.54	25.48	19.76
Percentage difference	0.57	0.08	1.08	0.40

Table 5.2: The periods (hr) of the Slichter modes for PREM

Author	Rotating			Non-rotating
	prograde	axial	retrograde	
Crossley et al. [17]	5.979	5.310	4.777	5.4206
Wu and Rochester [18]	5.979	5.310	4.767	5.4205
This work	5.979	5.310	4.779	5.4287

of the spheroidal modes is represented as

$$\mathbf{u}_k = \sum_{n=|m|}^{N_k} (\mathbf{S}_n^m)_k. \tag{5.1}$$

In equation (5.1), the toroidal $(\mathbf{T}_n^m)_k$ component of $\mathbf{u}_k$ is omitted because the spheroidal and toroidal modes are decoupled [90]. They are degenerate i.e., the eigenfrequencies of these modes for this model do not depend on the azimuthal order m. Table 5.1 shows the periods of some of the seismic modes (spheroidal modes) of this model. The seismic mode of the pth overtone period of harmonic degree n is denoted by ${}_pS_n$; where $p = 0, 1, 2, 3, \cdots$ and $p = 0$ corresponds to the fundamental mode. As it is clear from Table 5.1, our computed periods of the seismic modes agree very well with those cited in the literature [1].

Next, we compute the periods of the Slichter modes for both a non-rotating and a rotating Earth model. These results are given in Table 5.2 and are compared with the ones available in the literature for similar Earth models. Note that for the rotating model the displacement given in equation (2.22) or (2.23) is used. The periods of the Slichter modes from this work are nearly identical to those computed by Crossley et al. [17] using a perturbation technique, and with those by Wu and Rochester [18].

Table 5.3: Non-dimensional eigenfrequencies, $\sigma = \omega/2\Omega$, of some of the low order inertial modes for different Earth models. Except for the Poincaré core model (column 2) which is incompressible, the OC of the Earth models is considered as compressible and neutrally stratified. Note that BC means boundary conditions.

Modes	σ Poincaré model	σ sphere with rigid BC	σ sphere with elastic BC	σ shell with elastic BCs
(4,1,0)	0.6547	0.6573	0.6528	0.6661
(6,1,0)	0.4688	0.4715	0.4774	0.4742
(6,2,0)	0.8302	0.8308	0.8337	0.8341
(2,1,1)	0.5000	0.5000	0.4995	0.4995
(4,1,1)	-0.4100	-0.4213	-0.4208	
(4,2,1)	0.3060	0.3103	0.3150	0.3016
(4,3,1)	0.8540	0.8491	0.8587	0.8525
(6,1,1)	-0.7021	-0.7057	-0.7035	-0.6967
(6,2,1)	-0.2687	-0.2760	-0.2872	
(6,3,1)	0.2202	0.2242	0.2257	
(6,4,1)	0.6530	0.6517	0.6575	0.6595
(6,5,1)	0.9308	0.9282	0.9376	

In column 3 of Table 5.3, we show the frequencies of some the inertial modes computed using our method for a compressible, neutrally stratified spherical core model with rigid boundary. These frequencies are identical to those given by Seyed Mahmoud and Rochester [38] and Seyed Mahmoud et al. [37] for a similar core model. This represents yet another test of our method.

5.2 Inertial modes of realistic Earth models

In this section we report our computed non-dimensional frequencies, σ, for some of the low order inertial modes of different spherical Earth models. Note that there are two truncation levels involved for each layer: N_k represents the truncation level along θ, and L_k represents the truncation level along r, where $k = 1,2,3$ for an IC, OC and MT, respectively. Firstly, we ensure that for a given set of N_k's the frequency of a mode converges by increasing L_k's as necessary, therefore, in the Figures 5.1 and 5.2 we do not show L_k's.

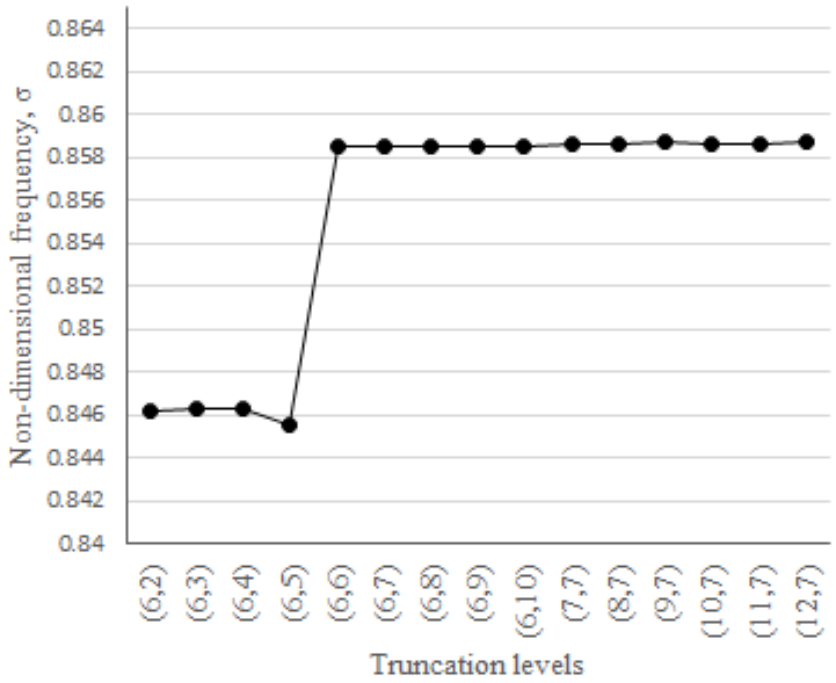

Figure 5.1: The convergence pattern for the (4,3,1) mode of a spherical Earth model with a compressible, inviscid, neutrally stratified fluid core with an elastic mantle. The numbers on the horizontal axis are the truncation levels (N_2,N_3) for the fluid core and mantle respectively.

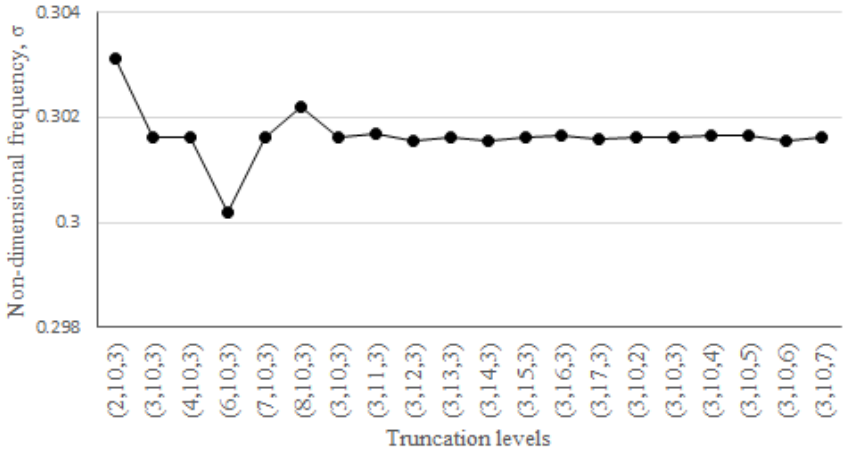

Figure 5.2: The convergence pattern for the (4,2,1) mode of a spherical fluid shell contained between an elastic inner core and mantle. The numbers on the horizontal axis are the truncation levels (N_1,N_2,N_3) for the inner core, fluid core and mantle respectively.

To ensure convergence in the θ direction, first low values of N_k's are chosen and a frequency is computed. We then keep N_2 and N_3 fixed and increase N_1 until the frequency converges. We then keep N_1 and N_3 fixed and N_2 is increased, and so on. This process is repeated until the frequency is converged for the set of N_k's. For example, the convergence pattern of the (4,3,1) mode for a spherical Earth model with a compressible OC and elastic MT is shown in Fig 5.1. The frequency of this mode is converged at $N_2 = 6$ for the OC and $N_3 = 6$ for the MT, whereas this mode for a spherical compressible OC with rigid boundary converges at $N_2 = 4$ [see Table 1 in [37]].

We identify a mode using three criteria: (1) the frequency of the mode is converged; (2) the displacement pattern of the mode must satisfy the boundary conditions, be regular at $r = 0$, and in the outer core of the Earth model, has displacement pattern similar to its counterpart for a Poincaré core model [38]; (3) the gravitational potential must be continuous across the interfaces. We use Greenspan's [80] notation to identify an inertial mode using labels (n,c,m), where n, and m refer to, respectively, the degree and order of the spherical harmonics; where $c = 1,2,3,\cdots$, and $c = 1$ corresponds to the smallest value of the frequencies of modes for a given n and m.

Table 5.3 shows the non-dimensional frequencies $\sigma = \omega/2\Omega$ for the some low order ($m = 0$ and $m = 1$) inertial modes of different spherical Earth models. We have chosen these wavenumbers because $m = 0$ corresponds to changes in the Earth's rotation rate and $m = 1$ to the Earth's wobble and nutation. In column 2 of Table 5.3 we show the frequencies of inertial modes of a Poincaré core model for which analytical solutions exist [80]. The frequencies of the inertial modes for a compressible spherical core model with an associated elastic mantle are given in column 4 of this table. Note that in column 3 are the frequencies of the inertial modes for a core model with a rigid boundary. It is clear that the frequency of the (4,2,1) mode is more affected by the elasticity of mantle, and the frequency of the SOM [the (2,1,1) mode] is less affected. The frequency of the FCN is changed from ≈ 0.50144 for an Earth model with a rigid mantle and inner core [91, 40] to ≈ 0.50116 for an elastic

Earth model [72, 39, 45, 84]. The corresponding period of the FCN for an Earth model with a rigid MT and IC is 346 sidereal days (sd) while that for an elastic Earth's model is 460 sd. It is clear that the change in the frequency of the SOM from 0.5000 for an Earth model with rigid mantle and inner core to 0.4995 for an Earth model with elastic mantle and inner core is consistent with the change in the frequency of the FCN, as the FCN is the counterpart of the SOM in a wobbling Earth model [36]. This is also significant as the frequency of the (2,1,1) mode is not affected by the compressibility [37] and density stratification [41, 42] of the OC. In column 5 of Table 5.3 we show the frequencies of the modes of a spherical fluid shell with elastic boundaries. A blank entry in this column means that the frequency of that mode did not converge and the corresponding mode of a sphere may not exist in a fluid shell (see [37]).

The displacement patterns in the fluid core for some of the inertial modes for a spherical Earth model with a compressible, inviscid, neutrally stratified fluid core and an elastic mantle are shown in Fig 5.3. These displacement patterns are similar to those for a Poincaré model [80] which are also similar to those of a compressible core model with a rigid boundary [37]. This is expected as the mantle is nearly rigid compared to the fluid core. In figure 5.4 we show the displacement eigenfunctions of a spherical fluid shell contained between an elastic inner core and mantle. Recall that the truncation levels N_k correspond to degree $2N_k$ of the spherical harmonics in equations (2.22) and (2.24) or (2.23) and (2.25). The truncation levels (N_2, L_2) of the OC for the convergence of the frequencies of the inertial modes depend on the spatial structure of these modes [37]. We would like to emphasize that the maximum degree of spherical harmonics considered in the traditional approach is 5 [45]. This is the main reason why the traditional approach does not yield the frequencies of the (long period) inertial modes, except for the purely toroidal modes like the SOM.

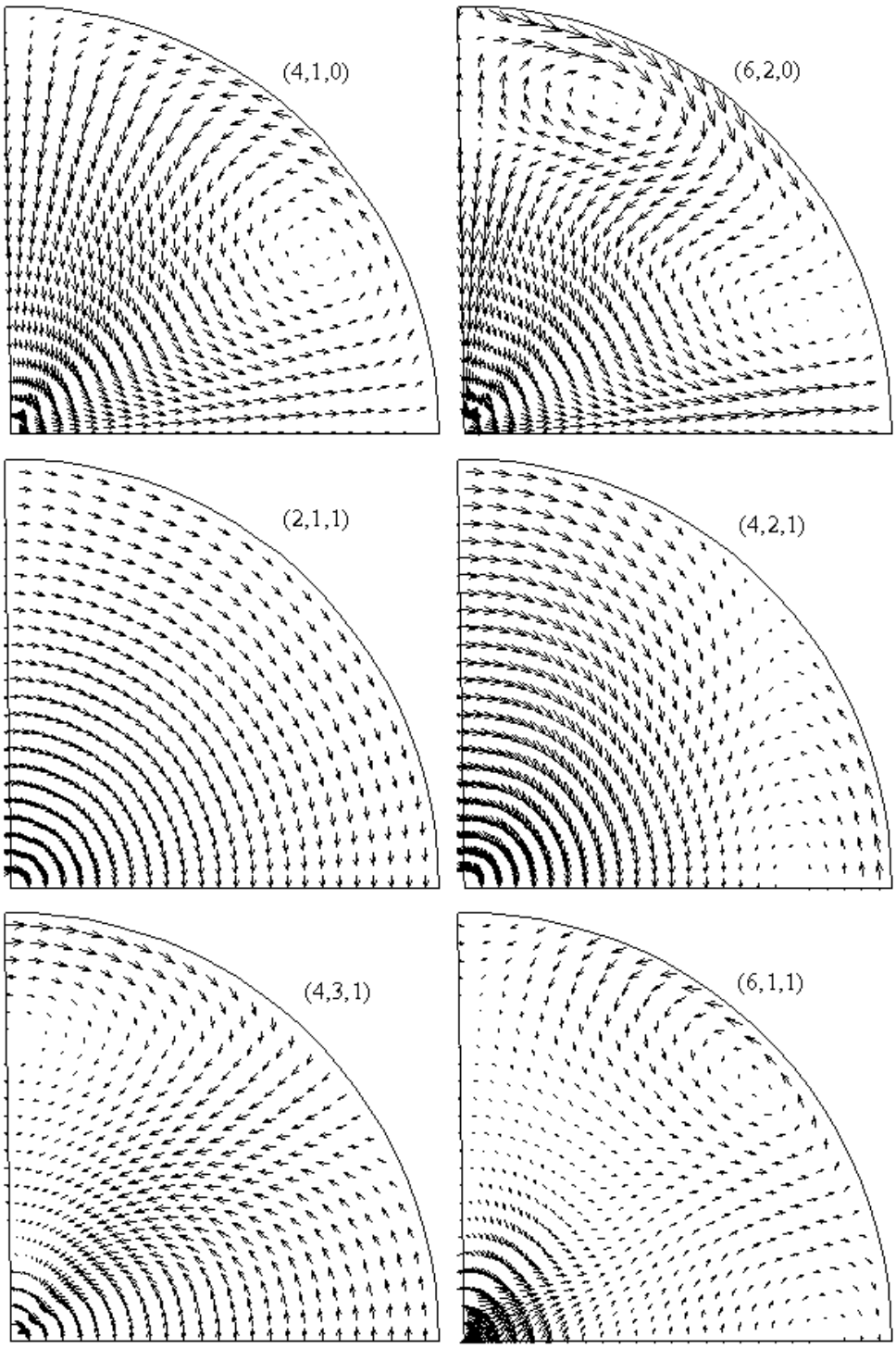

Figure 5.3: The displacement eigenfunctions in a meridional plane of fluid core for some of the inertial modes of a spherical Earth model with a compressible, inviscid, neutrally stratified fluid core with an elastic mantle. The eigenfrequencies of these modes are given in column 4 of Table 5.3.

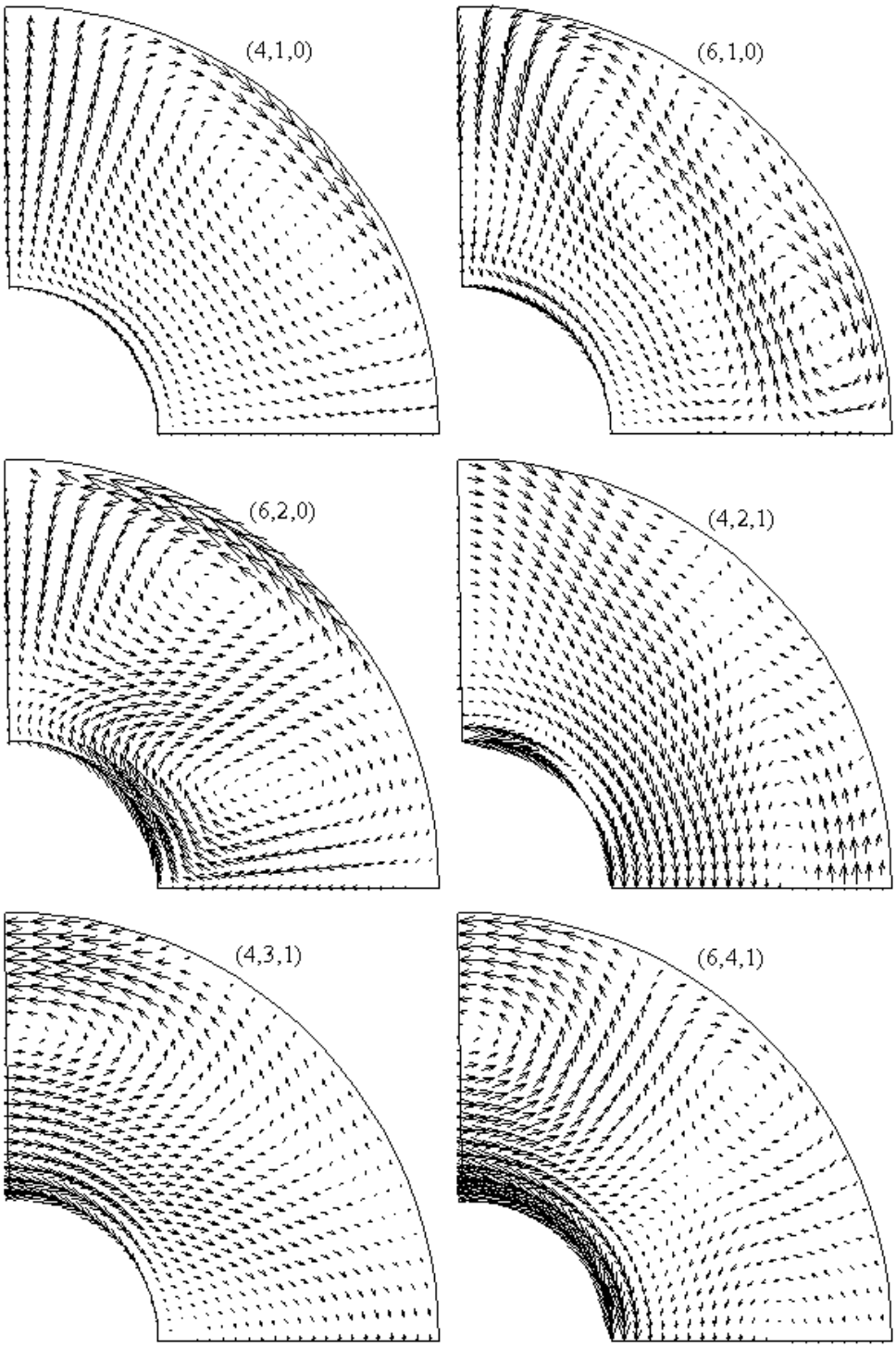

Figure 5.4: The displacement eigenfunctions in a meridional plane of fluid core for some of the inertial modes of a spherical fluid shell contained between an elastic inner core and mantle. The eigenfrequencies of these modes are given in column 5 of Table 5.3. Note that the mantle and the inner core are nearly rigid compare to the OC.

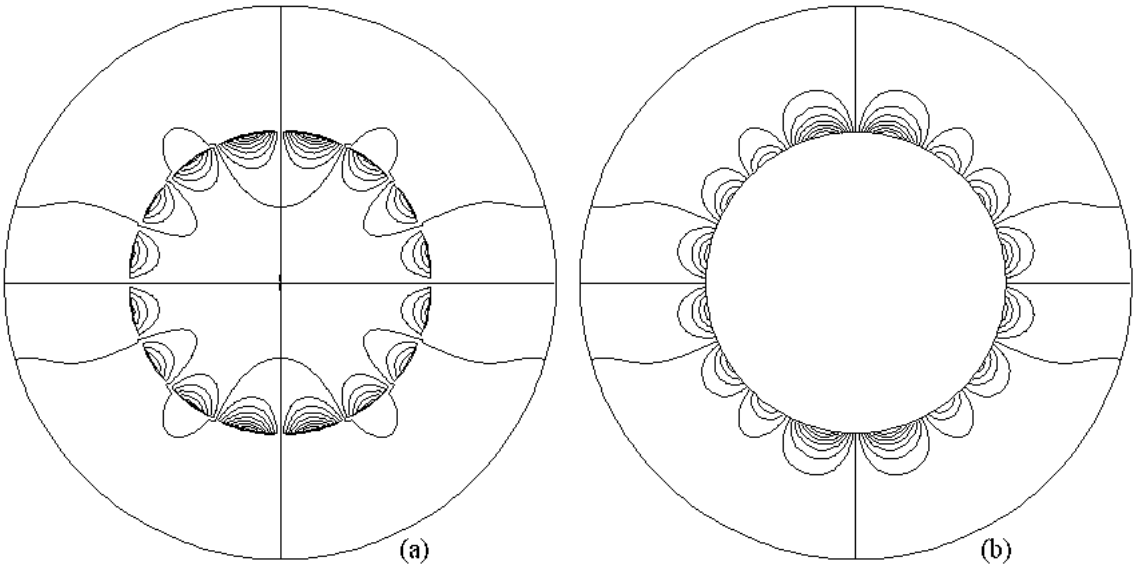

Figure 5.5: The gravitational potential contour of the (4,2,1) mode for the Earth model: (a) with a compressible core and an elastic mantle, and (b) zoomed in of the gravitational potential in the mantle. The contours clearly show the continuity of the gravitational potential at the CMB.

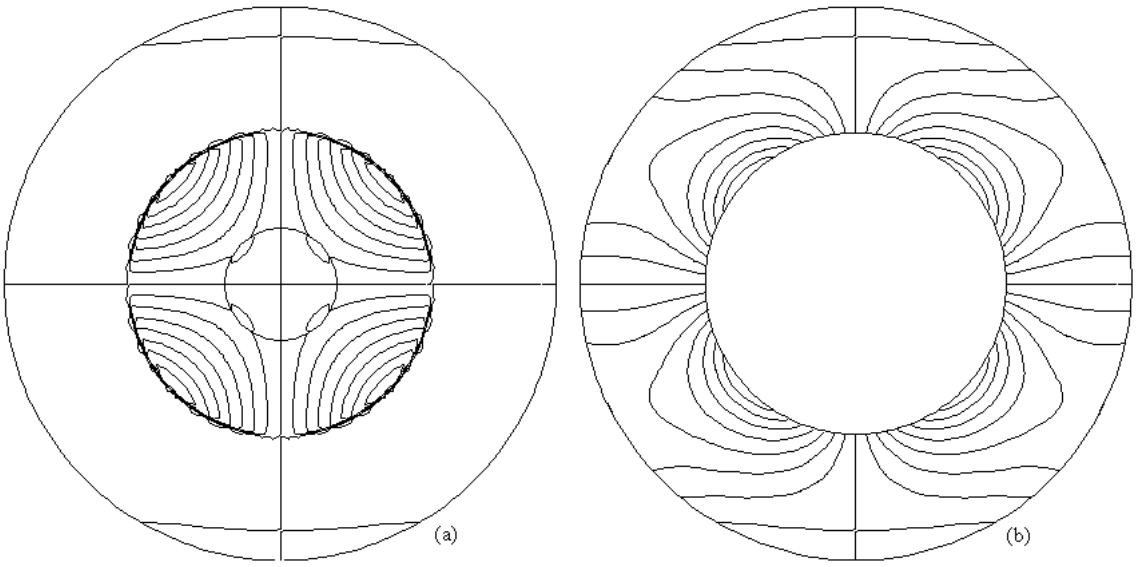

Figure 5.6: (a) The gravitational potential contour of the (4,2,1) mode for a three layer spherical Earth model with a compressible outer core, and elastic mantle and inner core. Fig 5-b shows the gravitational potential contours in the mantle (zoomed-in). The contours clearly show the continuity of the gravitational potential at the ICB and CMB.

Part II

Numerical Results for Spheroidal Earth Models

In this part, we compute the eigenfrequencies of the inertial modes of the OC with a rigid boundary for the spheroidal Earth models. Next, we compute the periods of the wobble and nutation modes of the realistic Earth models.

5.3 Numerical Validation

In order to justify our approach as well as our FORTRAN code, we consider a rotating spheroidal compressible and neutrally stratified OC with a rigid mantle, and compute non-dimensional eigenfrequencies σ of the inertial modes for this model. Table 5.4 shows the non-dimensional frequencies for some of the low order inertial modes of an incompressible fluid spheroid (the Poincaré model), and a compressible and neutrally stratified fluid spheroid. In Table 5.4, column 1 represents some of the low order modes of azimuthal wavenumber 0 and 1 and degree up to 6; column 2 shows our non-dimensional frequencies of these modes, which are identical to analytical solutions [92] for the Poincaré core model. In column 3 of this table, we show our computed eigenfrequencies of the above modes for a compressible and neutrally stratified OC with a rigid mantle. The non-dimensional frequencies (column 4) of these inertial modes for the same modified neutrally stratified spheroidal core model were computed by Seyed-Mahmoud and Moradi [87]. Although they used the 3PD, the results are nearly identical. Note that the procedure to identify a mode is described in Section 5.2.

5.4 Wobble and Nutation Modes of Realistic Earth Models

We have computed the periods of the CW and the FCN for an ocean-less PREM and a neutrally stratified outer core (PREMN) discussed in details in section 2.5. We compare our computed periods of the CW and the FCN with those of other authors for similar Earth models in Tables 5.5 and 5.6, respectively. In Tables 5.5 and 5.6, column 2 refers to the method used, AMD or LMD. Columns 4 and 5 of these tables show the computed periods of the CW and the FCN for the PREM and PREMN models, respectively. From

Table 5.4: Non-dimensional eigenfrequencies, $\sigma = \omega/2\Omega$, of some of the low order inertial modes for the spheroidal Earth models. Except for the Poincaré core model (column 2) which is an incompressible, the OC of the Earth model is considered as a compressible and neutrally stratified with a rigid mantle.

Modes	σ Poincaré model	σ spheroid This work	σ spheroid [87]
(4,1,0)	0.6556	0.6577	0.657
(6,1,0)	0.4698	0.4715	
(6,2,0)	0.8309	0.8310	0.831
(2,1,1)	0.5013	0.5013	0.5013
(4,1,1)	-0.4108	-0.4221	-0.419
(4,2,1)	0.3068	0.3111	0.307
(4,3,1)	0.8546	0.8505	0.851
(6,1,1)	-0.7030	-0.7063	-0.706
(6,2,1)	-0.2692	-0.2765	-0.277
(6,3,1)	0.2208	0.2248	0.225
(6,4,1)	0.6540	0.6527	0.653
(6,5,1)	0.9312	0.9286	0.928

column 3 of these tables, we see that in previous work the maximum degree of the spherical harmonics considered in the traditional approach of solving the dynamical equations for similar Earth models is 5, and there is no proof of convergence. We are confident our results are converged (see Fig 5.7).

In Table 5.5, we show that Rogister and Valette [39] find the period of CW to be about 403 sd for PREM and 406 sd for PREMN. Smith [52] computed the periods of the CW as 403.5 sd and noted that the outer fluid core stratification would not affect the period of CW significantly (see also Crossley and Rochester [45]). Our computed period of the CW is 403.52 sd for both PREM and PREMN models i.e., the period of the CW is not affected by the density stratification of the fluid core.

Jeffreys and Vicente [56] computed the period of the FCN for a two-layer Earth model, a homogeneous liquid core and an elastic, radially inhomogeneous mantle to be about -460 sd. Molodensky [57], and Shen and Mansinha [58] extended this model to add compress-

Table 5.5: The period (sd) of the Chandler Wobble (CW) of a spheroidal Earth model. AMD refers to angular momentum description, and LMD refers to linear momentum description.

Author	Description	Truncation	PREM	PREMN
Mathews et al. [72]	AMD		401.8	
Rochester and Crossley [78]	AMD		400.3	
Rogister and Valette [39]	LMD	T_3	403.2	406.6
		S_4	402.6	406.3
Crossley and Rochester [45]	LMD	T_3	401.69	401.69
		T_5	401.69	401.69
This work	LMD	converged	403.52	403.52

Table 5.6: The period (sd) of the Free Core Nutation (FCN) of a spheroidal Earth model. AMD refers to angular momentum description, and LMD refers to linear momentum description.

Author	Description	Truncation	PREM	PREMN
Mathews et al. [72]	AMD		-458.0	
Rogister and Valette [39]	LMD	T_3	-459.3	-459.3
		S_4	-459.4	-459.4
Crossley and Rochester [45]	LMD	T_3	-456.00	-455.98
		T_5	-456.05	-456.05
Zhang and Huang [84]	LMD	T_3	-431.2	
This work	LMD	converged	-432.28	-432.28

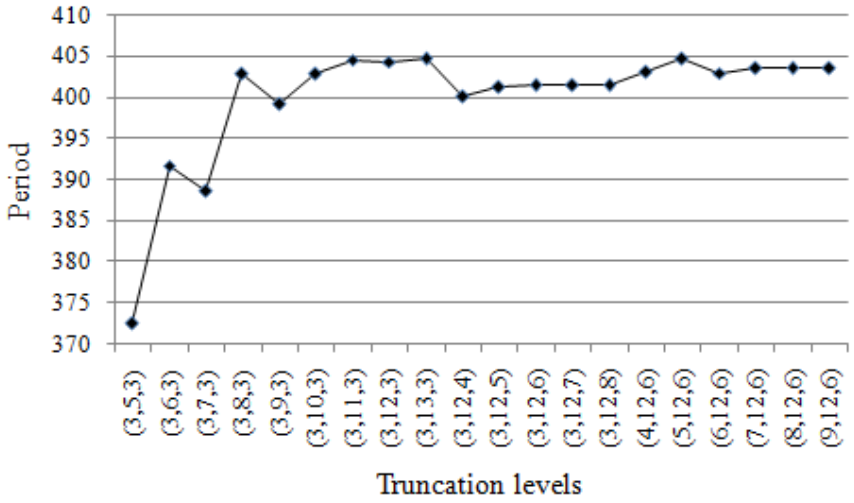

Figure 5.7: The convergence pattern for the Chandler Wobble of PREM . The numbers on the horizontal axis are the truncation levels (N_1,N_2,N_3) for the inner core, fluid core and mantle, respectively.

ibility of the liquid core and computed the same period for this mode. Rosat et al. [93] analyzed data from superconducting gravimeters and found the observed period of this mode to be (-428 ± 3) sd. Koot et al. [51] used VLBI (Very Long Baseline Interferometry) data and found the period of (-429.07 ± 0.07) sd for this mode. Our computed period of the FCN is -432.28 sd (see Table 5.6). Our result agrees with Zhang and Huang [84]. From Table 5.6, we show that the period of the FCN is the same for both PREM and PREMN models. This is consistent with the theory. Seyed Mahmoud et al. [41] and Kamruzzaman [42] show that the period of the (2,1,1) mode (the SOM) of the fluid core is independent of the density stratification of the fluid core. The FCN is the counterpart of the SOM of a wobbling Earth model [36]. Our approach does not yield the periods of the FICN and the ICW. We believe this is due to the fact that our results are correct to first order in the ellipticity. To compute the FICN and ICW, the boundary boundary conditions must be correct to second order in the ellipticity (see Eq. (27) in [40]).

Chapter 6

Conclusions

In this thesis, we have used the linear momentum description (LMD) of the dynamics of the Earth in order to study the Earth's normal modes. The advantage of the LMD is that we have used directly the S- and P-wave speeds and the density profiles of the Earth's layers, whereas the Love numbers are used mostly when a Lagrangian view is adopted and the angular momentum description (AMD) is considered. The main disadvantage of using the Love numbers is that another six differential equations are needed to solve for calculating the Love numbers [94].

A Galerkin method is applied to solve the momentum and Poisson's equations including the boundary conditions at the interfaces. It is clear that an important advantage of a Galerkin method is that the application of the divergence theorem replaces the volume integrals involving second-order derivatives with surface and volume integrals involving first-order derivatives. Another advantage is that the singularity of the differential equations (2.4) and (2.5) at $r = 0$ is removed using this method. The most important advantage, however, is that the convergence of the results may be checked. Note that the computed periods of wobble/nutation modes of the Earth in existing methods of previous studies lack proven convergence (e.g., [52, 62, 39, 45]). The heavy truncation involving in all previous studies was not able to answer for the question of whether or not the computed periods have actually converged. We have shown that our computed periods of wobble/nutation modes are converged using the Galerkin method. We have derived the vector and scalar operations, which involve the Galerkin formulation of the dynamical equations, by applying the

Clairaut coordinate system. We have expanded the Galerkin formulation of the dynamical equations correct to first order in the ellipticity. To integrate the Galerkin functional forms with respect to θ, we have used the orthogonality relation and the linear independence properties of the spherical harmonics to develop an algorithm based on the work of Seyed-Mahmoud [81]. After integrating the Galerkin functional forms with respect to θ, we have used the IMSL [83] subroutine DQDAG, which is an adaptive scheme based on the Gauss-Kronrod quadrature rule, to integrate the Galerkin functional forms with respect to r.

In order to find the P-wave and S-wave speeds, and the density profiles of the Earth's layers, the Preliminary Reference Earth Model (PREM) [1] is adopted as the base for our Earth model. We consider a one layer ocean-less MT and use the least squares method to modify density and seismic wave velocity profiles of this region. This is justified for our studies as the mantle is nearly rigid compared to the liquid core. In modifying PREM's mantle, we make sure that the P-wave and S-wave speeds, and the density profiles obey the law of mass conservation and meet the Adams-Williamson condition. Also, we have solved the Clairaut equation to find the Earth's ellipticity profile using the Runge-Kutta integration method.

We have considered a rotating spherical Earth model with a compressible, inviscid, stratified fluid OC with an elastic MT, and then a rotating spherical fluid shell contained between an elastic IC and an elastic MT, and have investigated the effects of mantle and inner core elasticity on the frequencies of some of the inertial modes of a spherical Earth model with a liquid core. Traditionally, a liquid core with rigid boundaries is considered to study these modes. We have validated our approach and numerical code by computing the periods of some of the seismic modes, the Slichter modes and some of the inertial modes of a compressible core model with rigid boundaries. Next, we have computed the frequencies, the displacement and gravitational potential eigenfunctions for some of the inertial modes of the fluid core for both models. We have shown that the frequencies of the inertial modes

may be significantly affected by the elasticity of an inner core and mantle. These modes are the long-period normal modes of a rotating Earth model and, because of rotation, in general their frequencies converge slowly. Our method allows us to increase the truncation levels and ensure that these frequencies are converged. For example, spherical harmonics of degree up to 24 were needed for the frequency of the (6,2,0) mode to converge. Up until now the maximum degree of the spherical harmonics considered in the traditional approach of solving the dynamical equations for a similar Earth model is 5, which would only yields the (2,1,1) mode. Seyed-Mahmoud et al. [40] show that spherical harmonics of degree up to 20 are needed for frequency of the FICN of a simple Earth model with rigid inner-core and mantle and an incompressible and homogeneous OC to converge to a mean value.

Next, we have considered a rotating spheroidal Earth model which has a compressible, inviscid, stratified fluid OC, an elastic IC and an elastic MT. To validate our approach and FORTRAN code, we have computed the non-dimensional frequencies of the inertial modes of an incompressible fluid spheroid (the Poincaré model), and a compressible and neutrally stratified fluid spheroid. Our results are nearly identical to those computed by Seyed-Mahmoud and Moradi [87]. Finally, we have computed the periods of the CW and the FCN for an ocean-less PREM and a neutrally stratified outer core (PREMN) models. Our computed periods of the CW and the FCN are 403.52 sd and 432.28 sd, respectively. Our result for the CW agrees with those predicted by other authors (see e.g., Smith [52], Rogister and Valette [39] and Crossley and Rochester [45]), and our computed period of the FCN agrees with observed values determined by both superconducting gravimetry and Very Long Baseline Interferometry (VLBI) data [93, 51], as well as the result of Zhang and Huang [84]. Our result indicates that the Earth is indeed in hydrostatic equilibrium and there is still merit in considering hydrostatic equilibrium as the reference configuration for a steadily rotating celestial body. However, Dehant and Defraigne [95] attempted to construct the Earth deviated from hydrostatic equilibrium which is completely internally inconsistent. Also, we show that the computed periods of the CW and the FCN are the same

for both PREM and PREMN models, i.e., the periods of these modes are not significantly affected by the density stratification of the fluid core. However, we are not able to compute the periods of the FICN and the ICW because we consider only first order of the ellipticity of the dynamical equations of the Earth's interior. As our approach is correct to first order in the ellipticity, it is not sufficient for computing periods of the FICN and the ICW.

In future work, we will take account of the following considerations:

(i) Expand the Galerkin formulation of the dynamical equations to include the 2nd order ellipticity because the frequency of the ICW is very low, and to compute the FICN and ICW, the boundary conditions must be correct to second order in the ellipticity (see Eq. (27) in [40]). Note that the ICW is not observed yet and the computed period of this mode is in the range 2410 sd to 2715 sd [71, 78]. Our method may give the actual period of this mode because our method makes sure whether or not the computed periods have actually converged.

(ii) Include the Lorentz force of the dynamical equations of the Earth's interior, and study the effects of the magnetic field on the frequencies of the Earth's normal modes such as inertial modes, Slichter modes and Earth's wobble/nutation modes. Note the observed and computed period of the FICN are 929 ± 31 sd [51] and 470 sd [45] respectively. The discrepancy of the observed and computed period of this mode may indicate a significant role of the magnetic field.

(iii) Include the viscosity of the fluid OC, and investigate the effect on the frequencies of the Earth's normal modes. The viscosity of the fluid OC may be responsible for the damping of the normal mode after excitation as a result of a large earthquake.

(iv) Include forces of other planets on the Earth, and study the forced wobble/nutation modes of the Earth.

References

[1] A. M. Dziewonski and D. L. Anderson. Preliminary Reference Earth Model. *Phys. Earth Planet. Inter.*, 25:297–356, 1981.

[2] D. L. Anderson. *Theory of the Earth*. : Blackwell Scientific Publications, Boston, 1989.

[3] I. Lehmann. Publications du Bureau Central Seismologique International, Srie A. *Travaux Scientifique*, 14:87–115, 1936.

[4] D. W. Vasco. A transformational approach to geophysical inverse problems. *Geophys. J. Int.*, 123:183 – 212, 1995.

[5] G. Masters, S. Johnson, G. Laske, and H. Bolton. A shear- velocity model of the mantle. *Philos. Trans. R. Soc. London*, A 354:1385 –1411, 1996.

[6] W. Su, R. L. Woodward, and A.M Dziewonski. Degree 12 model of shear velocity heterogeneity in the mantle. *J. Geophys. Res.: Solid Earth*, 99:6945–6980, 1994.

[7] M. Ishii and J. Tromp. Normal-Mode and Free-Air Gravity Constraints on Lateral Variations in Velocity and Density of Earth's Mantle. *Science*, 285:1231–1236, 1999.

[8] S. Zhong and X. Liu. The long-wavelength mantle structure and dynamics and implications for large-scale tectonics and volcanism in the phanerozoic. *Gondwana Res.*, 29:83–104, 2016.

[9] A. Alterman, H. Jarosch, and C. L. Pekeris. Oscillations of the Earth. *Proc. Soc. London*, A 252:80–95, 1959.

[10] D. Al-Attar, J.H. Woodhouse, and A. Deuss. Calculation of normal mode spectra in laterally heterogeneous earth models using an iterative direct solution method. *Geohyps. J. Int.*, 189:1028 – 1046, 2012.

[11] H. Benioff, F. Press, and S. Smith. Excitation of the free oscillations of the earth by earthquakes. *J. Geophys. Res.*, 66:605–619, 1961.

[12] F. Gilbert. Excitation of the normal modes of the earth by earthquake sources. *Geophys. J. R astron. Soc.*, 22:223–226, 1970.

[13] Z. S. Alterman, Y. Eyal, and A. M. Merzer. On free oscillations of the earth. *Surv. Geophys.*, 1(4):409–428, 1974.

[14] S. C. Webb. The earth's hum: the excitation of Earth normal modes by ocean waves. *Geophys. J. Int.*, 174:542–566, 2008.

[15] E. A. Okal and S. Stein. Observations of ultra-long period normal modes from the 2004 SumatraAndaman earthquake. *Phys. Earth Planet. Inter.*, 175:53–62, 2009.

[16] L. B. Slichter. The fundamental free mode of the earth's inner core. *Proc. Natl. Acad. Sci. U.S.A.*, 47:186 – 190, 1961.

[17] D. J. Crossley, M. G. Rochester, and Z.R. Peng. Slichter modes and Love numbers. *Geophys. Res. Lett.*, 19:1679–1682, 1992.

[18] W. J. Wu and M. G. Rochester. Gravity and slichter modes of the rotating Earth. *Phys. Earth Planet. Inter.*, 87:137–154, 1994.

[19] S. Friedlander. Internal oscillations in the earths fluid core. *Geophys. J. Int.*, 80:345 – 361, 1985.

[20] G. H. Bryan. The Waves on a Rotating liquid Spheroid of Finite Ellipticity. *Philos. Trans. A Math. Phys. Eng. Sci.*, 180:187–219, 1889.

[21] S. S. Hough. The Oscillations of a Rotating Ellipsoidal Shell Containing Fluid. *Philos. Trans. A Math. Phys. Eng. Sci.*, 186:469–506, 1895.

[22] H. Poincaré. Sur la précession des corps déformables. *Bulletin Astronomique, Serie I*, 27:321–356, 1910.

[23] K. Stewartson and J. A. Rickard. Pathological oscillations of a rotating fluid. *J. Fluid Mech.*, pages 759–773, 1969.

[24] K. D. Aldridge. Axisymmetric inertial oscillations of a fluid in a rotating spherical shell. *Mathematika*, 19:163–168, 12 1972.

[25] L. Kelvin. Vibrations of a columnar vortex. *Phil. Mag.*, 10:155–168, 1880.

[26] D.J. Ivers, A. Jackson, and D. Winch. Enumeration, orthogonality and completeness of the incompressible Coriolis modes in a sphere. *J. Fluid Mech.*, 766:468–498, 2015.

[27] S. Vantieghem. Inerial modes in a rotating tri-axial ellipsoid. *Proc. R. Soc.*, A470:20140093, 2014.

[28] D.J. Ivers. Enumeration, orthogonality and completeness of the incompressible Coriolis modes in a tri-axial ellipsoid. *Geophys. Astr. Fluid Dyn.*, 111:333–354, 2017.

[29] G. Backus and M. Rieutor. Completeness of inertial modes of an incompressible inviscid fluid in a corotating ellipsoid. *Phys. Rev.*, E95:053116, 2017.

[30] D.J. Ivers. Tilted incompressible Coriolis modes in spheroids. *J. Fluid Mech.*, 833:131–163, 2017.

[31] K. D. Aldridge and A. Toomre. Axisymmetric inertial oscillations of a fluid in a rotating spherical container. *J. Fluid Mech.*, 37:307–323, 6 1969.

[32] B. Seyed-Mahmoud, K. D. Aldridge, and G. Henderson. Elliptical instability in rotating spherical fluid shells: application to earths fluid core. *Phys. Earth Planet. Inter.*, 142(3-4):257–282, 2004.

[33] J. Boisson, D. Cébron, F. Moisy, and P. P. Cortet. Earth rotation prevents exact solid-body rotation of fluids in the laboratory. *EPL (Europhysics Letters)*, 198(3):59002–02, 2012.

[34] M. Rieutord. Inertial modes in the liquid core of the Earth. *Phys. Earth Planet. Inter.*, 91(13):41 – 46, 1995.

[35] M. Rieutord. Linear theory of rotating fluids using spherical harmonics part ii, time-periodic flows. *Geophys. Astrophys. Fluid Dyn.*, 59(1-4):185–208, 1991.

[36] M. Rieutord and L. Valdettaro. Inertial waves in a rotating spherical shell. *J. Fluid Mech.*, 341:77–99, 6 1997.

[37] B. Seyed-Mahmoud, J. Heikoop, and R. Seyed-Mahmoud. Inertial modes of a compressible fluid core model. *Geophys. Astrophys. Fluid Dyn.*, 101(5-6):489–505, 2007.

[38] B. Seyed-Mahmoud and M. G. Rochester. Dynamics of rotating fluids described by scalar potentials. *Phys. Earth Planet. Inter.*, 156(12):143 – 151, 2006.

[39] Y. Rogister and B. Valette. Influence of liquid core dynamics on rotational modes. *Geophys. J. Int.*, 176:368–388, 2009.

[40] B. Seyed-Mahmoud, M. G. Rochester, and C. M. Rogers. Truncation effects in computing free wobble/nutation modes explored using a simple Earth model. *Geophys. J. Int.*, 209:1455–1461, 2017.

[41] B. Seyed-Mahmoud, A. Moradi, M. Kamruzzaman, and H. Naseri. Effects of density stratification on the frequencies of the inertial modes of the Earth's fluid core. *Geophys. J. Int.*, 202(2):1146 – 1157, 2015.

[42] M. Kamruzzaman. Inertial modes of the Earth's fluid core. Master's thesis, The University of Lethbridge, AB, Canada, 2015.

[43] M. Kamruzzaman and B. Seyed-Mahmoud. Inertial modes of an Earth model with a compressible fluid core and elastic mantle and inner core. *J. Geod.*, 94(4):1–15, 2020.

[44] J. M. Ferrándiz, J. F. Navarro, A. Escapa, and J Getino. Earth's Rotation: A Challenging Problem in Mathematics and Physics. *Pure Appl. Geophys.*, 172:57–74, 2015.

[45] D. J. Crossley and M. G. Rochester. A new description of Earths wobble modes using Clairaut coordinates: 2. Results and inferences on the core mode spectrum. *Geophys. J. Int.*, 198(3):1878–1893, 2014.

[46] B.A. Buffet. Geodynamics estimates of the viscosity of the Earth's inner core. *Nature*, 388:571 – 573, 1997.

[47] S.M. Molodensky and E. Groten. On the upper bound of the liquid core viscosity. *Stud. Geophys. Geod.*, 45:12 – 36, 2001.

[48] J.Y. Guo, P.M. Mathews, Z.X. Zhang, and J.S. Ning. Impact of inner core rotation on outer core flow: the role of outer core viscosity. *Geophys. J. Int.*, 159:372–389, 2004.

[49] D.E. Smylie, V. Brazhkin, and A. Palmer. Direct observation of the viscosity of Earths outer core and extrapolation of measurements of liquid iron. *Phys.-Uspekhi*, 52:79–92, 2009.

[50] S.C. Chandler. On the variation of latitude, ii. *Astron. J.*, 11:97–101, 1891.

[51] L. Koot, M. Dumberry, A. Rivoldini, O. de Viron, and V. Dehant. Constraints on the coupling at the core-mantle boundary and inner core boundaries inferred from nutation observations. *Geophys. J. Int.*, 182:1279–1294, 2010.

[52] M.L. Smith. Wobble and nutation of the Earth. *Geophys. J. R. Astr. Soc.*, 50:103–140, 1977.

[53] L. Euler. Theoria motus corporum solidorum. *Litteris et impensis A.F. Rse, Rostochii*, 1765.

[54] S. Newcomb. On the dynamics of the Earth's rotation, with respect to the periodic variations of latitude. *Mon. Not. R. Astron. Soc.*, 52:336–341, 1892.

[55] A . E. H Love. The yielding of the Earth to disturbing forces. *Proc. R. Soc. London Ser.*, A 82:73–88, 1909.

[56] H. Jeffreys and R. O. Vicente. The Theory of Nutation and the Variation of Latitude. *Monthly Notices of the Royal Astronomical Society*, 117(2):142–161, 1957.

[57] M. S. Molodensky. The theory of nutation and diurnal Earth tides. *Comm. Obs. R. Belgique*, 188:25–56, 1961.

[58] P. Y. Shen and L. Mansinha. Oscillation, Nutation and Wobble of an Elliptical Rotating Earth with Liquid Outer Core. *Geophys. J. Int.*, 46(2):467–496, 1976.

[59] M. L. Smith. The Scalar Equations of Infinitesimal Elastic-Gravitational Motion for a Rotating, Slightly Elliptical Earth. *Geophys. J. R. Astr.l Soc.*, 37(3):491–526, 1974.

[60] M. G. Rochester, D. J. Crossley, and Y. L. Zhang. A new description of Earth's wobble modes using Clairaut coordinates: 1. Theory. *Geophys. J. Int.*, 198(3):1848–1877, 2014.

[61] J. M. Wahr. Body tides on an elliptical, rotating, elastic and oceanless earth. *Geophys. J. R. Astr. Soc.*, 64(3):677–703, 1981.

[62] J. M. Wahr. A normal mode expansion for the forced response of a rotating earth. *Geophys. J. R. Astr. Soc.*, 64(3):651–675, 1981.

[63] T. A. Herring, C. R. Gwinn, and I.I. Shapiro. Geodesy by radio interferometry: studies of the forced nutations of the earth, 1. Data. *J. Geophys. Res.*, 91:4745–4754, 1986.

[64] C. R. Gwinn, T. A. Herring, and I.I. Shapiro. Geodesy by radio interferometry: studies of the forced nutations of the earth, 2. Interpretation. *J. Geophys. Res.*, 91:4755–4766, 1986.

[65] J. M. Wahr and T. Sasao. A diurnal resonance in the ocean tide and in the Earths load response due to the resonant free core nutation. *Geophys. J. R. Astr. Soc.*, 64:635–650, 1981.

[66] J. M. Wahr and Z Bergen. The effects of mantle anelasticity on nutations, earthtides, and tidal variations in rotation rate. *Geophys. J. R. Astr. Soc.*, 87:633– 668, 1986.

[67] J. M. Wahr. The effect of the atmosphere and oceans on the Earths wobble, I. *Geophys. J. R. Astr. Soc.*, 70:349–372, 1982.

[68] J. M. Wahr. The effect of the atmosphere and oceans on the Earths wobble and on the seasonal variations in the length of day, II. *Geophys. J. R. Astr. Soc.*, 74:451–487, 1983.

[69] T.A. Herring. VLBI studies in the nutations of the Earth. *in Pro. of IAU Symposium 129, Kluwer, Dordrecht, The Netherlands*, edited by M.J. Reid and J.M. Moran:371–375, 1988.

[70] J. M. Wahr and D. de Vries. The Earth's forced nutations: geophysical implications, in Variations in Earth Rotation. *AGU monograph*, edited by D. McCarthy, 1990.

[71] P. M. Mathews, B. A. Buffett, T. A. Herring, and I. I. Shapiro. Forced nutations of the Earth: Influence of inner core dynamics: 1. theory. *J. Geophys. Res.: Solid Earth*, 96(B5):8219–8242, 1991.

[72] P. M. Mathews, B. A. Buffett, T. A. Herring, and I. I. Shapiro. Forced nutations of the Earth: influence of the inner core dynamics, 2: numerical results. *J. Geophys. Res.: Solid Earth*, 96(B5):8243–8257, 1991.

[73] B. Seyed-Mahmoud and Y. Rogister. Rotational modes of Poincaré Earth models. *Geophys. Astr. Fluid Dyn.*, 2021.

[74] P. M. Mathews, T. A. Herring, and B. A. Buffett. Modeling of nutation and precession: new nutation series for nonrigid Earth and insights into the Earths interior. *J. Geophys. Res.: Solid Earth*, 107(B), 2002.

[75] T. A. Herring, P. M. Mathews, and B. A. Buffett. Modeling of nutation-precession: Very long baseline interferometry results. *J. Geophys. Res.: Solid Earth*, 107(B), 2002.

[76] B. A. Buffett, P. M. Mathews, and T. A. Herring. Modeling of nutationand precession: effects of electromagnetic coupling. *J. Geophys. Res.: Solid Earth*, 107(B), 2002.

[77] C.L. Huang, V. Dehant, X.H. Liao, T. Van Hoolst, and M.G. Rochester. On the coupling between magnetic field and nutation in a numerical integration approach. *J. Geophys. Res.*, 116:1–18, 2011.

[78] M. G. Rochester and D. J. Crossley. Earth's long-period wobbles: a Lagrangean description of the Liouville equations. *Geophys. J. Int.*, 176(1):40–62, 2009.

[79] M. Dumberry. Influence of elastic deformations on the inner core wobble. *Geophys. J. Int.*, 178:57–64, 2009.

[80] H. P. Greenspan. *The Theory of Rotating Fluids*. Cambridge Monographs on Mechanics and Applied Mathematics. At the University Press, 1969.

[81] B. Seyed-Mahmoud. Wobble/nutation of a rotating ellipsoidal earth with liquid outer core: Implementation of a new set of equations describing dyanmics of rotating fluids. Master's thesis, Memorial University of Newfoundland, Canada, 1994.

[82] F. Birch. Elasticity and constitution of the Earth's interior. *J. Geophys. Res.*, 57(2):227–283, 1952.

[83] Rogue Wave Software. IMLS fortran Numerical Library: Mathematical Functions in Fortran. *www.absoft.com/Support/Documentation/MathV1.pdf.*

[84] M. Zhang and C. Huang. The effect of the differential rotation of the earth inner core on the free core nutation. *Geod. Geodyn.*, 10:146–149, 2019.

[85] S. Chandrasekhar and P. H. Roberts. The ellipticity of a slowly rotationg configuration. *Astophys. J.*, 138:801 – 808, 1963.

[86] A. C. Clairaut. Theori de la figure de la terre, tiree des principes de l'hydrostatique. *Paris*, 1743.

[87] B. Seyed-Mahmoud and A. Moradi. Dynamics of the earths fluid core: Implementation of a clairaut coordinate system. *Phys. Earth Planet. Inter.*, 227(0):61 – 67, 2014.

[88] Z. Kopal. Clairaut coordinates and the vibrational stability of distorted stars. *Astrophys. Space. Sci.*, 70:407 – 424, 1980.

[89] W. J. Wu. A new subseismic governing system of equations and its expansions. *Phys. Earth Planet. Inter.*, 75:289–315, 1993.

[90] F. A. Dahlen and J. Tromp. *Theoretical Global Seismology*. Chapter 8: Toroidal and spheroidal oscillations. Princeton University Press, 1998.

[91] D. de Vries and J. M. Wahr. The effects of the solid inner core and nonhydrostatic structure on the Earth's forced nutations and Earth tides. *J. Geophys. Res.*, 96(B5):8275–8293, 1991.

[92] K. D. Aldridge and L. I. Lumb. Inertial waves identified in the Earth's fluid outer core. *Nature*, 325:307–323, 1987.

[93] S. Rosat, N. Florsch, J. Hinderer, and M. Llubes. Estimation of the free core nutation parameters: sensitivity study and comparative analysis using linearized least-squares and bayesian methods. *J. Geodyn.*, 48:331–339, 2009.

[94] D. J. D. J. Crossley and M. G. Rochester. The subseismic approximation in core dynamics-II Love numbers and surface gravity. *Geophys. J. Int.*, 125:830–840, 1996.

[95] V. Dehant and P. Defraigne. New tranfer functions for nutations of a nonrigid Earth. *J. Geophys. Res.*, 102:27659–27687, 1997.

Appendix A

Algorithm for Integration with Respect to the θ

In the section 4.8, we explain a technique to remove the θ dependence from the Galerkin functional forms of the dynamical equations. We apply this technique to develop an algorithm based on the work of Seyed-Mahmoud [81]. Here, the algorithm for integration with respect to θ is as follows:

```
l=2*i2
if (i4.eq.3) goto 109 [This if statement separate the odd and even chain of the displacement
i.e., this if loop performs for the equation (2.23)]
if (l1.eq.2) then
l=l+4
az=0.0d0
ax=0.0d0
bx=0.0d0
cx=0.0d0
dx=0.0d0
ex=0.0d0
kx=Al(m,l-1)*GX(m,l-3)
lx=3.0d0*GX(m,l-1)*GX(m,l-2)*GX(m,l-3)
mx=2.0d0*l*Al(m,l-1)*GX(m,l-3)
nx=-l*Al(m,l-2)*GX(m,l-1)

    else if (l1.eq.1) then
l=l+2
az=0.0d0
ax=GX(m,l-1)
bx=-l*GX(m,l-1)
cx=Al(m,l)
dx=2.0d0*(l+1)*Al(m,l)
ex=6.0d0*cx-dx
kx=Al(m,l-1)*HX(m,l-3)+Bl(m,l-1)*GX(m,l-1)
lx=3*GX(m,l-1)*(GX(m,l-2)*HX(m,l-3)+GX(m,l-1)*HX(m,l-2)+GX(m,l)*HX(m,l-1)-1.0d0)
mx=2*l*Al(m,l-1)*HX(m,l-3)+3*Bl(m,l-1)*GX(m,l-1)
```

```
nx=(l-1)*Al(m,l)*HX(m,l-1)-l*Bl(m,l-2)*GX(m,l-1)

    else if(l11.eq.0) then
az=1.0d0
ax=HX(m,l-1)
bx=(l-1)*HX(m,l-1)
cx=Bl(m,l)
dx=3.0d0*Bl(m,l)
ex=6.0d0*cx-dx
kx=Bl(m,l-1)*HX(m,l-1)+Cl(m,l-1)*GX(m,l+1)
lx=3.0d0*HX(m,l-1)*(GX(m,l-1)*HX(m,l-2)+GX(m,l)*HX(m,l-1)+GX(m,l+1)*HX(m,l)-
1.0d0)
mx=3.0d0*Bl(m,l-1)*HX(m,l-1)-2*(l-1)*Cl(m,l-1)*GX(m,l+1)
nx=(l-1)*HX(m,l-1)*Bl(m,l)-l*GX(m,l-1)*Cl(m,l-2)

    else if(l11.eq.(-1)) then
l=l-2
az=0.0d0
ax=0.0d0
bx=0.0d0
cx=Cl(m,l)
dx=-2.0d0*l*Cl(m,l)
ex=6.0d0*cx-dx
kx=Cl(m,l-1)*HX(m,l+1)
lx=3.0d0*HX(m,l-1)*HX(m,l)*HX(m,l+1)
mx=-2.0d0*(l-1)*Cl(m,l-1)*HX(m,l+1)
nx= dfloat(l-1)*Cl(m,l)*HX(m,l-1)
end if
109 continue

    if (i4.eq.3) then [ This if loop performs for the equation (2.22)]
if(l1.eq.1) then
l=l+2
az=0.0d0
ax=0.0d0
bx=0.0d0
cx=Al(m,l-1)
dx=2.0d0*(l)*Al(m,l-1)
ex=6.0d0*cx-dx
kx=Al(m,l)*GX(m,l-2)
lx=3.0d0*GX(m,l)*GX(m,l-1)*GX(m,l-2)
mx=2.0d0*(l+1)*Al(m,l)*GX(m,l-2)
nx=-dfloat(l+1)*Al(m,l-1)*GX(m,l)

    else if (l1.eq.0) then
```

```
az=1.0d0
ax=GX(m,l)
bx=-dfloat(l+1)*GX(m,l)
cx=Bl(m,l-1)
dx=3.0d0*Bl(m,l-1)
ex=6.0d0*cx-dx
kx=Al(m,l)*HX(m,l-2)+Bl(m,l)*GX(m,l)
lx=3.0d0*GX(m,l)*(GX(m,l-1)*HX(m,l-2)+GX(m,l)*HX(m,l-1)+GX(m,l+1)*HX(m,l)-1.0d0)
mx=2.0d0*(l+1)*Al(m,l)*HX(m,l-2)+3.0d0*Bl(m,l)*GX(m,l)
nx=dfloat(l)*Al(m,l+1)*HX(m,l)-(l+1)*GX(m,l)*Bl(m,l-1)

    else if(l1.eq.(-1)) then
l=l-2
az=0.0d0
ax=HX(m,l)
bx=dfloat(l)*HX(m,l)
cx=Cl(m,l-1)
dx=-2*(l-1)*Cl(m,l-1)
ex=6.0d0*cx-dx
kx=Bl(m,l)*HX(m,l)+Cl(m,l)*GX(m,l+2)
lx=3.0d0*HX(m,l)*(GX(m,l)*HX(m,l-1)+GX(m,l+1)*HX(m,l)+GX(m,l+2)*HX(m,l+1)-1.0d0)
mx=3.0d0*Bl(m,l)*HX(m,l)-2.0d0*(l)*Cl(m,l)*GX(m,l+2)
nx=dfloat(l)*Bl(m,l+1)*HX(m,l)-(l+1)*GX(m,l)*Cl(m,l-1)

    else if(l1.eq.(-2)) then
l=l-4
az=0.0d0
ax=0.0d0
bx=0.0d0
cx=0.0d0
dx=0.0d0
ex=0.0d0
kx=Cl(m,l)*HX(m,l+2)
lx=3.0d0*HX(m,l)*HX(m,l+1)*HX(m,l+2)
mx=-2.0d0*(l)*Cl(m,l)*HX(m,l+2)
nx=dfloat(l)*Cl(m,l+1)*HX(m,l)
end if
end if

    if (i4.eq.1.and.i8.eq.1) then
F=az*S1+ax*S2+bx*S3+cx*S4+dx*S5+ex*S6+kx*S7+lx*S8+mx*S9+nx*S10
end if
```